AD-A071 814 DOUGLAS AIRCRAFT CO LONG BEACH CALIF F/G 1/3
HIGH SPEED BIRD IMPACT TESTING OF AIRCRAFT TRANSPARENCIES.(U)
JUN 78 M J COKER, R H MAGNUSSON F33615-75-C-3105
UNCLASSIFIED MDC-J7184 AFFDL-TR-77-98 NL

1 OF 3
AD
A071814

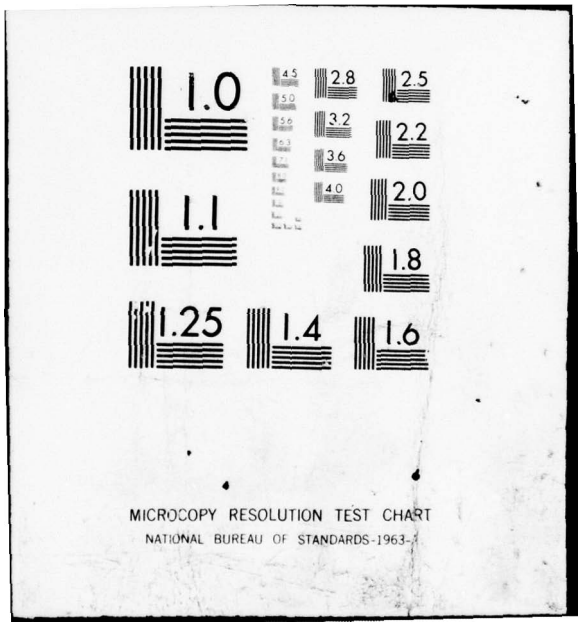
1.0
1.1
1.25
1.4
1.6
1.8
2.0
2.2
2.5
2.8
3.2
3.6
4.0
4.5
5.0
5.6
6.3
MICROCOPY RESOLUTION TEST CHART
NATIONAL BUREAU OF STANDARDS-1963-A

AFFDL-TR-77-98

LEVEL

HIGH SPEED BIRD IMPACT TESTING OF AIRCRAFT TRANSPARENCIES

R. H. Magnusson
Douglas Aircraft Company
McDonnell Douglas Corporation
3855 Lakewood Boulevard
Long Beach, California 90846

June 1978

TECHNICAL REPORT AFFDL-TR-77-98

Final Report Period July 1975-June 1978

Approved for public release; distribution unlimited

AIR FORCE FLIGHT DYNAMICS LABORATORY
AIR FORCE WRIGHT AERONAUTICAL LABORATORIES
AIR FORCE SYSTEMS COMMAND
WRIGHT-PATTERSON AIR FORCE BASE, OHIO 45433

NOTICE

When Government drawings, specifications, or other data are used for any purpose other than in connection with a definitely related Government procurement operation, the United States Government thereby incurs no responsibility, nor any obligation whatsoever; and the fact that the Government may have formulated, furnished, or in any way supplied the said drawings, specifications, or other data, is not to be regarded by implication or otherwise as in any manner licensing the holder or any other person or corporation, or conveying any rights or permission to manufacture, use, or sell any patented invention that may in any way be related thereto.

This report has been reviewed by the Information Office (OI) and is releasable to the National Technical Information Service (NTIS). At NTIS, it will be available to the general public, including foreign nations.

This technical report has been reviewed and is approved for publication.

Larry G. Moosman

LT. LARRY G. MOOSMAN
Project Manager
Improved Windshield Protection ADPO
Vehicle Equipment Division

Robert E. Wittman

ROBERT E. WITTMAN
Program Manager
Improved Windshield Protection ADPO
Vehicle Equipment Division

FOR THE COMMANDER:

Ambrose B. Nutt

AMBROSE B. NUTT
Director
Vehicle Equipment Division

Copies of this report should not be returned unless return is required by security considerations, contractual obligations, or notice on a specific document.

UNCLASSIFIED

SECURITY CLASSIFICATION OF THIS PAGE (When Data Entered)

REPORT DOCUMENTATION PAGE	READ INSTRUCTIONS BEFORE COMPLETING FORM
1. REPORT NUMBER: AFFDL-TR-77-98	2. GOVT ACCESSION NO. / 3. RECIPIENT'S CATALOG NUMBER
4. TITLE (and Subtitle): HIGH SPEED BIRD IMPACT TESTING OF AIRCRAFT TRANSPARENCIES	5. TYPE OF REPORT & PERIOD COVERED: FINAL REPORT July 1975 - June 1978
	6. PERFORMING ORG. REPORT NUMBER: MDC-J7184
7. AUTHOR(s): M. J. Coker, R. H. Magnusson	8. CONTRACT OR GRANT NUMBER(s): F33615-75-C-3105
9. PERFORMING ORGANIZATION NAME AND ADDRESS: Douglas Aircraft Company, McDonnell Douglas Corporation, Long Beach, California 90846	10. PROGRAM ELEMENT, PROJECT, TASK AREA & WORK UNIT NUMBERS: Project: 2202, Task: 02, Work Unit: 01
11. CONTROLLING OFFICE NAME AND ADDRESS: Air Force Flight Dynamics Laboratories/(AFFDL/FEW), Air Force Wright Aeronautical Laboratories, Air Force Systems Command, Wright-Patterson Air Force Base, Ohio 45433	12. REPORT DATE: June 1978
	13. NUMBER OF PAGES: 259
14. MONITORING AGENCY NAME & ADDRESS(if different from Controlling Office)	15. SECURITY CLASS. (of this report): Unclassified
	15a. DECLASSIFICATION/DOWNGRADING SCHEDULE

16. DISTRIBUTION STATEMENT (of this Report)

Approved for public release; distribution unlimited.

17. DISTRIBUTION STATEMENT (of the abstract entered in Block 20, if different from Report)

18. SUPPLEMENTARY NOTES

19. KEY WORDS (Continue on reverse side if necessary and identify by block number)

Aircraft Windshields	Impact Testing	Static Structural Analysis
Bird Impact	Laminated Plastics	Transparency
Dynamic Structural Analysis	Instrumentation	
Finite Element	Maintainability	

20. ABSTRACT (Continue on reverse side if necessary and identify by block number)

This report documents the test plans, test results and analyses of a series of high speed bird impact tests conducted on the B-1 X-5 Module windshield and on 36 x 36 inch simulated windshield test specimens as a portion of the work accomplished for the "Windshield Technology Demonstrator Program". The testing, analyses and development accomplished during this program involved a total system approach required for aircraft windshields in the context of the continuing Air Force generic windshield development programs. Tests were conducted to evaluate the bird impact resistance of glass and plastic

DD FORM 1 JAN 73 1473 EDITION OF 1 NOV 65 IS OBSOLETE

SECURITY CLASSIFICATION OF THIS PAGE (When Data Entered)

ABSTRACT:

windshield panels and associated supporting structure being considered for use in the B-1 aircraft. Strain and deflection measurements were made on the test panels and supporting structure on most of the tests. A description of the tests and the results obtained are presented.

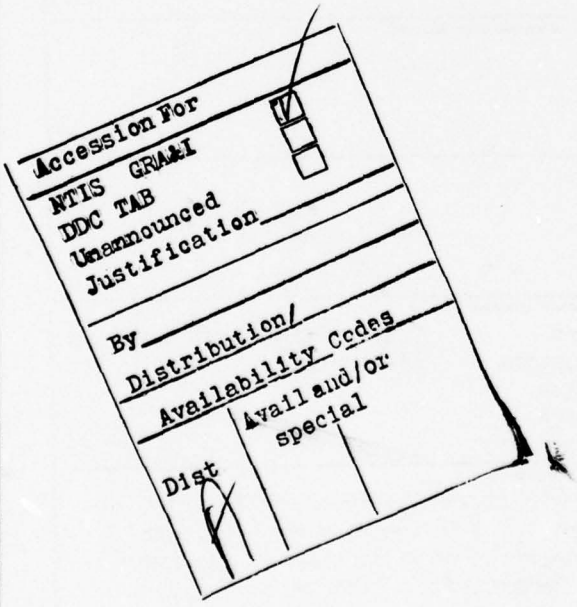

FOREWORD

This report is one of a series of reports that describes work performed by Douglas Aircraft Company, McDonnell Douglas Corporation, 3855 Lakewood Blvd., Long Beach, California 90846, under the Windshield Technology Demonstrator Program. This work was sponsored by the U.S. Air Force Flight Dynamics Laboratory, Wright-Patterson Air Force Base, under Contract F33615-75-C-3105, Project 2202/1926.

Capt. D. C. Chapin, USAF (Ret.), was the Air Force Project Manager during the conceptual phase of the work reported herein. Lieutenant L. G. Moosman (AFFDL/FEW) succeeded Captain Chapin during the conduct of the program.

Mr. J. H. Lawrence, Jr., was the Program Director for the Douglas Aircraft Company.

Principle investigators and contributing authors were:

M. J. Coker	-	Structures - Design
R. H. Magnusson	-	Structures - Stress
J. B. Hoffman	-	Structures - Design
L. R. Islander	-	Project Manager - Testing and Instrumentation
J. H. Lawrence	-	Structures - Design
J. W. Kozmata	-	Material and Process Engineering
V. G. Staar	-	Structures - Design

The authors wish to thank the many individuals in the commercial and military aircraft manufacturing industry and the aircraft windshield manufacturers for their excellent cooperation in sharing their experiences during the conduct of this work.

This report was first submitted to the Air Force in February 1978 and the time period covered by this report was from July 1975 through June 1978.

TABLE OF CONTENTS

TABLE OF CONTENTS (Continued)

LIST OF ILLUSTRATIONS

LIST OF ILLUSTRATIONS (Continued)

LIST OF ILLUSTRATIONS (Continued)

LIST OF TABLES

LIST OF SYMBOLS

c	Coefficient of viscous damping
D	Diameter of bird package
e	Natural logarithm base
$\bar{F}$	Effective force during impact
I	Impulse
K	Spring stiffness
L	Bird package length
$\bar{L}$	Effective bird length
M	Transparency mass in motion
P	Statically applied load
q	Disturbing force per unit mass
Q	Disturbing force
S_L	Equivalent static load
S_{L1}	Maximum static load ($t < t_d$)
S_{L2}	Maximum static load ($t_d < t$)
t	Time

t'	Dummy time variable
t_d	Time duration of impact
V	Bird impact velocity
W	Bird weight
x	Displacement of mass M in x-direction
$\dot{x}$	Velocty of mass M in x-direction
$\ddot{x}$	Acceleration of mass M in x-direction
x_o	Initial displacement of mass M in x-direction
$\dot{x}_o$	Initial velocity of mass M in x-direction
δ_i	Windshield deflection
ζ	Damping ratio
θ	Impact angle
ω_d	Damped natural frequency
ω_n	Natural frequency

SECTION I
INTRODUCTION

The impact of a bird on windshields of aircraft flying at high speeds represents a major structural problem for today's aircraft. The Douglas Aircraft Company's Windshield Technology Demonstrator Program is part of an effort by the Air Force Flight Dynamics Laboratory Improved Windshield Protection Program to develop technologies that will assist in the design of aircraft transparent enclosures to increase protection against bird-strikes.

Included in this report are the test plans, test results and analyses of a series of high speed impact tests conducted on test specimens of various windshield laminations and support structure designs. A basic consideration to this test series was the premise that for test results to be truly representative, the tests must be performed on structure which represents, simulates, or otherwise accounts for, actual aircraft structural stiffnesses. This consideration was followed throughout this test series.

Section II presents the test plans for a series of bird impact tests consisting of the following:

- B-1 Windshield Bird Impact Test Series
- Simulated Aircraft Windshield Bird Impact Test Series

The B-1 windshield was mounted in a crew module and subjected to a series of static loading/dynamic unloadings and bird impact tests on the original and on Douglas-modified windshield edge mountings. The purpose of this test series was twofold: (1) to demonstrate the relative merits of the various designs to defeat a four-pound bird at 565 KIAS (Sea Level) and to use this information in the design of simulated aircraft windshields and supporting structure, and (2) to collect windshield and support structure static, dynamic, and bird impact characteristic responses (both deflections and strains).

Five alternate simulated aircraft windshields were designed, fabricated and mounted on support fixtures which were designed to simulate the actual stiffness of the respective installation. The purpose of this test series was to demonstrate the capability of the Douglas alternate designs to defeat a four-pound bird at 565 KIAS (Sea Level) when subjected to operational temperature extremes. This provided data from which recommendations were made for a final USAF B-1 windshield and supporting structure design.

Section III establishes the requirements for strain measurements, deflection and temperature measurements, and high-speed motion picture coverage for the Windshield Bird Impact Tests. The test instrumentation required in the conduct of this series of high-speed bird impact tests was, in certain aspects, unique, and represented an advance in the state of the art. Detailed descriptions of the instrumentation utilized in this test series are presented, as is a recommended instrumentation checklist for Bird Impact Tests.

The bonding of strain gages on polycarbonate and acrylic window specimens, and on interlaminar plies, and then subjecting these specimens to high-speed bird impact, involved many instrumentation techniques which had to be developed for these applications. Previous investigators in this area expected crazing, with a resulting loss in impact resistance, on any polycarbonate part that had strain gage adhesive applied to it. Also, with the high G-level expected from a bird impact on the windshield, retention of externally mounted gages was a matter of concern. The candidate adhesives and installation techniques are also discussed in Section III.

The test results are presented and discussed in Section IV. In addition to the B-1 Windshield Bird Impact Test Results and the Simulated Windshield Bird Impact Test Results is a description of the Arnold Engineering Development Center (AEDC) data acquisition and reduction equipment, and an estimation of the data uncertainties. The test results include discussions of selected shots, tabular summaries, support structure behavior and strain and gage deflection tabulation.

It should be emphasized that this series of high speed impact tests is based on the approach to windshield design which considers the entire windshield structural system. By this is meant, the structure of the windshield coupled with the windshield supporting structure. Any evaluation of an aircraft windshield system must be systematically evolved from a review of past experience and available related industry design philosophies, design analyses, and test fixture development which are presented in Section V.

Section V also shows the results of Preliminary Design Methods utilized in these analyses which could be adapted to any windshield design effort involving bird impact.

Section VI presents a method for obtaining an equivalent static load on an aircraft windshield subjected to a bird impact and evaluates the effects on this load due to the relative stiffness of the impacted area. This bird impact study is an attempt to address the effects of total windshield system compliance on a rather simplistic level which may be conveniently used in the preliminary design phases of windshield systems.

Section VII presents conclusions and recommendations based on test results.

Two appendices are included in this report:

Appendix A contains detailed failure analyses of the windshield specimens utilized in these series of high speed bird impact tests. Specifically, for each specimen, detailed part and test information is listed, followed by a discussion of salient features of the failed specimen. Sketches are included which fully illustrate failure patterns and windshield fabrication details.

Appendix B contains B-1 windshield and simulated aircraft windshield strain maps, which were formulated from the high speed bird impact tests.

SECTION II
TEST PLANS

The test plans presented were used in two separate series of bird impact tests directed toward the B-1 aircraft windshield design. The first series, B-1 Windshield Bird Impact Tests, was conducted on actual B-1 windshields mounted in a crew module. Included in this test series were several static loading/dynamic unloading tests to determine the simple harmonic responses to the system when the edge configuration was altered.

The second series of tests was conducted on panels representing various windshield constructions mounted in support fixtures simulating the actual stiffness of the respective installation for correlation with analytical prediction techniques.

The purpose of the first test series was (1) to demonstrate the relative merits of the B-1 windshield installation and the same installation with modifications to defeat a four-pound bird at 565 KIAS and to use the test information for the design of simulated aircraft windshields and supporting structure, and (2) to collect windshield and support structure static, dynamic and bird impact characteristic response (both deflection and strain) data.

The purpose of the second test series was to demonstrate the ability of alternate simulated designs to defeat a four-pound bird at 565 KIAS when subject to operational temperature extremes for 8000 feet and below. This provided data from which recommendations were made for a final USAF B-1 windshield and supporting structure design.

B-1 WINDSHIELD BIRD IMPACT TESTING

With three windshields, one right hand and two left hand, available for these tests only four static and four impact tests were planned. As the testing progressed and little damage occurred two additional impact tests of a pass/fail response were performed.

The subsequent paragraphs define the test specimens, test loads, the test setup, and test procedure which had been planned to collect all pertinent data.

Test Specimens

Windshield Specimens

The test specimens were furnished by the Air Force and consisted of representative air vehicle windshields mounted in a Prototype B-1 Crew Module at AEDC.

The parts available were manufactured by Swedlow, Inc., per Rockwell International (RI) drawing L3000151, and were identified as:

*L3000151-001	Left Hand	SWU 108
L3000151-001	Left Hand	SWU 107
L300151-002	Right Hand	SWU 105

*Initially installed in Module.

The left hand part, SWU 107, had the bushing bolt attachments holes enlarged from 0.257 nominal to 0.300 minimum diameter, by AEDC/ARO, Inc. as described in Figure 1, before installation on the crew module. Each bushing was cleaned with Alaphatic naptha (TT-N-95), followed by cleaning with isopropyl alcohol. Dow Corning 1200 Primer was then applied to each bushing and the bushing cemented in the windshield hole with Dow Corning 93-007 sealant.

After testing, the test specimens were inspected for chipping, creep and deformation, and were then shipped to Douglas Aircraft Co., for Tracking and Data Acquisition (TDA). There coupon specimens were removed to establish mechanical and physical properties of the different materials.

B-1 Crew Module (X-5)

Prior to any testing in this series, repair to the X-5 Module was necessary as the upper right-hand windshield support near the module centerline had been damaged during prior B-1 bird impact qualification tests. The required repairs were accomplished by AEDC/ARO.

Bushing Requirements

AEDC obtained 116 bushings for the right-hand windshield installation. These bushings conformed to B-1 drawing dimensions and requirements. The 116 bushings obtained for the left-hand windshield installation were modified as shown in Figure 1.

After each bird impact test the bushings were reconditioned to prepare for the next test.

Retainer Modification

One set of left-hand windshield retainers were modified for a separate test as shown in Figure 2.

Test Requirements

To accomplish the required testing, AEDC provided facilities for static and bird impact testing. AEDC also provided a test support structure to mount the crew module for static loading and dynamic unloading (Figure 25, page 66) with the capability of applying a 2500-pound force normal to the windshield without interacting with it during the response phase.

The quick release mechanism and loading pad were designed and fabricated by Douglas Aircraft Co.

A goal of the windshield bird impact test was to obtain data from the same locations used to apply the static loads. Location A, Figure 3, for statically applying load was also a target for bird impact. Other points shown in Figure 3 were optional target points but were not utilized in this test series.

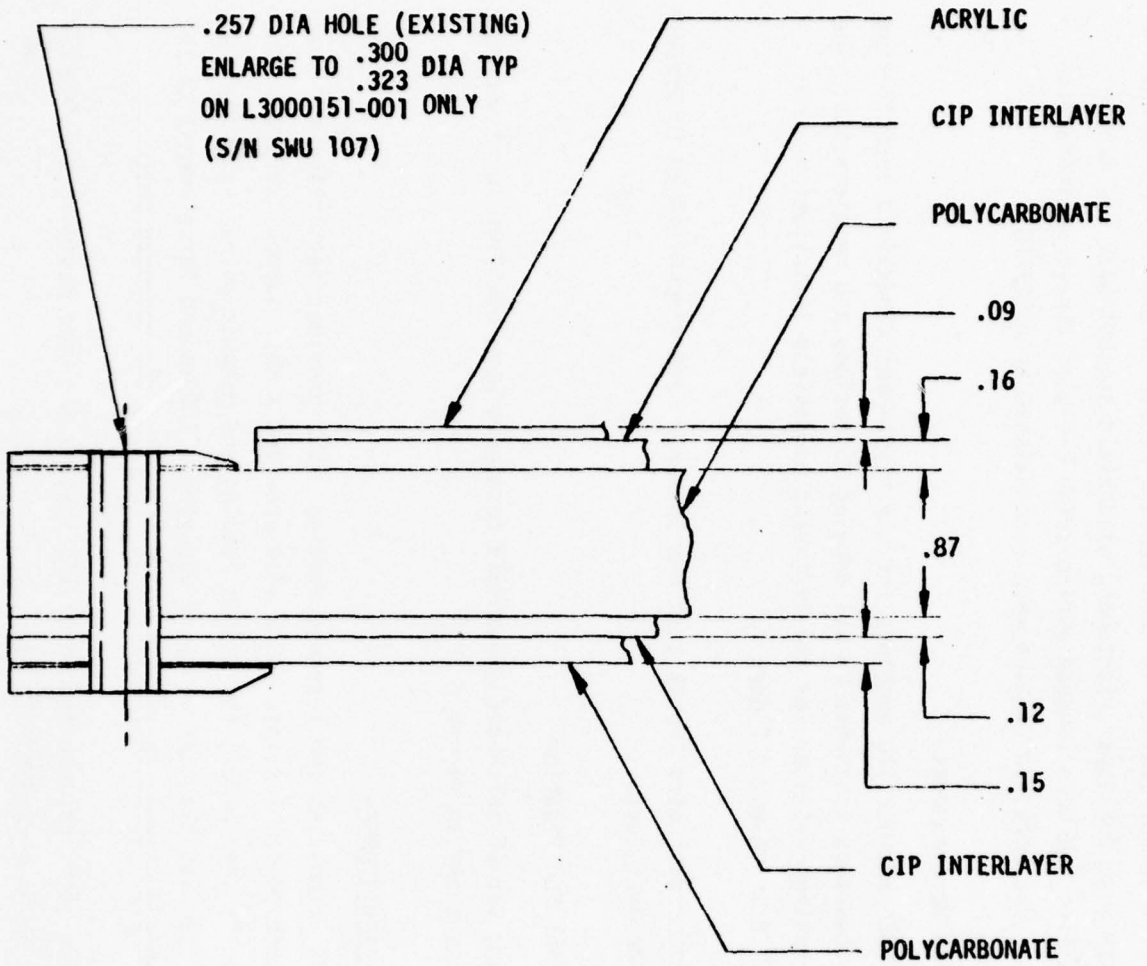

Figure 1. B-1 Crew Module Windshield (L3000151).

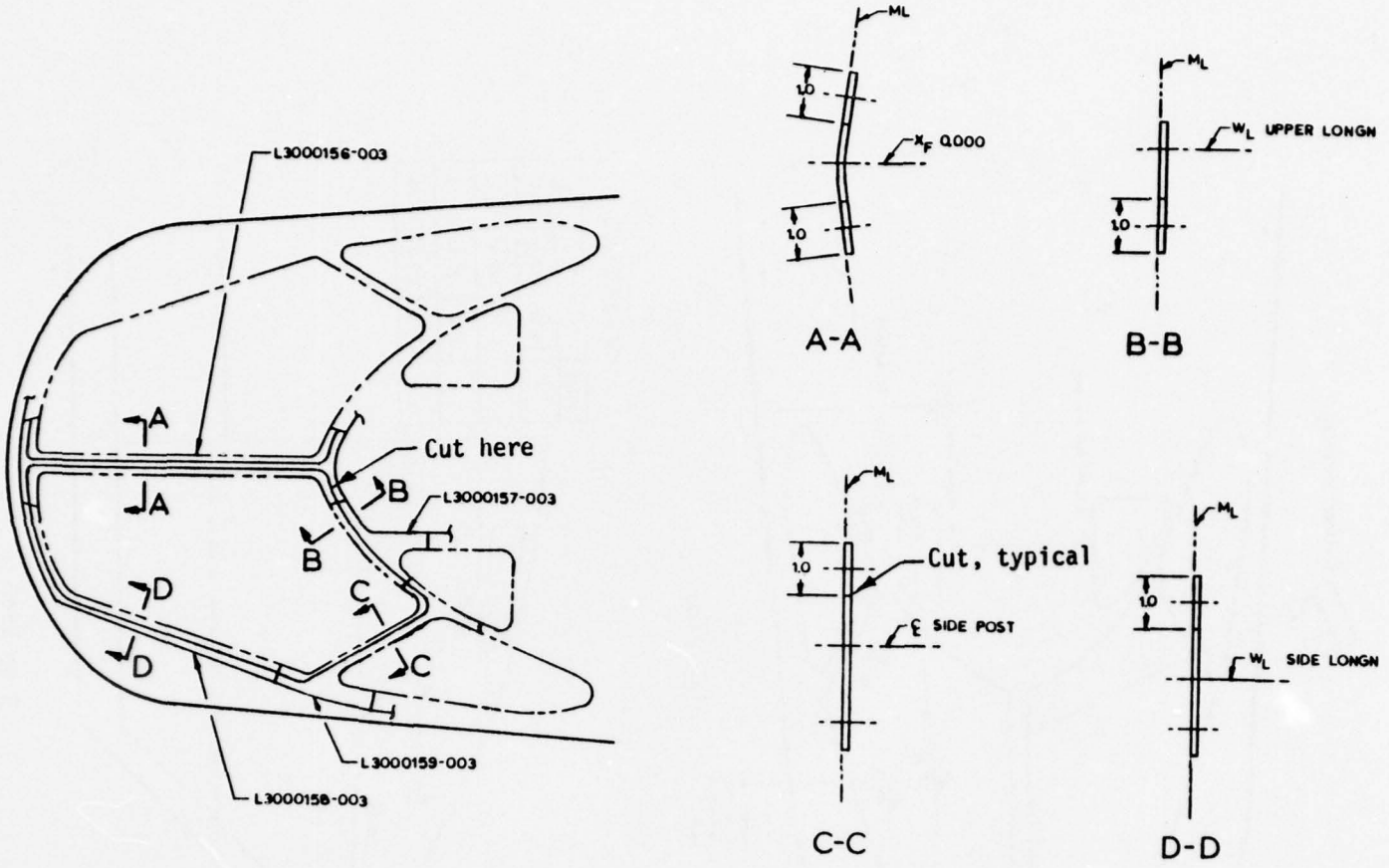

Figure 2. Retainer Modification. One Set of L.H. Outside Retainers Cut Lengthwise to Dimensions Shown.

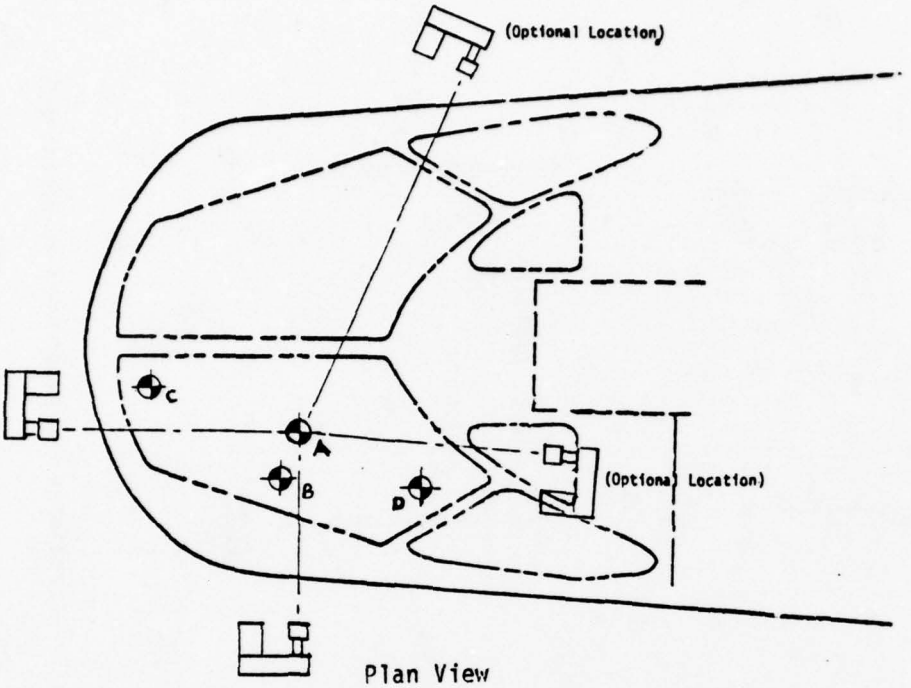

Plan View

POINT COORDINATES

POINT	X_F	Y_F	Z_F
A	18.58	252.31	81.87
B	24.14	247.61	75.46
C	7.00	227.88	76.05
D	24.76	270.75	85.68

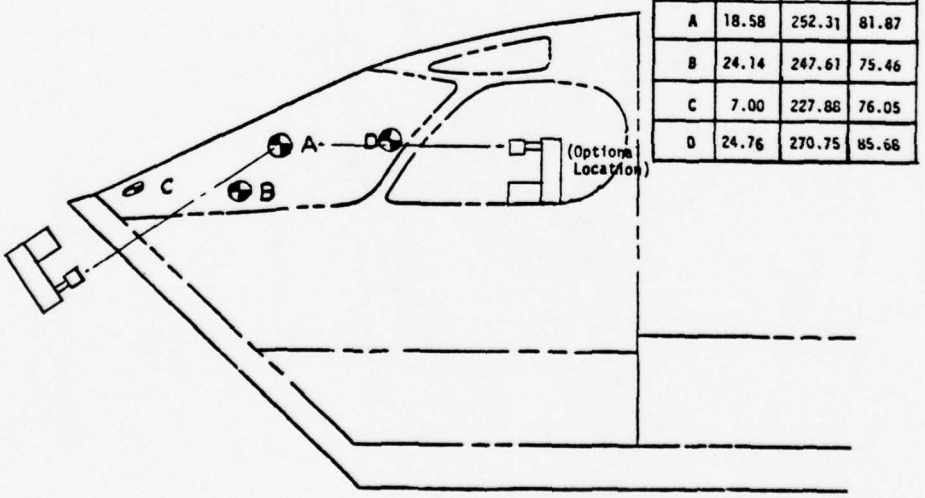

Side View

Figure 3. Bird Target and Camera Locations.

To ensure continuity and repeatability of the bird impact tests, rigid requirements were placed upon the bird weight, bird packaging and the bird accelerating equipment.

Structure Requirement

Modification of the test cell to accommodate the test assembly was accomplished by AEDC. The test assembly was positioned in a level attitude so that the windshield centerline beam would be at a 25-degree angle with respect to the bird gun horizontal axis to match the B-1 average flight angle. The module and its support fixture were elevated and positioned in a lateral direction to provide the appropriate alignment for the bird impact locations.

Installation of the windshields into the X-5 module was accomplished according to Rockwell procedure except for the bushings in the left-hand windshield.

Cameras

Results of each bird impact were recorded by 16MM high-speed cameras, furnished by the AEDC. Frame speed of high-speed cameras was sufficient (5000 frames/second) to clearly distinguish the bird during flight and to show structural deflections during and after impact. All cameras utilized color film and each camera viewing position had the test shot number prominently displayed within the field of view during the shot sequence. Module exterior camera coverage consisted of one high-speed camera located at an angle of approximately 30 degrees to the strike path showing an overall view of the approach and impact of the bird on the test specimen, and a second high-speed camera located 90 degrees to the strike path showing the flight of the bird, impact and windshield deflection. Figure 3 shows the approximate camera locations used throughout this series of tests.

Test Objectives

The objective of the initial test series was to collect sufficient deflection and strain data from bird impact to assist in the development and verification of, and correlation with, the bird impact analytical response prediction program documented in AFFDL-TR-77-99 (Bird Impact Math Model). After this had been accomplished the second objective was to demonstrate or verify the suitability of a recommended edge design for the B-1 windshield.

The second series of bird impact tests was made on simulated aircraft windshields with four-pound birds at 565 KIAS as required for the B-1 aircraft. The simulated windshields, five different concepts in number, represented constructions considered acceptable for the B-1. The specific objectives were to:

1. Demonstrate the various simulated windshield constructions
2. Obtain data on corner configuration sensitivity during bird impact
3. Obtain response data for the three support structure configurations when mated with the various panels.
4. Study the applicability of several instrumentation technqiues for deflection and strain measurements.

Test Procedure

To determine the deflection versus loading for the windshield system a series of loading tests were conducted in the following sequence:

1. A maximum of 1500 pounds static load was applied. Deflection data, strain gage data, thermocouple readings, sensing element readings, relative humidity, cell ambient temperature, and temperature inside the module before testing were recorded on data sheets. The load was quickly released and a record of the strain

gage data was made during specimen damping. High speed movie coverage was used during damping. The hydraulic cylinder was retracted to its original position.

Repeated test applying a maximum 2500 pound static load at Location A.

2. Examined strain gages and thermocouples for damage and removed deflectometers. Refurbished and/or replaced any damaged units.

3. Positioned module in test cell for Bird Shot No. 1 at Location A.

4. Attached all instrumentation lead wires from windshield to recording apparatus.

5. Performed calibration tests on recording apparatus with camera lights on five minutes prior to calibration. Recorded all calibration data.

6. Performed required Shot No. 1 bird impact test at Location A with a four-pound bird at 650 $\pm$ 17 MPH velocity. Recorded the condition of specimen before test, strain gage data before and after lights were turned on, and after impact. Recorded the bird weight, bird velocity, cell and module temperatures, thermocouples and sensing element readings before camera lights were turned on, and at time of impact. Deflection recordings of impact were accomplished with high speed movie cameras. Other high speed movies were used as required for testing coverage.

7. Examined strain gages, thermocouples, sensing element wiring, and test article structure for damage. Refurbished and/or replaced any units damaged. Reinstalled deflectometers.

8. Removed all retainers common to the left-hand windshield and installed reworked retainers noted in Figure 2. Torqued bolts common to windshield to 50-60 inch-pounds, including the center retainer for the right-hand windshield. All other portions of the retainers were installed and bolts torqued to 80-105 inch-pounds.

9. Applied a maximum of 1500 pound static load at Location A as described in Sequence 1.

10. Repeated Sequence 2.

11. Performed required Shot No. 2 bird impact test at Location A with a four-pound bird at 650 $\pm$ 17 MPH velocity. Recorded condition of specimen before test, strain gage data before camera lights were turned on, at time of, and during impact. Recorded bird weight, bird velocity, temperature, and relative humidity in test cell and inside module before camera lights were turned on, thermocouple and sensing element readings before camera lights were turned on and at the time of impact. Deflection recordings of impact were to be accomplished with high speed cameras. Other high speed movies were also required during impact.

12. After Shot No. 2, the instrumentation was disconnected and the windshield was removed. The retainers were saved for subsequent usage. The test structure was examined for damage and repaired as necessary.

13. Installed L3000151-001, Serial Number SWU 107, with R-I drawing retainers and all bolts common to the windshields were torqued to 50-60 inch-pounds and all other bolts were torqued to 80-105 inch-pounds. As each bolt was partially installed, PR 1422 sealant was applied around the bolt shank to fill the hol

Note: Under ambient temperature conditions above 70°F, it normally took 72 hours for the sealant to fully cure. For these series of tests, it was mandatory that the sealant was cured.

14. Installed on the windshield were strain gages, thermocouples, and sensing element wires; the lead wires were attached to recording devices.

15. Strain gages and thermocouples were calibrated before the camera lights were turned on and five minutes after lights were turned on. All data were recorded.

16. A maximum of 1500 pound static load was applied at Location A as described in Sequence 1.

    Repeated test applying a maximum 2500 pound static load at Location A.

17. Removed deflectometers and static load applicator.

18. Examined strain gages and thermocouples for damage. Refurbished and/or replaced any damaged units.

19. Repeated Sequence 5.

20. Performed required Shot No. 3 bird impact test at Location A as described in Sequence 6 except that strain gage data was noted during impact.

21. Repeated Sequence 7.

22. Repeated Sequence 8 except that bushing sealant was added as required.

23. Repeated Sequence 5. Performed calibration tests on recording apparatus with camera lights on five minutes prior to calibration. Recorded all calibration data.

24. Applied a maximum 1500 pound load at Location A as described in Sequence 1.

    Repeated test applying a maximum of 2500 pound static load at Location A.

25. Examined strain gages, thermocouples, sensing element wiring, and test article structure for damage, and removed deflectometers. Refurbished test article structure and/or replaced any damaged units.

26. Calibrated strain gages and thermocouples before camera lights were turned on and five minutes after lights were turned on. Recorded all data.

27. Performed required Shot No. 4 bird impact test at Location A as described in Sequence 11.

28. Reviewed data and test structure conditions from Shots 1 through 4 for subsequent assessment to ascertain which attachment should be employed for future production windshields.

29. Removed every other windshield attachment bolt.

30. Performed additional Shot No. 5 bird impact test at Location A with a planned four-pound bird at 650 $\pm$ 17 MPH velocity.

    Instrumentation: Replaced and repaired strain gages as required. Monitored all working strain gages, thermocouples, sensing elements similar to previous tests. All high-speed cameras were used. Appropriate still photos were taken after the shot.

31. Reviewed data and test structure from Shot No. 5. Repaired damage as required.

32. Performed Shot No. 6 bird impact test at Location A with planned six-pound bird at 650 ± 17 MPH velocity.

    Instrumentation: Same requirements as test Number 5.

    Special Requirements: Precautions were taken to minimize module interior damage due to possible bird penetration during this shot. Relocated interior camera, lights, etc., as required. Plastic sheeting was utilized to minimize possibility of bird debris residue in cockpit.

33. Reviewed data and test structure from shot Number 6.

After completion of Shot Number 6 (BM-009), the B-1 module, and both impacted windshield specimens with all removed retainers, hardware, bolts, etc., were shipped to Douglas.

Documentation

To ensure that maximum data were retained from the several static and impact tests, different methods of documentation were utilized.

For the static loading/dynamic unloading tests, this documentation included recording of pre- and post-test structural and environmental conditions, deflection versus time oscillograph recordings, digitized strain readings, and movies of the unloading and windshield dynamics. The greatest concern in determining the instrumentation and data recording methods was for strain gage failure during the activity. To ensure that maximum data points would be taken, the initial data points were in micro-seconds. The data were recorded in the following form:

Deflection: Displacement versus Time
and Displacement versus Load

Strain: μ in./in. versus Time (Printed and plotted)

The recording methods utilized for the static cases were supplemented with extensive camera coverage during the bird impact tests. The intent of camera coverage was:

1. To provide a means to accurately record the structural deflections occurring during and after the impact.

2. To provide an overview documentation of the impact that could be correlated with the recorded deflection and strain data.

3. To verify that the required condition of bird packaging was met.

SIMULATED AIRCRAFT WINDSHIELD BIRD IMPACT TESTING

This subsection describes a series of preliminary bird tests that were necessary to substantiate the materials selections and analyses formulated for alternate design concepts that could be utilized for design of B-1 Pilot's/Copilot's windshields and supporting structure.

The objectives of this series of tests were to assess:

- The adequacy of those materials selected
- The scaling effect of the selected instrumentation methods
- The effect of the adjacent structure on windshield panel stiffness.
- Aircraft operational and performance effects on the ability of a transparency to meet bird impact requirements.
- The effect of gussets and/or corner fittings on windshield panel response to the bird impact phenomena.
- Collection of test data for correlation with the bird impact math model for analysis validation.

- The effect of varying the transparency edge configuration on the transparency support structure.
- Selection of pertinent data for final transparency design determination.

The windshield specimens used were curved to a 60-inch radius to simulate the B-1 configuration. The initial testing was per the test plan of Reference 1.

Test Specimens

Ten specimens, simulating laminated glass windshields and laminated polycarbonate windshields, were built by transparency vendors and were tested as described in this report.

In determining what constructions would be viable candidates for the proposed B-1 design, several laminated designs of thin polycarbonate were estimated to be preferred over a single thicker (7/8 inch) polycarbonate ply. This resulted in the Z5942640-501, Z5942639-503, Z5942639-505 designs. To validate the theory that under low thermal conditions, the thicker monolithic layer would fail where as the multilaminate design would accept partial failure without penetration, a monolithic polycarbonate ply specimen (Z5942640-507) was required. The construction and edge configuration of these specimens are shown in Figure 4.

Three laminated glass specimens (Z5942639-501), Figure 5, were built to approximately simulate windshields that are currently in the Douglas DC-10 aircraft. Tests on and service usage of this windshield has shown that this construction has a high service reliability and reasonably high impact resistance.

Figures 4 and 5 also show the various specimens built with identifying numbers.

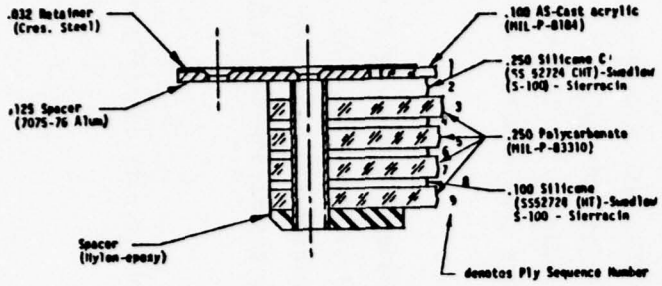

Figure 4a. Laminated Polycarbonate Windshield Design (Z5942640-501).

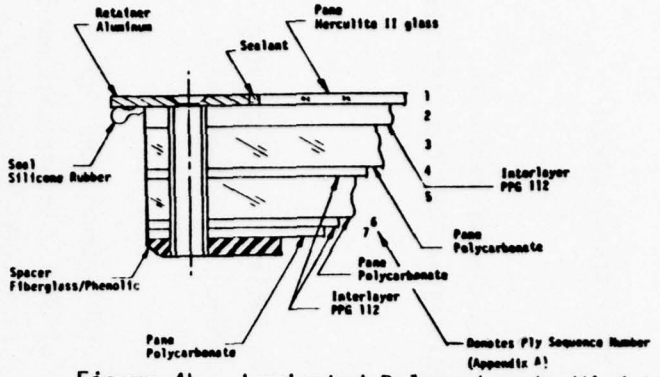

Figure 4b. Laminated Polycarbonate Windshield Design (Z5942639-503).

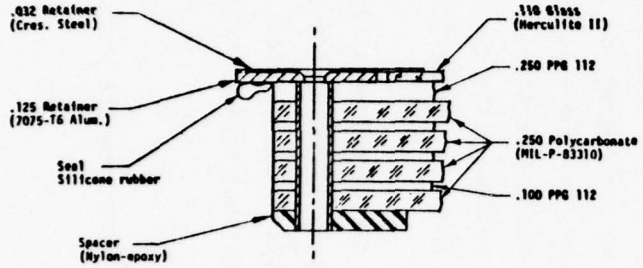

Figure 4c. Laminated Polycarbonate Windshield Design (Z5942639-505).

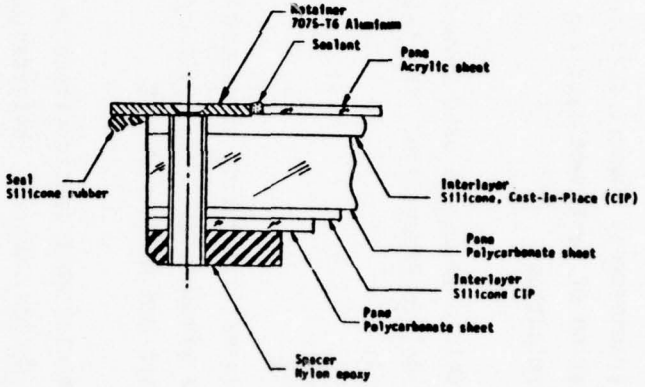

Figure 4d. Laminated Polycarbonate Windshield Design (Z5942640-517).

Figure 4.

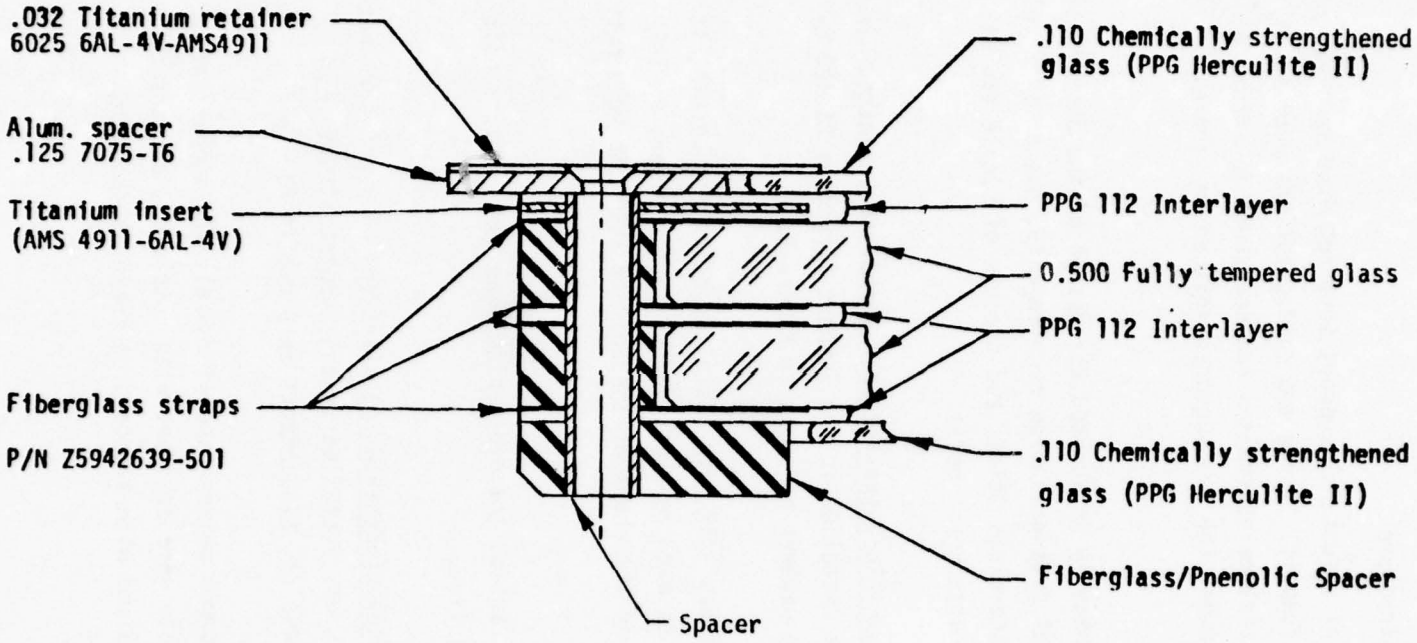

Figure 5. Laminated Glass Construction (Z5942639-501).

Test Specimen Support Structure

Two configurations of structural support were required to simulate current B-1 structural support. These two configurations were identified as Z5942638-1 and -501 fixture assemblies and are shown in Figure 6, with the differences between the two supports defined in Figures 6a, through Figure 6h.

Those factors that heavily influenced the design of the support structure were operational internal pressurization requirements, use of stiff glass and flexible polycarbonate windshields, and the use of single row attachment bolts and dual row attachment bolts.

Glass Laminated Windshield Installation - The Glass Laminated Windshield, Z5942639-501 was installed in the Support Structure Z5942638-1, using standard bolts, nuts and washers as shown in Figure 6.

The glass windshield has 1/16 inch oversized holes for bolting it to the structure fixture. As each bolt was partially installed, PR 1422 sealant was applied around the shank of the bolt to fill the void between the bolt and spacer.

For bolts that were reused, the old sealant was removed from bolt threads and sealant reapplied.

Polycarbonate Laminated Windshield Installation - The polycarbonate Windshield, Z5942640-501, was installed in the Support Structure, Z5942638-501, with two rows of attachments as shown in Figure 6.

The 84 attachments common between the windshield and support structure that were inaccessible were attached with nutplates, and the other 80 attachments were installed with standard hardware as shown in Figure 6.

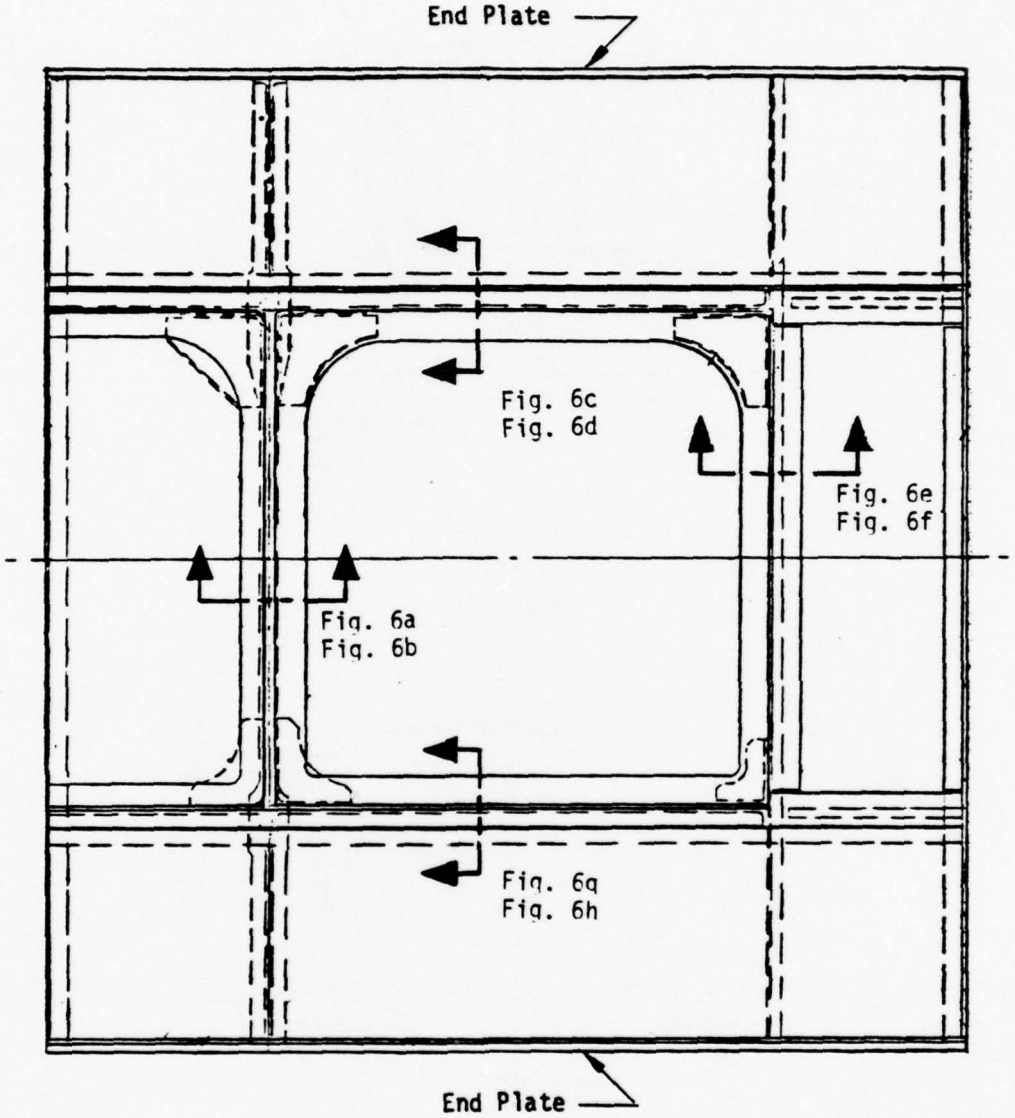

P/N Z5942638-1 for laminated glass

P/N Z5942638-501 for laminated polycarbonate

Figure 6. Windshield Support Structure Fixture Assemblies.

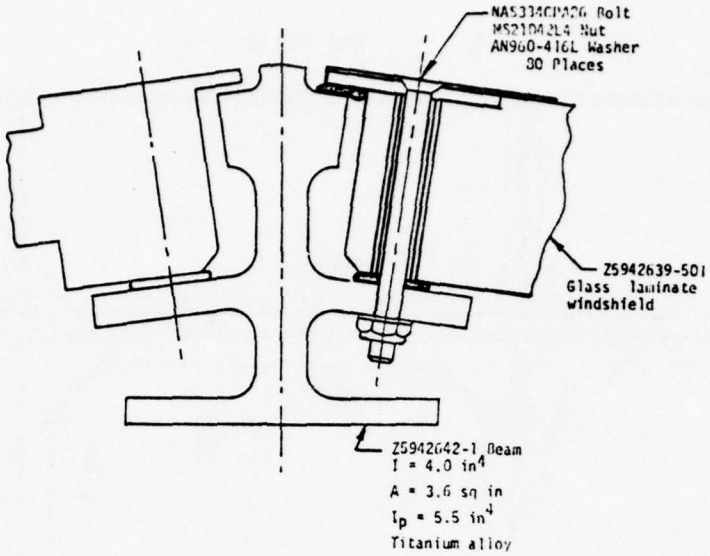

(-1)
Figure 6a.

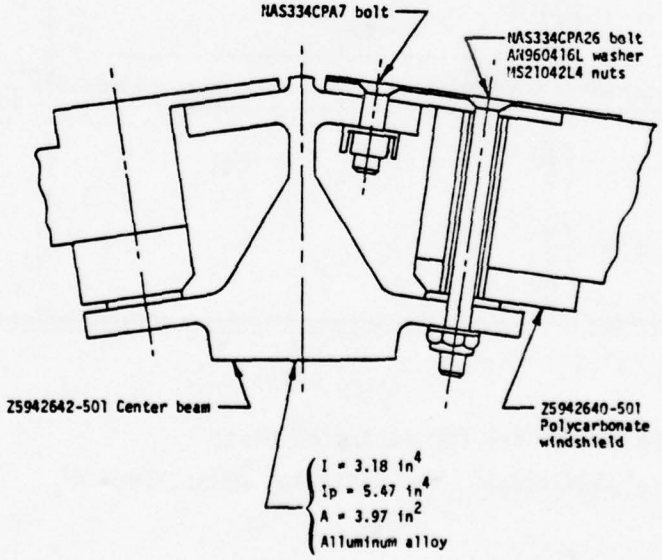

(-501)
Figure 6b.

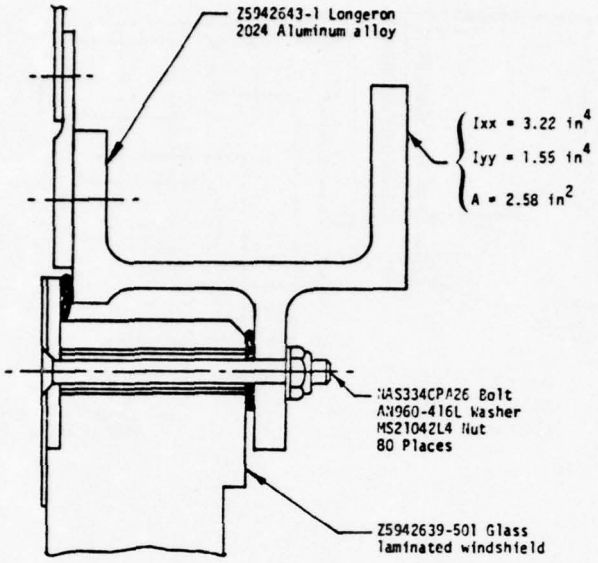

(-1)
Figure 6c.

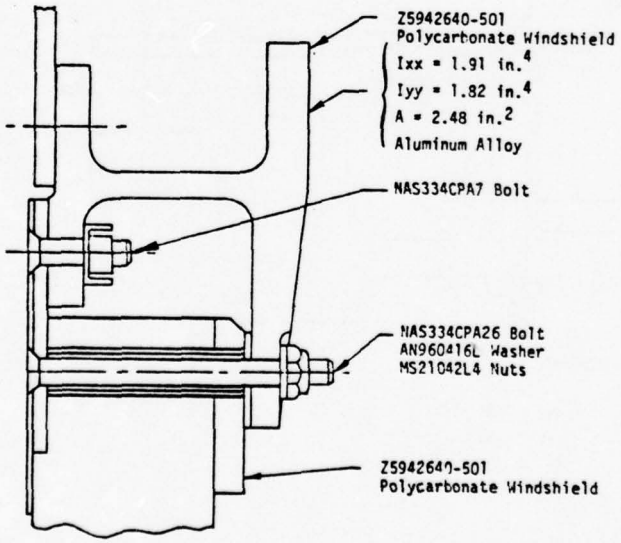

(-501)
Figure 6d.

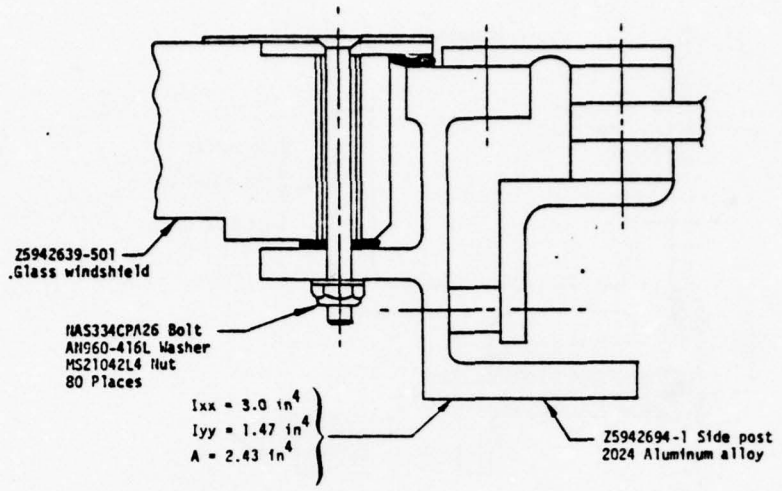

(-1)
Figure 6e.

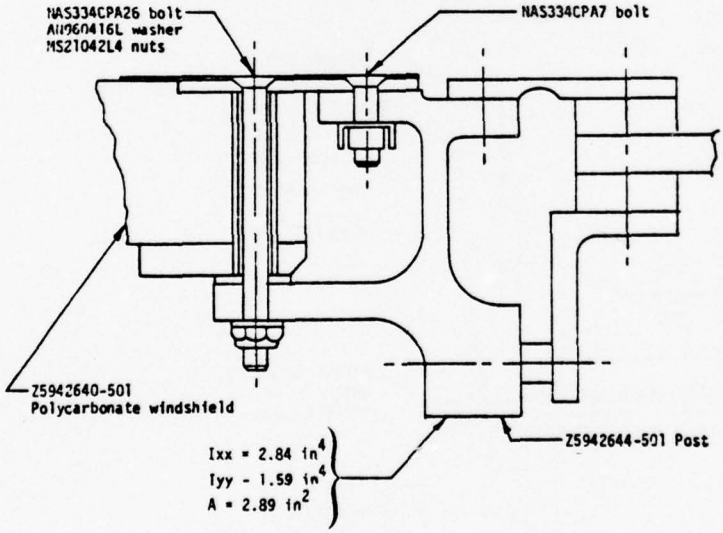

(-501)
Figure 6f.

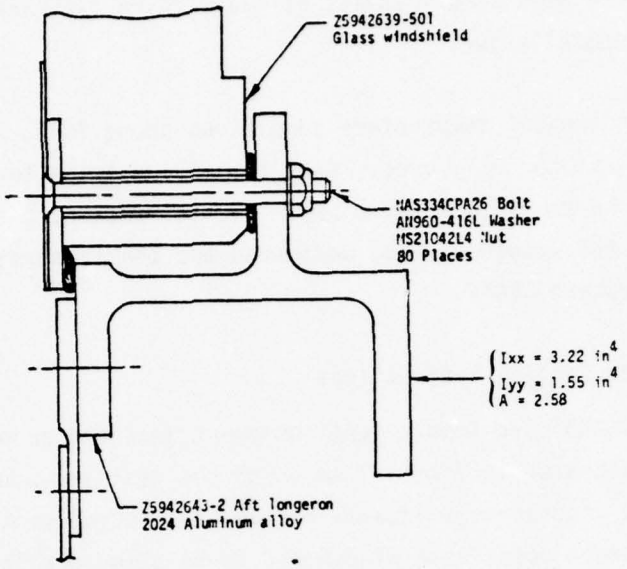

(-1)

Figure 6g.

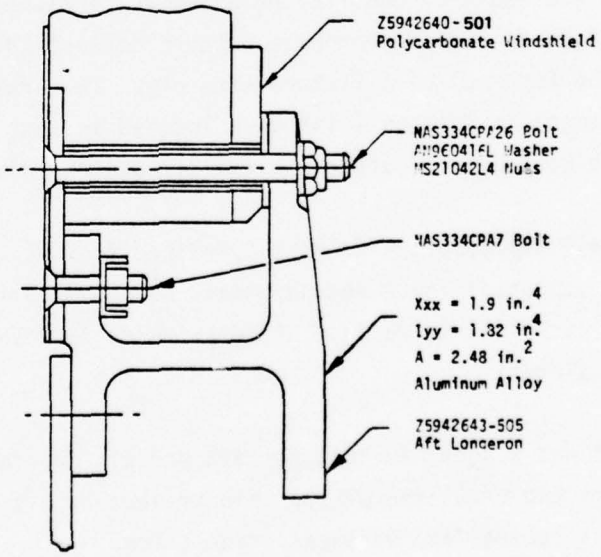

(-501)

Figure 6h.

As in the case with the glass windshield, each bolt hole was 1/16 inch oversize. The resulting void was filled with PR 1422 sealant during attachment installation.

NOTE: Under ambient temperature conditions above 70°F, it took 72 hours for the sealant to fully cure. Heat lamps were installed above the surface to provide the required temperature. The temperature on the structure adjacent to the windshield was monitored and the temperature was not allowed to exceed 120°F.

Test Specimen Rigging Instructions

The AEDC/ARO bird impact test equipment included an adjustable test bed, as illustrated in Figure 7 on which the test setup was installed. The test bed incorporated lateral and vertical adjustment capabilities which allowed a target point on a windshield to be aligned with the centerline of the bird cannon.

The bird shot test procedure required that the two configurations (Z5942638-1 and -501) of the fixture assembly be capable of being removed and reinstalled in a different hole pattern corresponding to 180 degree rotation (end for end) of a fixture assembly. To permit this rotation, two interchangeable hole patterns were located in each adapter which corresponded to the hole pattern in the fixture end plate.

To install the complete Douglas furnished test fixture including windshield, support fixture and adapters, ARO hoisted the unit into position to backdrill 1-1/2 inch diameter holes from VS110770 into the adapter end plates.

The unit was aligned so that forward and aft adapter exposed plates were vertical and that line of the bird trajectory hit target points "A" and "B" after lateral and vertical translation.

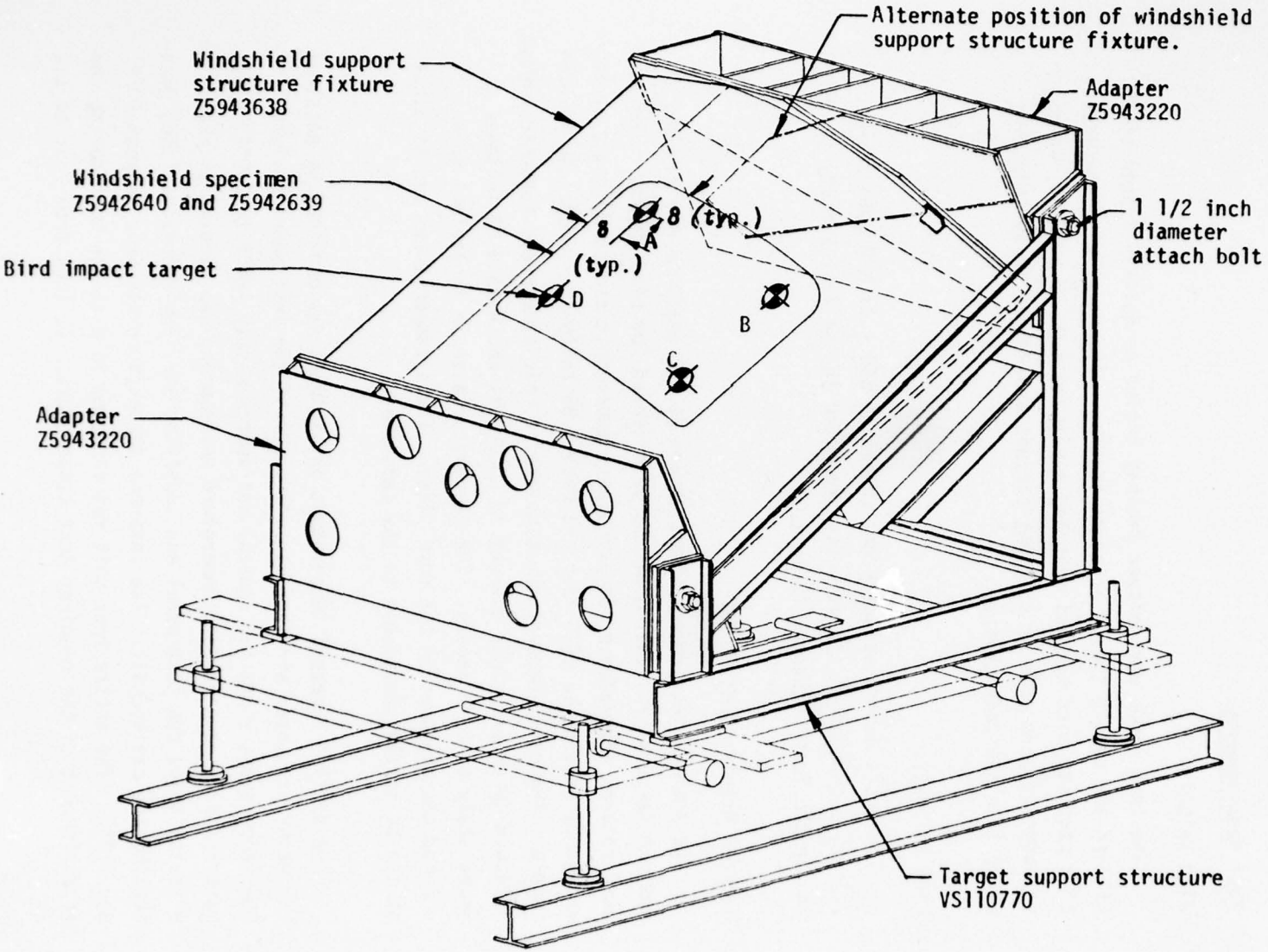

Figure 7. Bird Impact Test Equipment and Target Locations.

Test Requirements

Bird Weight

The test birds were either freshly killed or quickly frozen after killing and slowly thawed prior to testing. Each test bird consisted of a complete bird carcass weighing a planned 4.0 $^{+.2}_{-.0}$ pounds. Weight adjustments were made by clipping carcass appendages or by injecting water into the body cavity.

Bird Velocity

The basic design velocity was chosen as 650 $\pm$ 17 MPH (953.33 $\pm$ 25 ft/sec). Changes in the velocity are noted in the Test Summary in Section IV, and in the Test Sequence, Table 1.

Thermal Requirements

The thermal requirements were chosen as the absolute minimum and maximum temperatures that could be experienced for bird impact. The hot temperatures simulated a hot atmosphere supersonic cruise followed by an emergency descent to 8000 feet and Mach 0.85 followed immediately by bird impact. The cold temperatures simulated a cold atmosphere subsonic cruise followed by an emergency descent to 8000 feet and Mach 0.85 followed immediately by bird impact. The temperatures shown in Table 1 were planned temperatures on the core plies. These temperatures are as close as can be easily obtainable in the laboratory.

The desired external temperature environment was obtained by passing LN_2 vapor or heater air from manifolds across the test panel surface. The temperature range for control was approximately -85°F to 250°F. The interior crew compartment temperature environment was created by enclosing a cavity below the test panel and supplying air from pneumatic lines penetrating the cavity wall. The internal temperature was held between 40°F and 110°F. The entire test unit was enclosed in a canvas hood during the establishment of the required test temperature. It took from four to six

TABLE 1. TEST SEQUENCE AND TEMPERATURE REQUIREMENTS (°F)

PART NUMBER	TEST NO.	SPEC. NO.	SHOT LOC.	V (fps)	TYPE OF STR. (FIG 27)	T2-5 O.B.SFC	T6-9 T.C.INT	T10-13 I.B.SFC
Z5942640-501	BM10	SWU 001	A	941	b	-40°F	-20°F	40°F
Z5942640-501	BM11	SWU 002	A	960	b	85°F	78°F	93°F
Z5942639-501	BM12	PPG 001	A	943	a	-55°F	-28°F	7°F
Z5942639-501	BM13	PPG 001	A	948	a	80°F	80°F	80°F
Z5942639-501	BM14	PPG 002	C	939	a	87°F	87°F	87°F
Z5942639-501	BM15	PPG 002	E Center	515	a	90°F	90°F	90°F
Z5942640-501	BM16	SWU 002	C	369	b	82°F	82°F	82°F
Z5942640-501	BM17	SWU-001	C	737	b	97°F	-	91°F
Z5942640-501	BM18	SK 001	C	847	b	230°F	190°F	110°F
Z5942639-501	BM19	PPG 003	C	971	a	220°F	190°F	160°F
Z5942640-501	BM20	SK 001	A	958	b	74°F	80°F	76°F
Z5942640-501	BM21	SWU 003	A	960	b	-40°F	-20°F	38°F
Z5942640-501	BM22	SWU 003	C	846	b	75°F	76°F	71°F
Z5942639-503	BM23	PPG 004	C	953	c	194°F	159°F	130°F
Z5942639-505	BM24	PPG 005	C	877	c	205°F	191°F	132°F
Z5942639-505	BM25	PPG 005	C	951	c	200°F	195°F	145°F
Z5942640-507	BM26	SK 002	C	939	c	226°F	213°F	143°F
Z5942640-507	BM27	SK 002	B	920	c	-36°F	-41°F	31°F
Z5942639-503	BM28	PPG 004	B	940	b	-30°F	-33°F	38°F
Z5942639-505	BM29	PPG 005	B	931	b	-28°F	-21°F	39°F

hours to attain a steady state. Just prior to the bird impact firing the hood was dropped. See Figure 8.

Figures 9 and 10 show thermocouple locations for monitoring the thermal condition of the test specimens.

Test Procedure

The tests were conducted in the sequence listed in Table 1 with the velocities and temperatures as specified. Table 2 shows the Instrumentation Checklist used during the tests and Figure 7 shows the target locations.

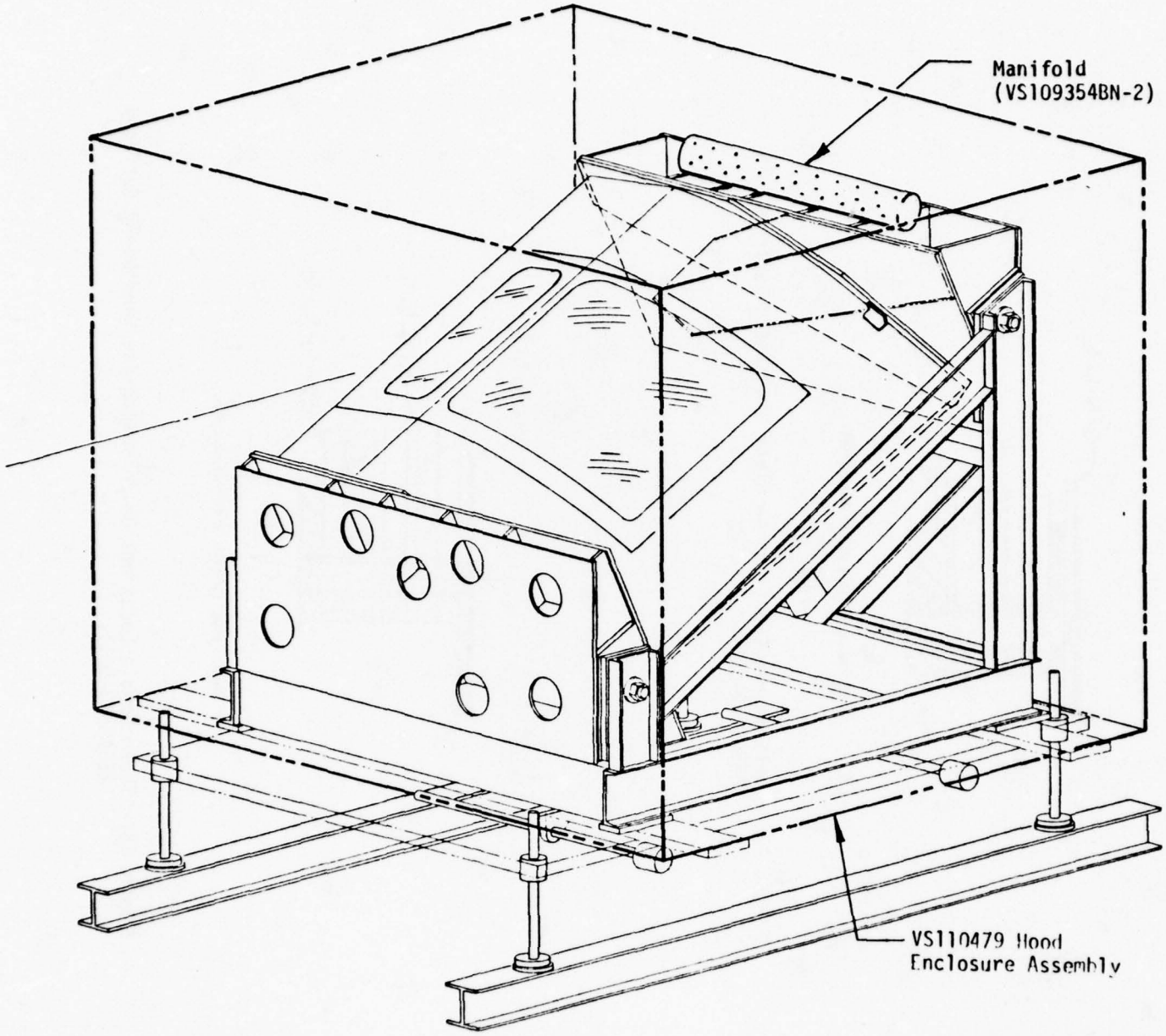

Figure 8. Heat Hood and Manifold.

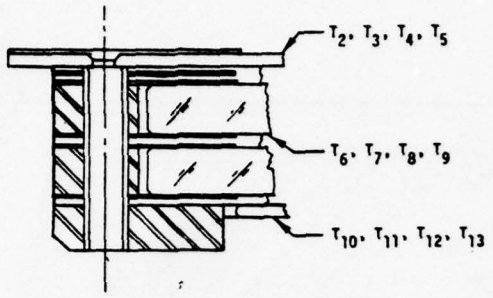

Note: Refer to Table 1 for temperatures

Figure 9. Thermocouple Locations on Glass Windshield Surfaces (Z5942639-501).

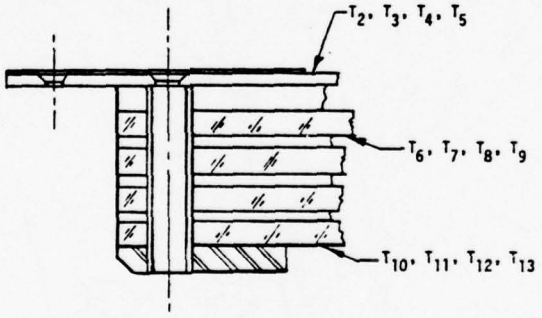

Note: Refer to Table 1 for temperatures.

Figure 10. Thermocouple Locations on Polycarbonate Windshield Surfaces (Z5942640-501).

TABLE 2

INSTRUMENTATION CHECKLIST

FOR BIRD STRIKE TESTS

1. Preparations (prepare gun for firing-trim and weight chicken).
   a. Equipment in position.
      1. Obtain still photos before every shot, showing camera positions and strain gage details.
      2. As accurately as possible determine position in space of camera of lens angles with window, etc., (distances, angles).
      3. Perform scale calibration of movie cameras for all cameras.
      4. Provide reference position markers (crosses, dots, etc.) for movies.
   b. Strain gages - check continuity, measure resistance at terminals, identify channel by channel, identify proper scaling for tape recorder (sensitivity settings, and shunt calibrations).
   c. Set up log for logging each record and event on o'graph recorders/ tape - mark on records where possible - record clock time (hours/ minutes) of events on the shot log.
   d. Set up temperature recorder - check identity of each channel.
   e. Prepare sheet, referencing each Strain Gage channel to recorder channel - include calibration resistor value and equivalent in strain.
   f. Obtain relative humidity reading from local source.
   g. Provide DAC with measurement system schematic showing identification, serial numbers, cable type and numbers, signal conditioner type and numbers, setting for equipment sensitivities and equipment calibration dates. (May be completed after test.)
2. Pre-test Environmental.
   a. Take zero record on tape/recorders.
   b. Take calibration record on tape/recorders.
   c. Start temperature recorder and continuously record or incremental time record if applicable during heating or cooling.

TABLE 2 cont'd.

2. Pre-test Environmental. (Continued)
   d. Incrementally time record (intervals TBD) strain gage channels on tape recorders. Correlate with temperature records.
   e. When target temperatures are reached and stabilized, take tape/recorders recordings. (If applicable.)
3. Bird Shot
   (Record event time of each step.)
   a. Take zero record on tape/recorders.
   b. Take calibration record on tape/recorders.
   c. Start temperature recorder at T-30 seconds.
   d. Monitor and record electrical sensing elements before test.
   e. 1) Start count down
      a) Turn on temperature recorder at T-30 seconds. Mark at T = 0
      b) Turn on oscillograph at T-5 seconds, 20 inch/second (if applicable).
      c) Turn on tapes at T-5 seconds, 120 in./sec.
      d) Mark T-lights on and T = 0 and T-15 seconds
      e) Turn on cameras T-1 second.
      f) Mark time correlation at T-1 second.
      2) Fire - Note time of firing.
4. Post Test.
   a. Tabulate data on Douglas Data Sheet and obtain test signatures.
   b. Obtain still photos of damage and condition of specimen.
   c. Strain gage data may be reviewed quick-look by playback on oscillograph. Check for scaling and qualitative results. Also, compare with digitized data for timing and magnitude.
   d. Data from digitizer and plotter to be available for review within 48 hours.
   e. Review movies and make notes.
   f. Assist in and obtain deflection data from optical reading system and computer program.
   g. Provide suggestions/changes for improving next test.
   h. During testing, Douglas will determine the data channels priorities requiring rapid digitizing and/or plotting. The number required will be kept to a minimum.

Test Provisions

The following facilities and equipment were provided at AEDC for these tests:

1. Bird gun with speed trap and appropriately packaged four and six pound chickens, were provided as required.
2. Structural assembly used to mount the Douglas furnished preliminary test fixtures (VS110770).
3. Liquid nitrogen (LN_2) for cooling the preliminary specimens to -60°F.
4. Heating system to obtain specimen temperatures to 230°F.
5. Completion networks, power supplies, balancing and sensitivity controls for resistance bridge measurements with outputs compatible to FM recording equipment.
6. Recording equipment for reading approximately 20 thermocouples in rapid sequence.
7. A minimum of three high speed movie cameras (5000 frames per second) to record specimen deflections versus time and to verify time of bird impact and bird speed.
8. FM tape recorders for up to 24 data channels. All tapes carried precision time code for data synchronization. An additional eight channel recording capability on oscillographs was available.
9. The format for data presentation was as mutually agreed and the acquisition was the responsibility of AEDC. The format absolutely required was the strain gage data presented in engineering units (μ in./in.) versus time correlated with initial impact (printed data and plots).

10. AEDC test engineers, cameramen, and personnel capable of removing, replacing and repairing test specimens (excluding major repair).

Documentation

Bird Impact Test Shots

Douglas required a data format for the bird impact test shots that would allow the recording of those items that required direct readings of instrumentation before, at-time-of, and after the shots. Such data included temperature and sensing element readings and other physical test parameters.

AEDC supplied oscillograph readings clearly identified regarding scale and calibration. The equipment used to record data from the 33 strain gage channels was required to be sufficient to supply strain gage data presented in engineering units, μ in/in versus time. The period of interest included the duration of impact, which was predicted to be about half a millisecond, and some 5 to 10 milliseconds subsequent to impact.

Test reduction data included:

- Strain gage data digitized and plotted.
- Deflections digitized and plotted as
  a) Vertical displacement versus horizontal displacement,
  b) Maximum displacement (x, y) versus time.
- Temperature recording trace and/or tapes.

Such data were generally made available for Douglas review soon after test.

SECTION III
TEST INSTRUMENTATION

The test instrumentation required in conducting these series of high-speed bird impact tests was, in certain aspects, unique, and represented an advance in the state of the art. Descriptions of the instrumentation equipment and methods for the measurement of strain deflection and temperature are included in this section. Also discussed is the camera coverage for the bird impact sequences.

The bonding of strain gages on polycarbonate and acrylic window specimens, and on interlaminar plies, and then subjecting these specimens to high-speed bird impact involved many testing techniques which had to be developed for these applications. Previous investigators in this area expected crazing with a resulting loss in impact resistance, on any polycarbonate part that had any strain gage adhesive applied to it. Also, with the high G-level expected from a bird impact on the windshield, retention of externally mounted gages was a matter of concern. These concerns are discussed and the means to reduce the adverse effects of the instrumentation are presented.

STRAIN MEASUREMENT INSTRUMENTATION

The strain gage instrumentation used for both the B-1 bird impact tests and the simulated aircraft windshield bird impact tests was to meet the following requirements and conditions:

- Instrumentation shall yield position and velocity data for that section of surface near the area of impact, and preferably for other parts as well, of a windshield or transparency. For the area of impact, strain measurements were to be obtained until high elongation would open the strain gages.

- The motion to be measured was lightly damped oscillation with a period of about 15 milliseconds. Peak velocities were anticipated

in the region of 2000 cm/sec, with peaks as great as 10,000 cm/sec.

- The period of interest included the duration of impact, which is about half a millisecond, and some 5 to 10 milliseconds subsequent to impact.

- The test method shall permit these measurements to be made without interfering with the bird strike test. There was to be free access to the test surface for the projectile, and the test apparatus was not to affect the free movement of the test surface.

These requirements were met for both test specimens after several iterations and reviews of the problems inherent in instrumenting material that is flexible, in a highly transient environment, and very sensitive to surface conditions.

Many problems were foreseen in attempting to collect strain data during a bird impact on the transparency. The main concern was surface degradation from cementing strain gages to the unprotected polycarbonate transparency. The physical effect of many gage adhesives is detrimental as they contain solvents which can plasticize the polycarbonate. It is believed that the solvents cause the polycarbonate molecules to rotate and align forming crystalline or ordered planes. This may explain the loss of the amorphous structure with ensuing brittleness.

To eliminate this problem, the cement used throughout the test series was Micro-Measurements M-Bone AE10/15. It is compatible with plastics since it is 100 percent epoxy and contains no solvents. A clamping pressure of no more than 20 psi was used. This resulted in an adhesive thickness of about 0.005 to 0.010 inch.

Another problem is the flexing of polycarbonate. When under load it can elongate over 100 percent. As usually installed no strain gage system will survive this environment. Initially the use of a sealant

encapsulated shock block installation was considered adequate, Figure 11, as the block would allow movement of the transparency without causing hyper-extension of the ribbon tab. The first three bird impact tests on the B-1 windshield revealed that gage failure was occurring in some areas of the transparency. Close examination of the high-speed film showed that on bird impact the whole sealant capsule would deflect causing the strain gage lead to stretch and fail. To resolve this difficulty the sytrofoam block was discarded and the gage ribbon lead was looped, as shown in Figure 12. This allowed transparency elongation and proved satisfactory on subsequent tests.

Strain Gage Installation

Sixteen (16) EP-08-125AV-120 (Option B-64) Micro-Measurement strain gages were installed on the inside surfaces of the two left-hand full-size windshield specimens. Figure 13 shows the strain gage locations on the B-1 windshields. For tests 1, 2 and 3 the shock block installation was used for all strain gages. For tests 4, 5 and 6, the ribbon tab loop installation was used in the impact area at Locations 3, 4, 15 and 16, (Figure 13).

For the simulated windshield bird impact tests, strain gages were located internally on the transparencies at locations shown in Figure 14. The gages were part Number EP-08-125TM-120 (Option 276). The planned capability was for 20 measurements at each of two opposite corners on each transparency. Additionally, one 90-degree two element rosette strain gage was located on the inside surface of the transparencies at each of two opposite corners, in line with the center gage of the internally mounted strain gage pattern. Sixteen single active leg strain gages were located at points in the window frame structure. A typical wiring harness assembly installed on each specimen which connected with AEDC provided terminals is shown in Figure 15. Figure 16 illustrates the strain measuring system circuit. AEDC provided system wiring, completion bridges, signal conditioning and FM tape recorders, all integrated with the DAC instrumented specimen. Table 3 shows the planned strain gage channel numbering per test

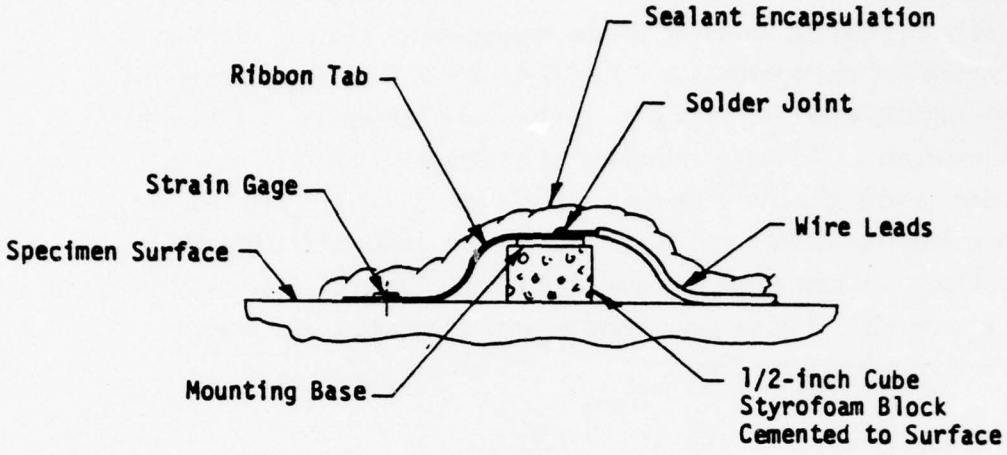

Figure 11. Styrofoam Block Shock Absorber.

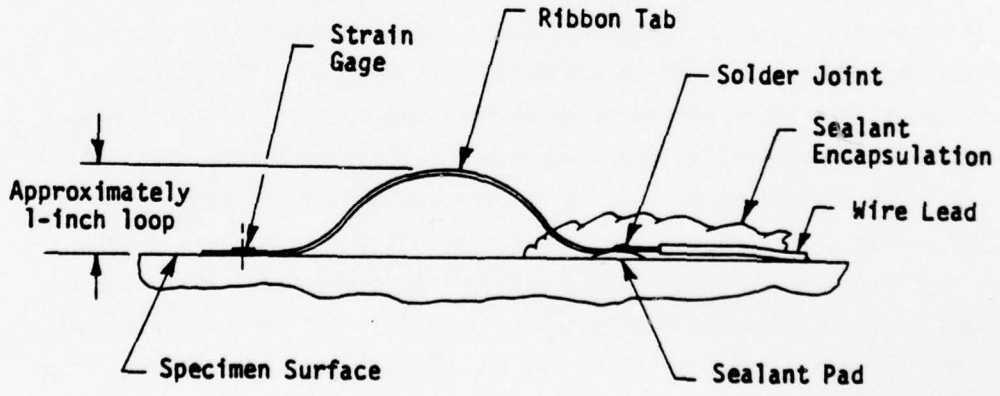

Figure 12. High Impact Shock Resistant Gage Installation.

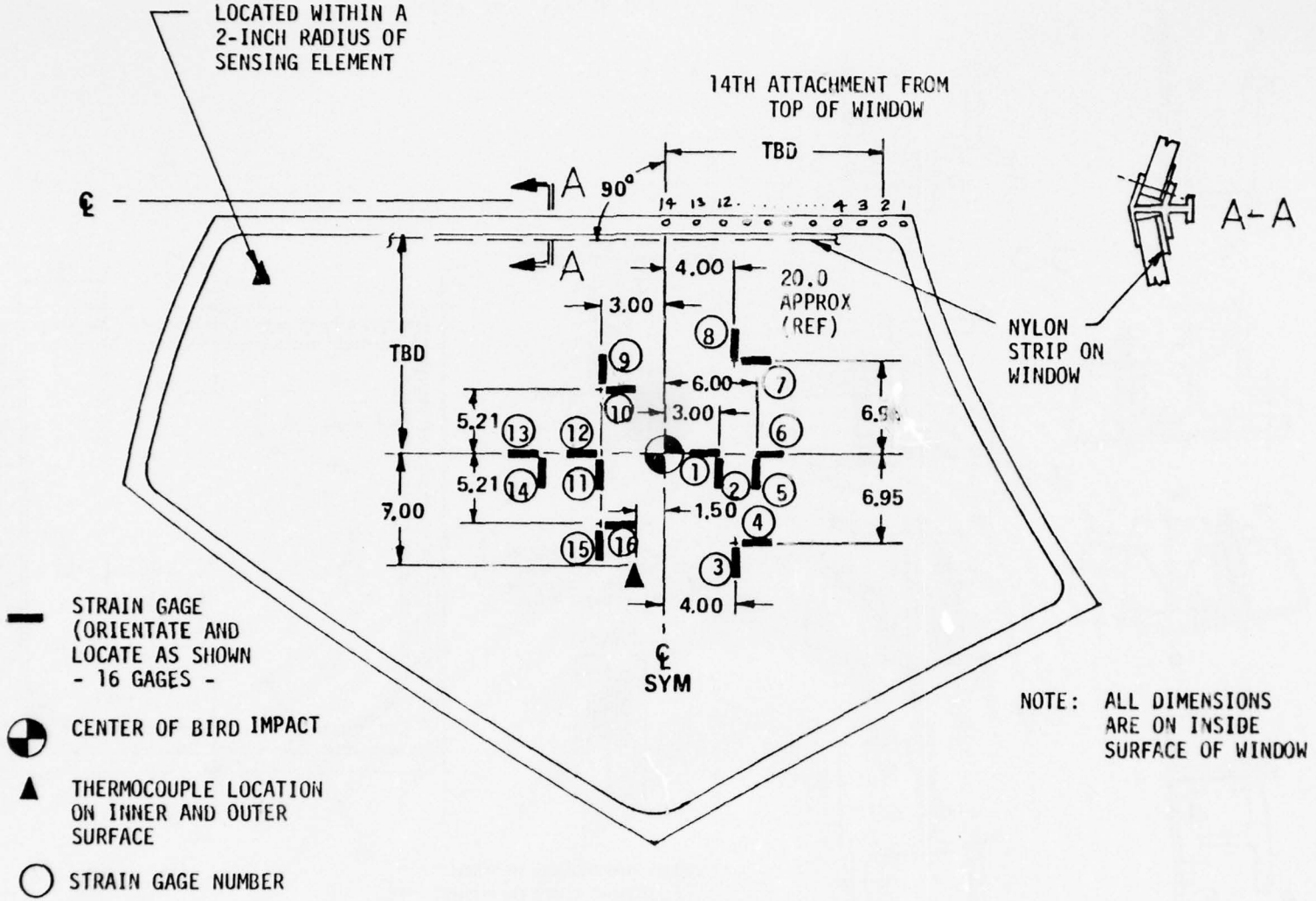

Figure 13. Strain Gage and Thermocouple Locations.

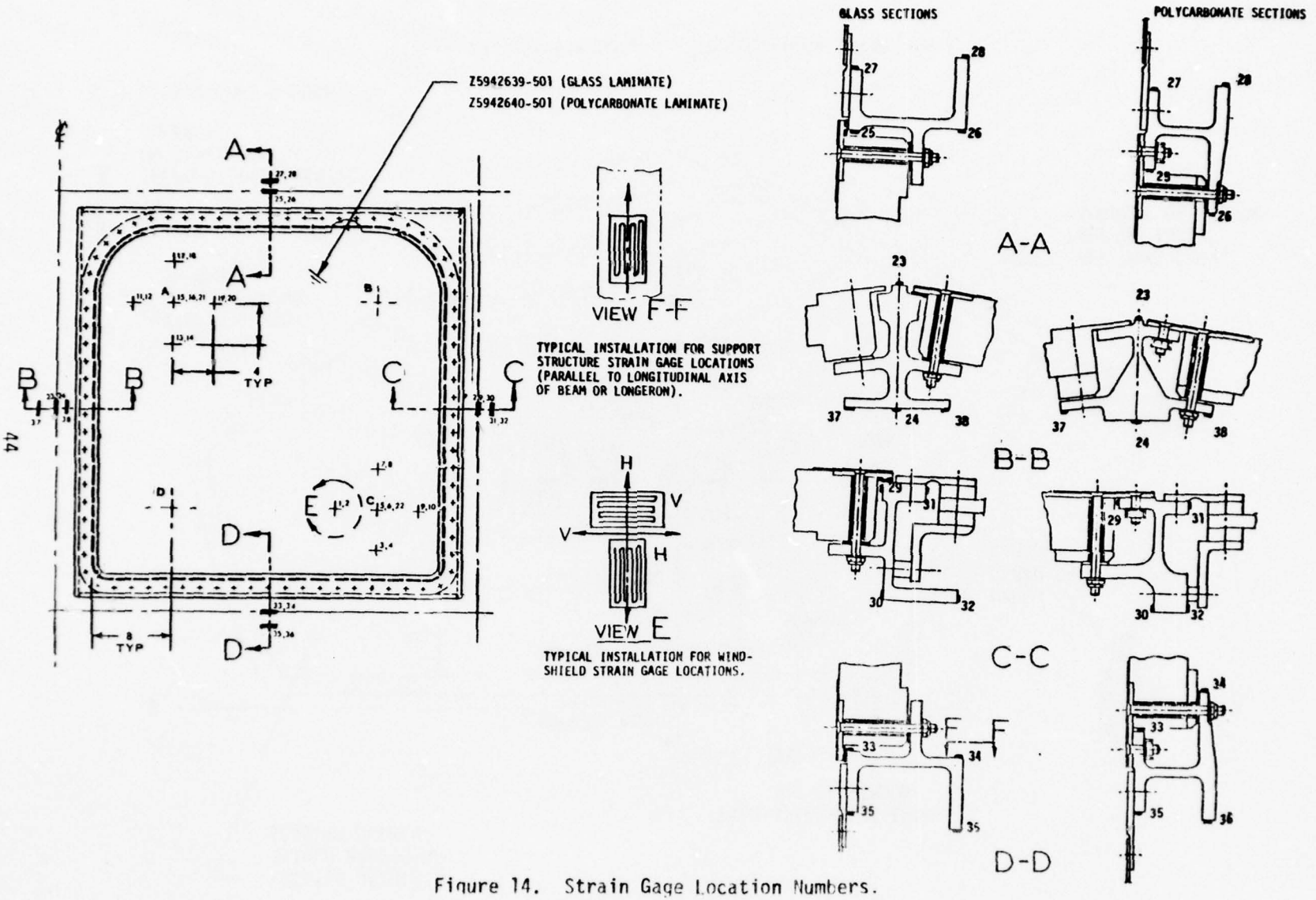

Figure 14. Strain Gage Location Numbers.

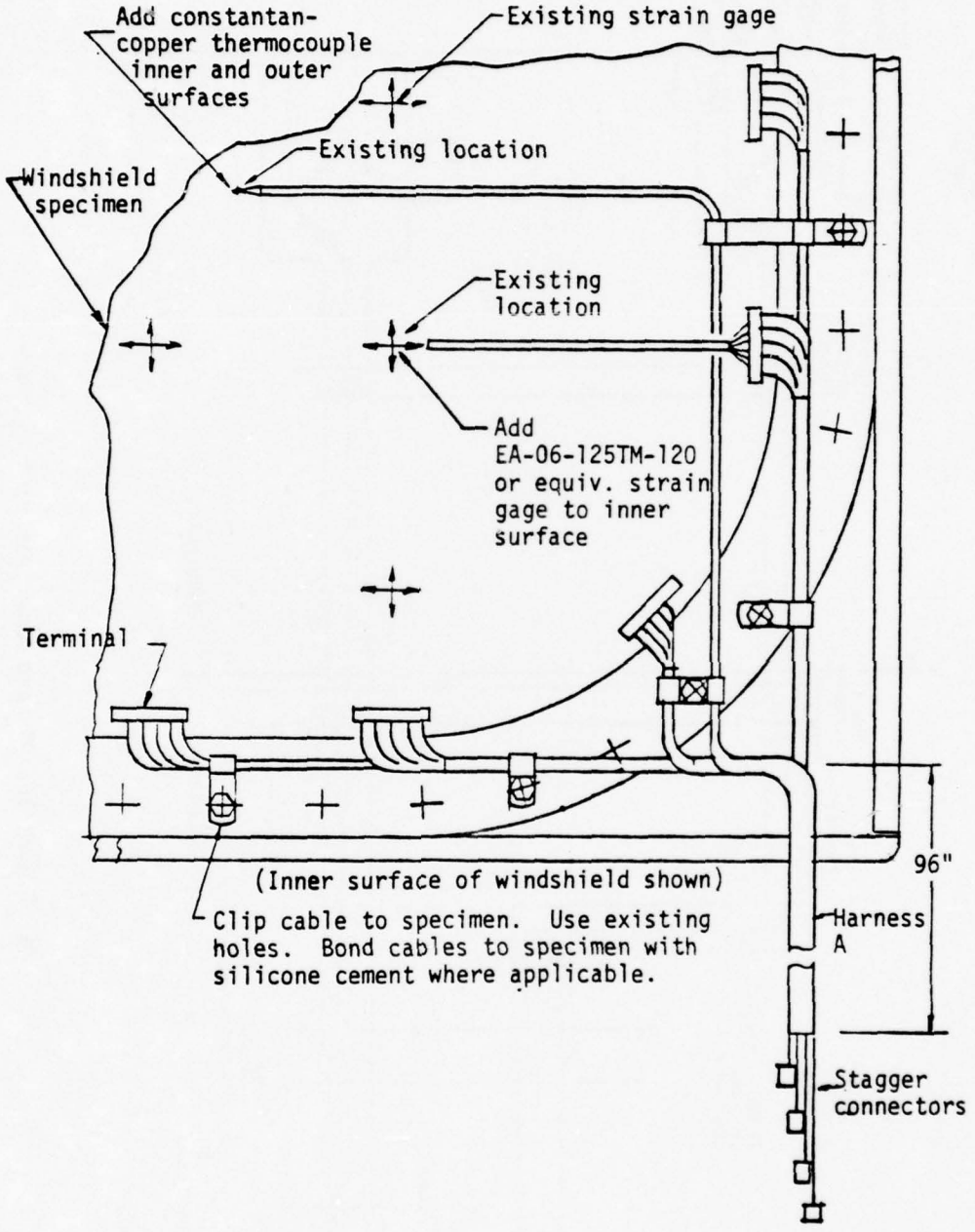

Figure 15. Strain Gage and Thermocouple Wiring Typ for Two Corners.

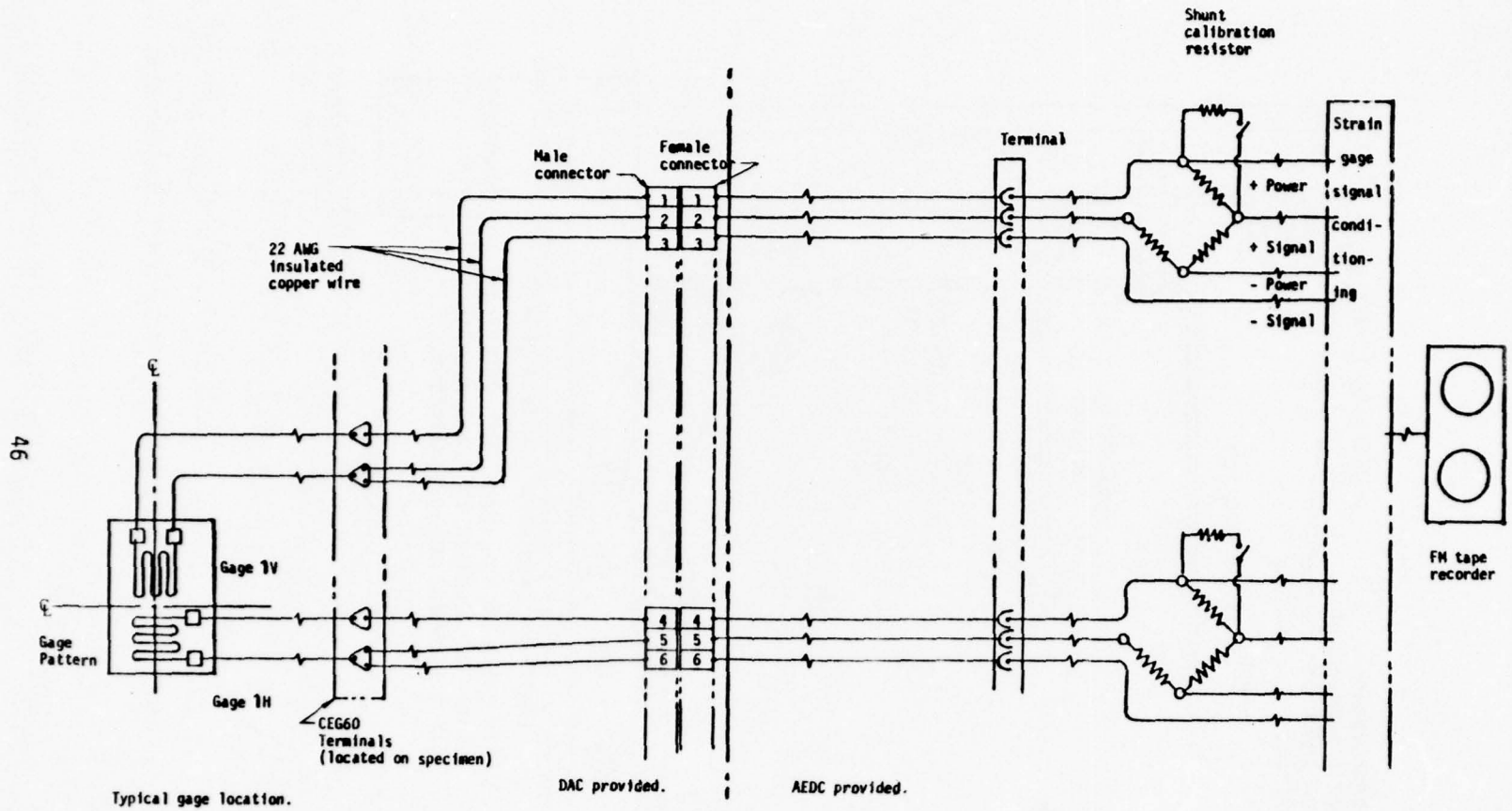

Figure 16. Strain Gage Measuring System.

TABLE 3. STRAIN GAGE LOCATION AND RECORDING CHANNEL SEQUENCE NUMBERS PER SHOT LOCATION

Strain Gage Location			Channel Sequence No.			
Location No. and Gage Dir.	On Ply No.	Side	Shot Location A	B	C	D
* 1 H	-9	Outer			*	*
1 V	-9	Outer			1	1
* 2 H	-9	Inner			*	*
2 V	-9	Inner			2	2
3 H	-7	Outer			3	
3 V	-7	Outer			4	
4 H	-7	Inner			5	
4 V	-7	Inner			6	
5 H	-7	Outer		1	7	3
5 V	-7	Outer		2	8	4
6 H	-7	Inner		3	9	5
6 V	-7	Inner		4	10	6
7 H	-7	Outer		5	11	
* 7 V	-7	Outer		*	*	
8 H	-7	Inner		6	12	
* 8 V	-7	Inner		*	*	
9 H	-9	Outer			13	
9 V	-9	Outer			14	
10 H	-9	Inner			15	
10 V	-9	Inner			16	
11 H	-9	Outer	1			
11 V	-9	Outer	2			
12 H	-9	Inner	3			
12 V	-9	Inner	4			
13 H	-7	Outer	5			7
*13 V	-7	Outer	*			*
14 H	-7	Inner	6			8
*14 V	-7	Inner	*			*
15 H	-7	Outer	7	7		9
15 V	-7	Outer	8	8		10
16 H	-7	Inner	9	9		11
16 V	-7	Inner	10	10		12
17 H	-7	Outer	11			
17 V	-7	Outer	12			
18 H	-7	Inner	13			
18 V	-7	Inner	14			
*19 H	-9	Outer	*	*		
19 V	-9	Outer	15	11		
*20 H	-9	Inner	*	*		
20 V	-9	Inner	16	12		
21 H	Inner Ply	Inner	17	13		13
21 V	Inner Ply	Inner	18	14		14
22 H	Inner Ply	Inner		15	17	15
22 V	Inner Ply	Inner		16	18	16
23 H		Supt. Structure	19			17
24 H		Supt. Structure	20			18
25 V		Supt. Structure	21	17		
26 V		Supt. Structure	22	18		
*27 V		Supt. Structure	*	*		
*28 V		Supt. Structure	*	*		
29 H		Supt. Structure		19	19	
30 H		Supt. Structure		20	20	
*31 H		Supt. Structure		*	*	
*32 H		Supt. Structure		*	*	
33 V		Supt. Structure			21	19
34 V		Supt. Structure			22	20
35 V		Supt. Structure			23	21
36 V		Supt. Structure			24	22
37 H		Supt. Structure	23			23
38 H		Supt. Structure	24			24

NOTE: Strain gages/channels marked with * may be monitored with oscillograph, if available.

shot. All strain gages required dummy bridge completion networks. AEDC recorded strain measurements from the structural gages and any other specimen strain gages on FM tape or by oscillograph.

AEDC ran a full set of calibration tests on the strain gages before each instrumented bird impact. The camera lights were activated at least five (5) minutes before the strain gages were zeroed and calibrated to eliminate any transient thermal effects on the strain gages.

Calibration of instruments was required to verify that total systems requirements have been satisfied. Evidence of recent certification was provided to the Douglas test representative.

Strain Recording Equipment

The equipment used by AEDC to record data from the strain gages was sufficient to supply Douglas strain gage data, presented in engineering units, μ in./in. versus time, with both printed data and plots. As it was anticipated that strain gages in the impact areas would fail due to high elongation, it was deemed important that initial time increments during the digitizing process be as small as possible (micro-seconds).

Temperature Measurements Methods

Appropriate critical operating temperatures were determined for typical high-speed high performance aircraft. To accurately monitor these temperatures at critical locations, appropriate thermocouples were used. All thermocouples were of copper-constantan construction calibrated to I.S.A. or equivalent standard.

Several temperature measurements were made on the B-1 windshield. Four (4) foil copper constantan thermocouples with 10 ft. leads, Part Number 20-114-L10, available from RdF Corporation, 23 Elm Avenue, Hudson, New Hampshire 03051, were cemented with AE-15 by the AEDC on the outer and inner surfaces of each windshield specimen as noted in Figure 13.

The thermocouples were read and recorded prior to turning the camera lights on and at the moment of impact to monitor all thermal responses. Neither high response, nor rapid acquisition, was required; hence, this information was recorded on a data logger whose scan rate was one-half second.

AEDC attached equipment on the two left-hand windshields' sensing element, then read and recorded the resistance of each sensing element prior to turning on the camera lights and at the moment of impact. A sensing element (AVK1160) resistance-temperature conversion chart is shown in Figure 17. This provides a convenient, built-in check on the thermocouple readings.

For the simulated windshields four thermocouples were located in the interior of each specimen. Leads from these were terminated near the inside surface of the window specimens. Eight thermocouples were located on the exterior and interior surface of the transparency, and on the surrounding structure. Temperature measurements utilizing thermocouples were also made of the temperature chamber air, pilots head air, and ambient outside air. Thermocouple locations were as shown in Figure 18.

AEDC installed thermocouples not provided by DAC and completed the measurement circuit as required for recording temperatures. A recorder for monitoring and recording temperatures at maximum of one second intervals between temperature points was required. Continuous monitoring and recording was necessary during heating and cooling and during bird impact testing for each test shot. Test events were recorded on the temperature records as they occurred. Thermocouple wiring schematic and connectors for hookups between the windshield/support structure and the instrumentation equipment is shown in Figure 19.

Deflection Measurement Methods - Bird Impact

High speed cameras were used to measure deflections at selected time intervals during impact. Five thousand frames/second cameras were set

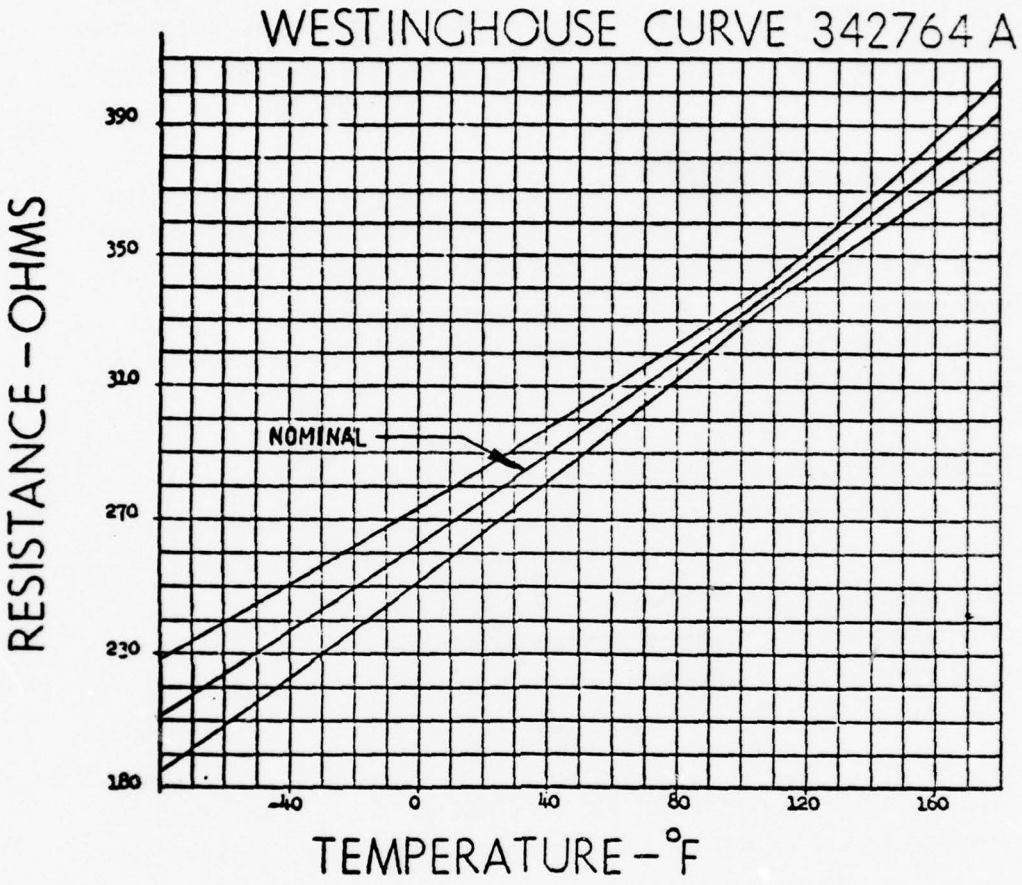

Figure 17. Sensing Element Resistance Chart.

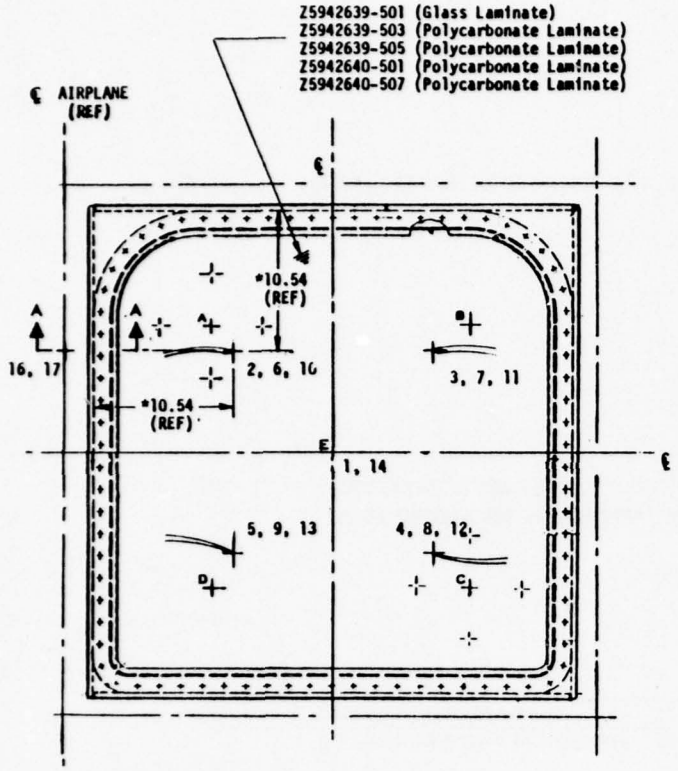

* THERMOCOUPLES ON BOTH SURFACES TO BE IN-LINE WITH THERMOCOUPLES IN TEST SPECIMEN.

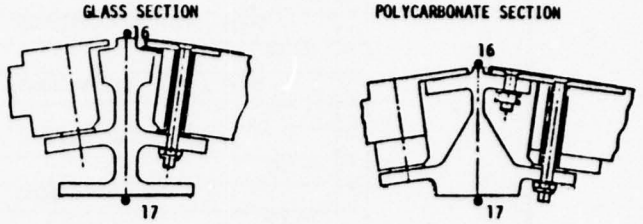

SECTION A-A

THERMOCOUPLE NO.	LOCATION
1	CHAMBER AIR TEMP - 3" ABOVE 'E'
2	OUTER PLY SURFACE TEMP - NEAR 'A'
*3	OUTER PLY SURFACE TEMP - NEAR 'B'
4	OUTER PLY SURFACE TEMP - NEAR 'C'
*5	OUTER PLY SURFACE TEMP - NEAR 'D'
6	CORE PLY TEMP - NEAR 'A'
7	CORE PLY TEMP - NEAR 'B'
8	CORE PLY TEMP - NEAR 'C'
9	CORE PLY TEMP - NEAR 'D'
10	INNER PLY SURFACE TEMP - NEAR 'A'
*11	INNER PLY SURFACE TEMP - NEAR 'B'
12	INNER PLY SURFACE TEMP - NEAR 'C'
*13	INNER PLY SURFACE TEMP - NEAR 'D'
14	COCKPIT AIR TEMP - 3" BELOW SURFACE AT 'E'
15	TEST CELL AMBIENT TEMP
16	STRUCTURAL TEMP - ℄ BEAM - OUTSIDE ADJACENT TO T/C 2
17	STRUCTURAL TEMP - ℄ BEAM - INSIDE ADJACENT TO T/C 10

NOTE: (*) Indicates optional recording documentation.

Figure 18. Thermocouple Locations.

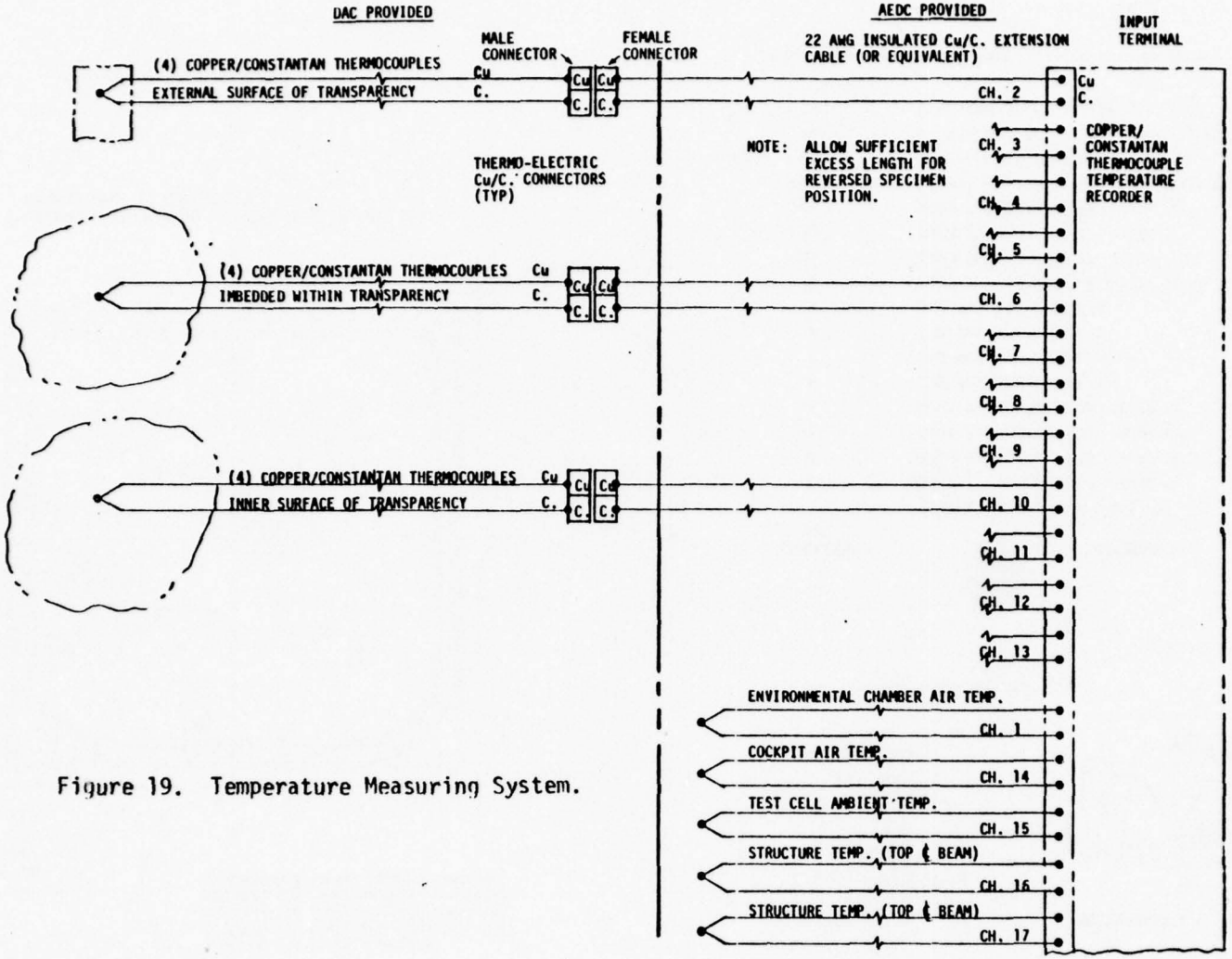

Figure 19. Temperature Measuring System.

along an inboard-outboard segment, with camera locations as shown in Figures 20, 21, 22 and 23. Both cameras were located to view the external and the interior surface of the transparency. A minimum of thirteen target deflection points, nine on the transparency and four completing the segment geometry on the structure were required. For this deflection measurement evaluation, it was anticipated that during impact, the determination of all target point deflections may not be attainable, but sufficient definition was still expected to be obtained from those which remained in view. The results were not entirely satisfactory, although a camera was located for an overall view of the bird impact and test specimen.

Deflection measurements were made using cameras No. 2, 3 and 4 shown in Figure 21 and cameras No. C1 and C2 shown in Figure 23. The points on the windshield for which measurements were made on deflection during impact were the same points for which the measurements were made in the static tests using the deflectometers. These points are shown in Figure 24. Deflection measurements were made in the following manner: points to be measured were marked on the windshield with a cross made of white tape with the center of the cross marked with colored tape. A scale was attached to the deflection point and positioned to lie in the vertical plane. A calibration film was obtained with the scale in position. The scale was removed and, with the camera position unchanged, movies were obtained of the actual shot. Measurements were then made by first placing the calibration film on a digitized film reader and determining a scale factor for points in the plane of the scale. The film made during the actual shot was then placed on the film reader and measurements of deflection were recorded for each millisecond of elapsed time (every five frames for a frame rate of 5000 frames/second).

Camera No. 4 was mounted inside the module, and as a result, was subject to movement resulting from the bird impact. In order to correct the error that this movement could introduce, a point on the module structure was used as a reference and the difference between the movement of points on the windshield and this reference point on the structure was then taken

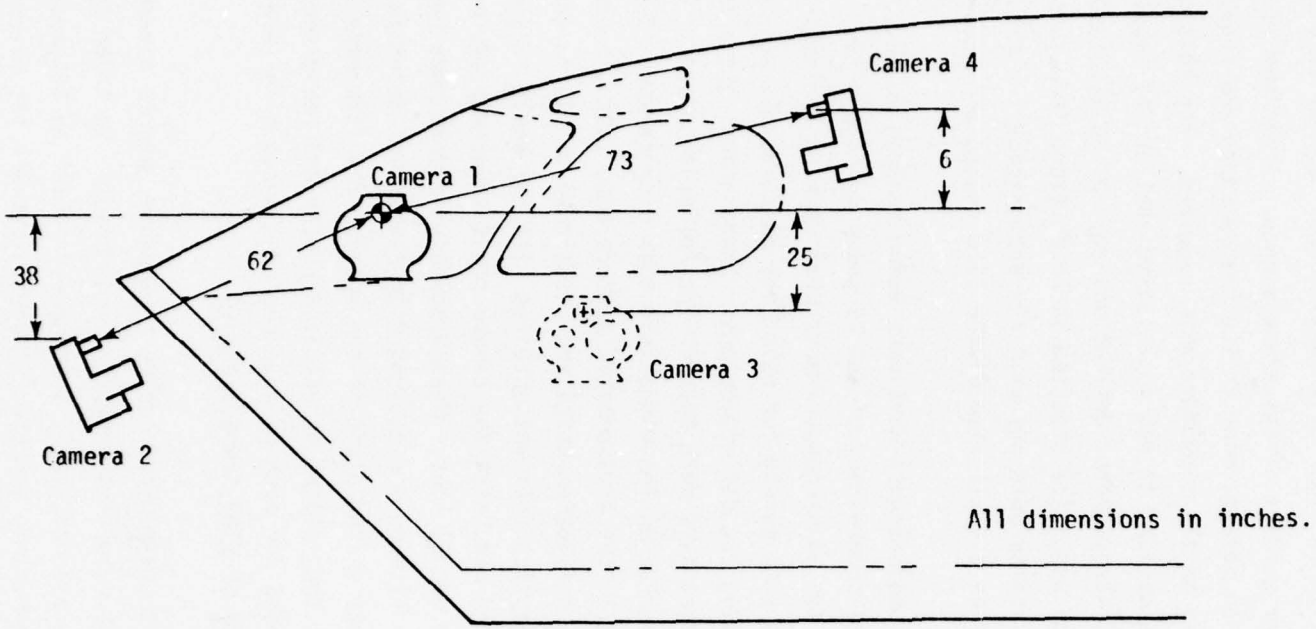

Figure 20. B-1 Windshield Bird Impact Test, Side View of Camera Locations.

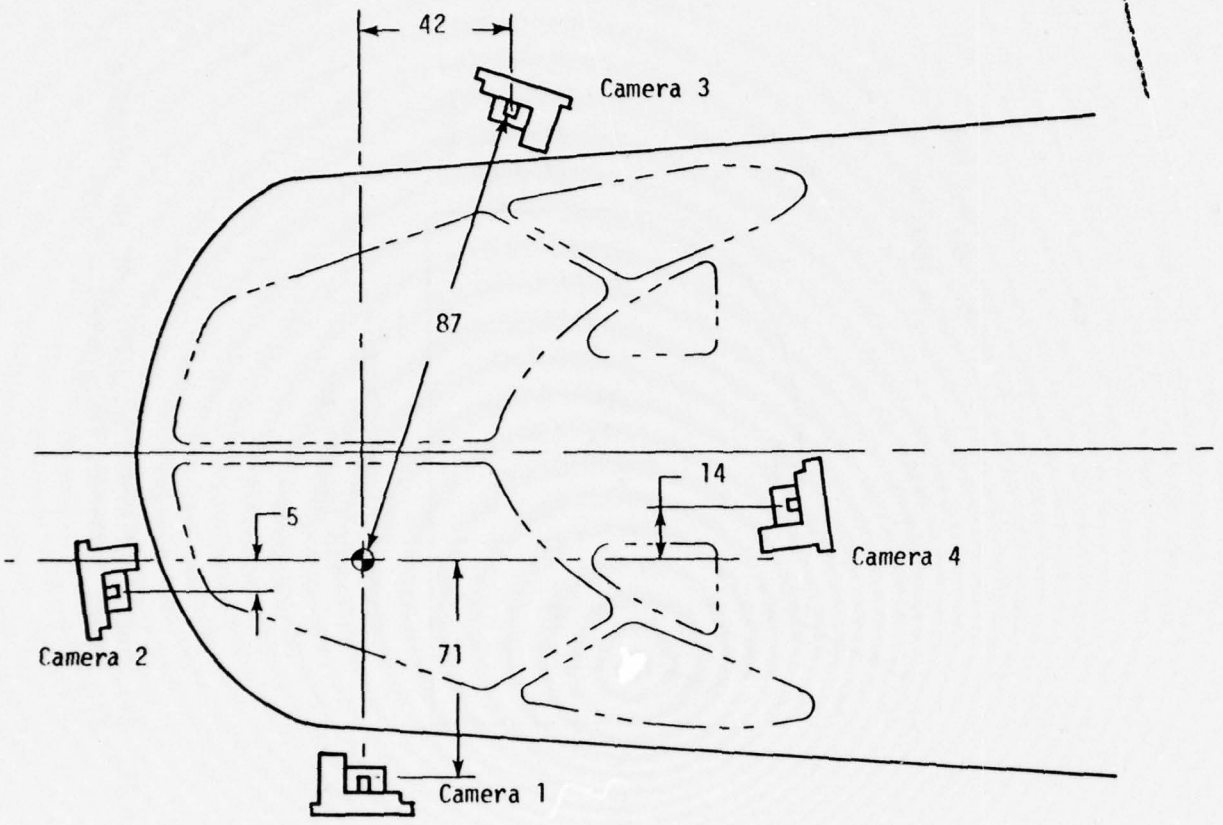

Figure 21. B-1 Windshield Bird Impact Test, Plan View of Camera Locations.

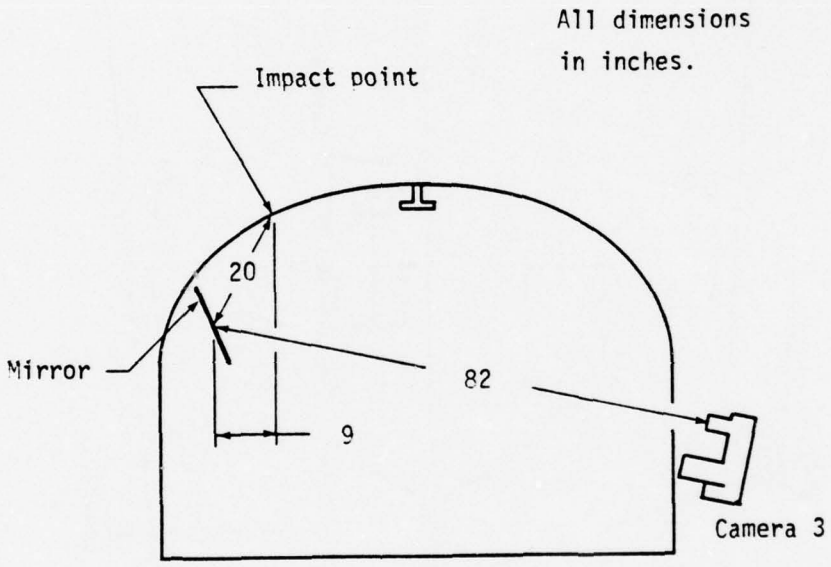

Figure 22. B-1 Windshield Bird Impact Test, Mirror Location for Camera Number 3, Tests BM005 - BM009.

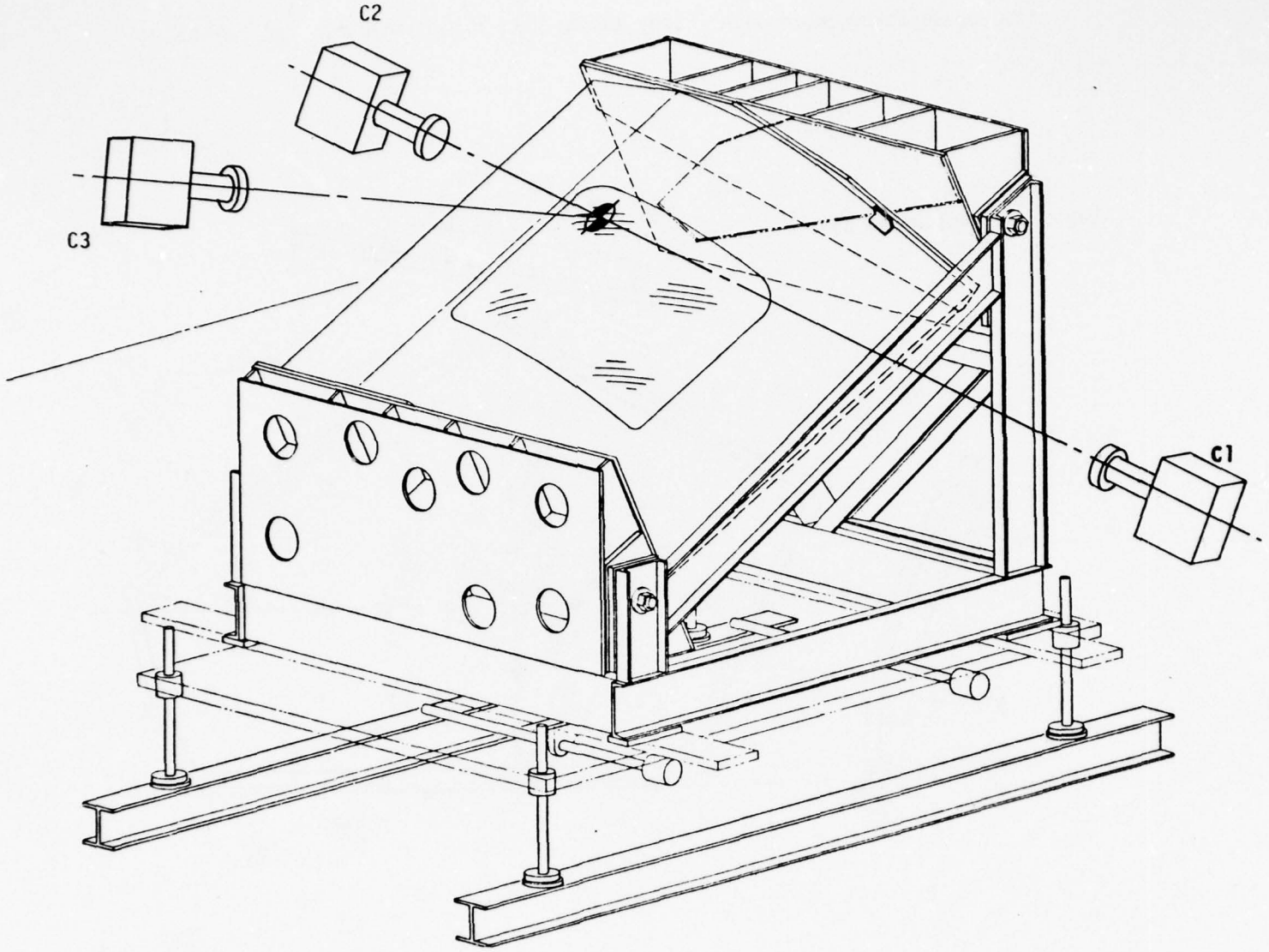

Figure 23. Camera Locations.

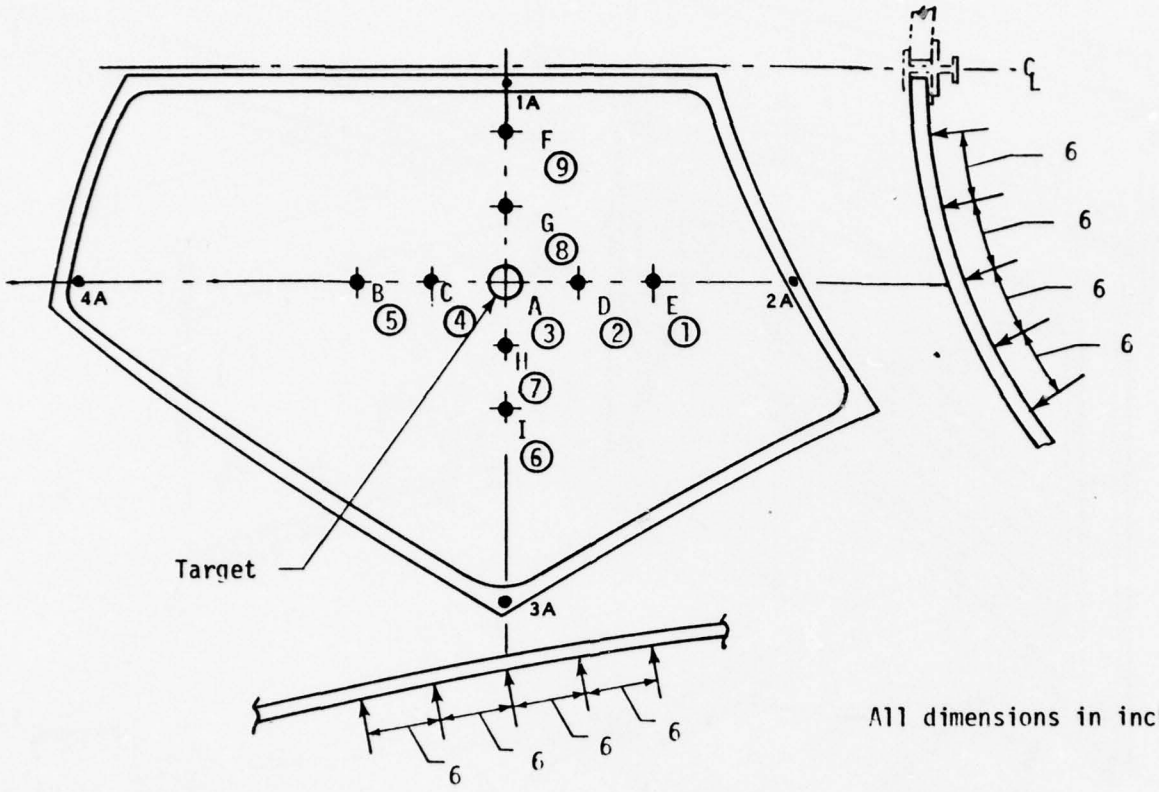

All dimensions in inches.

Figure 24. B-1 Windshield Bird Impact Test, Deflection Measuring Points.

as the actual windshield deflection. The difference between the measurement of deflection of a certain point on the windshield by cameras 2, 3 and 4 can be attributed to errors in this correction and the correction for viewing angle.

Deflection Measurement Methods - Static

Deflection readings were required at several points for the static loading conditions. Maximum deflections at the target point were required for both B-1 specimens at impact.

Deflectometer Installation

Nine (9) deflectometers were mounted by the AEDC on the inside of each left-hand windshield at locations noted in Figure 24 to determine deflections during static loading tests. These were Bourn Model 109 linear potentiometers.

These deflectometers were capable of deflecting at least two (2) inches before bottoming out. The deflection gages A through E were mounted on a structural beam that had been secured at the aft longeron member and the forward bulkhead. The deflection gages F through I were mounted on a structural beam that had been secured to the center beam and outboard beam. Any deflection of both ends of deflectometer support beam was measured with peripheral deflectometers 1A, 2A, 3A and 4A.

Deflectometer Recording Equipment

The measurements were made using a Bourns Model 109 linear potentiometer as the active leg in a wheatstone bridge circuit. The potentiometer shafts were spring-loaded to insure intimate contact with the inside surface of the windshield and to cause the shaft to follow the windshield movement during rapid unloading of the applied force. The oscillograph readings were recorded before, during and after the maximum static load was applied, and upon release. The deflection data were supplied in inches versus applied load and inches versus time. Thirteen channels of deflectometer data were recorded on oscillographs.

Photographic Coverage

The purpose of camera coverage was threefold:

1. To provide a means of accurately recording structural deflection under impact conditions.
2. To provide an overview documentation of the shots.
3. To verify that the bird package was intact.

AEDC provided high speed 16 mm camera (5000 frames/second) to measure specimen deflection, in inches, versus time during bird impact. A medium speed camera (200 frames/second) which varied in location, was used on some shots to provide a more real time record of the bird impact event.

Both black and white, and colored high speed film were used along with appropriate lighting.

For the B-1 bird impact deflection camera locations in the test area are shown in Figures 21, 22 and 23. Camera Number 3 was mounted such that it viewed the interior of the module through an opening in the side below the transparency. This camera viewed the windshield directly on shot No. 1, but was positioned to view the windshield through a mirror on shots 2 through 6 in order to obtain a better angle from which to view windshield movement (Figure 22).

For the windshield simulation impact test two cameras, Figure 23, C1 and C2, were utilized for the deflection measurements. A third camera, Camera C3, was positioned to provide the best overall view of the test specimen and fixture.

AEDC supplied Douglas with camera lens coordinates, camera viewing angle, and edited, unspliced copies of the film.

One copy of color photographs of the specimen, environmental fixtures, and pertinent pre-test and post-test items were provided Douglas and the Air Force.

Still color photographs were made of the test setup, including the interior of the module, deflectometer setup, static loading device, camera setup, inner and outer views of the windshield, and general overall views. Color photographs were also made of the test article after impact to record any damage to the windshields or supporting structure.

SECTION IV
TEST RESULTS

This section presents the results of the high speed bird impact tests and static loading/dynamic unloading tests on the B-1 windshield. Also presented are the results of the high speed bird impact tests on the simulated aircraft windshield specimens. All of the acquired test results data are not presented in this volume, but these additional data may be found in their entirety in the AEDC Reports, References 2 and 3. The following paragraphs present a discussion of the data acquisition and reduction, test data uncertainties (which are expanded in Reference 2), test specimens and supporting structure behavior, and strain gage and deflection tabulation.

DATA REDUCTION AND UNCERTAINTIES

Data Reduction

Projectile velocity was determined from three X-ray stations located along the flight path between the launcher muzzle and the target. The velocity measuring system was mounted on an instrumentation dolly with the first station located approximately one foot from the muzzle of the stripper tube. The X-ray pulsers were triggered when the chicken broke a 24 gauge copper wire in an electrical break-wire system. The time between firings of the pulsers was recorded with a digital chronograph, and using the time together with the distance measured between images of the projectile on the X-ray film (after corrections for point source emission), the velocity was determined.

Strain gage and deflectometer data obtained during the static portion of the static loading/dynamic unloading tests of the B-1 tests only were provided to Douglas in the form of oscillograph traces together with their respective calibration traces. Strain gage data obtained during the dynamic unloading portion of the tests and the actual bird shot tests for both series were digitized, then plotted as a function of time.

Photographic data consisting of motion picture film and still photographs were also transmitted to Douglas for evaluation.

Data Uncertainty

Estimated total uncertainties associated with data obtained during these tests were as follows (Reference 2):

Parameter	Uncertainty
Velocity	± 0.5 percent
Bird Weight	± 0.1 percent
Strain Gage Readings	± 10.0 percent
Deflection (using deflectometers)	± 12.0 percent
Deflection (using cameras)	± 0.2 inch
Temperature	± 1.78°F

Sources of uncertainty considered for strain gage measurements include: (1) gage factor and gage resistance, (2) calibration resistor value, (3) signal conditioner gain (static calibration/dynamic operation), and (4) magnetic tape record/reproduce system gain (static calibration/dynamic operation). The bias of the instrumentation equipment used to record was estimated to be negligible.

B-1 WINDSHIELD BIRD IMPACT TEST RESULTS

Test Specimens

The tests included the original R-I windshield design and installation requirements utilizing two rows of tight attachments, then revised for two rows of attachments with loose holes, one row of attachments with tight holes, one row of attachments with loose holes, and one test with every other attachment left out. To accomplish the variances, two sets of bushings and a new set of retainers for the left-hand windshield were required. One set of these bushings were fabricated according to Rockwell Drawing No. L3000645, and the other set fabricated according to the same drawing but modified appropriately. Before each bushing was installed, it was cleaned with alaphatic naptha, followed with cleaning with isopropyl

alcohol. Dow Corning 1200 primer was applied to each bushing and then the bushing was cemented in the windshield hole with Dow Corning 93-007 sealant. The new retainers were modified by cutting as shown in Figure 2.

During the previous Rockwell International B-1 windshield test (Reference 4) the right-hand longeron, near the centerline of the module, was damaged. A large piece of the longeron was torn off during bird impact and cracks were formed in the web. Most of the damaged section of the longeron was removed and a new section made of steel was installed (Reference ARO Drawing No. VST0409401). The right-hand windshield, No. 105, was installed before the tests began and remained for all the shots.

Static Loading/Dynamic Unloading Tests

Static loading/dynamic unloading tests were conducted before each of the first four bird impact shots.

The loading was accomplished by means of hydraulically operated loading pad, Figure 25, which was mounted with its axis normal to the impact point. A quick-release mechanism was incorporated as an integral part of the device to remove the load with a minimum of damping action attributable to the device itself. The loading device was calibrated for loads up to 2500 pounds.

The test procedure was to obtain deflection measurements using the deflectometers at several different load levels, then dynamically release the load and obtain strain versus time measurements and high-speed motion picture coverage of the event. High-speed motion picture coverage was provided to obtain a visual record of the releasing of the loading pad and to measure the deflection of the windshield for comparison with deflectometer measurements. The center deflection measurements taken during the static loading tests prior to the first four bird shots are presented in Table 4.

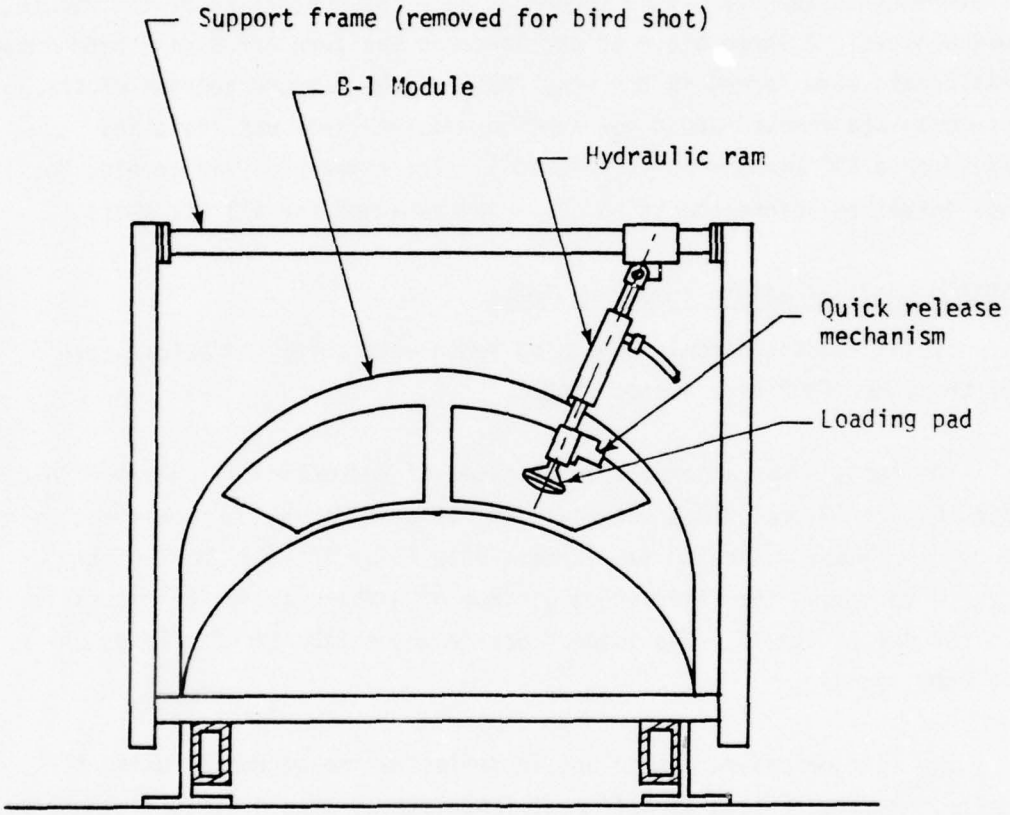

Figure 25. B-1 Windshield Static Loading/Dynamic Unloading Test Setup.

TABLE 4. STATIC LOADING/DYNAMIC UNLOADING TESTS

TEST NO.	PART NO.	TEMPERATURE (°F)			LOAD (LBS)	CENTER DEFLECTION (INCHES)	RETAINER/ATTACH. HOLES CONDITION
		AMB.	W/S	COCKPIT			
1	SWU-108	71.0	71.5	-	1500	0.25	Original B-1 Instl. (Full retainer-tight holes in bushings. W/S attach bolt torque 80-105 inches). Heat bubble damage on inner ply near SG 9.
2	SWU-108	61.2	72.0	55.2	1500	0.25	One bolt design simulation. Retainer cut between attach bolts (1 inch). Tight holes in bushings. W/S bolt T = 50-60 inches.
3	SWU-108	55.3	60.0	-	2500	0.43	
4	SWU-107	60.0	65.2	69.5	1500	0.22	Full retainer (2-bolt design) Bolt holes in bushings are o/s + sealant. W/S bolt T = 50-60 inches.
5	SWU-107	59.4	71.7	71.2	2500	0.38	
6	SWU-107	45.0	55.5	53.7	1500	0.27	One bolt design simulation. Retainer cut between attach holes. Bolt holes in bushings are o/s + sealant. W/S bolt T = 50-60 inches
7	SWU-107	45.0	61.0	56.1	2500	0.46	

Bird Impact Tests

A tabulation of the test results is presented in Table 5 and the following paragraphs discuss the test results.

The outer acrylic ply of Panel No. 108 spalled and cracked as the result of shot Number 1, but there did not appear to be any damage to the polycarbonate structural ply. There were several cracks in the polycarbonate inner ply that appeared to emanate from an area that was damaged by excessive heat being applied to the windshield during the installation of the strain gages. Strain gages were checked and damaged ones repaired in preparation for the static test.

On shot Number 2, there was some additional spalling of the outer ply but no visible damage to the structural ply or any additional cracking of the inner ply. The strain gages failed in the impact area and were replaced in preparation for the static test.

On shot Number 3, using windshield panel Number 107, the outer acrylic ply spalled and cracked, but there was no visible damage to the polycarbonate structural ply or cracking of the inner ply. Again the damaged strain gages were repaired or replaced in preparation for the next static test.

Shot Number 4 produced very little damage to windshield panel Number 107. There was some additional cracking and peeling of the outer ply, but no visible damage to the structural core ply or inner ply.

Before shot Number 5, every other bolt common to the windshield panel was removed. The ends of the top aft retainer (L3000157-003) and the forward end of the lower aft retainer (L3000159-003), which were not secured with bolts, were bent outwards as a result of the hydraulic forces of the bird. As an aid in preventing this from occurring on the following shot, bolts were moved from adjacent holes to the ends of the retainer,

TABLE 5. BIRD IMPACT TEST RESULTS ON X-5 MODULE

SEQ	SHOT NO	PART NO.	BIRD IMPACT						REMARKS		
			TEMPERATURE			WT (lb)	V (fps)	CENTER DEFL	RETAINER/ATTACH HOLES CONDITION	TRANSPARENCY COND. AFTER TEST	SUPPORT COND. AFTER TEST
			AMB.	W/S	COCKPIT						
1	BM004	L3000151-001 SWU-108	73.5°	83.5°	74.6°	4.00	953	2.15"	Original B-1 Instl. (Full retainer-tight holes in bushings. W/S attach bolt torque 80-105"#) Heat bubble damage on inner ply near SG 9.	Outer ply fracture over lg. area near impact. Inner ply fracture start at heat bubble. No damage to core ply.	No structural damage. Bolts did not rotate.
2	BM005	L3000151-001 SWU-108	48.5°	63.8°	49.2°	4.07	951	2.40"	One bolt design simulation. Retainer cut between attach bolts (1"). Tight holes in bushings. W/S bolt T = 50-60"#	More spalling of outer ply. No further damage to inner ply. No damage to core ply.	No damage.
3	BM006	L3000151-001 SWU-107	57.6°	64.4°	60.0°	4.02	967	2.05"	Full retainer (2-bolt design.) Bolt holes in bushings are o/s, + sealant. W/S bolt T= 50-60"#	Much crack & spalling of outer ply. No damage to core ply or inner ply.	No damage.
4	BM007	L3000151-001 SWU-107	62.9°	71.0°	68.6°	4.00	936	2.15"	One bolt design simulation. Retainer cut between attach holes. Bolt holes in bushings are o/s, + sealant. W/S bolt T=50-60"#	Additional cracks & peeling of outer ply. No damage to core ply or inner ply.	No damage.
5	BM008	L300151-001 SWU-107	62.9°	71.4°	65.7°	4.02	930	2.25"	Same as previous test, except every other w/s attach bolt removed.	Additional cracks & peeling of outer ply. No damage to core ply or inner ply.	Unsupported end of top retainer bent up 1". Also, bottom fwd end of rear retainer bent up 3/4".
6	BM009	L3000151-001 SWU-107	72.4°	78.4°	74.4°	6.00	970	4.55"	Same as previous test. Bent retainer straightened and replaced.	Additional peeling of outer ply. No damage to core ply. Inner ply cracks originated at point of maximum deflection.	14" crack in radius of long'n above side post. 3" crack in radius of lower sill 12" fwd of side post.

leaving two successive holes without bolts. This bolt configuration was successful in securing the ends of the retainer during the impact of shot Number 6.

On shot Number 6 (six-pound chicken), the inner ply cracked but did not spall. The progressive damage to the outer ply, and the crack pattern of the inner ply are shown in the Failure Analysis of Appendix A; as well as a complete failure analysis based upon crack propagation. Structural damage to the module also occurred as the result of this shot. Cracks appeared in the aft longeron and in the outboard sill structure. Also, a few bolts failed, but there was no penetration of the bird into the interior of the module.

Documentation of the tests is illustrated in Figure 26 for vertical deflection (BM006). The strain gage maps for the B-1 windshield and the 36 x 36 inch test specimens are located in Appendix B.

Strain Gage Installation

Strain gages were attached at strategic locations as shown in Figure 13 for the windshield and in Figures 3 and 5 of Reference 5 for the structure. As described in Section III, gages were installed on each of the two windshields, and six gages were selected from those attached to the structure to be monitored during the tests.

Strain measurements were made using a data acquisition system comprised of bridge completion networks, signal conditioners, recording magnetic tape machines and recording oscillographs. Twenty-two recording channels were used in acquiring data on deflection tests and on the actual test shots. These data were presented as oscillograms and were digitized and converted to the desired units. The bandwidth of the recording system was DC to 4 KHz.

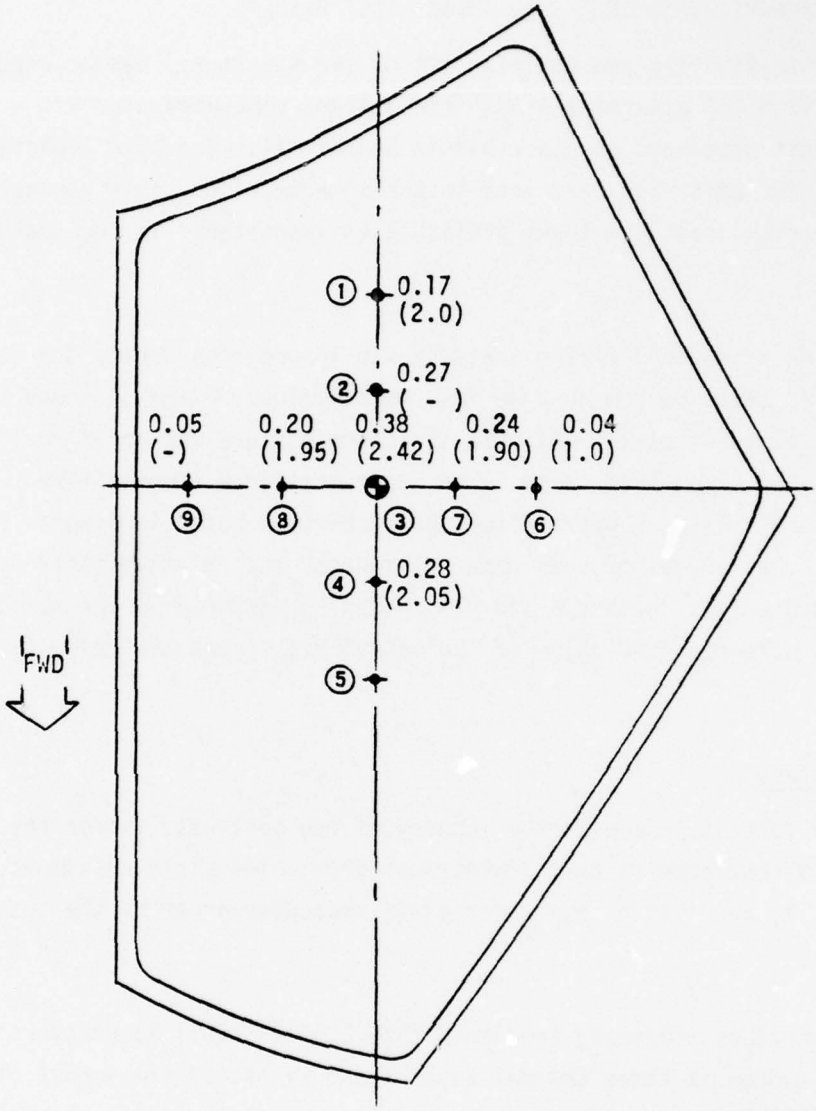

WINDSHIELD DEFLECTION MAP

Top number is deflection from 2500 pounds static load.
(Bottom Number) is deflection from bird impact.
Reference 2, Camera 2

Figure 26. Windshield Deflections - B-1 Windshield Bird Impact Test Specimen SWU 107, Test No. BM006.

SIMULATED AIRCRAFT WINDSHIELD BIRD IMPACT TEST RESULTS

In order to finalize and optimize all of the structural design aspects for a full sized B-1 alternate windshield design, simulated aircraft windshield test specimens as described in Section II, were bird impacted according to the test plan described in the same section. This subsection details the actual test and those difficulties encountered in the course of the test.

A computer windshield sizing analysis was in progress during the design and early bird tests on the 36 x 36 inch windshields. Based on these analyses the glass windshield support structure fixture was modified for five of the last seven bird tests. The lower stiffener flanges were removed on three of the support structure members as noted in Figures 28 through 30. The removal of this material reduced the relative stiffness of the structure near corners B and C as noted on Figure 27. The reduced stiffness is more representative of the actual B-1 structure (refer to Section V).

Bird Impact Tests

Noted in Table 6 is a complete summary of the test results for the 20 bird shots conducted on the simulated aircraft windshield specimens. The results, in this table, are arranged in ascending order of the test sequence.

The three glass laminated specimens (P/N Z5942639-501) manufactured by PPG were tested at three thermal regimes and withstood the impact of a four-pound bird at V_c = 565 knots without excessive damage.

The one specimen of four 1/4-inch plies of polycarbonate laminated by Sierracin was successfully tested at V_c = 502 knots at maximum hot temperatures and cracked only one ply. Subsequently, this specimen was tested at V_c = 565 knots at room temperature and passed. Since the elasticity of silicone interlayer does not change significantly at the

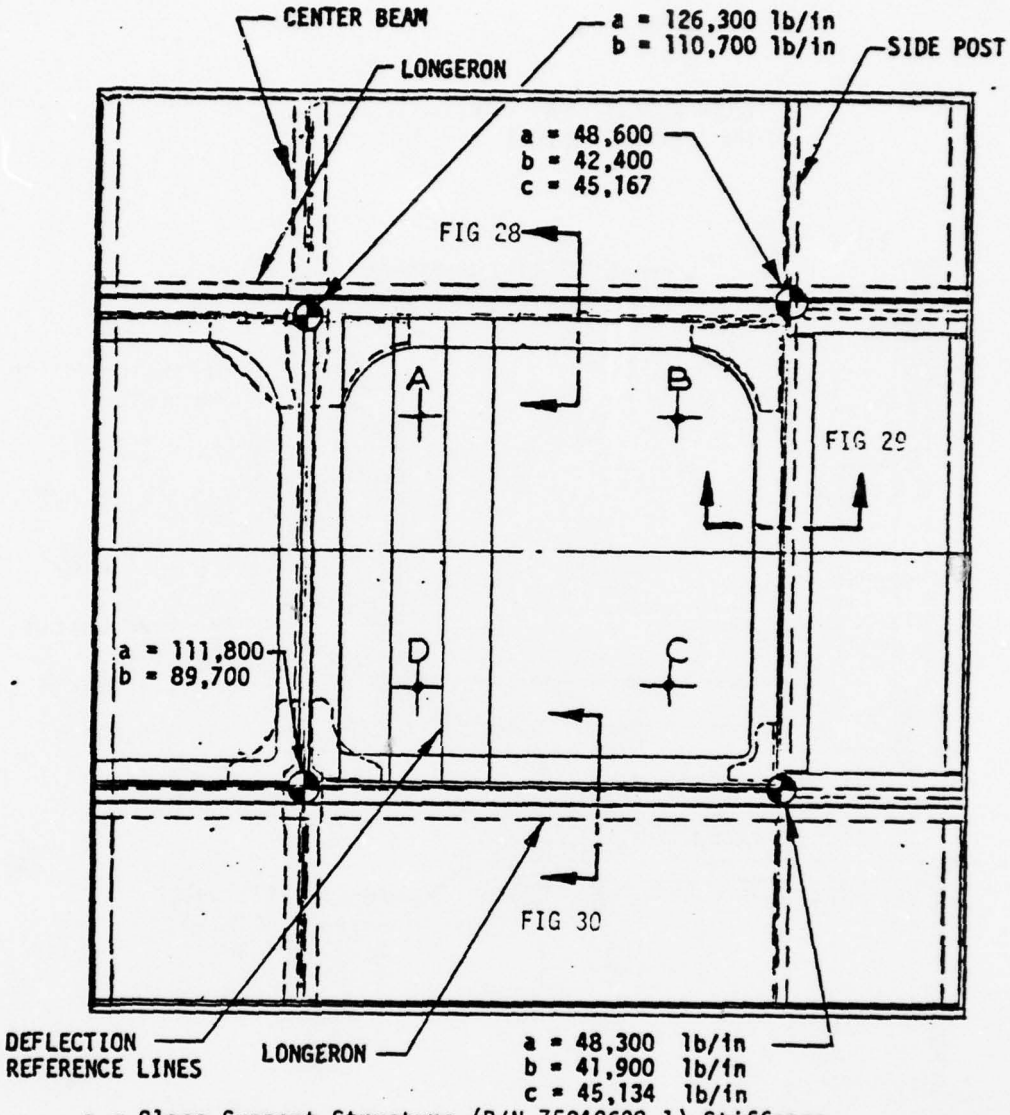

a = Glass Support Structure (P/N Z5942633-1) Stiffness

b = Polycarbonate Support Structure (P/N Z5942638-501) Stiffness

c = Modified Glass Support Structure (P/N Z5942638-1) Stiffness

Figure 27. Windshield Support Structure Fixture Assemblies.

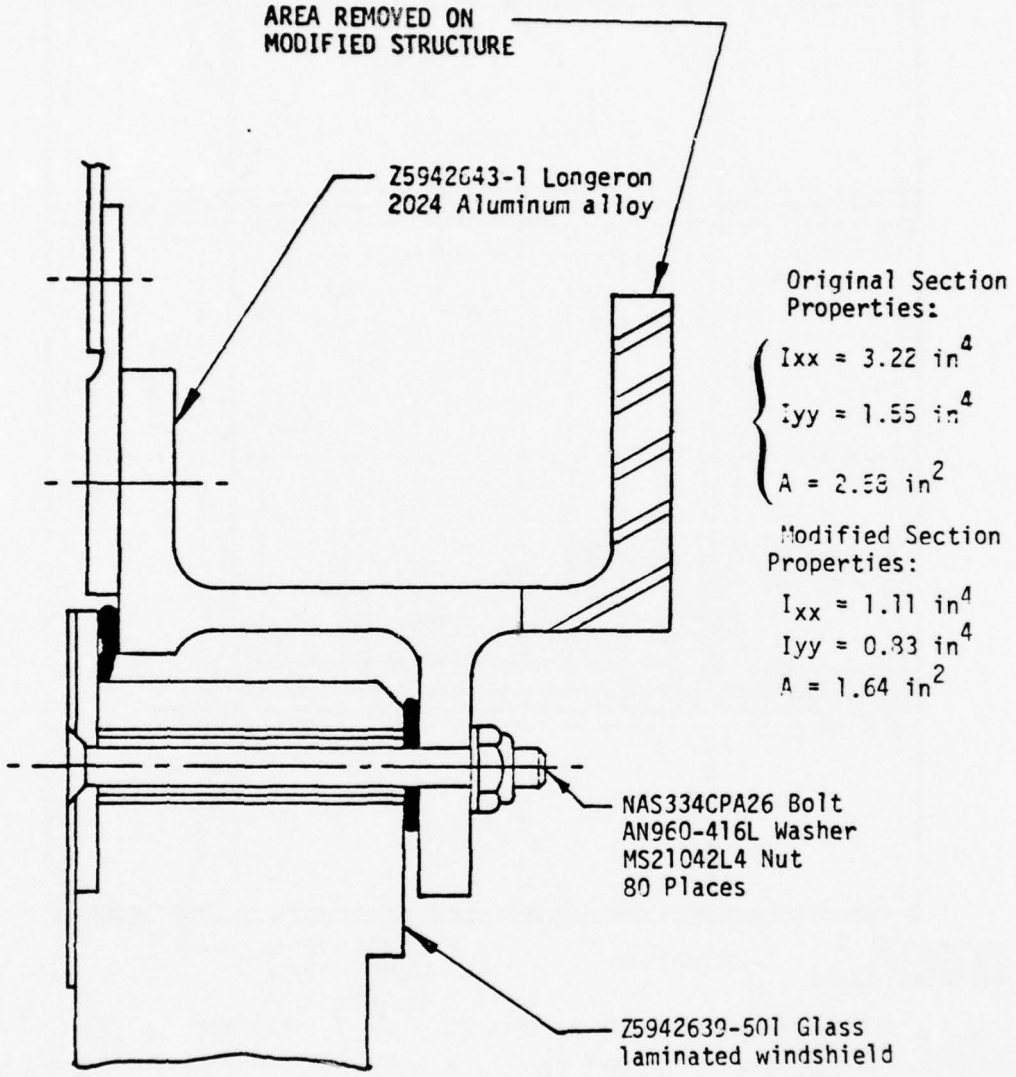

Figure 28. Representative Aft Longeron Support Structure.

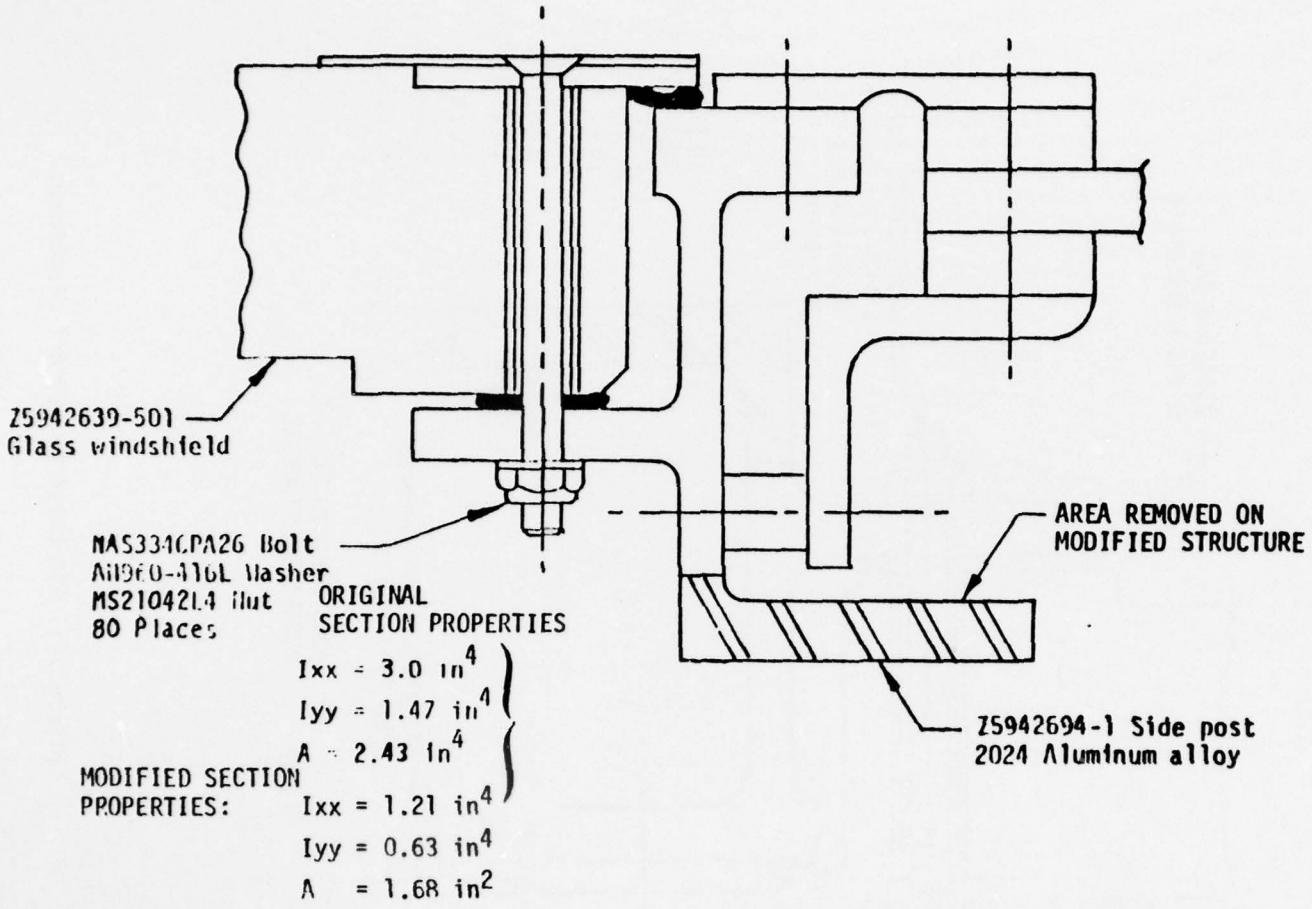

Figure 29. Side Post Support Structure.

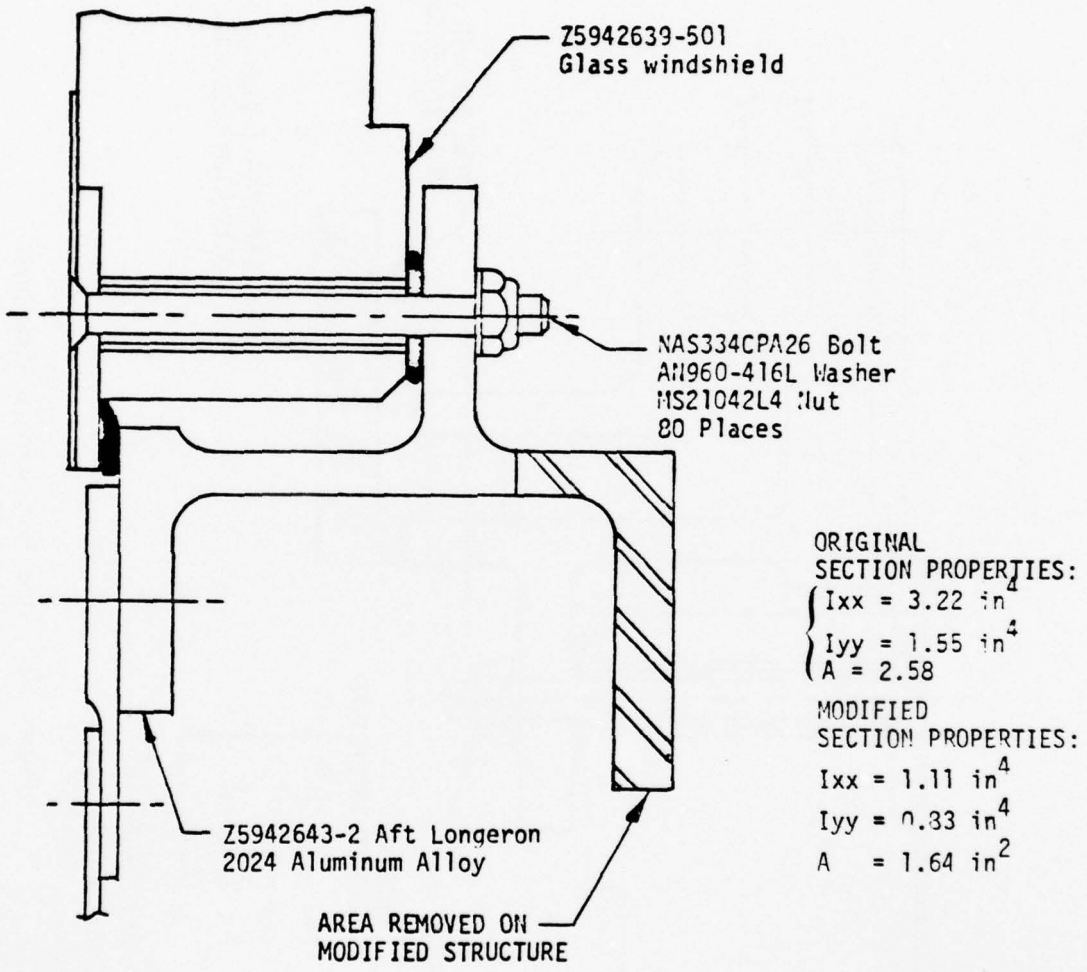

Figure 30. Aft Longeron Support Structure.

TABLE 6. TEST SEQUENCE AND TEMPERATURE REQUIREMENTS (°F)

PART NUMBER	TEST NO.	SPEC. NO.	SHOT LOC.	V (fps)	TYPE OF STR. (FIG 140)	T2-5 O.B.SFC	T6-9 T.C.INT	T10-13 I.B.SFC	ROWS OF BOLTS	REMARKS
Z5942640-501	BM10	SWU 001	A	941	b	-40°F	-20°F	40°F	Two	Cracked specimen near edge of support structure - Bird penetration.
Z5942640-501	BM11	SWU 002	A	960	b	85°F	78°F	93°F	Two	Cracked through specimen near point or impact - Bird penetration.
Z5942639-501	BM12	PPG 001	A	943	a	-55°F	-28°F	7°F	One	Cracked outer 1/2 inch ply only - No penetration.
Z5942639-501	BM13	PPG 001	A	948	a	80°F	80°F	80°F	One	Bagged bird - Depth 4-6 inches - Broke remaining 3 glass plies - No penetration.
Z5942639-501	BM14	PPG 002	C	939	a	87°F	87°F	87°F	One	Cracked both 1/2 inch glass plies - No penetration.
Z5942639-501	BM15	PPG 002	E Center	515	a	90°F	90°F	90°F	One	No additional damage.
Z5942640-501	BM16	SWU 002	C	369	b	82°F	82°F	82°F	Two	Bounced bird - No additional cracking from BM11 - No penetration.
Z5942640-501	BM17	SWU-001	C	737	b	97°F	-	91°F	One	Cracked all plies - No penetration.
Z5942640-501	BM18	SK 001	C	847	b	230°F	190°F	110°F	One	Locally cracked #3 P.C. ply.
Z5942639-501	BM19	PPG 003	C	971	a	220°F	190°F	160°F	One	All plies cracked - No penetration - Cracked through specimen 9-inch length at back edge of structure.
Z5942640-501	BM20	SK 001	A	958	b	74°F	80°F	76°F	One	Cracked all four 1/4 P.C. plies - Passed - No penetration.
Z5942640-501	BM21	SWU 003	A	960	b	-40°F	-20°F	38°F	One	Cracked through specimen near edge of support structure - Bird penetration.
Z5942640-501	BM22	SWU 003	C	846	b	75°F	76°F	71°F	One	Installed in glass support structure - Completely shattered inner P.C. ply - A section of laminate 3 x 6 inches went into cavity - Very little bird penetration.
Z5942639-503	BM23	PPG 004	C	953	c	194°F	159°F	130°F	One	Shattered outer glass ply - No other damage tested in modified glass structure.
Z5942639-505	BM24	PPG 005	C	877	c	205°F	191°F	132°F	One	Shattered outer glass ply similar to BM23 - Velocity low - Tested in modified glass structure - Decision made to re-shoot.
Z5942639-505	BM25	PPG 005	C	951	c	200°F	195°F	145°F	One	Repeat of BM24 - Removed additional outer ply glass - No additional plies cracked.
Z5942640-507	BM26	SK 002	C	939	c	226°F	213°F	143°F	One	Removed outer ply in impact area - No damage to core ply - Cracked support flange locally, approximately 5 inches in length (modified glass str.).
Z5942640-507	BM27	SK 002	B	920	c	-36°F	-41°F	31°F	One	Very little damage - Several additional cracks in outer acrylic ply - No damage to core ply - Cracked support flange, locally approx. 9 inches (modified glass str.)
Z5942639-503	BM28	PPG 004	B	940	b	-30°F	-33°F	38°F	One	Broke both 1/2 inch P.C. core plies aft of impact point - Bird penetrated! (Tested in P.C. structure).
Z5942639-505	BM29	PPG 005	B	931	b	-28°F	-21°F	39°F	One	Much spalling of outer ply of glass with no apparent damage to core plies. (Tested in P.C. Structure).

lower temperatures, it is believed that this specimen design would also withstand the bird impact at lower thermal extremes.

The one specimen identified as Z5942639-505, of four 1/4-inch plies of polycarbonate laminated by PPG was successfully tested at maximum thermal extremes and withstood the impact of a four-pound bird at V_c = 565 knots.

The 7/8-inch ply of polycarbonate laminated specimen, identified as Z5942640-507 and installed with one row of attachments, was tested at maximum thermal regimes and withstood the impact of a four-pound bird at V_c = 565 knots.

Instrumentation and Documentation

Strain measurements were made using a data acquisition system comprised of bridge completion networks, signal conditioners, recording magnetic tape machines and recording oscillographs. Twenty-two recording channels were used very successfully in acquiring data on static loading/dynamic unloading tests and on the actual bird impact test shots. These data were presented as oscillographs and were digitized and converted to desired units and replotted as a function of time.

This strain data were further analyzed by taking time cuts on the digitized plots and summarizing all the strain values as a function of time as each strain gage peaked. The strain data are summarized and presented in full in Reference 3 and in part in Appendix B. The strain maps in Appendix B show the strain gage measurements at pertinent locations for each specimen.

Deflection data consisting of motion picture film edited such that all camera views of the impact and adjacent areas were reduced into deflection versus time data for each shot and punched on IBM cards. It was the original intent that the IBM cards, thus punched, were to be used to plot deflection versus time plots for four predetermined individual lines on the surface of the windshield, as shown in Figure 27.

A Douglas proprietary program was utilized to use these IBM cards and plot deflections (as a function of time for all four lines) to simultaneously show relative deflections and windshield shape at any instant in time. This information could be used to verify the bird impact model described in Section V. A sample output of deflection at time = 0 milliseconds, and time = 3 milliseconds, is shown on Figures 31 and 32. This latter figure shows a typical lack of deflection detail in the area of impact. This is due to the nature of the deflection data collection process. When the film analyst can not discern the motion of the target lines, no deflection data can be punched on the IBM cards. On this series of tests, meaningful deflections in the area of impact were difficult or impossible to obtain due to obscuring of this area due to chicken debris, or in cases involving cold tests, the "cold-air fogging" of the area and/or ice and frost flakes.

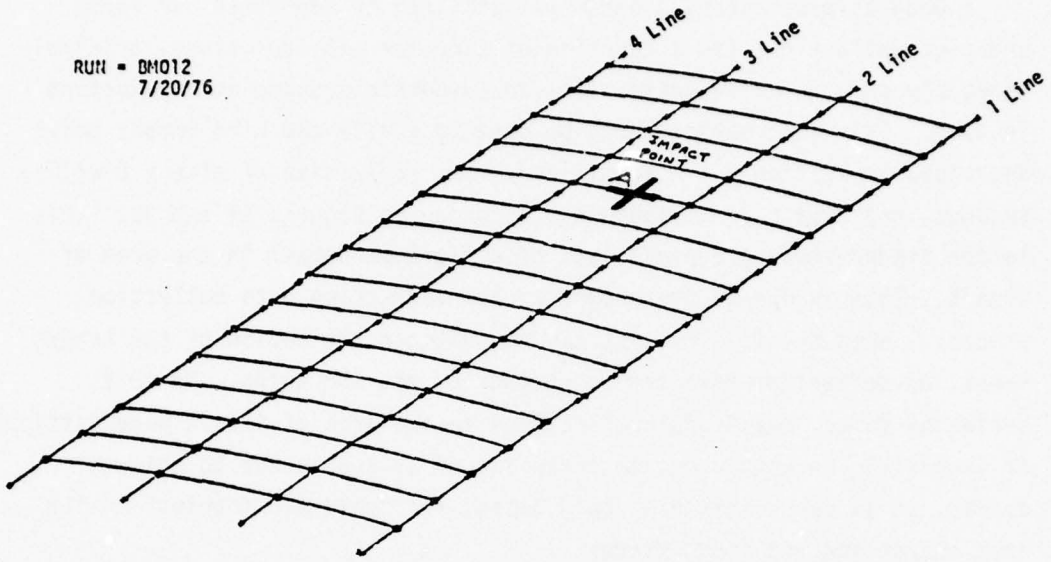

Figure 31. Relative Deflection and Windshield Shape at T-0 Milliseconds After Impact.

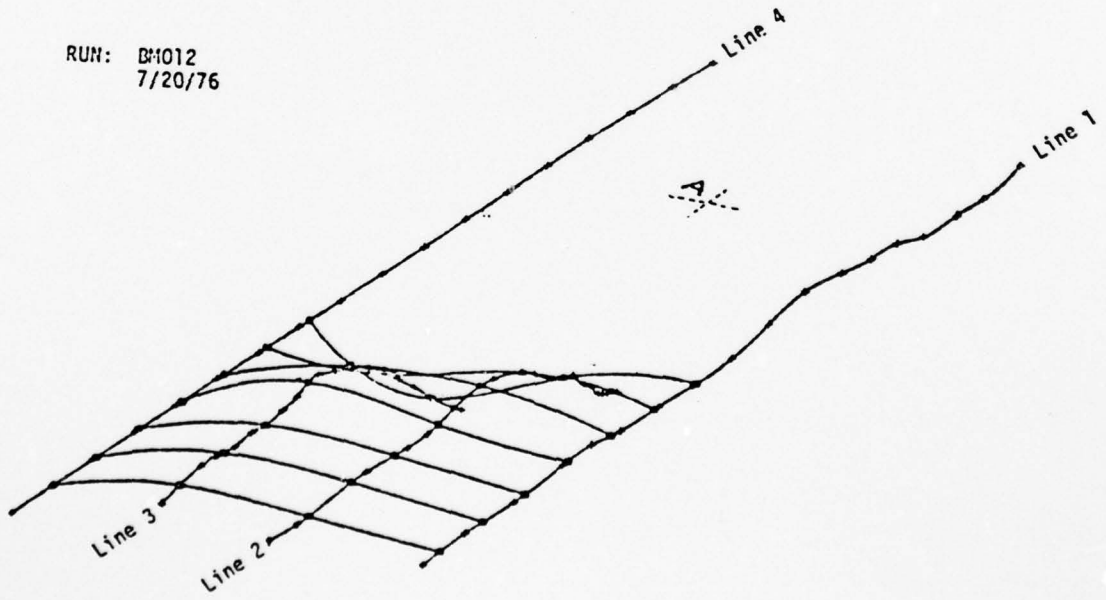

Figure 32. Relative Deflection and Windshield Shape at Time = 3 Milliseconds After Impact

SECTION V
WINDSHIELD SYSTEM DESIGN STUDIES

This series of high speed bird impact tests is based on a proper approach to windshield design, that of considering the entire windshield system. By this is meant the structure of the windshield itself coupled with the windshield supporting structure. Any evaluation of an aircraft windshield system must be systematically evolved from a review of past experience and available related industry design philosophies, design analyses, and test fixture development. These items are presented in this section.

This section also correlates the results of this series of high speed bird impact tests as relating to, and affecting the goal of this program: demonstration of windshield design technologies using parameter guidelines based on the B-1 aircraft.

DESIGN PHILOSOPHIES

In recent years windshields were designed to meet the same basic requirements; yet, differences taken in the design approaches and material selections have resulted in the introduction of problem areas such as maintenance problems, marginal service lives, failure modes that result in aircraft flight speed restrictions in accordance with FAA bird impact requirements, and in the extreme, the loss of USAF aircraft due to bird strikes.

Meaningful data that were available for an initial review for the Windshield Technology Demonstrator Program included:

- Air Force furnished F-111 bird impact data
- Air Force furnished A-10 and A-37 bird impact data
- Goodyear Aerospace reports AFML-TR-74-234 Parts I and II
- Rockwell International B-1 data and drawings
- Airlines service experience data for the L-1011 and B-747 aircraft windshields

- FAA bird impact study reports
- Douglas DC-8/DC-9/DC-10 service experience, test and development data
- Vendor furnished data

Subsequently it became readily apparent that the windshield design for the B-1 aircraft should be directed toward combining the best features of the Rockwell International B-1 design and the Douglas DC-10 design. Results of other transparency tests performed by various manufacturers were also evaluated in determining an optimum design. These evaluations are discussed in the subsequent subsections.

Alternate B-1 Windshield System Design Approach

In an endeavor to develop an alternate B-1 windshield design, basic design philosophies and guidelines were established as presented in the following discussion.

Since the B-1 windshield is part of an existing air vehicle system, certain R-I design philosophies and requirements were maintained, including the following:

- Aerodynamic shape
- Structural member locations
- Reacting pressurization carry-thru loading between the windshield and support structure
- Crew compartment pressurization criteria

It was determined that primary consideration must be given toward defining the acceptable failures during the design of the windshields and supporting structure during bird impact conditions. Historically, on Air Force aircraft the resultant effects of a bird strike were destroyed windshields, destroyed structure and frequently a complete loss of aircraft and crew. It is believed that the windshield should be, at worst, disposable after a bird impact, but still should be capable of meeting operational requirements for mission completion. The

windshield structural supporting members should not be disposable or have permanent deformation because of high maintenance costs to replace the structure.

The existing B-1 windshield designs make use of retainers that are common to more than one transparency. Frequently, during a windshield replacement, the adjacent windshield and retainers were damaged and the pressure seal was destroyed. As a design objective, this program has been directed toward utilizing only one row of attachments and an integral retainer around the entire periphery of the windshield for ease of installation. Also, for ease of maintenance, loose hardware such as retainers, shims, fittings, and fasteners that are difficult to account for during a windshield change-out, should be kept to a minimum. The attaching bolts should be the same length, nutplates attached to the structure, and the retainers and dry seals a permanent part of the windshield.

Also, since it is virtually impossible for a transparency vendor to manufacture a curved windshield to an exact shape, attachment holes should be oversized to allow maintenance personnel to readily align the windshield on the aircraft and maintain interchangeability.

Industry Windshield Design Approach

In an effort to test only the most promising windshield designs, certain engineering judgments were made as to windshield materials (structural plies and interlayers), the thickness and number of plies. The basis for these judgments are discussed in this subsection.

A method of calculating bird penetration capability for a glass windshield was based on an informal test by Douglas Aircraft on the DC-10 glass windshield. The DC-10 windshield and supporting structure had been successfully bird impact tested to 776 FPS. Using a mathematical analysis based on an equation for bird impact force from Reference 6:

$$P = K\,(W)^{2/3}\,(V)^2 \sin A \qquad (1)$$

where P = peak normal force, lbs.,
K = test constant,
W = bird weight, lbs.,
V = bird relative velocity, FPS,
A = impact angle, degrees.

Assuming the same peak force and other constants hold, then the DC-10 glass windshield rotated from 41° to 25° would withstand an impact velocity of

$$V = \left[(776)^2 \frac{\sin 41^\circ}{\sin 25^\circ}\right]^{1/2} = 967 \text{ FPS } (659 \text{ MPH})$$

This analysis showed that a glass windshield was structurally feasible; hence, other test data involving glass windshields were investigated.

PPG made some high-speed bird impact test data available (Reference 7). The impacted test panel consisted of two glass plies .50 inches thick using CIP 64 interlayer and a .110 inch thick outer glass shield. The test temperature was -16°F, the bird impact angle was 25 degrees, and the impact velocity was 895 FPS (610 MPH). The bird did not penetrate. Minor glass spall was visible on the inner ply. The configuration of Figure 5 is based on this tested design.

An effort was made to determine the effect of the number of structural plies on bird penetration velocity for polycarbonate laminates. Reference 3 indicates that the penetration velocity for a four-ply laminate is approximately 17 percent higher than for a 1" monolithic panel. These results apply to a flat panel at room temperature and a 45 degree bird impact angle. This report also compares the effect of multiple plies on penetration velocity. A four-ply laminate with CIP 0.10 inch urethane is approximately 20 percent better than a three-ply laminate at room temperature, 45 degree angle and flat. The configurations of Figures 4a and 4c are based on this tested design.

An additional comparison from this report may be made for a two-ply laminate with 0.50 inch plies and CIP 0.10 inch urethane interlayer by applying the ratio of 0.10 inch urethane to .025 inch Ethylene Terpolymer (ETP) to the curve for the 0.50 inch plies with ETP interlayer. The new configuration would have a penetration velocity greater than 766 FPS (522 MPH) and slightly less than the four-ply (0.25 inch per ply) configuration at room temperature, 45 degree angle and flat. The configuration of Figure 4b was based on this design.

From this report (Reference 8), Goodyear makes these observations: 1) while additional plies increase the penetration velocity, doubling the number of plies does not double the penetration velocity; 2) doubling the plies does, however, more than double the kinetic energy defeated; 3) the relationship between impact velocity and impact angle is shown in Figure 33. The results of the current B-1 tests are shown superimposed on it.

Windshield Mounting Design Approach

Two divergent mounting philosophies have been used throughout the aircraft industry. One mounting philosophy is to isolate the windshield from the aircraft structural loads. The second is to carry fuselage loads through the windshield.

In the first mounting philosophy, it is necessary to design the surrounding structure to the airframe's fatigue life requirements without depending on the windshield for any support. This philosophy dictates a heavy, stiff structure. Most industry studies and testing is based on this design philosophy.

The second approach allows a lighter weight structure to meet the fatigue life requirements. This approach, which was adopted for the alternate B-1 windshield system design, involved a constant analytical study, throughout the design process, of the relative stiffnesses of all

AD-A071 814 DOUGLAS AIRCRAFT CO LONG BEACH CALIF F/G 1/3
HIGH SPEED BIRD IMPACT TESTING OF AIRCRAFT TRANSPARENCIES.(U)
JUN 78 M J COKER, R H MAGNUSSON F33615-75-C-3105
UNCLASSIFIED MDC-J7184 AFFDL-TR-77-98 NL

2 OF 3
AD
A071814

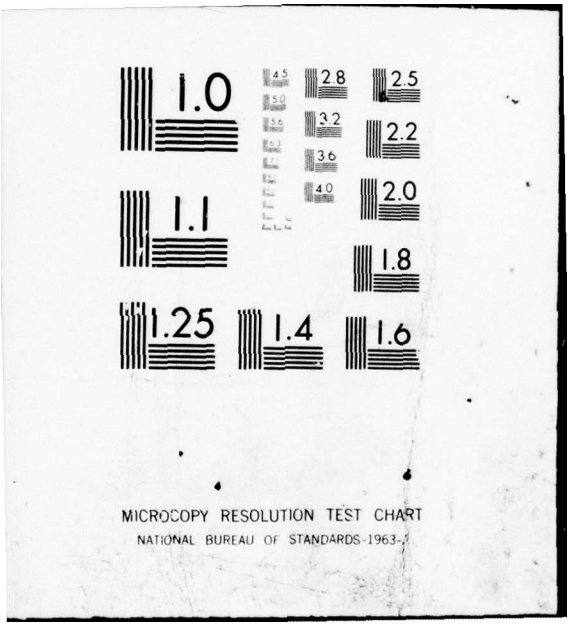
1.0
1.1
1.25
1.4
1.6
1.8
2.0
2.2
2.5
2.8
3.2
3.6
4.0
4.5
5.0
5.6
6.3
MICROCOPY RESOLUTION TEST CHART
NATIONAL BUREAU OF STANDARDS-1963-

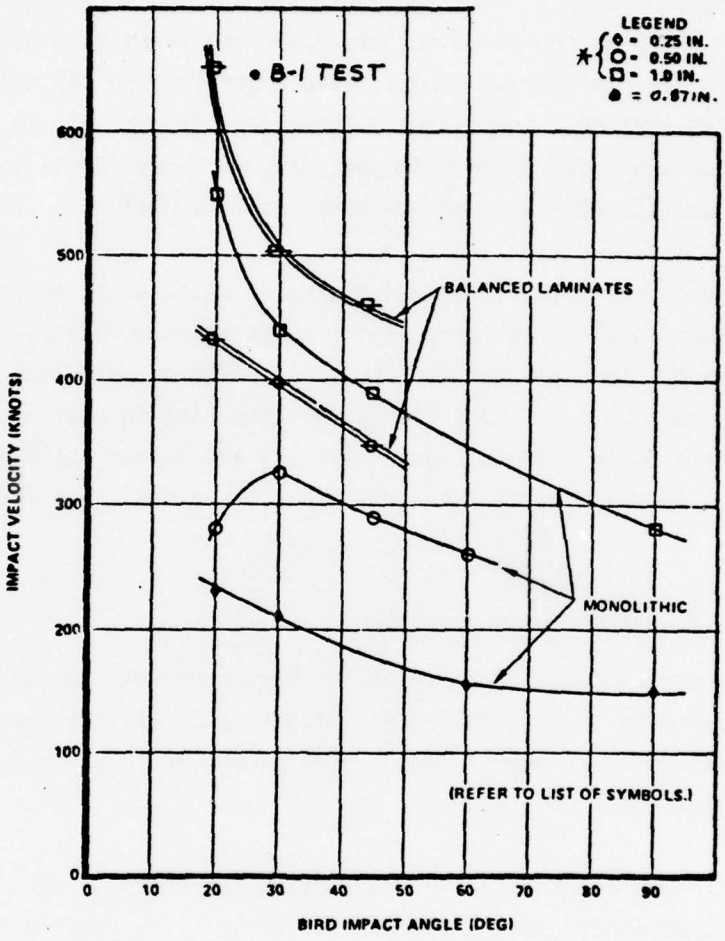

(Reference 2, 8)

* NOTE:
LAMINATED PANELS HAVE 0.10 IN. CIP URETHANE INTERLAYERS.

Figure 33. Effect of Impact Angle on Penetration Velocity for Optically Treated Polycarbonate at 75°F.

elements of the windshield system. Douglas utilization of this design approach in these series of tests, with the necessary emphasis on proper support structure stiffnesses, is presented subsequently in this section.

STRUCTURAL SUPPORT SIZING ANALYSIS

The purpose of this analytical effort was to conduct a study of the B-1 baseline support structure with a glass-face transparency cross section using designs composed of a single thick ply of polycarbonate, and multilaminate polycarbonate and glass transparency cross sections to provide the optimum structure to resist bird impact.

This study includes the following areas:

- Identification of those structural elements which cause undesirable changes in stiffness at any point throughout the transparency and support structure. This is, essentially, an investigation of sensitivity to changes in the structural stiffness of the various elements of the design.
- Refinement of support structure that is required to provide the flexibility necessary to be compatible with the transparency for bird impact.
- The influence of windshield support structure corner gussets/ fittings on the impact sensitivity.
- The effects of using one row of attachments versus two rows on impact response.

Finite Element Model

The approach taken to accomplish this study was based on utilizing a Douglas redundant force analytical computer program. The resize finite element model of the B-1 baseline (AV4) support structure, Figure 34, contains the structure from the canted bulkhead at Y_F = 293.3 aft to

Index to Substructure Diagrams - Overall

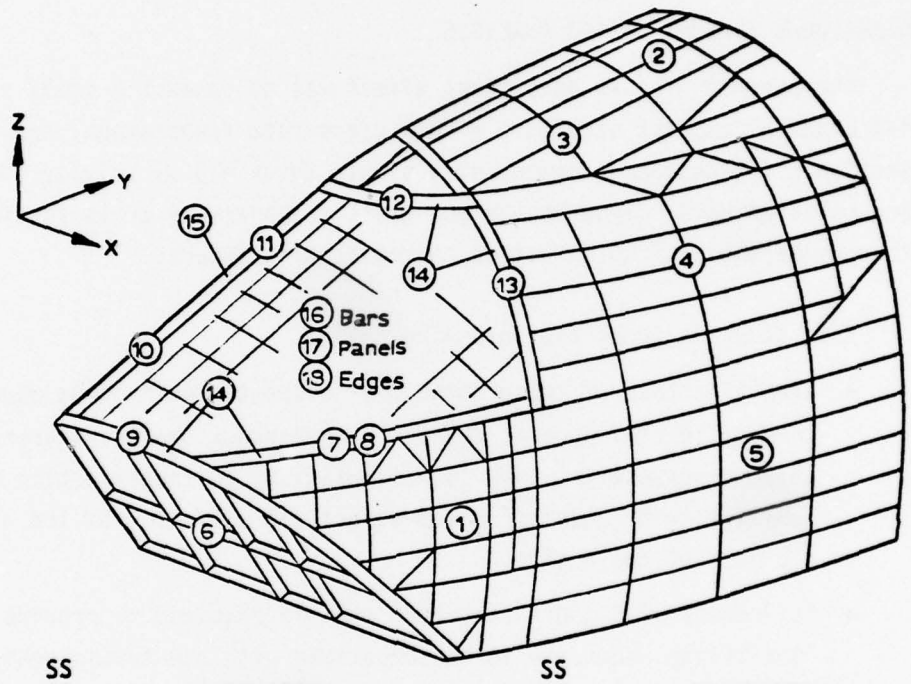

SS NO.	DESCRIPTION	SS NO.	DESCRIPTION
1.	Forward Lower Fuselage	10.	Center Beam (Part 1)
2.	Aft Upper Fuselage	11.	Center Beam (Part 2)
3.	Eyebrow Window	12.	Upper Longeron
4.	Aft Side Fuselage	13.	Side Post
5.	Aft Lower Fuselage	14.	Retainer
6.	Canted Forward Bulkhead	15.	Retainer
7.	Lower Longeron (Part 1)	16.	Windshield (Bars)
8.	Lower Longeron (Part 2)	17.	Windshield (Panels)
9.	Forward Bulkhead Fitting	18.	Windshield to Edge Member Attachment

Figure 34. B-1 (AV4) Modeling.

Y_F - 317.00 and above the pressure panel at Z_F = 26.5. This model consists of approximately 5,000 elements.

The system was modeled with the greatest detail at the transparency support flange. The transparency and edge attachments were modeled on a coarser scale, reflecting the need for relatively less detail in areas of uniform construction.

Specifically, the modeling of the structure included support flanges modeled to account for local bending and bolt simulation. Modeling of the attachments in the flange area was simplified by grouping four attachments together, then varying the stiffness of each group to simulate one or two attachment rows.

A detailed discussion of the modeling and CASD computer program utilized in this study is contained in Volume 2 of Reference 14.

Support Structure to Transparency Compatibility Evaluation

A basic premise in designing structure to efficiently take impact loads is that there should not be areas of sudden stiffness discontinuities. Hence, an evaluation of the support structure and transparency compatibility was made. The initial evaluation took place during the preliminary design phase so that necessary adjustment to support structure stiffnesses could be made. This evaluation was accomplished by analyzing the finite element model with a unit load at each of the 105 transparency nodes to determine the stiffness of the transparency support structure at different locations. These stiffnesses were mapped for each of the candidate transparencies listed so that an overall view of the stiffness change can be seen and the relative compatibility determined.

As indicated in Table 7, Figures 35, 36, 37, 38 and 39 show the transparency/structural support compatibility plot for the indicated configurations. The plots show lines of equal stiffness, calibrated in

kips per inch, which are developed with consideration for the effects of both transparency and support structure. These compatibility plots may be substantiated by comparing the actual stiffness of a windshield of given configuration with the plotted stiffness generated for the compatibility plots. Specifically, for the B-1 configuration (Configuration C in Table 7), the actual stiffness of the windshield, as measured during the static loading tests of test number BM006 is 9124 lbs/inch (refer to Equation 29, Page 146). This value compares well with the stiffness of 9500 lbs/inch taken from the compatibility plot of the corresponding configuration, Figure 37.

TABLE 7. DESIGN CONFIGURATION.
POLYCARBONATE/GLASS LAMINATES

CONFIG.	STRUCTURAL PLIES			NO. BOLTS	REMARKS	REF. FIGURE
	NO.	MATERIAL	t PLY			
a	4 ply	PC	0.25"	2		35
b	2 ply	PC	0.50"	1		36
c	1 ply	PC	0.87"	2	B-1 Design	37
d	2 ply	GLASS	0.50"	1		38
e	4 ply	PC	0.25"	1		39

The general plan was to establish a baseline with the extremes being a flexible transparency and a stiff transparency with compatible structures for each. This baseline was then used to compare transparencies with intermediate stiffnesses. As a result of the compatibility evaluation, it was determined that the preliminary bird impact test specimens, 4-ply polycarbonate windshield, Figure 35, was the flexible transparency, and the glass windshield, Figure 38, was the stiff transparency.

The edge attachment for the flexible transparency was originally the two-bolt configuration (see Figure 35) as it was most effective for pressure loading. Also, this provided a test as to whether the two-bolt design could reasonably be used. The method to determine if a two-bolt configuration was acceptable was by evaluation of the test specimens

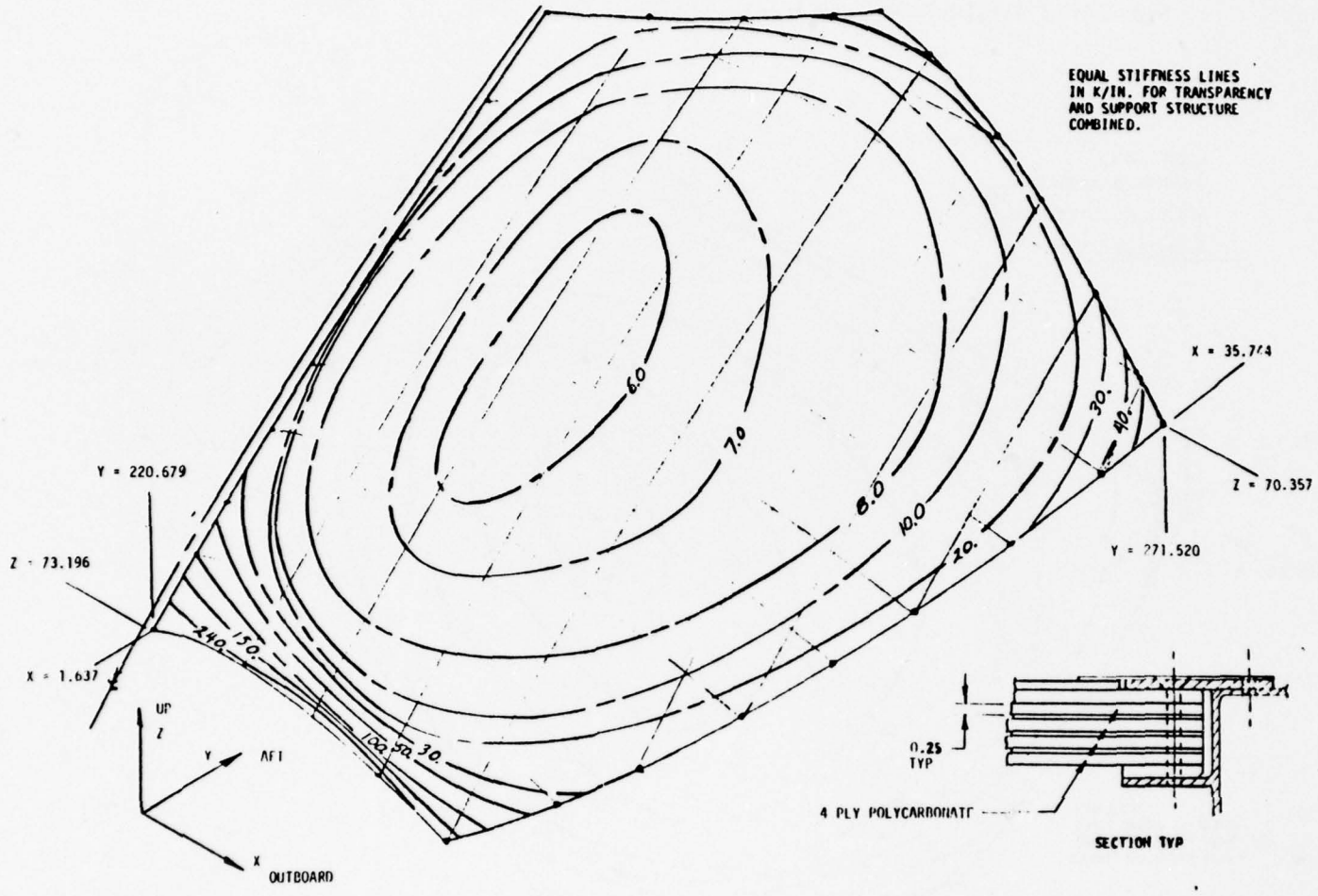

Figure 35. Transparency/Support Structure Compatibility Plot 4-Ply Polycarbonate Design - 2 Bolts at Edges.

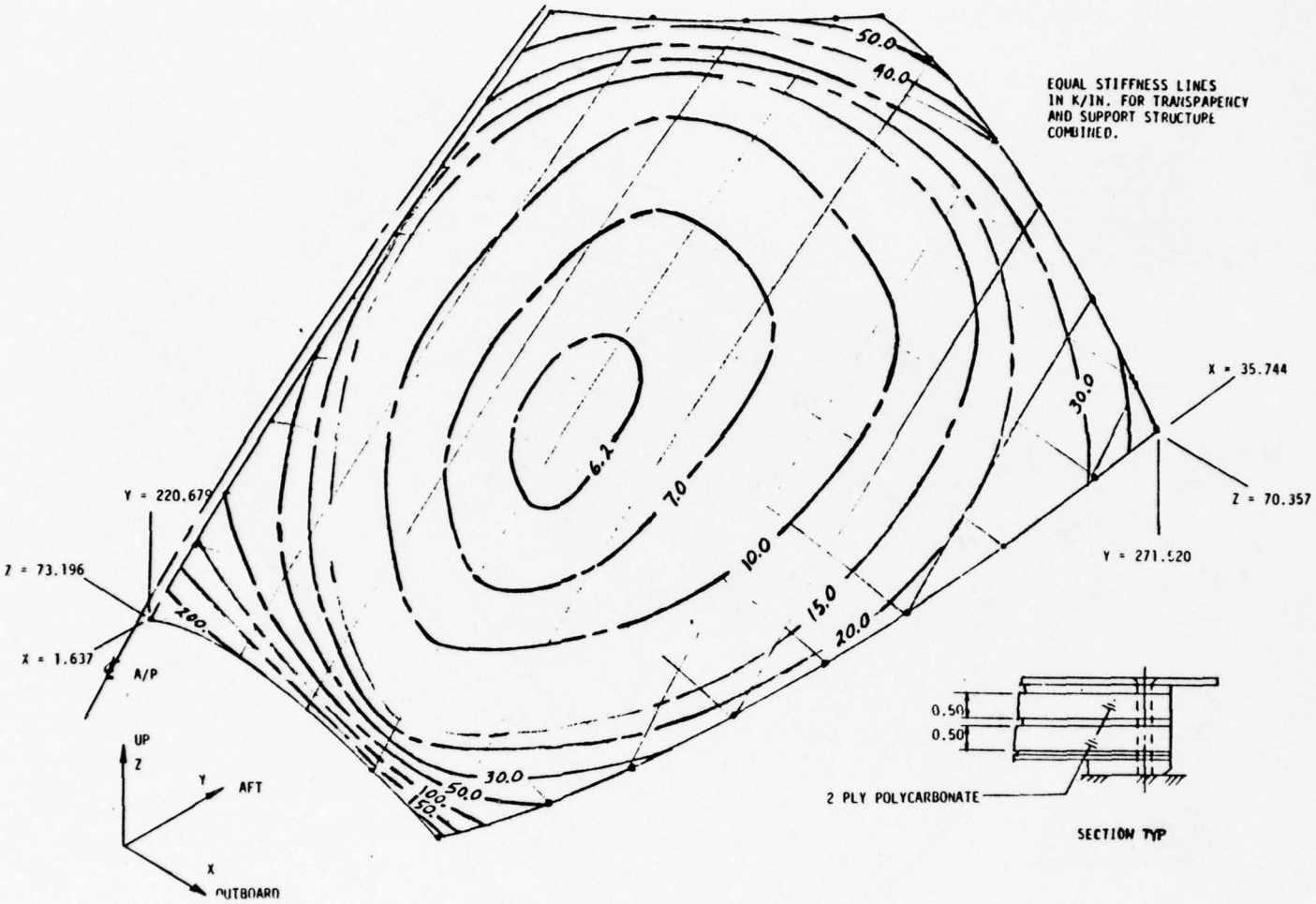

Figure 36. Transparency/Support Structure Compatibility Plot 2-Ply Polycarbonate Design - 1 Bolt at Edges.

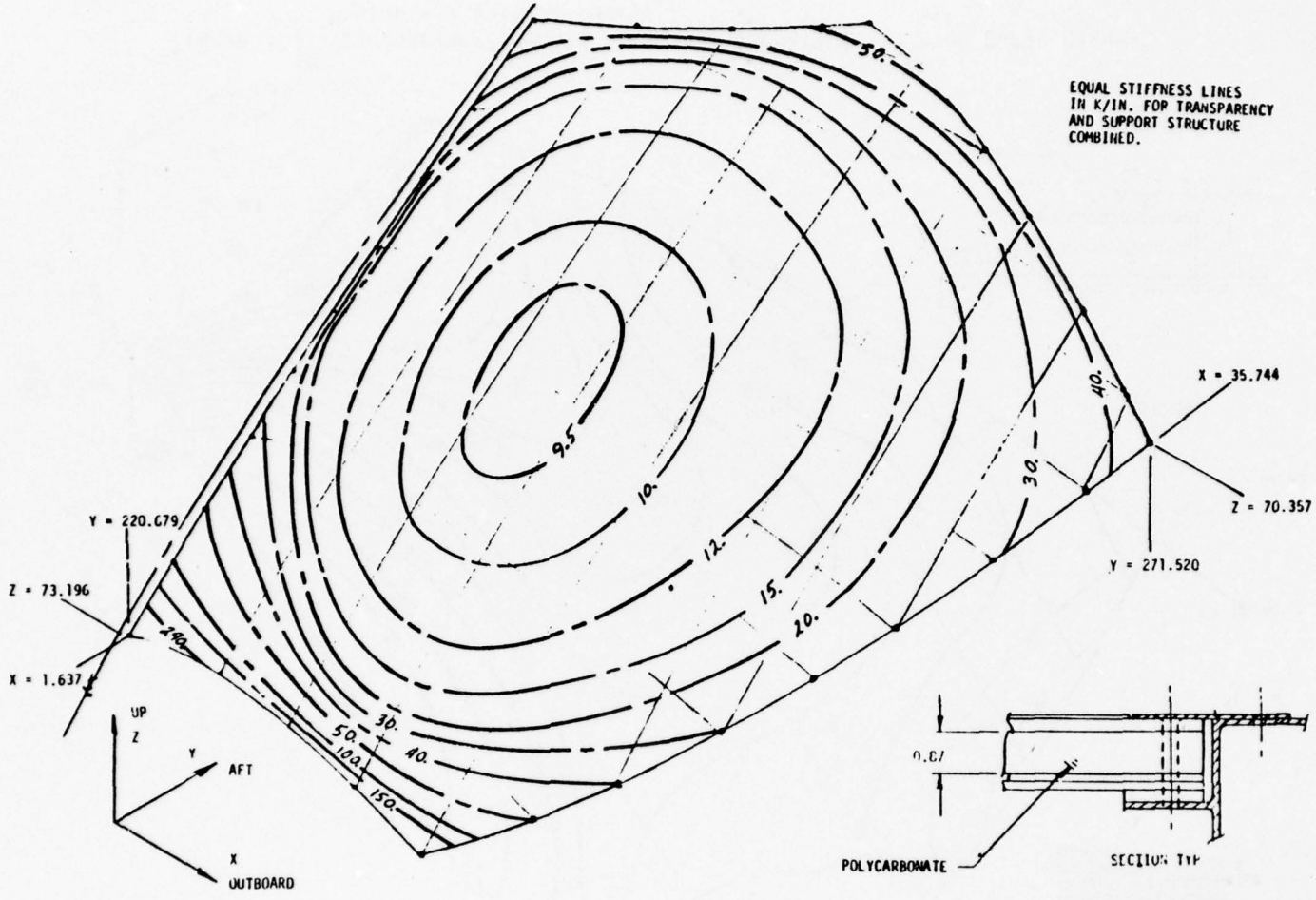

Figure 37. Transparency/Support Structure Compatibility Plot 1-Ply Polycarbonate Design - 2 Bolts at Edges.

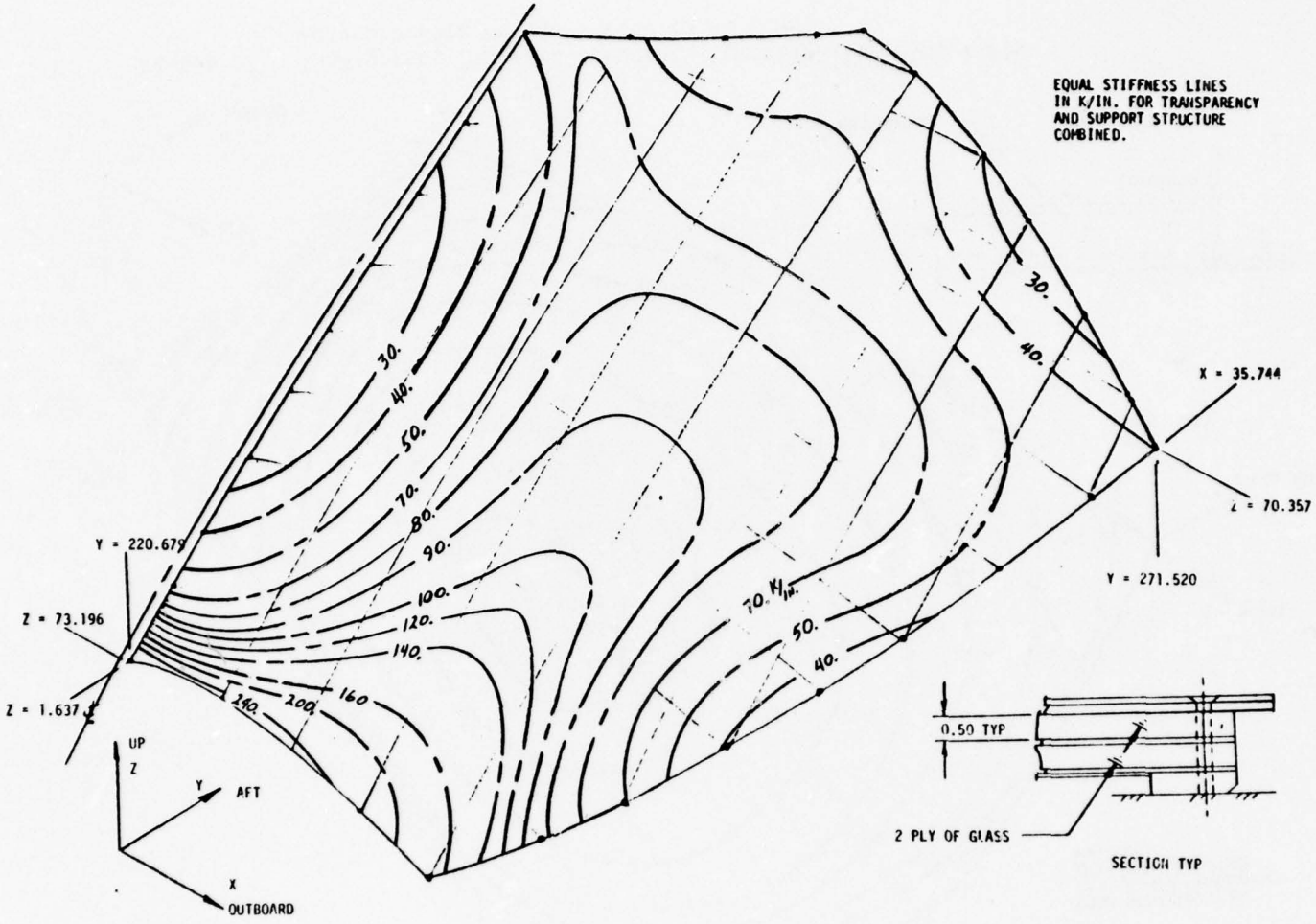

Figure 38. Transparency/Support Structure Compatibility Plot 2-Ply Glass Design - 1 Bolt at Edges.

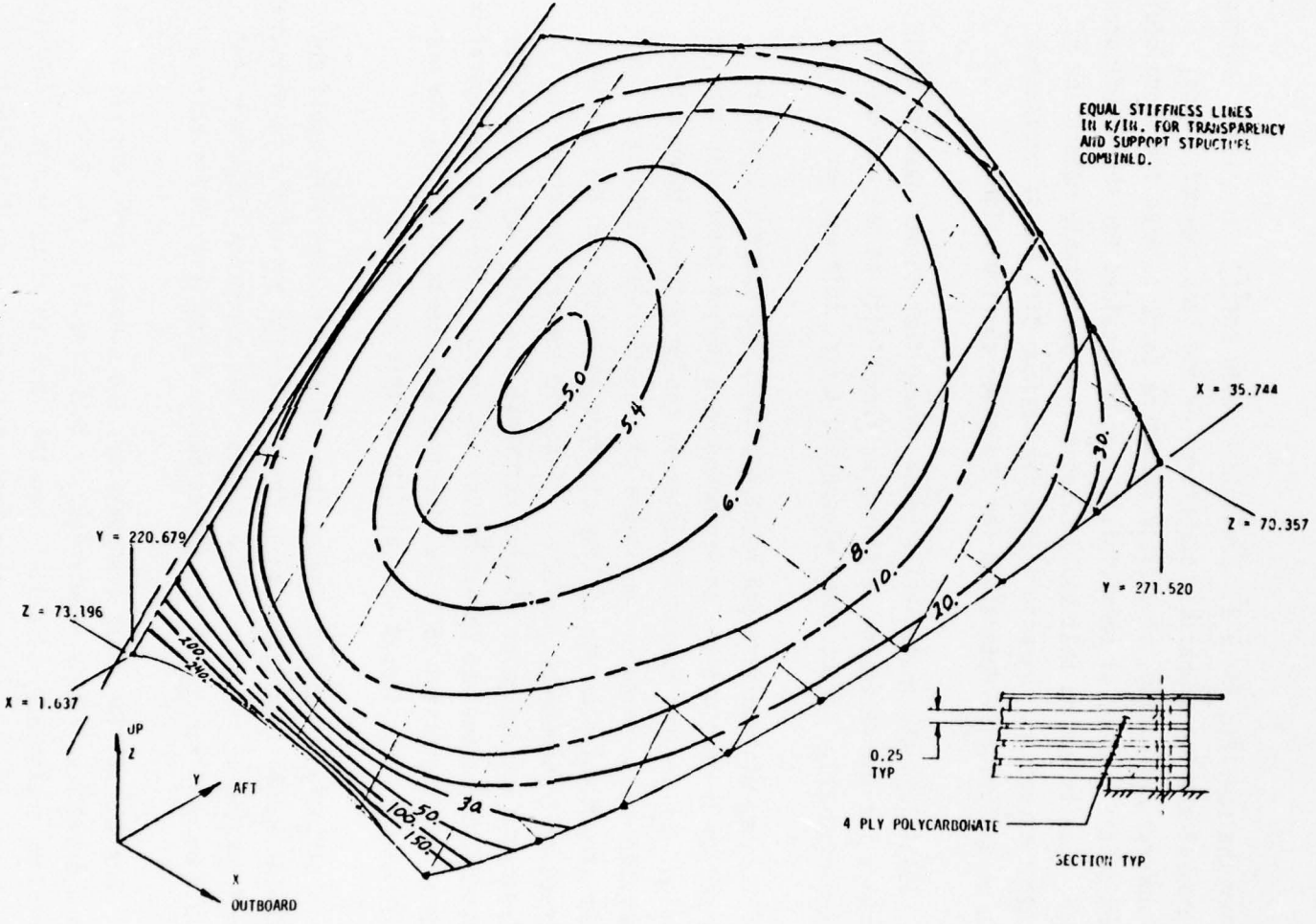

Figure 39. Transparency/Support Structure Compatibility Plot 4-Ply Polycarbonate Design - 1 Bolt at Edges.

after the specific 36" x 36" preliminary bird tests. This is an "autopsy" method of showing compatible structure, or the lack thereof; since, by natural definition, compatible structure tends to make for successful bird tests. Hence, if compatibility can be obtained for this configuration, then structure that would respond in a predictable manner and of optimal structural characteristics for maximum bird impact resistance can be analytically determined for the other configurations.

Initially, the analytical studies showed that corner gussets would provide for the necessary stiffness or flexibility at the corners of the windshield. During these windshield tests, this was not verified.

Because minimum strength requirements of the support structure (based on 2P pressure and an estimated bird impact load) dictated its design, the desired compatibility could not be obtained through the computer resize method. Conditions of compatibility could be met only when structural elements of like-stiffnesses existed at the support structure transparency juncture. Since the support structure was already at its design of minimum stiffness, the only way to partially accomplish the desired compatibility was to use a one-bolt configuration. Subsequent successful 36" x 36" specimen bird tests utilizing the one-bolt design demonstrated the validity of this approach.

Initially it was anticipated that the support structure would not provide enough flexibility to be compatible with any of the polycarbonate configurations. However, the end result was a support structure that could be used for <u>any</u> of the polycarbonate windshield configurations.

For the stiffer glass transparency, the support structure was sized to a minimum stiffness requirement as determined from the 36" x 36" specimen preliminary bird tests and the strength requirements. A minimum stiffness was used because this test structure is more flexible in its critical corners than the corners of the B-1 support structure. This tends to compensate for the increased weight of the transparency.

It should again be noted that the strength requirements dictate a support structure design with a certain minimum stiffness. This may be quantitatively represented as $(EI)_{\text{edge req'd}}$. Now, $(EI)_{\text{edge req'd.}} \propto (EI)_{\text{sup. struc.}} + (EI)_{\text{transp. edge}}$. Hence, it may be seen that in the case of polycarbonate transparencies, where $E_{\text{trans}} << E_{\text{sup struc}}$, there is virtually no stiffness contribution from the transparency edge, so the stiffness of the support structure governs. In the case of glass transparencies, however, $E_{\text{trans edge}}$ and $E_{\text{sup struc}}$ are of same order of magnitude, hence, the transparency can add to the stiffness of the support structure. So, for compatibility, the stiffness of the glass windshield support structure is less than that for the polycarbonate windshields.

Identification of Structural Elements That Cause Undesirable Changes in Stiffness

A survey of industry-wide windshield bird impact testing relative to support structure design, as well as observed design tendencies on this program, indicates that an overly stiff support structure tends to be designed and utilized for purposes of durability during a series of impact tests. This is sometimes rationalized because the utilization of very stiff support structure tends to place maximum load on the transparency. Results of the present analyses, as well as the 36 x 36 inch specimen bird impact test program, indicate that while this "stiff" approach may be acceptable for center shots, it is very unrealistic for determining bird impact capability at a location which will ultimately be mated to existing airframe structure whose stiffness is significantly different than that tested.

The previously described analysis (pages 89 through 96) was used to determine the areas in which stiffness changes occur. In order to identify the structural members which contribute to the change in stiffness, the resize capability of Douglas' computer program was used. This program allows the insertion of a load and deflection at a preselected location, and the program will resize the structure to obtain the given deflection with minimum weight.

The resize program for the 4 ply 1-bolt polycarbonate configuration was completed. Minimum areas and minimum depths were used for the windshield support structure. Even with these greatly reduced sections, (to provide more flexibility) the corners were still too stiff to be compatible with any of the polycarbonate windshield configurations as originally designed. Therefore, a different attachment design was indicated to reduce the stiffness link between the support structure and the transparency. This was accomplished by utilizing the one-bolt concept.

From the results of this analysis, the moments of inertia and areas were calculated for the support members. These were compared to the 36 x 36 inch test fixture. It was found that the stiffness would be within the limits of the test fixture but the area would not. For this case, the model was modified with the ability to either add or subtract areas in such a way as to not change the stiffness significantly. The model was resized again using these new areas and a one-bolt edge attachment.

Utilizing this resizing approach in an attempt to optimize the support members, the four-ply polycarbonate laminate analysis, utilizing one row of attachments, was completed and the results were the basis for reworking the 36 x 36 inch specimen support structure members as shown in Figure 27, Page 73.

Attachment Evaluation

The one-row versus two-row attachment evaluation was accomplished by repeating the compatibility evaluation of the support structure to transparency analysis as previously described. It was noted during the preliminary 36 x 36 inch specimen bird impact tests that the shearing of the polycarbonate structural plies was directly related to the degree of edge corner stiffness. Hence, using the one-bolt concept significantly reduces corner stiffness allowing successful subsequent shots on the simulated windshield panels.

Pressure Considerations

In addition to bird impact forces, the support structure design must accommodate the aircraft internal pressure.

Polycarbonate Windshield Support

The structural cross sections for the polycarbonate support structure configuration were evolved from conventional stress analysis techniques per methods of this section. The moment of inertia is approximately 3 to 7 percent greater than the existing Rockwell B-1 design. The depth is shallower in order to reduce the stress in the outer flanges. The rotational stability has been increased. The area of this support structure is approximately twice the area of the original B-1 design. The cross sections selected for the simulated aircraft windshield tests are representative of the proposed production design. The bolt hole spacing for this prototype approach was approximately 1.625 inches.

Glass Windshield Support

The support structure for the glass windshield was sized by a 2P pressure condition (21.2 PSI) and was designed to carry fuselage loads around the windshield opening. The stiffness of the center post for this configuration is approximately twice the Rockwell B-1 design to insure the necessary low stresses in the glass plies. This concept requires only one row of bolts for attachment of the transparency to the structure and improves maintainability considerably.

The hole spacing is approximately 1.625 inches, and each window may be removed individually. The weight (250 lbs.) of the glass windshield is approximately twice that of the polycarbonate windshield configuration.

The glass configuration was pursued because of its strength at high temperature, its excellent optical qualities, and its capability to defeat the bird. Suitability of a glass configuration to meet these requirements has been established by prior tests performed at Rockwell and Douglas Aircraft which are reported in References 9 and 10.

Windshield Deflection Comparison

A comparison was made between a 4-ply polycarbonate windshield, a 3-ply polycarbonate windshield, and the Rockwell B-1 windshield using deflection as a basis for comparison (Table 8). Analytical studies which required finite element techniques were conducted by Rockwell to determine the structural deflection under pressure. The model used a one-inch strip of structure with two-bolt attachments for the simulation. When the comparison was made for a loading condition of 10.6 PSI pressure, the difference in deflection for the three configurations was less than 10 percent. The same configurations modeled in the same manner but with a single bolt deflected approximately 23 percent more than the two-bolt installation. Confidence in the simulation exists since the B-1 analytical two-bolt deflection of .202 inches compares favorably with R-I test data of .208 inches as shown in the bottom row of Table 8.

The deflection of the these panels is a function of the total cross section area as well as the moment of inertia. Solid section panels have a higher moment of inertia than multi-ply panels because the interlayer has a very low capability to transfer shear between plies. The deflections, however, are almost equal. For the solid panel, the deflection and stress is dependent on the moment of inertia and the hoop tension capability. As the stiffness decreases with a multi-ply panel, the hoop tension capability predominates.

The results of the one-bolt method require that the bolt spacing be reduced from 1.625 inches on center to approximately 1.250 inches on center for .25 inch diameter bolts to reduce the bolt bending to an acceptable level. The total number of bolts was reduced from 232 to 147, a 37 percent reduction. Since use of multi-layer laminates reduce light transmission and degrade optical quality, further optical studies were conducted on two-ply composites for polycarbonate and glass transparencies, using both CIP silicone and PPG 112 interlayer. Refer to Section II of Reference 14 for these studies.

TABLE 8. DEFLECTION FOR COMPOSITE WINDSHIELDS SIZED TO FIT THE B-1 GEOMETRY

	PRELIMINARY DEFLECTION ~ INCHES	
	10.6 PSI PRESSURE 50 INCH RADIUS	
	1 Row of Bolts	2 Rows of Bolts
4-Ply Polycarbonate .25 inch per ply (Figures 4a, 4c)	0.379	0.197
3-Ply Polycarbonate .25 inch per ply (Figure 4a)	0.412	0.218
2-Ply Polycarbonate .50 inch per ply (Figure 4b)	0.305	--
1-Ply Polycarbonate .87 inch (Figure 4d)	0.248	0.202
2-Ply Glass .50 inch per ply with .120 interlayer (Figure 5)	0.078	--
1-Ply Polycarbonate .87 inch B-1 A/V #3 (RI Test 1-25-75)	--	0.208

PRELIMINARY DESIGN METHODS

Several independent approaches to analytical substantiation of test data were devised and utilized in the design phases of the alternate B-1 windshield. These methods were used to advantage in this program and are described in this subsection.

Deflection and Stress Calculations in a Laminated Beam

Reference 11 describes and documents the theory and procedures for calculating the elastic deflection and stress distribution of a flat, laminated beam with fixed ends or simply-supported ends comprised of transparency materials subjected to a normal point load at the midpoint of the beam. The development of a computer program using the basic theory is presented along with illustrative examples and a "user's manual". The program results have been favorably compared with actual test data, including data of this test series, and with a finite element method. This subsection presents salient features of Reference 11.

Beam configurations used as a basis for the included illustrative examples are as follows:

Case A - 4-ply polycarbonate laminated beam
Case B - 2-ply glass laminated beam
Case C - 1-ply polycarbonate laminated beam
Case D - 2-ply polycarbonate laminated beam

Deflections for these cases are generated using a unit load and are as shown in Figure 40 for beams of varying lengths. This figure shows the deflection comparison of a laminated beam to a multi-ply beam without interlayer.

Being able to ascribe a stiffness value to a laminated beam is of great importance in any comparative evaluation. Techniques of Reference 11 readily allow a calculation of the "effective stiffness" of any laminated beam. This effective stiffness value is calculated from the

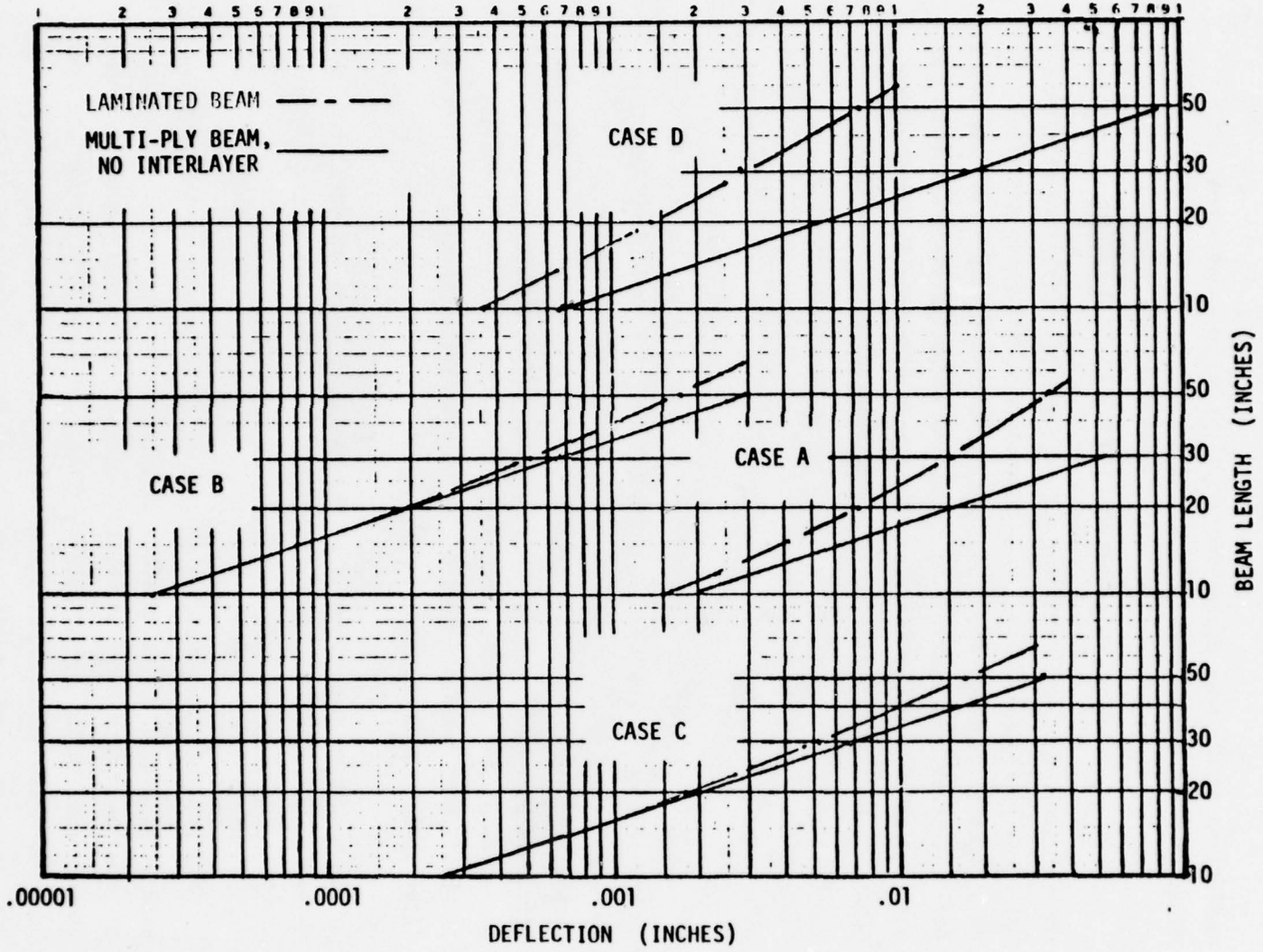

Figure 40. Deflection Versus Beam Length. (Reference 11)

deflection at the beam centerline using the formula for a beam with fixed ends and a center point load which is:

$$EI(EFF) = \frac{FL^3}{192V} \qquad (2)$$

where F is load, L is length and V is deflection. Effective stiffness varies with length. Table 9 is a comparison of effective stiffness, at various lengths for the four cases, to the stiffness if all the plies acted as individual beams. The reason why effective stiffness increases with length is that the interlayers are more effective in transferring shear between structural plies, as length increases. Thus, the behavior of the longer beams approaches monolithic. Figure 41 shows a plot of the effective stiffness for the B-1 configuration (Case C) as a function of length.

The analysis and computer program presented by the methods of Reference 11 were developed to provide a tool for evaluating laminated combinations of transparent materials during initial design of windshields and windows. Historically, formulas and theories from engineering handbooks have been used for this purpose, but these methods are highly approximate, for the most part. Application of "handbook" formulas, as modified by considerations of "effective stiffness" will be discussed later in this section.

It should be appreciated that the laminated beams analyzed per Reference 11 could represent a strip cut from a typical aircraft windshield transparency remote from bulkhead supports.

The primary characteristic of such a laminated beam is the relative ease of structural plies to slide past each other because of the softness of interlayer materials. Also, this method has a solid theoretical base because equilibrium and compatibility equations are written for the beam, based upon assumptions that preserve the important features of laminated beam behavior. The resulting set of differential equations is solved exactly.

TABLE 9. EFFECTIVE STIFFNESS (POUNDS-INCHES SQUARE)

	OUTPUT FROM PROGRAM				SINGLE ACTING BEAMS (NO INTERLAYER)
LENGTH OF BEAM - (INCHES)	10	20	30	50	
CASE A					
4-Ply Polycarbonate	3,397	5,683	9,238	19,212	2,600
CASE B					
2-Ply Glass	217,500	237,900	270,600	366,000	209,100
CASE C					
1-Ply Polycarbonate	20,700	23,450	27,500	37,900	19,720
CASE D					
2-Ply Polycarbonate	14,326	29,370	48,175	89,080	7,900

(Reference 11)

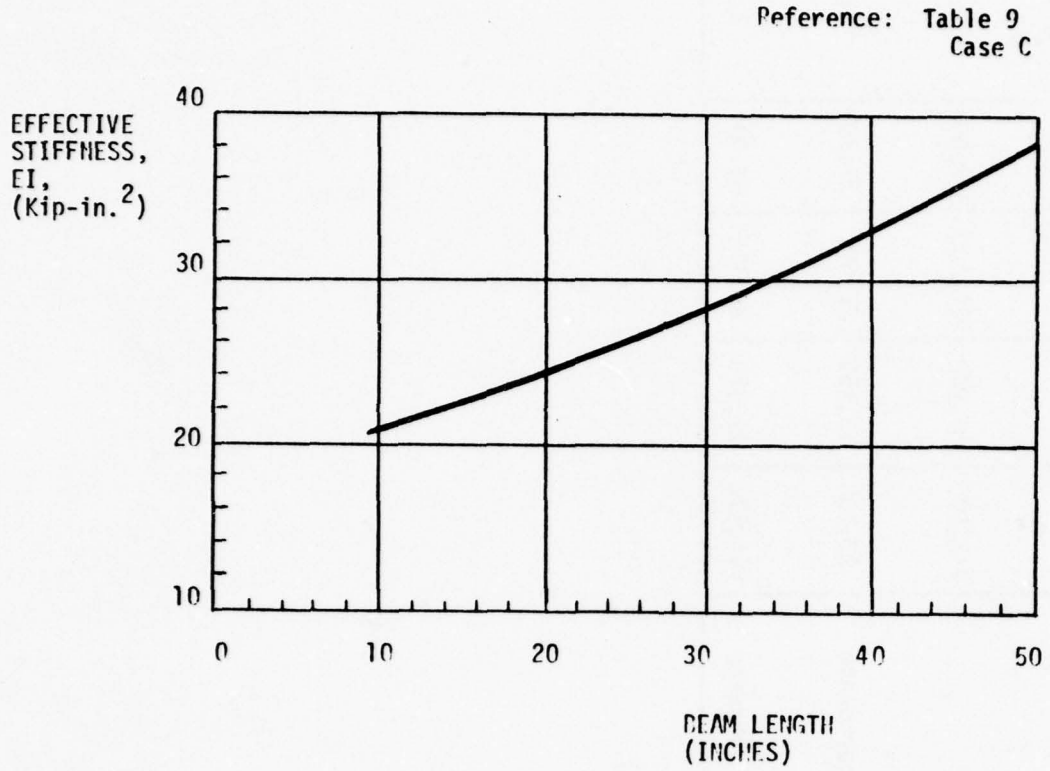

Figure 41. Effective Stiffness as a Function of Beam Length - B-1 Configuration Beams.

Flat Plate Deflection Analyses

For relative ease in arriving at pertinent preliminary design parameters, utilization of published "handbook" formulas would be desirable. This subsection presents analyses utilizing "handbook" flat plate formulas, and presents data indicating their suitability for preliminary design purposes. A comparison of the "handbook" approach with test values is made.

Flat Plate Analyses - Pressure Loading

Table 10 presents analyses that were performed on a windshield of typical construction (2-ply glass per Figure 5) utilizing "handbook" flat plate techniques. Formulas and coefficients from Roark (Reference 12, Article 59) were used which account for bending as well as in-plane tension. The analysis in Table 10 is shown in two parts. Part A shows a typical handbook approach: the structural plies are assumed to act separately with each ply supporting half the pressure. Part B shows a more realistic approach: the structural plies are assumed to act together through a consideration of interlayer effectiveness. An equivalent thickness is thus obtained. This thickness is the thickness of a single ply which acts the same as the laminated panel. The total pressure is then applied to the effective panel as shown.

The analyses shown consider both pinned-edges and fixed-edges for comparison purposes. The value of deflection for Case B-2, Table 10 is in close agreement with the finite element model deflection for this configuration as discussed on page 100 and shown as follows:

HANDBOOK ANALYSIS DEFLECTION (CASE B-2, TABLE 10)	FINITE-ELEMENT MODEL DEFLECTION (2-PLY GLASS CASE, TABLE 3)	% DIFFERENCE
0.086 in.	0.078 in.	9%

Such close correlation as this tends to lend credence to "handbook" analyses of laminated transparent panels, providing all parameters are truly representative.

TABLE 10. DEFLECTIONS AND STRESS FOR B-1 TYPE WINDSHIELD USING FORMULAS FOR FLAT PLATES UNDER UNIFORM LOAD

A. Handbook Analysis (Reference 12, Article 59)

Structural plies act separately.

No interlayer shear assumed.

Material: 2-ply glass, t = .50 in. per ply (Ref. Figure 5).

Modulus of elasticity: $E = 10 \times 10^6$ PSI.

Panel load: 10.6 PSI (total uniform pressure on 2-plies);

$$W = \frac{10.6}{2} = 5.3 \text{ PSI per ply.}$$

Average panel width: b = 33 inches.

Handbook length-to-width increment: 1.5 (actual is 1.8).

Handbook value for Poissons ratio: .316 (actual is .25).

Handbook values:

a/b \ $\frac{wb^4}{Et^4}$	12.5
1.5 (Edges Pinned)	$K_2 = .625$ $K_3 = 4.48$
1.5 (Edges Fixed)	$K_2 = .28$ $K_3 = 5.75$

Case A-1 - Edges Pinned:

The above handbook coefficients must be adjusted to account for a lesser value for wb^4/Et^4:

$$\bar{K}_1 = \frac{wb^4}{Et^4} = \frac{5.3\ (33)^4}{10^7\ (.5)^4} = 10.06$$

$$\bar{K}_2 = \frac{\bar{K}_1}{K_1} K_2 = \frac{10.06}{12.5} (.625) = .503$$

$$\bar{K}_3 = \frac{\bar{K}_1}{K_1} K_3 = \frac{10.06}{12.5} (4.48) = 3.606$$

TABLE 10. (continued)

Deflection, $y = \bar{K}_2 t = .503\ (0.50) = 0.252$ in.

Stress, $S = \bar{K}_3 \frac{Et^2}{b^2} = 3.606 \frac{10^7\ (.50)^2}{(33)^2} = 8294$ PSI (at panel center)

Case A-2 - Edges Fixed:

$\bar{K}_1 = 10.06$, $\bar{K}_2 = \frac{10.6}{12.5}\ (.28) = 0.225$, $\bar{K}_3 = \frac{10.6}{12.5}\ (5.75) = 4.63$

Deflection, $y = \bar{K}_2 t = .225\ (.50) = 0.113$ in.

Stress, $S = \bar{K}_3 \frac{Et^2}{b^2} = 4.63 \frac{10^7\ (.50)^2}{(33)^2} = 10{,}623$ PSI (at center of long sides)

B. Handbook Analysis (Reference 12, Article 59)

Structural plies act together.
Interlayer shear is effective.
Same conditions as Part A, and same panel (Figure 5), except effective stiffness considerations, Table 9, are used to calculate an equivalent thickness. The total pressure (w - 10.6 PSI) acts on this equivalent thickness.

Equivalent thickness:

$EI = 270{,}600$ lb-in^2 (Table 9, Case B, length = 30")

$$t = \left[\frac{270{,}600 \times 12}{10^7}\right]^{1/3} = 0.687 \text{ inch}$$

Case B-1 - Edges Pinned:

$$\bar{K}_1 = \frac{wb^4}{Et^4} = \frac{10.6\ (33)^4}{10^7\ (.687)^4} = 5.64$$

$$\bar{K}_2 = \frac{5.64}{12.5}\ (.625) = 0.28, \quad \bar{K}_3 = \frac{5.64}{12.5}\ (4.48) = 2.02$$

Deflection, $y = .28\ (.687) = 0.192$ inch

Stress, $S = 2.02 \frac{10^7\ (.687)^2}{33^2} = 8754$ PSI

TABLE 10. (continued)

Case B-2 - Edges Fixed:

$\overline{K}_1 = 5.64$, $\overline{K}_2 = \frac{5.64}{12.5}(.28) = .126$, $\overline{K}_3 = \frac{5.64}{12.5}(5.75) = 2.59$

Deflection, $y = .126\ (.687) = .086$ inch

Stress, $S = 2.59\ \frac{10^7\ (.687)^2}{33^2} = 11{,}255$ PSI

Flat Plate Analyses - Central Static and Bird Impact Loading

This subsection will present methods and techniques which indicate that the B-1 bird impact problem can be solved utilizing "handbook" techniques, coupled with test results.

When considering the preliminary design of windshield panels for bird impact, the actual width of the panel is a critical factor. It is difficult to arrive at a correct value for this width without supporting test data. From a typical B-1 windshield static load and bird impact test, BM006 (Reference 2), deflection measurements were taken with deflectometers for the former test and photographically for the latter test. These deflections were plotted and are shown in Figure 42 as a function of location. By extrapolating the deflection curve to the position of zero-deflection, the windshield effective panel size is determined. Table 11 presents these effective panel sizes for the static load case, and for the bird impact case. Note that the "effective panel" has that size which allows it to behave analytically as does the entire windshield under test.

Before flat plate formulas can be utilized in these cases, realistic values for the loads must be obtained. In our case of the 2500 pound static load on the B-1 windshield, the load is already determined, and a flat plate formula is utilized as shown in Table 12, Part A, to arrive at the required deflection calculation. However, the determination of a bird impact load has been nebulous at best. Utilizing bird impact equations such as Equation (1), page 84, results in the following calculation for a static bird impact force:

$$F = 0.0558\, w_b^{2/3}\, V^2 \sin\theta$$

where the terms are as defined on page 84. Hence,

$$F = 0.0558\, (4)^{2/3}\, (953)^2 \sin 25^\circ = 53{,}969 \text{ lbs.}$$

This is too high a force for impacts on typically compliant structure, as will be shown below.

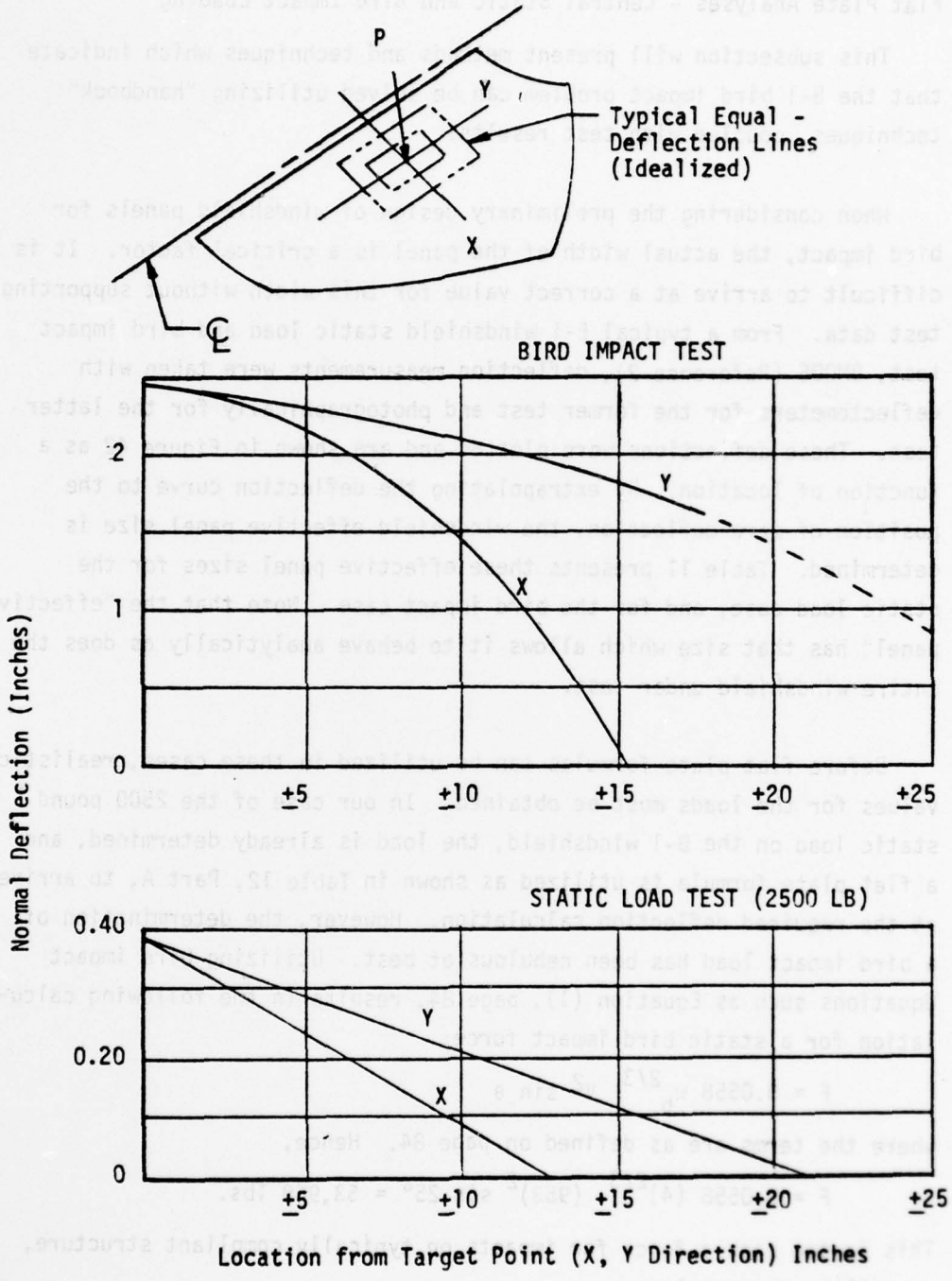

Figure 42. B-1 Windshield Deflection, Test Number BM006.

TABLE 11. B-1 WINDSHIELD EFFECTIVE PANEL SIZE, STATIC LOAD AND BIRD IMPACT LOAD

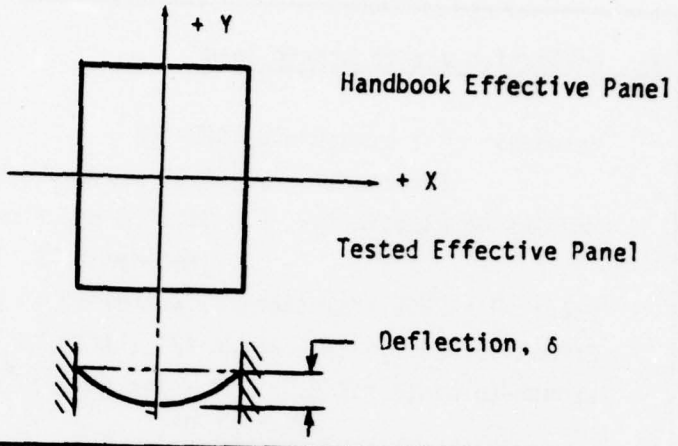

TEST	LOCATION OF $\delta = 0$*		EFFECTIVE PANEL SIZE**	
	±x	±y	b (= 2x)	a (= 2Y)
BM006, Static Load	13	21	26	42
BM006, Bird Impact	15 1/4	30	30 1/2	60

NOTES: * Reference Figure 42.

** Effective panel size is determined by the location of the zero-deflection line.

TABLE 12. DEFLECTION FOR B-1 WINDSHIELD USING FORMULAS FOR FLAT PLATES WITH CONCENTRATED LOAD

A. Deflection due to static load

Material: B-1 windshield, SWU-107

Structural ply = 0.87 polycarbonate

Modulus of Elasticity: E = 350,000 psi (low strain-rate value)

(Reference 13, Table 13)

Load: P = 2500 lbs. statically applied at center.

Effective Panel Size: 26" x 42" (Refer to Table 11)

Length-to-width ratio: 1.62 (size ratio)

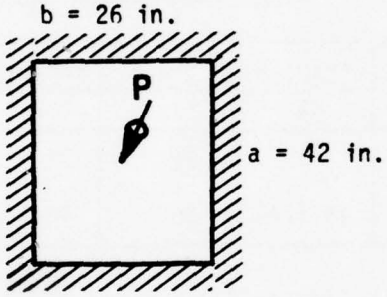

Equivalent thickness:

EI = 26,500 (Reference Figure 41 for length = 26 inches)

$$t = \left[\frac{26{,}500 \times 12}{350{,}000}\right]^{1/3} = 0.968 \text{ inches}$$

Deflection:

$$y = \alpha \frac{Pb^2}{Et^3}$$ (Reference 12, Table 10, Case 42)

where $\alpha = 0.0773$, based on size ratio, a/b = 1.62

P = 2500 pound, static load from B-1 test no. BM1006

TABLE 12. DEFLECTION FOR B-1 WINDSHIELD USING FORMULAS FOR FLAT PLATES WITH CONCENTRATED LOAD (Continued)

hence $y = 0.0778 \left[\frac{(2500)\ (26)^2}{(350 \times 10^3)\ (.968)^3} \right]$

$= 0.41$ inches

B. Deflection due to bird impact

Material: B-1 windshield, SWU-107

Structural ply = 0.87 polycarbonate

Modulus of Elasticity: E = 384,00 psi (high strain-rate value)
(Reference 13, Table 22)

Load: P = 11,000 pounds (Equivalent static load from 4 pound bird impact on target with spring-rate K = 9124 pound/inch.)
Refer to Figure 58 on page 151.

Effective Panel Size: 30 1/2" x 60" (refer to Table 12)

Length-to-width ratio: 1.98

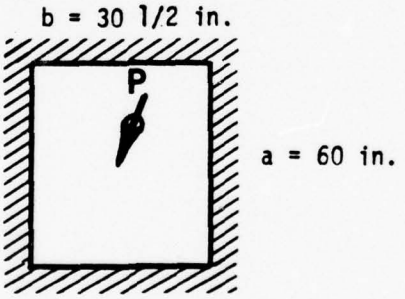

Equivalent thickness:

EI = 27,500 (Reference Figure 41 for length = 30 1/2 inches)

$t = \left[\frac{25,500 \times 12}{384,000} \right]^{1/3} = 0.95$ inches

Deflection:

$y = \alpha \frac{Pb^2}{Et^3}$ (Reference 12, Table 10, Case 42)

TABLE 12. DEFLECTION FOR B-1 WINDSHIELD USING FORMULAS FOR FLAT PLATES WITH CONCENTRATED LOAD (Continued)

where $\alpha = .079$, based on size ratio, $a/b = 2$

hence $$y = .079\left[\frac{(11{,}000)\ (30.5)^2}{(384 \times 10^3)\ (.95)^3}\right] = 2.46 \text{ inches}$$

To alleviate impact force conservatism, a method for determining a static bird impact force equivalent to the dynamic force would be highly desirable. Such a method should consider the compliance of the windshield and supporting structure to be most effective. An analytical study is presented in Section VI, which describes a method for obtaining an equivalent static load on an aircraft windshield system subjected to a bird impact and evaluates the effects on this load due to the relative stiffness of the impact area. Hence, for a bird impact on the B-1 windshield (Test number BM006, Reference 2) which has an effective stiffness at the point of impact equal to 9124 pound/inch (refer to Figure 37, and Equation 29), the equivalent static load from Figure 58 on page 150 is 11,000 pounds. This force is 19 percent of the force calculated using Equation (1) on page 34. Justification for the method which generated this lower, and more realistic load is contained in Section VI. Table 12, Part B, calculates the deflection due to bird impact on a given panel utilizing flat plate formula.

The "Flat Plate" deflections calculated are listed below and compared with actual as-tested B-1 windshield deflections:

LOAD CONDITION	CALCULATED B-1 WINDSHIELD DEFLECTION	TESTED B-1 WINDSHIELD* DEFLECTION	% ERROR
Static Load	.41"	.38"	+8%
Bird-Impact	2.46"	2.42"	+2%

*Reference 2, Test BM006.

Thus it is seen that handbook-type preliminary design values for laminated panels may be quite accurate if the input parameters, such as stiffness, effective thickness, and load, are truly representative.

In addition, the close agreement of bird impact test-versus-analysis deflections lends credence to the validity of the equivalent static force method presented in Section VI.

Math Model Computer Program

This subsection briefly describes a Douglas-developed bird impact dynamic math model computer program and presents applications that have been accomplished to support the alternate B-1 windshield design. This work was accomplished employing a preliminary version of the Math Model computer program ("IMPACT"). This preliminary analysis is described in Volume 1 of Reference 14 and in this section. The Math Model computer program, as finally submitted, is documented in Reference 15.

Part 1 of Reference 15 describes the theoretical basis of the program, as completed, and presents applications to classical problems and actual windshield systems. The approach is based upon a finite element model of the multilayered transparency and supporting structure, subjected to time-varying loads representing bird impact. The equation of motion for the model is derived, considering geometric and material nonlinearities. The approach to geometric nonlinearities is based upon the method of fictitious forces and deformations. The approach to material nonlinearities is based on the Von Mises yield criterion, and the Pandtl-Reuss equation. The scope of the computing effort is minimized by introducing a modal transformation. The transformed nonlinear differential equation of motion is solved incrementally in time and iteratively within each time step. Calculated results produced by the program are shown to correlate accurately with exact solutions for simple dynamically loaded structures that exhibit large geometrically nonlinear effects.

Part 2 of the report is a "User's Manual", and Part 3 is a "Programming Manual."

Since the use of the Math Model is not generally considered to be a preliminary design method, the applications in this section are included to illustrate its demonstrated partial utility. As discussed in Section I of Reference 15, this computer program is not fully operational for all types of transparency design. However, its usage for laminated transparent

panels of the simulated aircraft windshield general shape is shown in this section.

Math Model Applications

Applications of the Math Model technique pertaining to the modeling and/or analyses of the B-1 windshield, and curved-and-flat-models of the simulated aircraft windshield are presented below. The pertinent test number/s are noted.

These analyses were run concurrently with the testing described in this report. The version of the Math Model computer program utilized was not considered operational and the results thus generated were treated as preliminary.

B-1 Windshield Specimen

The finite element model of the B-1 module is shown in Figure 43. Cross sections of pertinent structure are shown in Figure 44. These figures illustrate some structural complexities which may be adequately represented. A complete analysis of the B-1 windshield was not accomplished due to other program commitments.

Simulated Aircraft Windshield Specimen, Curved Model

Figure 45 shows a finite element of a laminated glass specimen which has been prepared by the Math Model. The specimen modeled is PPG-002 as tested per test number BM014. The specimen and test are described in Sections II and IV. A model of the affected structure was made which included the transparency and supporting structure. Figure 46 is a cross section of the transparency showing the modeling of the four glass plies and three interlayers.

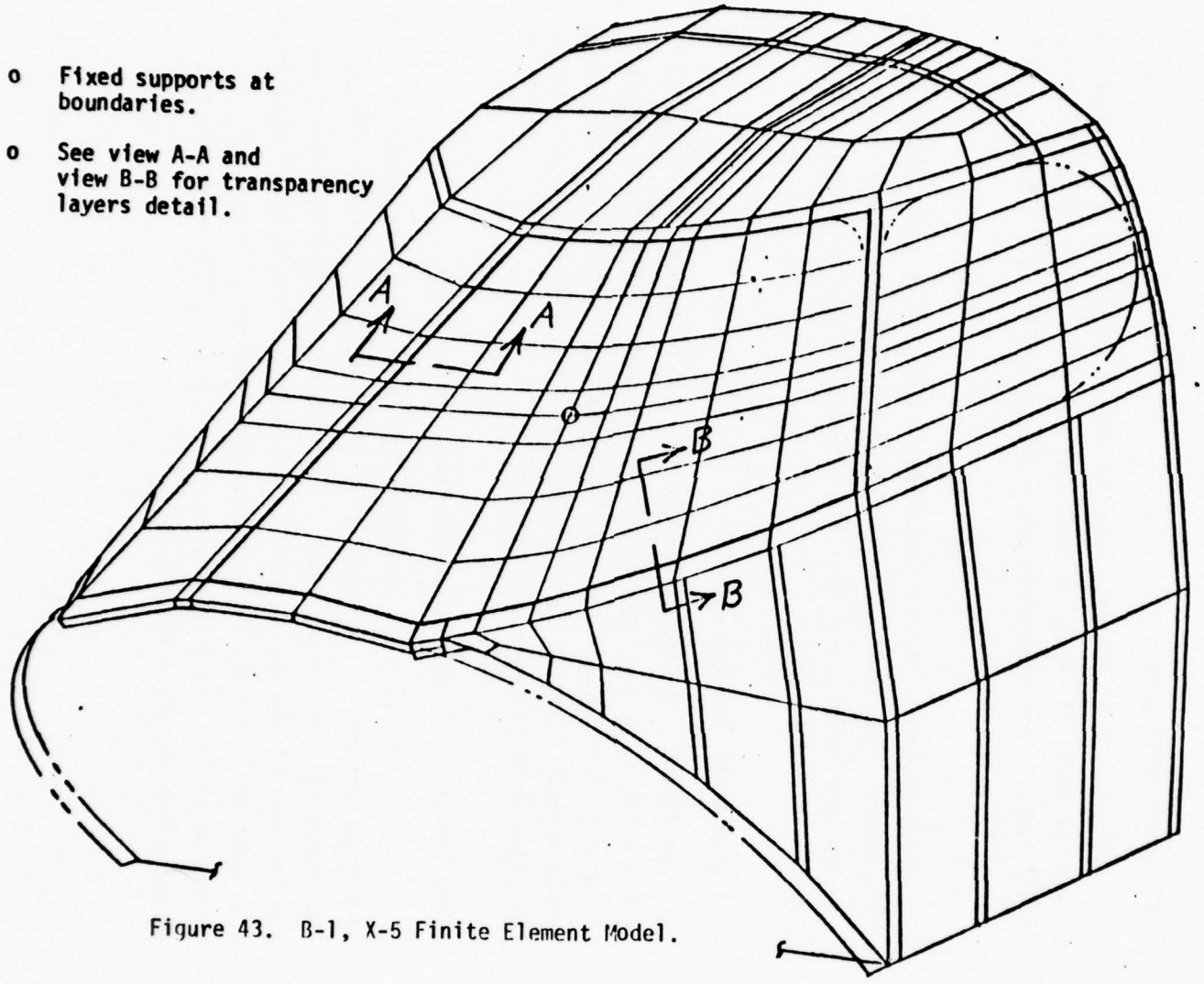

Figure 43. B-1, X-5 Finite Element Model.

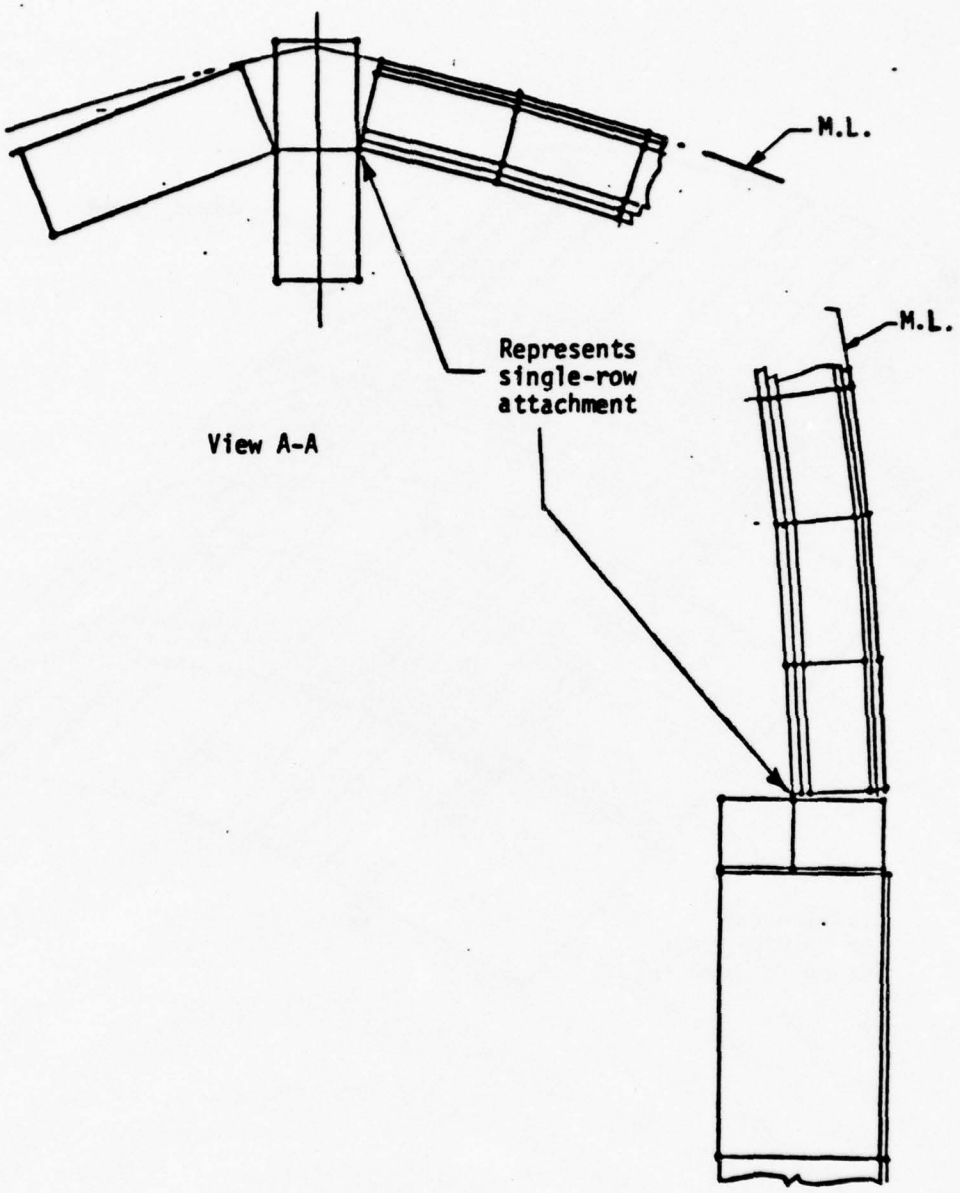

Figure 44. B-1, X-5 Model Cross Sections.

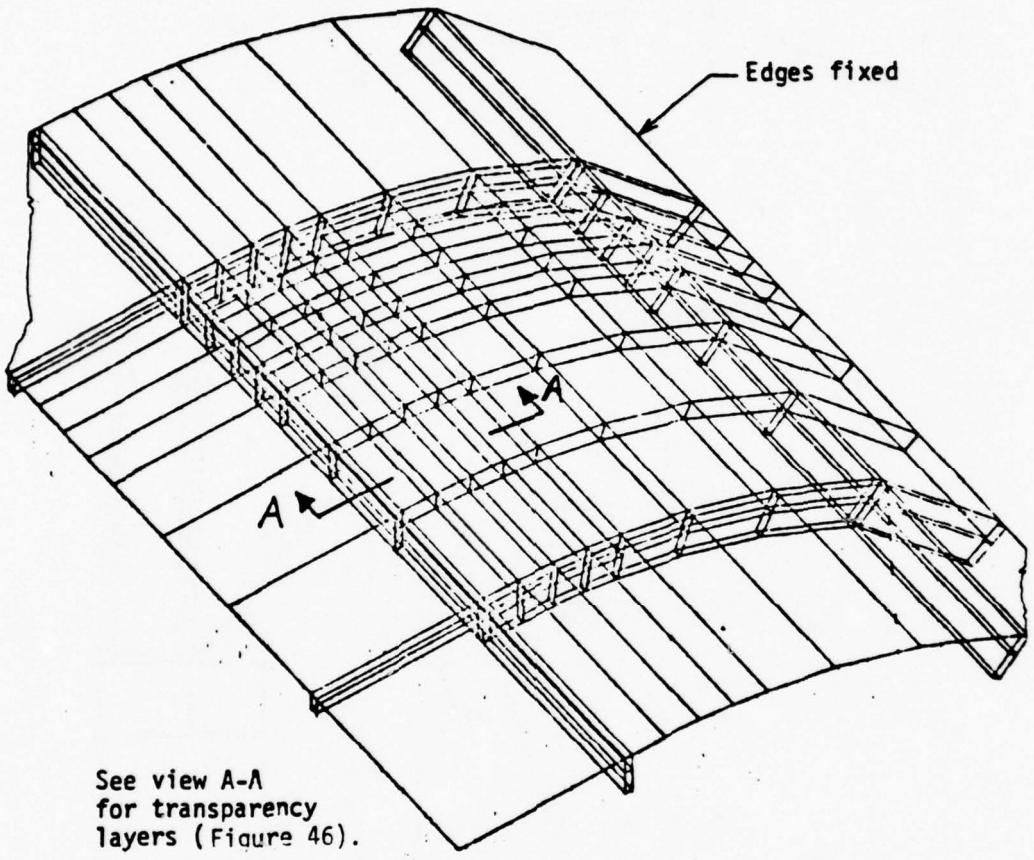

Figure 45. Simulated Aircraft Windshield Specimen Model.

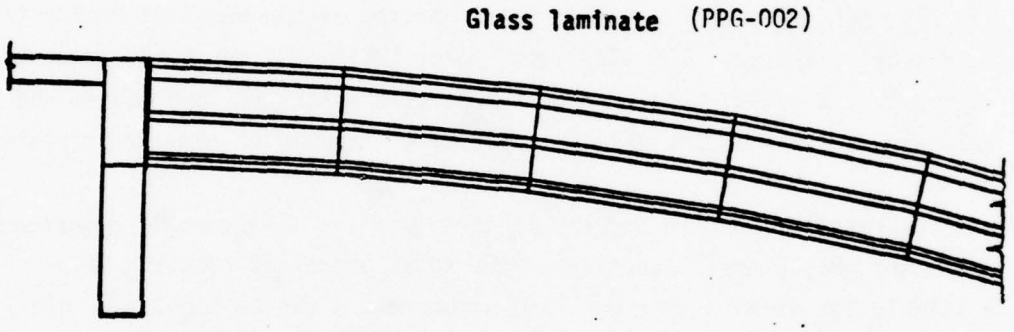

View A-A
(Enlarged)

Figure 46. Simulated Aircraft Windshield Specimen Model Section.

Simulated Aircraft Windshield Specimen, Flat Models

Flat finite element models of the simulated aircraft windshield test specimens were prepared at a time when a preliminary model generator applicable to flat models only was available, and before the final generator applicable to curved models was completed. Figure 47 shows such a model, comprising a transparency and supporting structure. The modeling is done to the same degree of detail as the curved model of Figures 45 and 46. These models were analyzed with the aid of the math model linear analysis option, rectangular pulse load. Applications of the program to Flat Model numbers 2 and 3 are as follows:

Flat Model Number 2 - A flat panel version of the model of Figure 47 representing specimen PPG-002 (test number BM014), as described in Section II and IV, is called Model number 2. The bird weight is four pounds and bird velocity is 939 fps. Material properties correspond to room temperature.

The results shown in Figures 48 through 52 as subsequently described, represent only a small fraction of the total amount of computed data available for Model number 2. This demonstrates the methodologies which were utilized in this design effort.

Figure 48 shows displacement for Model number 2. The figure shows how a wave traverses the panel, starting at the point of impact at time t = 0.002 second after first contact. The wave travels diagonally across the panel, and reaches the opposite corner at t = 0.008 second. The displacements shown correlate with test results as well as can be determined from available test data.

Figure 49 shows time histories of the total load and displacements at selected points. The total load is 18,719 pounds applied as a rectangular pulse for 0.00208 second. This load is distributed to four nodes of the model adjacent to the center of impact. The displacement near the center of impact reaches a maximum at approximately the end of the load pulse, and then damps out in a sinusoidal manner. The presence of at least two vibration modes can be observed. The displacement at the panel center and

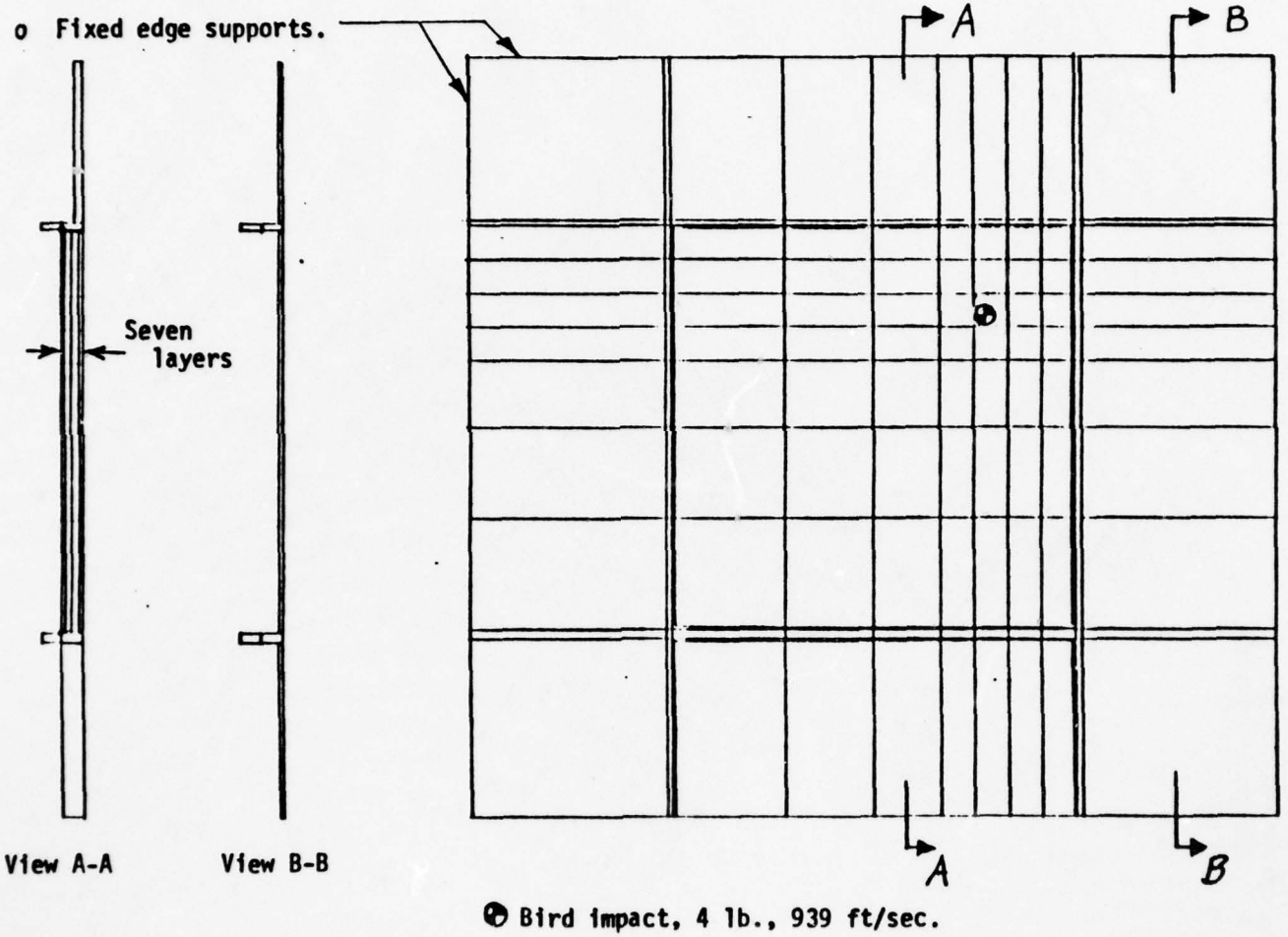

Figure 47. Simulated Aircraft Windshield Flat Model, Model Number 2.

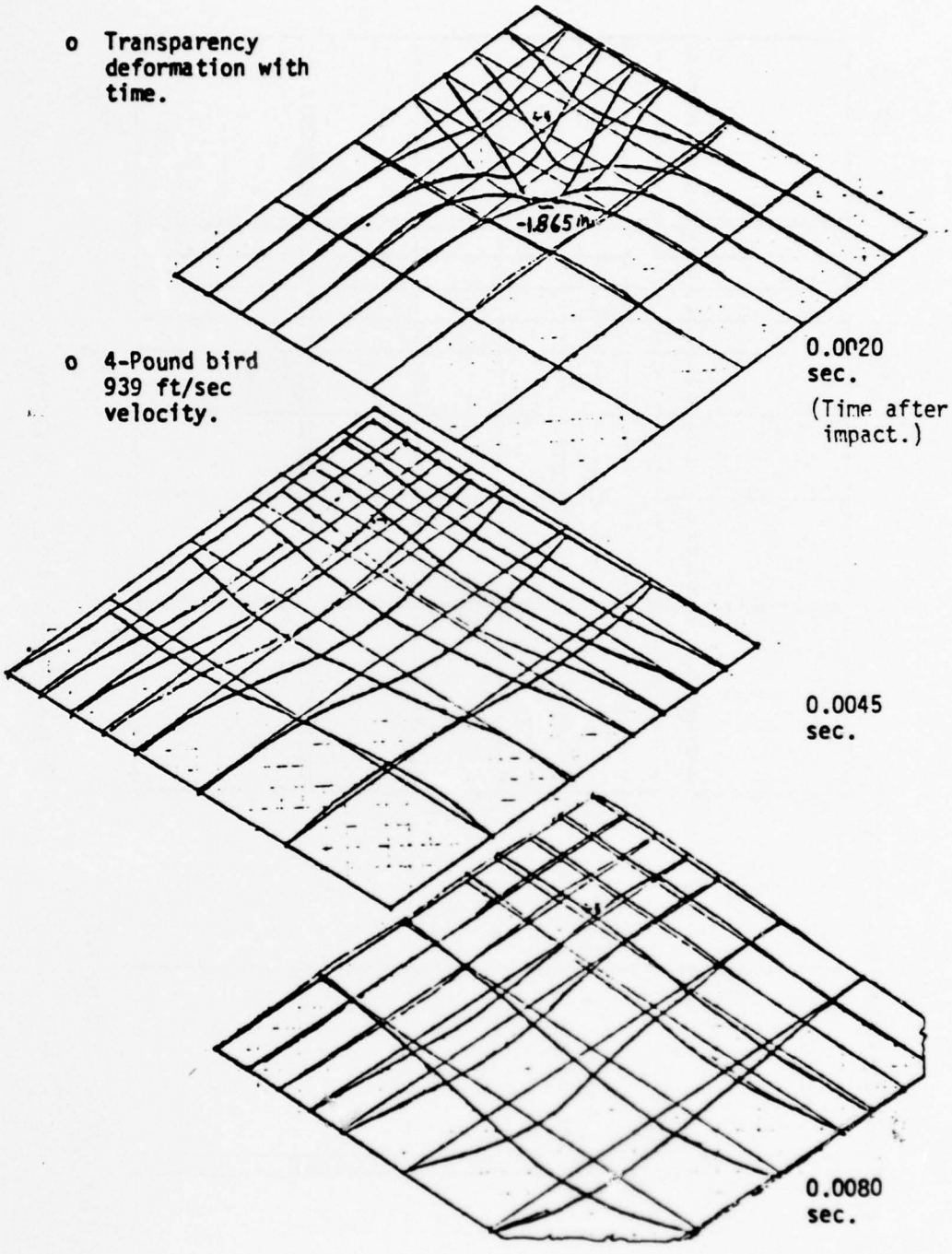

Figure 48. Displacements After Impact, Simulated Aircraft Windshield Specimen Flat Model, Model Number 2.

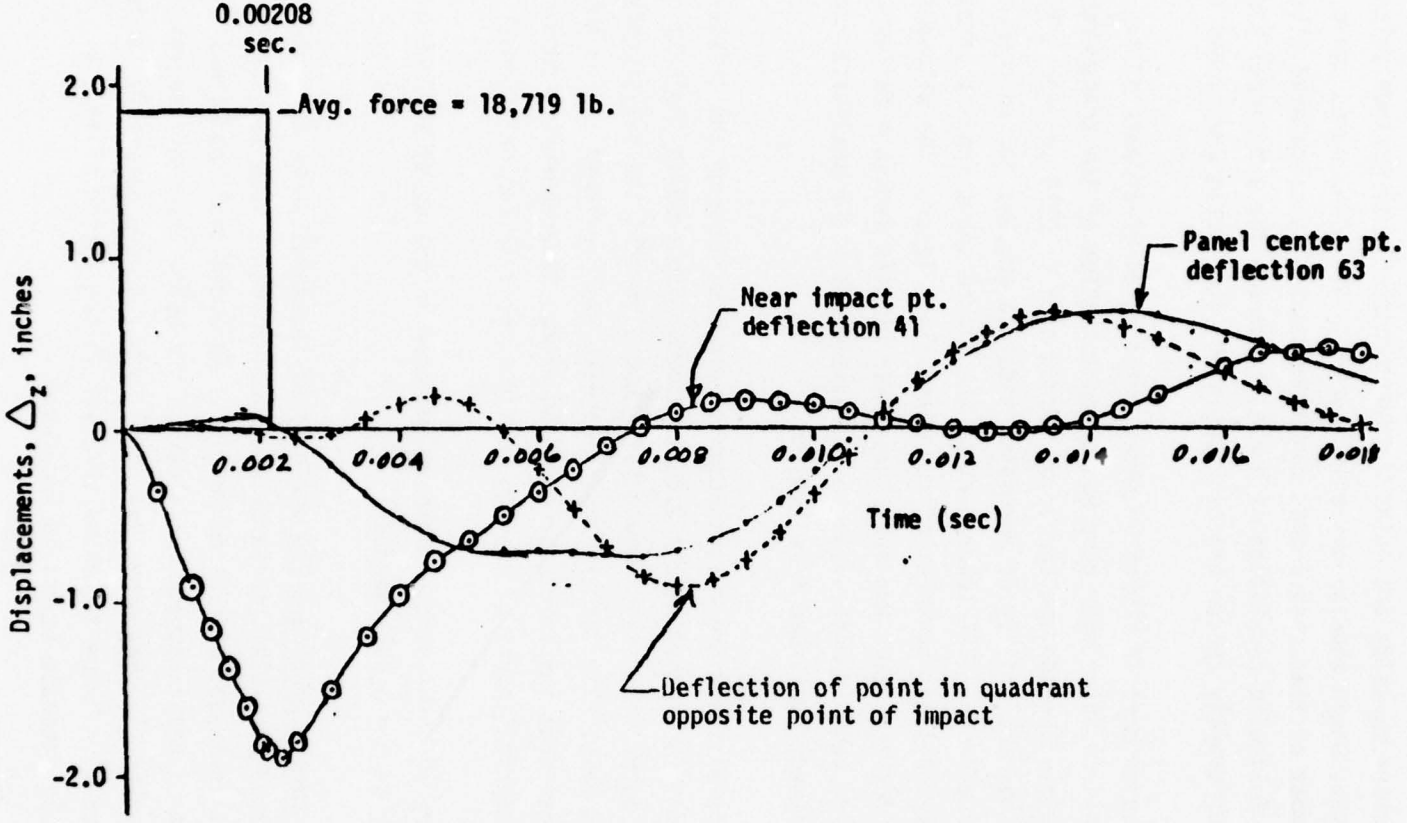

Figure 49. Load and Displacement as Function of Time, Simulated Aircraft Windshield Flat Model, Model Number 2.

at the corner opposite the point of impact reach lower maximum values at later times, again showing the existence of a traveling wave. Note the large number of time points that can be economically calculated with this option. Following completion of a run, responses for additional time points arbitrarily chosen can be calculated with little additional expense.

The upper part of Figure 50 shows relative displacements of the layers resulting from interlayer compression on a section of the transparency approximately through the center of impact at t = .0024 seconds. These results show the ability of the match model to account for through-the-thickness effects. The lower part of the figure shows bending stresses in the upper and lower surfaces of the outer glass layer. The allowable stresses for the glass are such that these results indicate failure of the layer. The test (BM014), which was conducted after the analytical results were obtained, confirmed this finding.

Figure 51 shows the distribution of stresses through the thickness of the vicinity of impact at t = 0.0021 second. The results indicate not only that the outer glass layer would fail, but also that the polycarbonate layers would not fail. The latter prediction also was confirmed in the subsequent test. Note that the layers are bending almost independently, showing that the engineering theory of bending does not apply to laminate construction.

Figure 52 shows stress contours computed in the upper surface of the glass ply at t = 0.0021 second.

Flat Model Number 3 - The analysis of the model shown in Figure 47 was repeated with CIP interlayer material, which is much less stiff than the PPG interlayer material of Model 2. An additional change was the substitution of polycarbonate for glass as the outer layer of the revised model (number 3). Responses for Model number 3 were generally larger than for number 2. Figure 53 shows stresses in the region of impact. Failure of the polycarbonate layers is indicated.

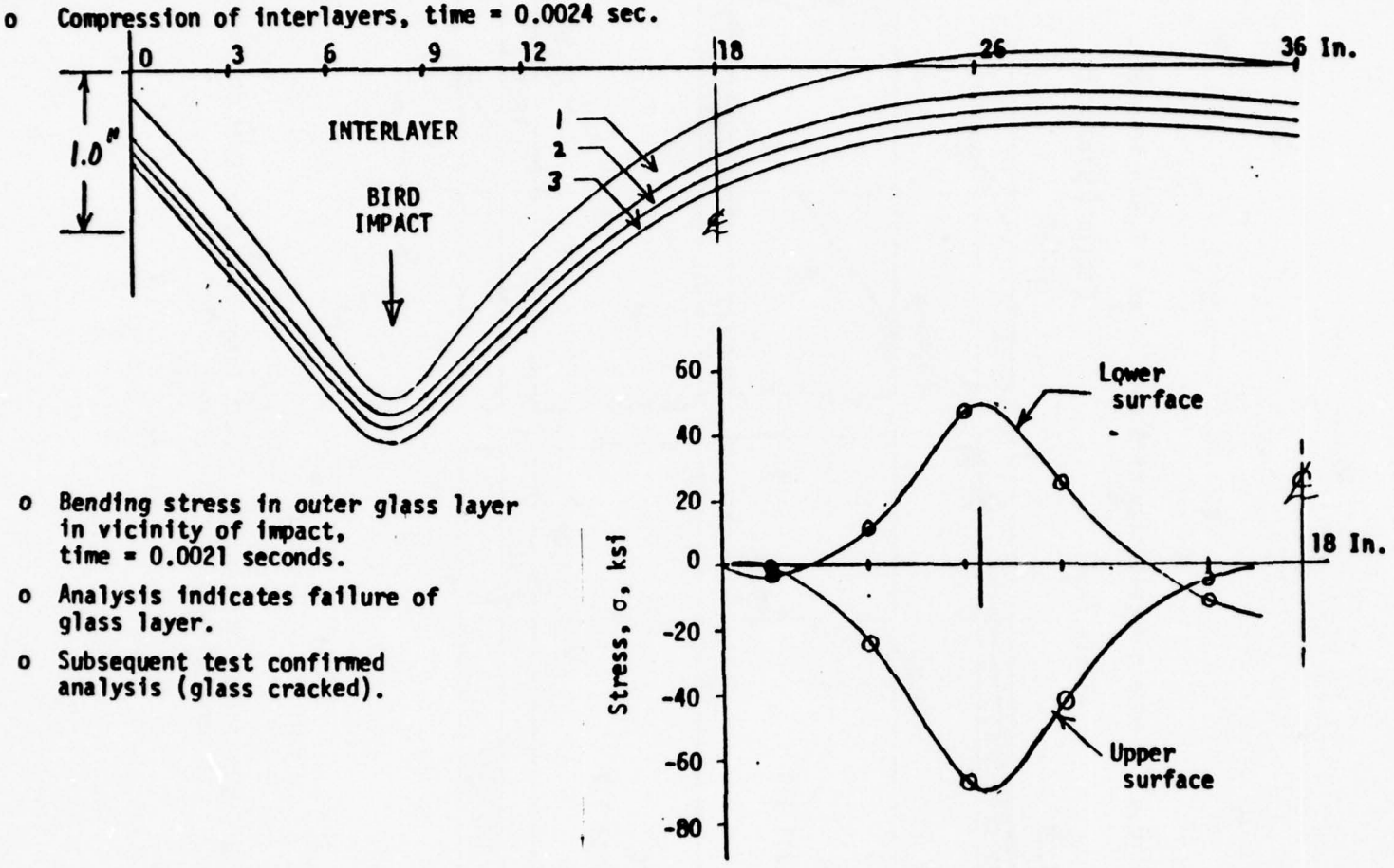

Figure 50. Interlayer Compression and Bending Stresses Simulated Aircraft Windshield Flat Model, Model Number 2.

o Stress and strain in vicinity of impact, time = 0.0021 seconds.

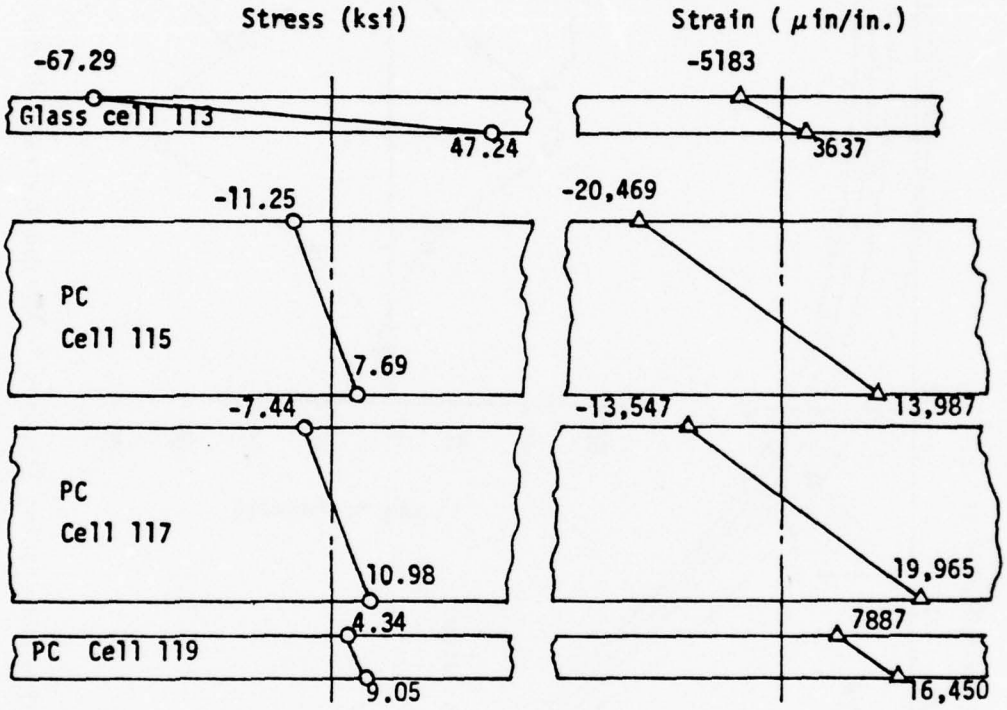

Figure 51. Stress Distribution Across Thickness, Simulated Aircraft Windshield Flat Model, Model Number 2.

o Stress contour, glass, upper surface, time = 0.0021 seconds.

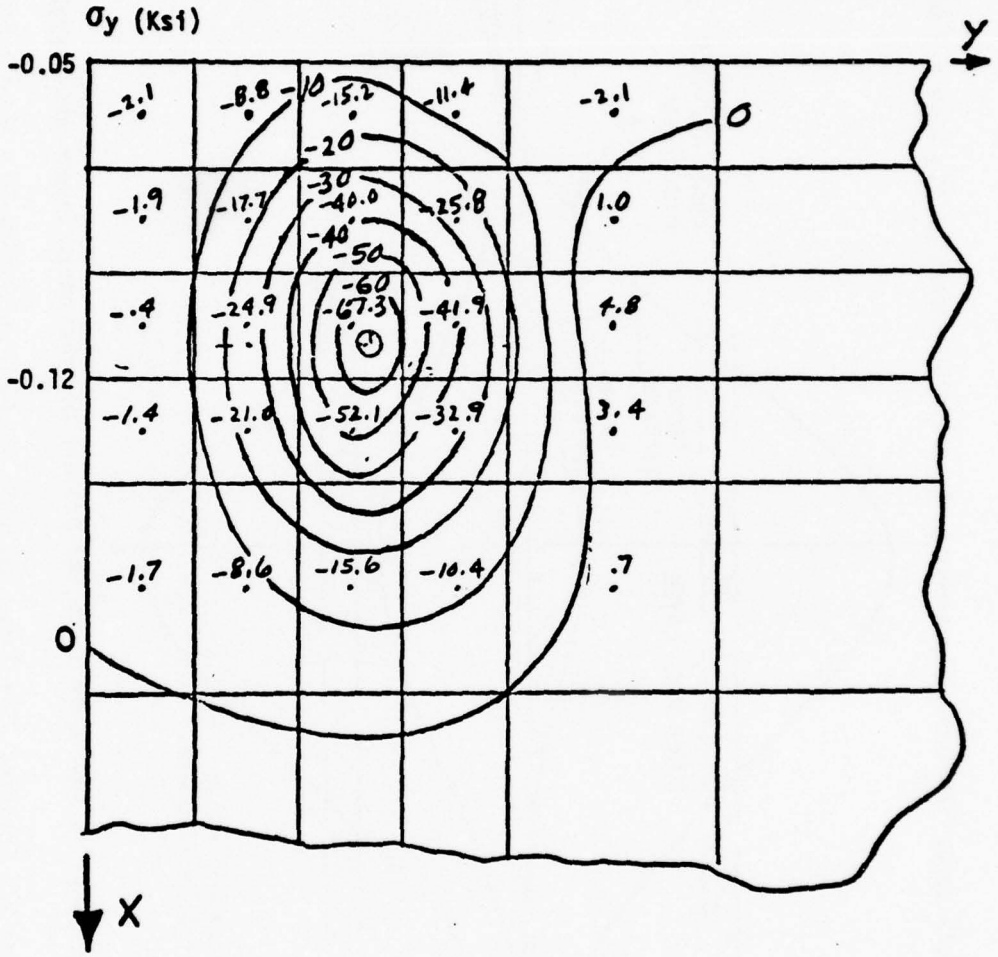

Figure 52. Stress Contour, Simulated Aircraft Windshield Flat Model, Model Number 2.

o Stress in outer and upper 1/2-inch polycarbonate layers near impact point; time = 0.0026 seconds.

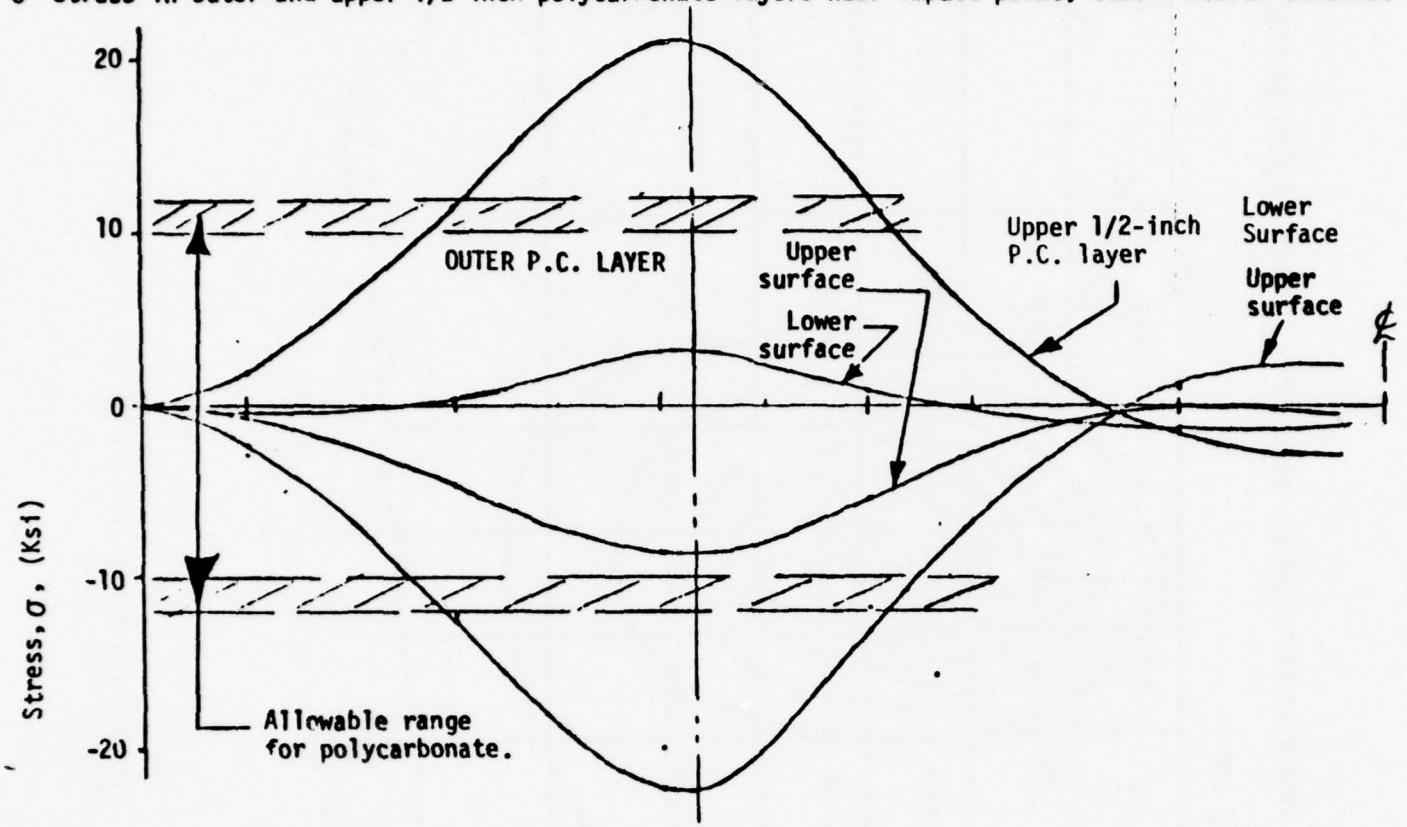

o Failure of transparency is indicated since the primary polycarbonate layers are overstressed.

Figure 53. Critical Ply Stresses, Simulated Aircraft Windshield Flat Model, Model Number 3.

SECTION VI
WINDSHIELD SYSTEM BIRD IMPACT STUDY

This section presents a method for analytically determining a static load on the B-1 aircraft windshield equivalent to the actual dynamic load of a bird impact. This method evaluates the effects on this load due to the relative stiffness of the impacted area. Equivalency of the load determined by this method to an actual dynamic load is established by comparing the ensuing windshield responses (displacements) for several actual B-1 tests (page 117). The structural stiffness of both windshield and supporting structure are included.

In the previous section, a method was presented which modeled and analyzed the B-1 windshield by transformation into an equivalent flat plate. An example of flat plate analyses using "handbook" formulas was shown (Table 12). This was accomplished using both an actual static load (used in Test BM006), and a dynamically equivalent static load which was determined using methods of this section.

BACKGROUND

High speed bird impact tests have, in the past, been performed to accomplish either of the following:

1. Provide a basis on which to judge the effectiveness of a particular windshield to defeat the birdstrike. (This has been done, generally, without consideration or duplication of actual aircraft windshield supporting structure.)

2. Provide a means whereby forces or pressures exerted on a target may be determined when subjected to various impact velocities, impact angles, and bird sizes.

As is well known, the effects of impact on structure are less severe when the impacted structure is mounted on relatively flexible supports. However, transparency support structures have been designed most generally by loading conditions which considered aircraft inertia and pressure only. Although bird impact loading is one of the primary parameters for transparency design, it has received only secondary consideration relative to design of support structure, and then only if the support structure failed during bird impact tests of the transparency.

It is generally true that the transparency impact capability is higher when impact is near the center than near any of the support structure. The F-111 windshield system is a good example. In the center it can withstand a four pound bird impact at velocities over 780 knots; however, near the support structure it could only withstand a four pound bird impact below 500 knots (Reference 16). There should be a ready explanation for this decrease in the windshield capability to withstand impact near the support structure. If a plate is loaded statically, the plate stresses are higher when loaded in the center than near the edges. This implies a structural response which is apparently opposite to the observed results of bird impact tests.

These observations coupled with results from a survey of industry-wide bird impact tests show the following:

- The bird penetration velocity is much lower when the impact is near the support structure rather than at the center of the transparency.
- The optimum transparency/support structure system would seem to be one which has the same impact capability at any location on the transparency.

On the basis of these two observations, an analytical approach was developed which would (1) consider bird impact loading on the transparency/support structure system in a manner adaptable with other types of design

loading, and (2) would provide a method whereby the bird impact capability of the transparency could be quantitatively studied when bird impact is adjacent to the support structure. This analytical approach is presented in this section. Though the derivation of the method is generally rigorous, its application is shown based on certain test results from the B-1 windshield bird impact tests.

This bird impact study is an attempt to address the effects of total windshield system compliance on a rather simplistic level which may be conveniently used in the preliminary design phases of windshield systems.

It should be noted that since this is a static approach rather than a dynamic approach, the static effects of inertia and pressure loading may be included in the final analysis. The simplification of the time parameter inherent in a static analysis reduces the complexity of the problem for an initial approach. This leads to economies during these initial design efforts where basic design trade-off analyses should occur. The use of a complex computer program for the dynamic analysis becomes most cost-effective when used in the final stages of design in order to 1) eliminate problem areas that are not readily apparent in a static analysis and 2) to determine the exact capabilities of the prospective final configurations.

It will be demonstrated in this section that in bird impact situations, the immediate structural response is primarily dependent upon the natural frequency of the transparency/support structure system. This natural frequency is a function of both the mass and the stiffness. The transparency unit mass is relatively fixed by available materials and is fairly constant, hence, in the original design phase only the transparency stiffness can be readily varied. Using this static impact method, curves are generated which show the relationship of the equivalent static load to the stiffness of the impacted transparency system.

STRUCTURAL RESPONSE

To ascertain the effects of stiffness on the structural response and force transmission of a windshield system subjected to a disturbing force, a model of the active structural elements involved was made. This is shown in Figure 54, together with the attendant disturbing force, Q(t):

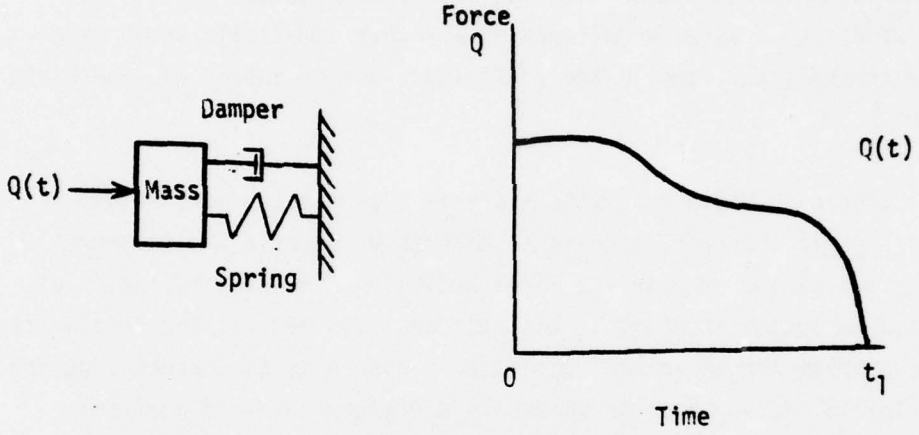

Figure 54. Mass-Spring-Damper System and Arbitrary Disturbing Force.

The equation of motion for such a system is

$$M\ddot{x} + c\dot{x} + Kx = Q(t) \qquad (3)$$

where M = effective mass being moved
c = viscous damping coefficient
K = spring stiffness
x = displacement of mass in x-direction
$\dot{x}$ = velocity of mass in x-direction
$\ddot{x}$ = acceleration of mass in x-direction
Q(t) = arbitrary disturbing force as a function of time, t

To simplify, divide the equation by the mass, M. Hence equation (3) becomes

$$\ddot{x} + \frac{c}{M}\dot{x} + \frac{K}{M}x = \frac{Q(t)}{M} \tag{4}$$

This is again put in a more convenient analytical form by rearranging and redefining terms, thusly:

$$\ddot{x} + 2\zeta\omega_n\dot{x} + \omega_n^2 x = q(t') \tag{5}$$

where ζ = damping ratio = $c/2\sqrt{KM}$

ω_n = natural frequency of system = $\sqrt{K/M}$

q = load per unit mass

t' = dummy time variable

To arrive at a structural response to this system of applied loads, impulse considerations are employed. Whenever two bodies contact and rebound, the change of momentum of either is the value of impulse on the other, whether or not the impact is elastic. Using previously defined terms, the impulse I, in this system is

$$I = M d\dot{x} = \int_0^t Q\, dt'$$

Rearranging and substituting $q = Q/M$, this equation reduces to the following expression:

$$d\dot{x} = \int_0^t q\, dt' \tag{6}$$

This is defined as the incremental impulse and is shown in Figure 55:

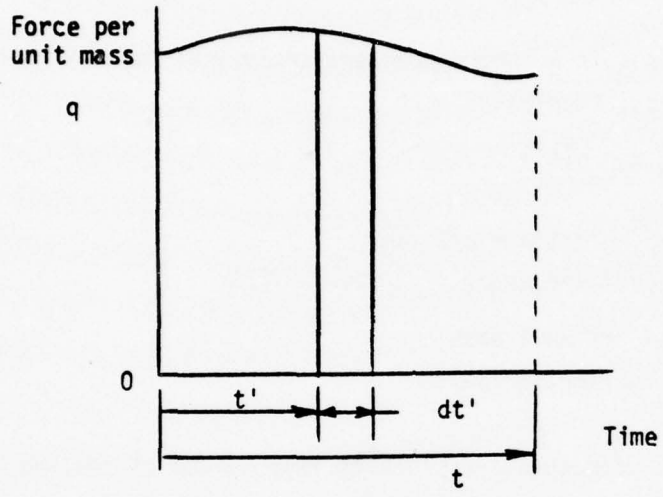

Figure 55. Incremental Impulse.

The solution of the homogeneous portion of Equation (5) is

$$x(t) = e^{-\zeta\omega_n t}(x_o \cos \omega_d t + \dot{x}_o + \zeta\omega_n \; x_o \sin \omega_d t) \qquad (7)$$

where x_o = initial displacement

$\dot{x}_o$ = initial velocity

$\omega_d = \sqrt{1-\zeta^2}\,\omega_n$ = natural frequency-damped

This solution is equivalent to the response in a free-vibration-with-damping system subjected to the above initial displacement and velocity. Under impact conditions, where the time t' is so short that there is virtually no displacement of the spring (refer to Figure 54) then, at time t' = o,

$$x = e^{-\zeta\omega_n t}\left(\frac{\dot{x}_o}{\omega_d}\sin\omega_d t\right) \tag{8}$$

This equation of motion is identical to that in a freely vibrating system with subcritical damping and negligible spring displacement (Reference 22 , Equation (8-46)).

If the increment of velocity is taken as initial velocity at any time t', then the increment of displacement produced by the increment of impulse, q dt', acting (suddenly) at t = t' is

$$dx = e^{-\zeta\omega_n(t-t')}\left(\frac{q\,dt'}{\omega_d}\right)\sin\omega_d(t-t') \tag{9}$$

or in integral form:

$$x(t) = \frac{1}{\omega_d}\int_o^t e^{-\zeta\omega_n(t-t')}\, q\sin\omega_d(t-t')dt' \tag{10}$$

This expression is the total displacement produced by the disturbing force Q acting on the system for a time t = o to t = t. This response is referred to as Duhamels Integral.

The total solution to Equation (5) is obtained by the summation of Equations (7) and (10). This response considers all initial, steady-state, and transient conditions:

$$x(t) = e^{-\zeta\omega_n t}\left(x_o\cos\omega_d t + \dot{x}_o + \zeta\omega_n x_o\sin\omega_d t\right) + \frac{1}{\omega_d}\int_o^t e^{\zeta\omega_n(t-t')}\, q\sin\omega_d(t-t')\,dt' \tag{11}$$

For further equation simplicity, the damping ratio, ζ, is set equal to zero. For purposes of this analysis, this simplification is valid since the amount of damping present in windshield systems composed of state-of-the art laminated transparency materials has been found to be small. (Reference 18). In particular, for a windshield beam of B-1 transparency materials the damping ratio, $\zeta \cong 0.7$ at room temperature. Also, since the period of interest during and subsequent to a bird impact is so short, the amount of windshield damping has negligible effect on response in the period of interest. Hence, Equation (11) reduces to

$$x(t) = x_o \cos \omega_n t + \frac{\dot{x}_o}{\omega_n} \sin \omega_n t + \frac{1}{\omega_n} \int_0^t q \sin \omega_n (t-t') \, dt' \qquad (12)$$

In a problem involving bird impact, we may properly assume the initial displacement, x_o, and the initial velocity, $\dot{x}_o$, of the system are both equal to zero. Hence, Equation (12) reduces to its final form as

$$x(t) = \frac{1}{\omega_n} \int_0^t q \sin \omega_n (t-t') \, dt' \qquad (13)$$

IMPACT LOADING

To find the equivalent static load, S_L, at any time t, Equation (13) representing structural displacement, is multiplied through by the spring stiffness, K. Hence,

$$S_L(t) = Kx(t) = \frac{K}{\omega_n} \int_0^t q \sin \omega_n (t-t') \, dt' \qquad (14)$$

The assumed arbitrary disturbing force, Q, which is representative of bird impact is shown in Figure 56.

Note that for mathematical simplification, a rectangular pulse is used rather than the triangular pulse suggested by the University of Dayton in their bird impact studies of References 19 and 20.

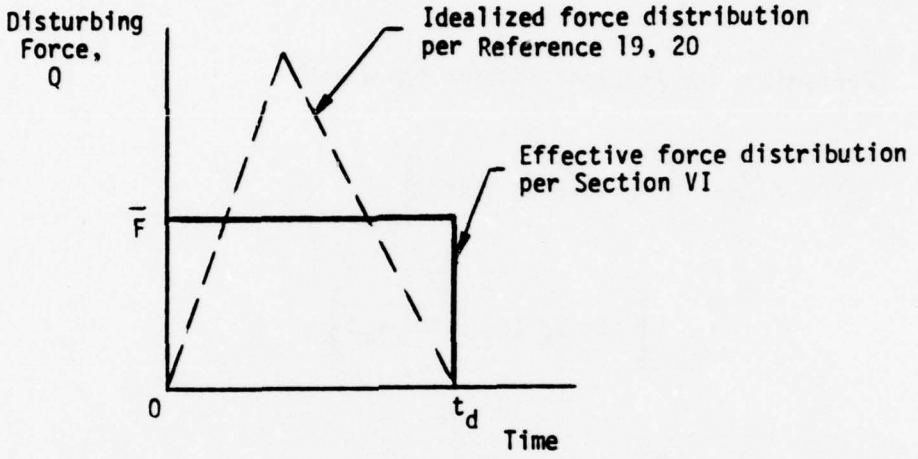

Figure 56. Disturbing Force and Duration for Bird Impact.

This force Q(t) is described as follows:

$$Q(t) = \begin{cases} \bar{F} & , \quad o<t<t_d \\ 0 & , \quad t>t_d \end{cases}$$

where $\bar{F}$ = effective force during period of bird impact
t_d = time duration of bird impact

Now, the force per unit mass, q(t') is then equal to

$$q(t') = \frac{Q(t)}{M} = \begin{cases} \frac{\bar{F}}{M} & , \quad o<t<t_d \quad (15) \\ 0 & , \quad t>t_d \quad (16) \end{cases}$$

where M = effective transparency mass (per definition on page 136).

Now, from Equations (14) and (15), the equation for the static load in the time period from $t' = o$ to $t' = t_d$ is

$$S_L(t) = \frac{K\bar{F}}{M\omega_n} \int_o^t \sin \omega_n (t-t')\, dt', \quad o<t<t_d \tag{17}$$

Performing the required integration gives

$$S_L(t) = \frac{K\bar{F}}{M\omega_n} \left[-\frac{1}{\omega_n} \cos \omega_n (t-t') \right]_o^t$$

$$= \frac{K\bar{F}}{M\omega_n^2} \left[\cos \omega_n (o) - \cos \omega_n t \right]$$

$$= \frac{K\bar{F}}{M\omega_n^2} \left[1 - \cos \omega_n t \right] \tag{18}$$

Since, by definition, $\omega_n^2 = \frac{K}{M}$, then Equation (18) reduces to

$$S_L(t) = \bar{F} (1 - \cos \omega_n t), \quad o<t<t_d \tag{19}$$

The equation for the static load for any time t, greater than t_d is

$$S_L(t) = \frac{K\bar{F}}{M\omega_n} \int_o^{t_d} \sin \omega_n(t-t')dt' + \frac{K(o)}{M\omega_n} \int_{t_d}^t \sin \omega_n(t-t')dt', \quad t_d<t \tag{20}$$

This equation reduces to the following:

$$S_L(t) = \frac{K\bar{F}}{M\omega_n} \left[\frac{1}{\omega_n} \cos \omega_n (t-t') \right]_0^{t_d}$$

$$= \bar{F} \left[\cos \omega_n (t-t_d) - \cos \omega_n t \right] \quad , \quad t_d < t \qquad (21)$$

By using Equations (19) and (21), the University of Dayton bird impact studies, (References 19 and 20) and appropriate empirical data from actual B-1 static and dynamic bird impact testing (reference Section IV), the relationship between stiffness and equivalent static load during bird impact will be presented.

WINDSHIELD SYSTEM IMPACT

The presentation of the relationship between windshield system stiffness and equivalent static load during bird impact follows in this subsection. This method is illustrated through utilization of test data obtained in the B-1 Windshield Bird Impact Tests as described in this volume in Section IV.

Impact Time Duration

It has been determined by test that during a high speed bird impact, the deceleration of the bird is negligible (Reference 19, Section III). The duration of the force-time pulse is equal to the time it takes for the bird to "squash up." This time is, then, the effective bird length divided by its velocity, as follows:

$$t_d = \frac{\bar{L}}{V} \qquad (22)$$

where t_d = time duration of impact (sec)

$\bar{L}$ = effective bird length (ft)

V = bird velocity (ft/sec)

The effective length of the bird, $\bar{L}$, is calculated per the following equation:

$$\bar{L} = (L + D/\tan\theta)/12 \qquad (23)$$

where L = length of bird package (inches)
D = diameter of bird (inches)
θ = impact angle (degrees)

These parameters are as shown in Figure 57:

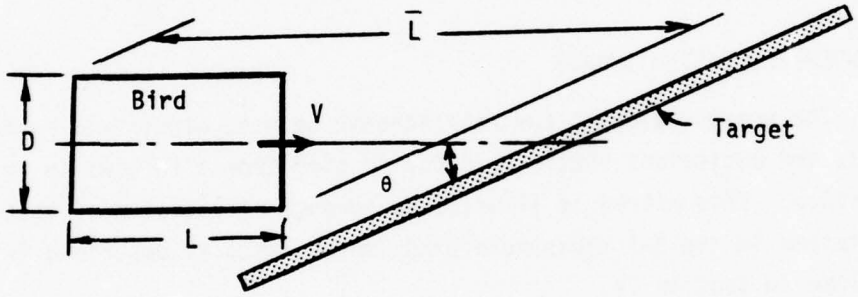

Figure 57. Bird Mass Impact Parameters.

The following data was collected in the B-1 windshield bird impact test number BM006, Reference 2:

V = 967 fps
θ = 21°
W = 4.0 lbs

The length, L, and the diameter, D, of the bird was obtained from representative measurements made in conjunction with bird impact testing

of the DC-10 windshield, Reference 21. These dimensions are L = 8.5 inches, and D = 5.25 inches for a 4.0 lb bird. The effective length, $\bar{L}$, is then calculated from Equation (23) as

$$\bar{L} = (8.5 + 5.25/\tan 21)/12 \quad (24)$$
$$= 1.85 \text{ feet}$$

and, the time duration of impact is calculated from Equation (22):

$$t_d = \frac{\bar{L}}{V} = \frac{1.85}{967} = 0.002 \text{ sec.} \quad (25)$$

Effective Force

The effective force is calculated by the following equation (Reference 20):

$$\bar{F} = \frac{\bar{M}V^2 \sin\theta}{\bar{L}} \quad (26)$$

where $\bar{M}$ = bird mass = bird wt/32.2 ft/sec^2
V = 967 fps
θ = 21°
$\bar{L}$ = 1.85 ft

Therefore

$$\bar{F} = \frac{4}{32.2} \frac{(967)^2 \sin 21°}{1.85} = 22{,}500 \text{ lbs} \quad (27)$$

Effective Spring Stiffness

The effective spring stiffness at a particular point of the transparency system is the ratio of a known applied load at that point to its corresponding deflection. For purposes of this study, the average deflection of the area of impact is utilized.

During test number BM006 of the B-1 windshield bird impact test series, a static load of 2500 pounds was applied normal to the windshield at the center of the bird impact area. Ensuing deflections were read at selected points with appropriate deflectometers. (Refer to Section IV.) The deflections in the bird impact area were: 0.38 inches, 0.28 inches, 0.27 inches, 0.24 inches, 0.20 inches. The effective spring stiffness is expressed mathematically as

$$K = \frac{\bar{P}}{\frac{1}{n}\sum_{i=1}^{n} \delta_i} \tag{28}$$

where $\bar{P}$ = applied load = 2500 pounds

n = number of deflection readings in target area = 5

δ_i = deflection readings, as noted above

Hence, from Equation (28):

$$K = \frac{2500}{\frac{1}{5}(.38 + .28 + .27 + .24 + .20)}$$

$$= 9124 \text{ pound/inch} \tag{29}$$

Effective Transparency Mass

From the graphs of deflection vs. time of B-1 test BM006 (refer to Reference 2, Figure 14), the natural frequency of the transparency is measured to be 40 cycles per second or 251.33 rad/sec. Furthermore, since $\omega_n^2 = K/M$, then the effective transparency mass, M, is

$$M = \frac{K}{\omega_n^2}$$

$$= \frac{9124 \text{ pound/inch}}{(251.33)^2} = 0.144 \frac{\text{pound-second}^2}{\text{inch}} \tag{30}$$

This mass corresponds with the definition on page 136.

Maximum Static Load Versus Windshield System Stiffness

The equivalent static load, S_L, is a load that, when applied statically, will produce the same structural response as occurs dynamically during bird impact at a given time t.

Maximum Static Load, $t<t_d$

The maximum static load, S_{L1}, that can occur in the interval from time, t=o to $t=t_d$ will occur at $t=t_d$, providing that the period of structural response is such that $\omega_n t_d < \pi$. It should be noticed that this reservation is of little concern considering the anticipated relatively large periods of real aircraft windshield systems. Impact Time - Response Ratios, t_d/T_n ($=\omega_n t_d$) is shown in Table 13 over an indicated natural frequency regime.

TABLE 13. IMPACT TIME - RESPONSE RATIOS, t_d/T_n, FOR t_d = .002 SEC.

NATURAL FREQUENCY		PERIOD	IMPACT TIME	$\frac{t_d}{T_n}$
f_n (HZ.)	ω_n (rad/sec)	T_n (sec)	t_d (sec)	
20	125	.0080	.002	0.25
40	251	.0040	.002	0.50
60	377	.0027	.002	0.74
80	503	.0020	.002	1.0
159	1000	.0010	.002	2.0
238	1500	.00067	.002	3.0
250	1571	.00064	.002	π

The maximum static load, S_{L1}, from Equation (19) is:

$$S_{L1} = \bar{F}(1-\cos \omega_n t_d)$$

Substituting the calculated results from Equations 27 and 30 and using the relationship $\omega_n = \sqrt{K/M}$ results in

$$S_{L1} = 22{,}500\ (1-\cos \sqrt{\frac{K}{.144}}\ (.002)) \tag{32}$$

Maximum Static Load, $t>t_d$

To obtain the maximum static load, S_{L2}, that will occur at times $t>t_d$, use Equation (21), and optimize. The maximum static load will occur when

$$t = \frac{\pi}{2\omega_n} + t_d. \tag{33}$$

Hence, the maximum static load from Equation (21) is

$$S_{L2} = \bar{F}\ \left[\cos\ \omega_n\ (t-t_d)\ -\cos\ \omega_n t\right]\quad t>t_d$$

$$= 22{,}500\ \left[\cos\ \omega_n\ (\frac{\pi}{2\omega_n} + t_d - t_d)\ -\ \cos\ \omega_n\ (\frac{\pi}{2\omega_n} + t_d)\right]$$

$$= 22{,}500\ \left[-\cos\ (\frac{\pi}{2} + \omega_n\ t_d)\right]$$

Therefore,

$$S_{L_2} = 22{,}500\ \left[-\cos\ (\frac{\pi}{2} + \sqrt{\frac{K}{0.144}}\ (.002)\right] \tag{34}$$

where the parameter definitions are the same as used in deriving Equation (32).

Load Versus Stiffness Curves

Curves relating the maximum equivalent static loads, S_{L1} and S_{L2}, as a function of the B-1 windshield system stiffness, K, for a system natural frequency, f_n = 40 cps are shown in Figure 58. These curves were developed using the theory as developed in this section and the empirical data for the particular windshield system parameters utilized in B-1 test number BM006. For K = 9124 lb/in., it may be seen that the maximum equivalent load is 11,000 lbs.

Expanding the basic conditions to observe the behavior of S_L-versus-K with changing B-1 windshield system natural frequency results in the family of curves shown in Figure 59. These curves show the maximum static load as a function of both the windshield system stiffness and natural frequency.

Curves of this nature may be generated in like manner for other windshield systems providing sufficient supporting analytical or test parameters may be generated.

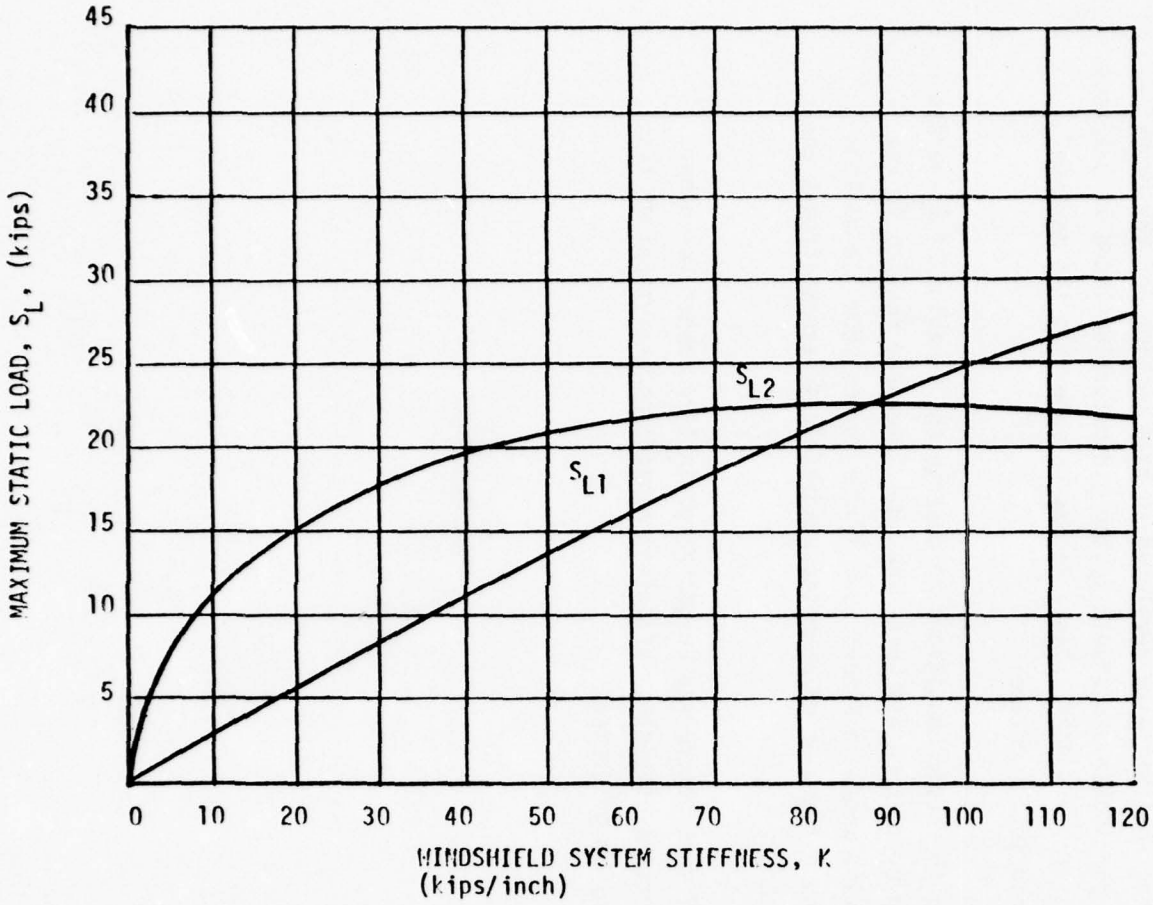

Figure 58. Maximum Static Load as Function of Windshield System Stiffness (f_n = 40 cps).

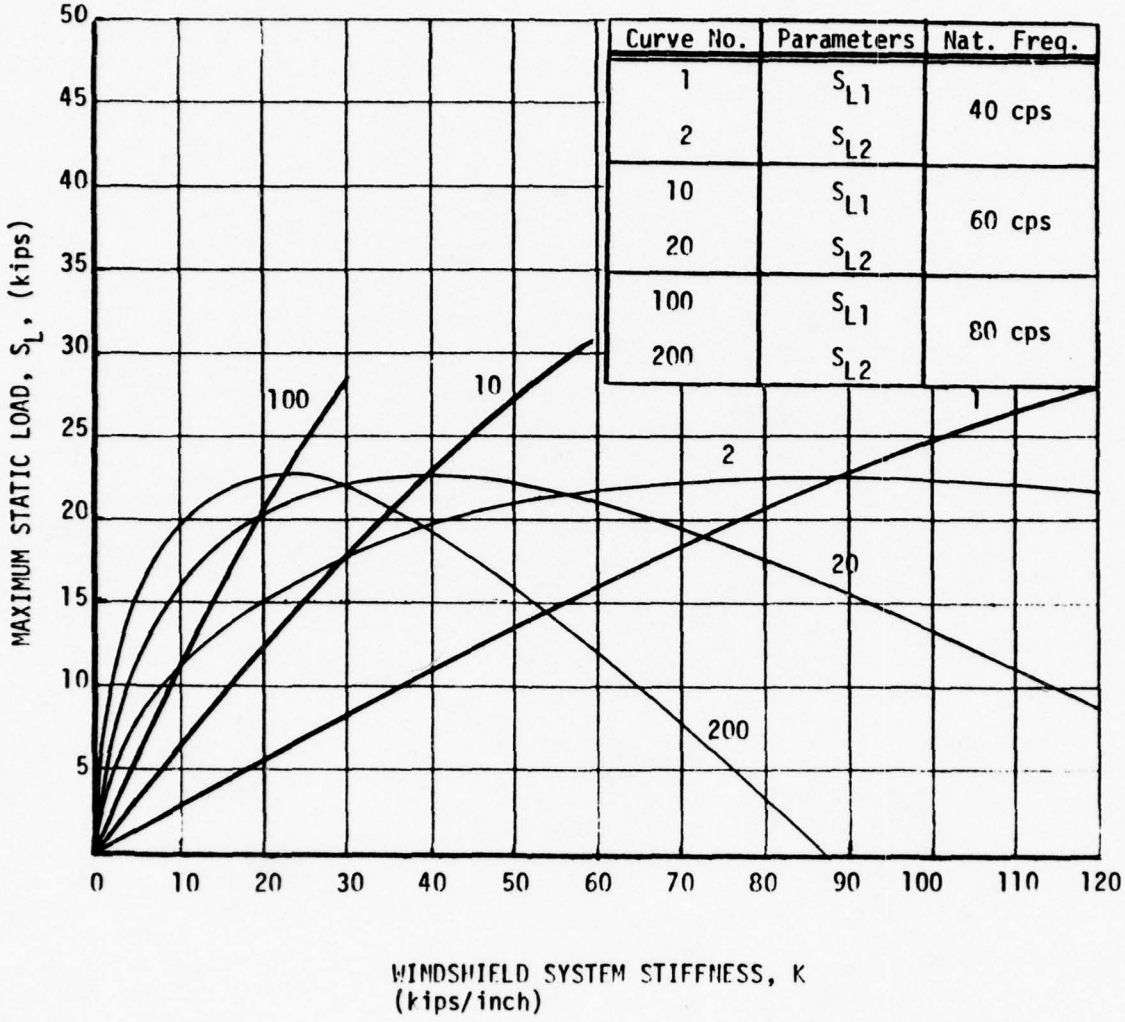

Figure 59. Maximum Static Load as Function of Windshield System Stiffness and Natural Frequency.

SECTION VII
CONCLUSIONS AND RECOMMENDATIONS

CONCLUSIONS

B-1 Windshield Bird Impact Test Series

Test results show that the existing windshield design on the B-1 aircraft will survive bird impact without hazard to the crew. The test temperatures were limited between 55.5°F and 72.0°F windshield temperature; therefore the results are valid only for that range.

The R-I designed windshields were determined to be a very high cost item from the standpoint of installation. Each edge of the windshield had to be installed with two rows of attachments and on several edges the exterior retainers were common to another transparency involving an additional row of attachments. As a result of the number and close fit of the attachment holes, the installation and removal of the windshield was time consuming. To eliminate the need for common exterior retainers, reduce the total number of attachments and difficulty of installing attachments, Douglas modified the windshield installation design to utilize only one row of attachments installed in loose holes with wet sealant.

A series of six bird impact shots were made with four and six pound birds at velocities up to 562 knots. The test results show that the B-1 windshield with the modified edge attachment design will meet bird impact requirements at room temperatures.

Simulated Aircraft Windshield Bird Impact Test Series

To optimize the design of the windshields, structural support and edge designs, a series of five simulations were designed utilizing materials proprietary to three transparency vendors for bird impact testing. Two specimens of each design, 36 x 36 inches in size and curved to a 60-inch radius, were tested. Each design represented various laminates of

polycarbonate or glass plies. Two structural fixtures, one for glass the other for polycarbonate, were used to support the simulated windshields for the impact tests. The fixtures were designed analytically to be compatible structurally with windshield specimens.

As a result of the impact tests, it is believed that a successful design of laminated glass or laminated polycarbonate could be developed and installed on production aircraft. A glass, as compared to a polycarbonate laminate, would have prohibitive weight, yet the glass laminate would be highly reliable, have good optical quality, and potentially meet maximum anti-icing requirements. It would have the disadvantage of having only one vendor able to supply production windshields with the desired vision envelope. The polycarbonate laminates also can be made reliable, have maximum anti-icing capabilities and it is felt that good optical quality can be developed by the two vendors.

The laminated specimen with 7/8-inch thick polycarbonate can be installed on a production airplane as demonstrated by the existing B-1 design.

RECOMMENDATIONS

The recommended windshield is the end result of a progressive design system of optimization which utilized the work documented in this report and in Reference 14.

Tests were run with a progressive series of different edge restraints and stiffnesses, and/or various transparency designs at extreme temperature conditions. The specimens involved in these tests utilized all current state-of-the-art transparency, structural and interlayer materials commercially available for high-performance aircraft. There were five final candidate windshield designs in this program. A primary point of test specimen evaluation was the determination whether the ensuing specimen failure was cohesive (within a ply itself), or adhesive (at the bond line between interlayer and structural ply). A cohesive failure ensures

that the maximum possible load is carried by a particular ply configuration. Of the tested specimens, the two-ply glass design provided the most desired combination of strength and stiffness; however, the weight of this design was prohibitive for high-performance aircraft. The four-ply polycarbonate design, as tested per this report, represents the structural optimum in lightweight windshield design and is recommended as an alternate B-1 windshield design.

A windshield laminate with a 7/8-inch thick structural ply cannot be recommended since the ply is comprised of two or more individual plies fusion bonded. Laboratory testing indicates that fusion bonded material may delaminate and cause objectionable visibility problems for a flight crew. Also, because of the stiffness of this configuration, more load is transferred to the support structure locally. The support flange near the impact point was cracked in each of two tests (possibly the cumulative effect of previous shots conducted on corners).

Support structure corner gussets are not recommended as test results indicate conclusively that they did not contribute to the success of the specimens withstanding the bird impacts.

As a result of analyses made relating to these tests, a semi-empirical method for obtaining an equivalent static load on an aircraft windshield subjected to a bird impact has been developed. This method is characterized by a mathematical analysis using various stiffness loadings derived from either test data or a computer supported finite element math model. The method also permits the evaluation of the effects of impact load due to the relative stiffness of the impacted area. This bird impact study is an attempt to address the effects of total windshield compliance by means of an analytical method which may be conveniently used in the preliminary design of aircraft transparencies.

APPENDIX A

WINDSHIELD FAILURE ANALYSES

APPENDIX A
WINDSHIELD FAILURE ANALYSES

This appendix contains detailed failure analyses of the windshield specimens utilized in these series of high speed bird impact tests. Specifically, for each specimen, detailed part and test information is listed, followed by a visual examination and discussion of salient features of the failed specimen. Sketches are included which fully illustrate failure patterns and windshield fabrication details.

All specimens were returned to Douglas after the bird impact testing for this series of visual examination. After this examination and failure analyses, selected parts had specimens cut from them such that material properties could be determined by further test. (Reference 17).

An index is included which relates specific tests to the related failure analysis tables and figures.

FAILURE ANALYSES INDEX

Test Series	Vendor No.	Test No.	Table No.	Figure No.
B-1 Bird Impact Testing	B-1 SWU-108	BM-004 BM-005	A.1	A.1
	B-1 SWU-107	BM-006 BM-007 BM-008 BM-009	A.2	A.2 A.3 A.4 A.5
Simulated Aircraft Windshield Bird Impact Testing	SWU-001	BM-010 BM-017	A.3	A.6 A.7
	SWU-002	BM-011 BM-016	A.4	A.8 A.9
	PPG-001	BM-012 BM-013	A.5	A.10 A.11
	PPG-002	BM-014 BM-015	A.6	A.12
	PPG-003	BM-019	A.7	A.13 A.14
	SK-001	BM-018 BM-020	A.8	A.15 A.16
	SWU-003	BM-021 BM-022	A.9	A.17 A.18
	PPG-004	BM-023 BM-028	A.10	A.19 A.20 A.21
	SK-002	BM-026 BM-027	A.11	A.22 A.23 A.24
	PPG-005	BM-029	A.12	A.25 A.26 A.27

TABLE A.1.

FAILURE ANALYSIS
OF
WINDSHIELD SPECIMENS
(B-1 SWU-108)

TEST ENCLOSURE	P/N L3000151-001
PART NUMBER	SWU-108
TEST NUMBER	BM-004 and BM-005
SHOT LOCATION	Center
V (Fps)	951-953
TEST TEMPERATURE	Ambient
WINDOW TEMPERATURE	Ambient
NO. BOLT HOLES	
TYPE OF ENCLOSURES	Laminate polycarbonate/silicone windshield.
TEST RESULTS	No Bird Penetration

Discussion

On Shot No. 1 (BM-004), the outer acrylic ply of Panel No. 108 spalled and cracked but there was no damage to the polycarbonate structural ply. There were several cracks in the polycarbonate inner ply that emanated from a damaged area appeared to be a "heat bubble" where a 3-inch circle of the inner ply delaminated from the interlayer and warped out approximately 1/4-inch.

On Shot No. 2 (BM-005), there was some additional spalling of the outer ply but no visible damage to the structural ply or additional cracking of the inner ply.

Both shots were with a 4-pound bird.

No detailed examination or failure analysis was performed on this test enclosure at the Douglas facilities.

Material Identification and Dimensional Verification

The material identification and dimensional verification was very close to the requirements specified in P/N-L3000 151-001 Drawing. See Figure A.1 for detailed comparisons.

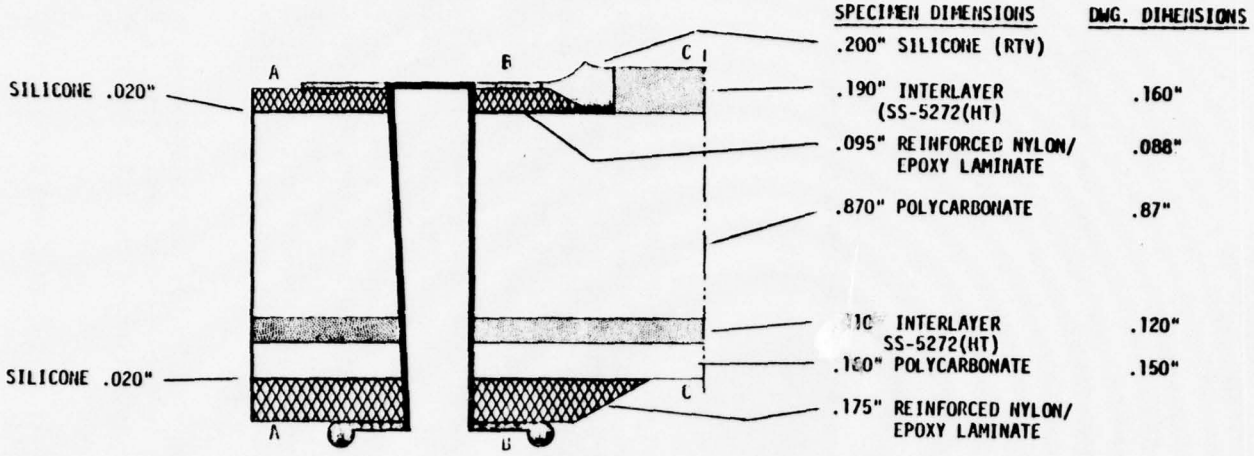

Figure A.1. Material identification and dimensional verification, test specimen L3000151-001 (SWU108).

TABLE A.2.

FAILURE ANALYSIS
OF
WINDSHIELD SPECIMENS
(B-1 SWU-107)

TEST ENCLOSURE	P/N L300151-001
PART NUMBER	SWU-107
TEST NUMBER	BM-006, BM-007, BM-008 and BM-009
SHOT LOCATION	Center
V (Fps)	930-970
TEST TEMPERATURE	Ambient
WINDOW TEMPERATURE	Ambient
NO. BOLT HOLES	
TYPE OF ENCLOSURES	Laminated Polycarbonate/Silicone Windshield
TEST RESULTS	No Bird Penetration

Discussion

On Shot No. 3 (BM-006), using windshield panel No. 107, the outer acrylic layer spalled and cracked, but there was no visible damage to the polycarbonate structural ply or cracking of the inner ply. On Shots 4, 5 and 6 (panel No. 107) there was little additional damage to the windshield; the outer ply did not appear to be damaged. On shot No. 6 (6-pound chicken) the inner ply cracked but did spall (Figure A.2, A.3).

Every other bolt common to the windshield was removed for shot No. 5. On shot No. 5, the ends of the top aft retainer (L3000157-003) and the forward end of the lower aft retainer (L3000159-003), which were not secured with bolts, were bent outwards as a result of the hydraulic forces of the bird. As an aid in preventing this from happening on the following shots, bolts were moved from adjacent holes to the ends, leaving two successive holes without bolts. This bolt configuration was successful in securing the ends of the retainer during the impact of shot No. 6 (Figure A.4).

Structural damage occurred on shot No. 6; cracks appeared in the left eyebrow longeron and in the left sill structure. Also, a few bolts failed, but there was no penetration of the interior of the module by the bird.

No detailed examination or failure analysis was performed on this enclosure at the Douglas facilities.

TABLE A.2 (Continued)

Material Identification and Dimensional Verification

The material identification and dimensional verification was very close to the requirements specified in P/N L3000151-001 Drawing. See Figure A.5 for detailed comparisons.

NOTES:

1. All damage is from Test BM006, except as indicated: 7 indicates damage from BM007
   8 indicates damage from BM008
2. All cracks are in the outer acrylic ply. Gouges in the outbd C-I-P interlayer as noted.
3. No damage to core ply or to spall shield
4. Indicates acrylic pieces torn out (on BM008)
5. (1) indicates deflectometer location
6. A indicates target point
7. * indicates tool damage (pre BM006).

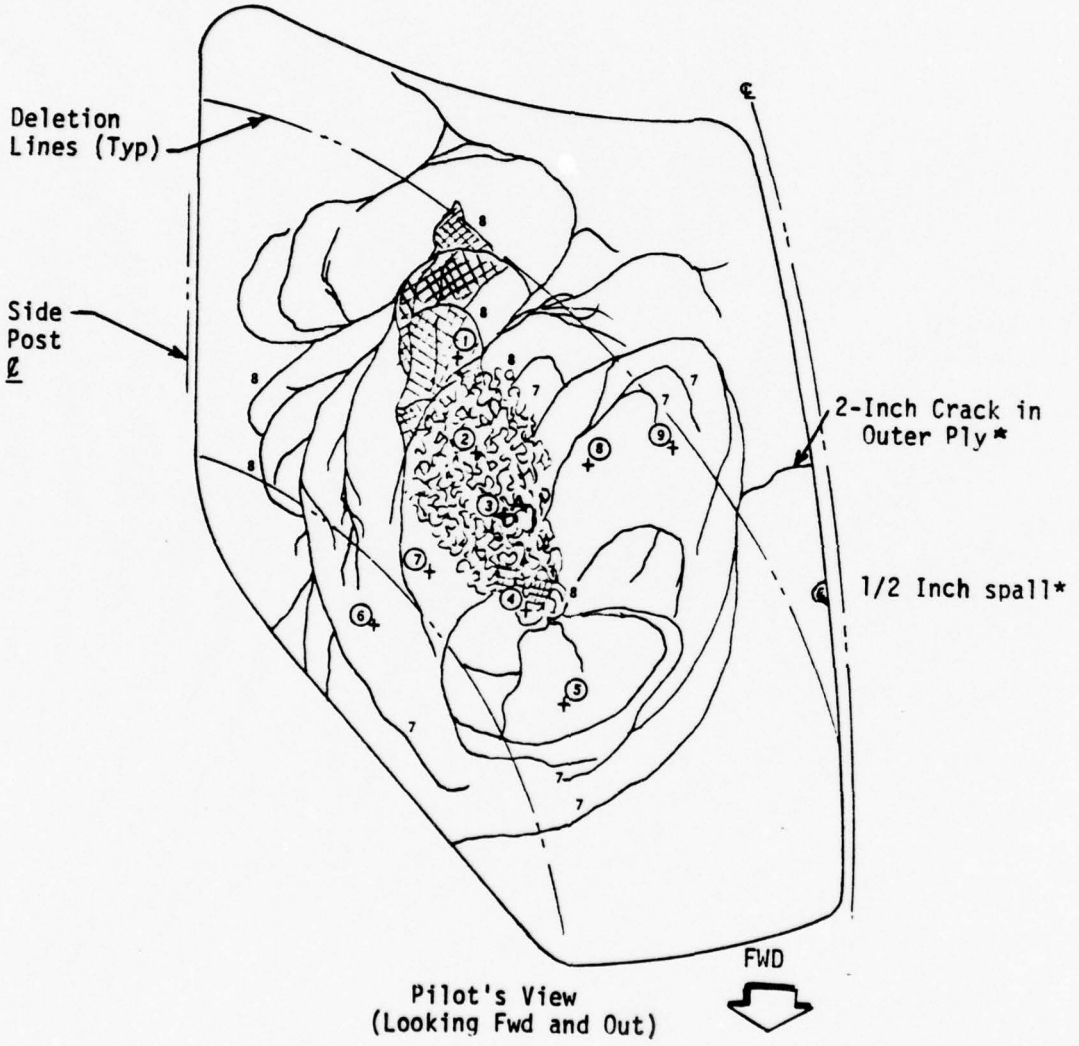

Figure A.2. B-1 windshield test specimen (SWU107) test BM006 to BM008.

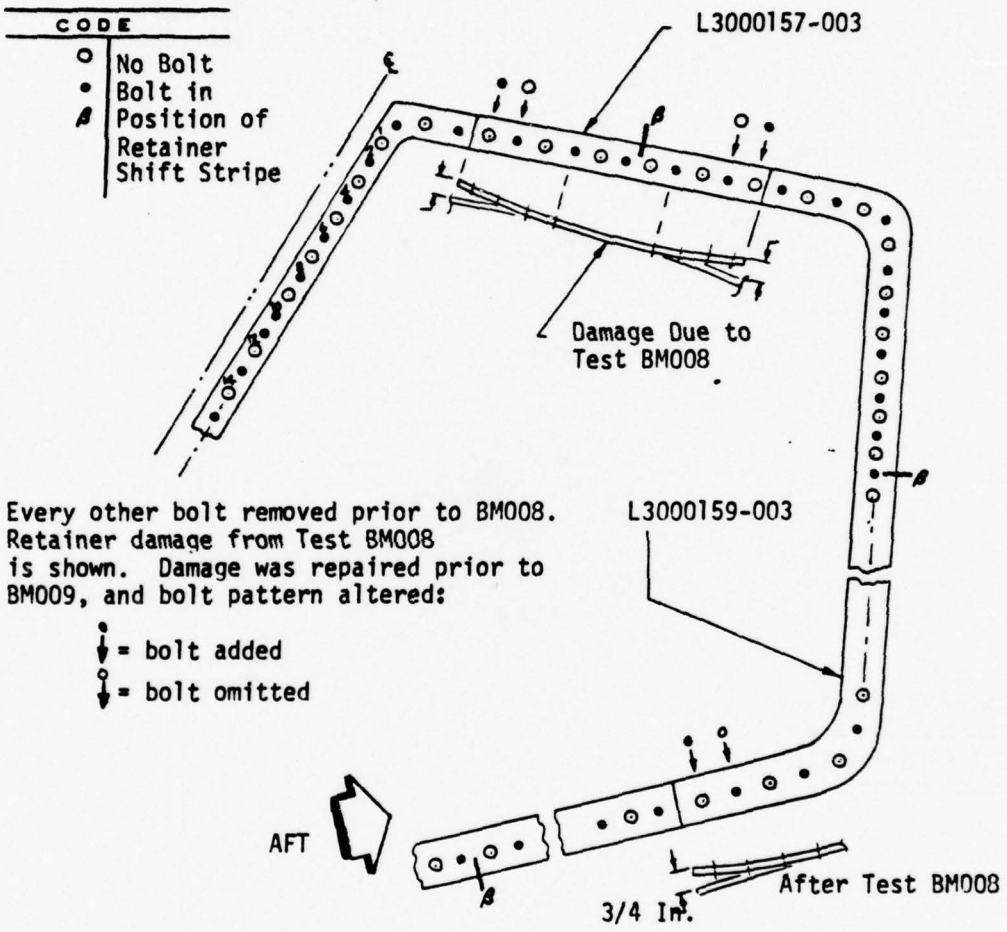

Figure A.3. B-1 windshield retainer modification Test BM008.

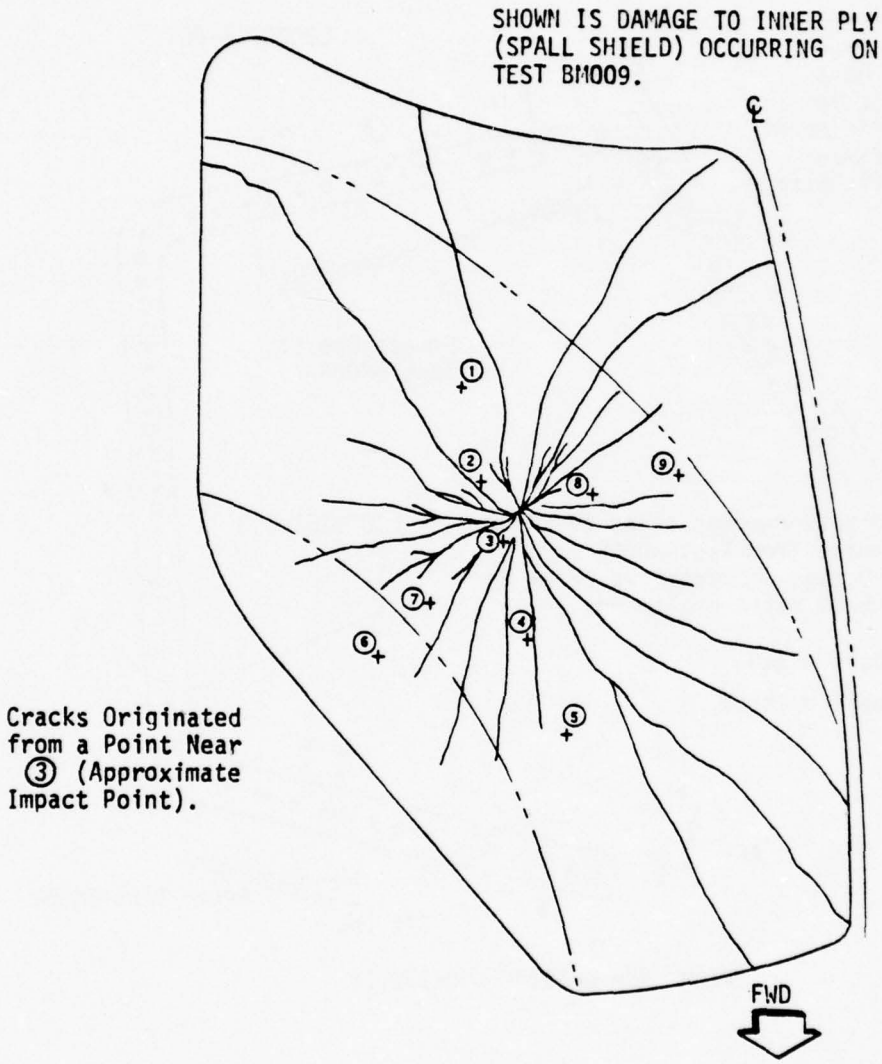

Figure A.4. B-1 windshield test specimen (SWU107), inner ply surface, post-test BM009.

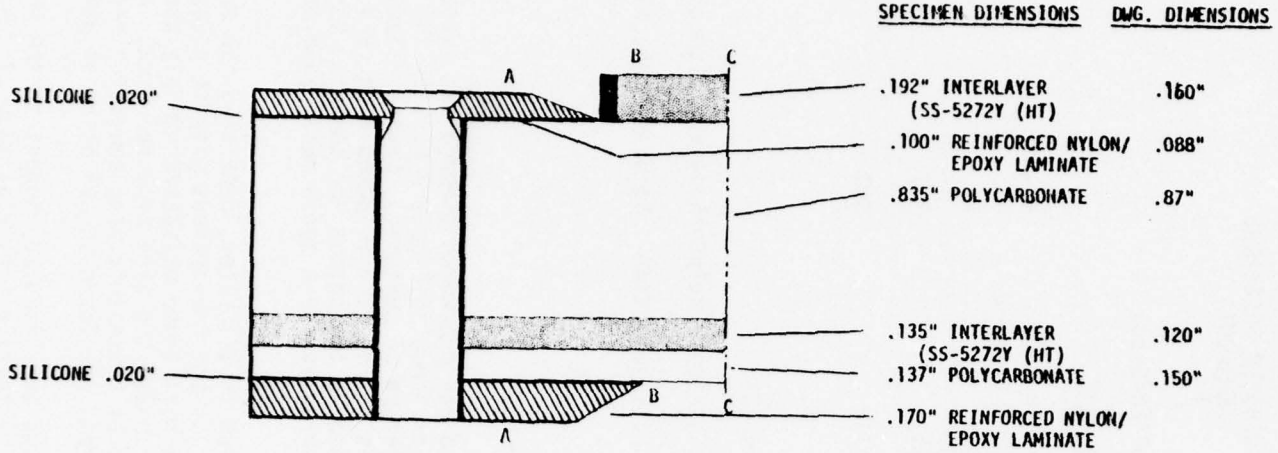

TOTAL THICKNESS	DWG. THICKNESS
A. 1.434"	1.423 ± .020
B. 1.293"	
C. 1.303"	

Figure A.5. Material identification and dimensional verification, test specimen L3000151-001 (SWU107).

TABLE A.3.

FAILURE ANALYSIS
OF
WINDSHIELD SPECIMENS
(SWU-001)

TEST ENCLOSURE	Z5942640-501	
PART NUMBER	SWU-001	
TEST NUMBER	BM-010	BM-017
SHOT LOCATION	A	C
IMPACT VELOCITY (fps)	941	737
TEST TEMPERATURE	Cold	Hot
WINDOW TEMPERATURE		
NO. BOLT HOLES	Two (2)	
TYPE OF ENCLOSURE	Multi-layer Polycarbonate/Silicone Laminate	
TEST RESULTS	Bird Penetration	No Bird Penetration

Test BM-010

Visual Examination

The 4-pound bird penetrated and punctured through the extreme upper corner of the test enclosure, as shown in Figure A.6. All the polycarbonate plies were either cracked or ruptured. Severe delamination occurred in all laminated plies in the bird impacted area, and some fringes of delamination extended to the bottom "D" corner. Noticeable and isolated delamination occurred at the A and D metal edge attachment retainer.

Severe delamination occurred in all plies, depicting the poor adhesion of the silicone interlayer to the transparent plastic plies of material. Large pieces of the most inner polycarbonate ply was completely removed, extending directly below the bird impacted area. A series of primary cracks, in the form of concentric arcs emanating from the center of the bird impacted area, was found in all plies of polycarbonate.

A series of secondary cracks and fissures tangent to the primary arc cracks was found primarily to be tensile (brittle) type of cracks,

occasionally with chevron fissures emanating from the cracks. Typical shear and tensile/shear concentric cracks that appeared around the impacted area are shown in Figure A.6. The fracture topography of tensile, tensile/shear ductile, and brittle failure is shown in Figure A.6.

The origin of secondary cracks and fissures usually occurred at a point tangent to the concentric cracks or fissure; usually initiated by an internal "flaw" or inclusion found in the polycarbonate material.

Material Identification and Dimensional Verification

The material identification and dimensional verification were very close to the requirements specified in P/N Z5942640-501 Dwg. See Figure A.7 for detailed comparisons.

Discussion

The rational for the failure mechanism for the BM-10 bird penetration is that severe interlayer (silicone) delamination occurred in all plies of interlayers, and delamination increased in area to the internal portion of the laminate. The individual transparent plastic plies ruptured or fractured in shear and combination of shear/tensile failure. The majority of primary cracks failed in shear, since less load is required to produce this type of failure.

The primary cracks and fissures consisting of a series of concentric arcs emanating from the impacted area and are formed by a cylindrical package impacting a ductile low modulus composite polycarbonate laminate.

Test BM-017

Visual Examination

The bird impacted the "C" corner, however, bird penetration was not evidenced. All polycarbonate plies exhibited some cracks and fractures and interlayer delamination. There was much less primary and secondary cracks and fractures as compared to the upper BM-010 shot. Edge attachment holes appear to be in good condition. The shear cracks and fracture topograph appears to be ductile in nature - as shown in Figure A.6. The secondary tensile and tensile/shear crack and fracture topograph appeared to be smooth, which usually indicates brittle failure. Most of crack and fracture did not reach the periphery of the test enclosure. The acrylic face plies exhibited primary shear failure mode and cohesive failure of the interlayer ply, due to high velocity mechanical erosion as a result of bird impact.

TABLE A.3. (Continued)

Material Identification and Dimensional Verification

The material identification and dimensional verification was very close to the requirements specified in P/N Z5942640-501 Dwg. See Figure A.7 for detailed comparison.

Discussion

The lower impact speed produced less delamination and, therefore, initiated less primary and secondary polycarbonate cracks and fissures, and no bird penetration was evidenced. The attachment holes looked very good relative to internal smoothness, alignment, and crazings. All strain gauge were intact and bonded.

Although all the polycarbonate plies were cracked, the test enclosure was capable of withstanding the bird impact due to the limited delamination of the interlayer between the various plies of polycarbonate.

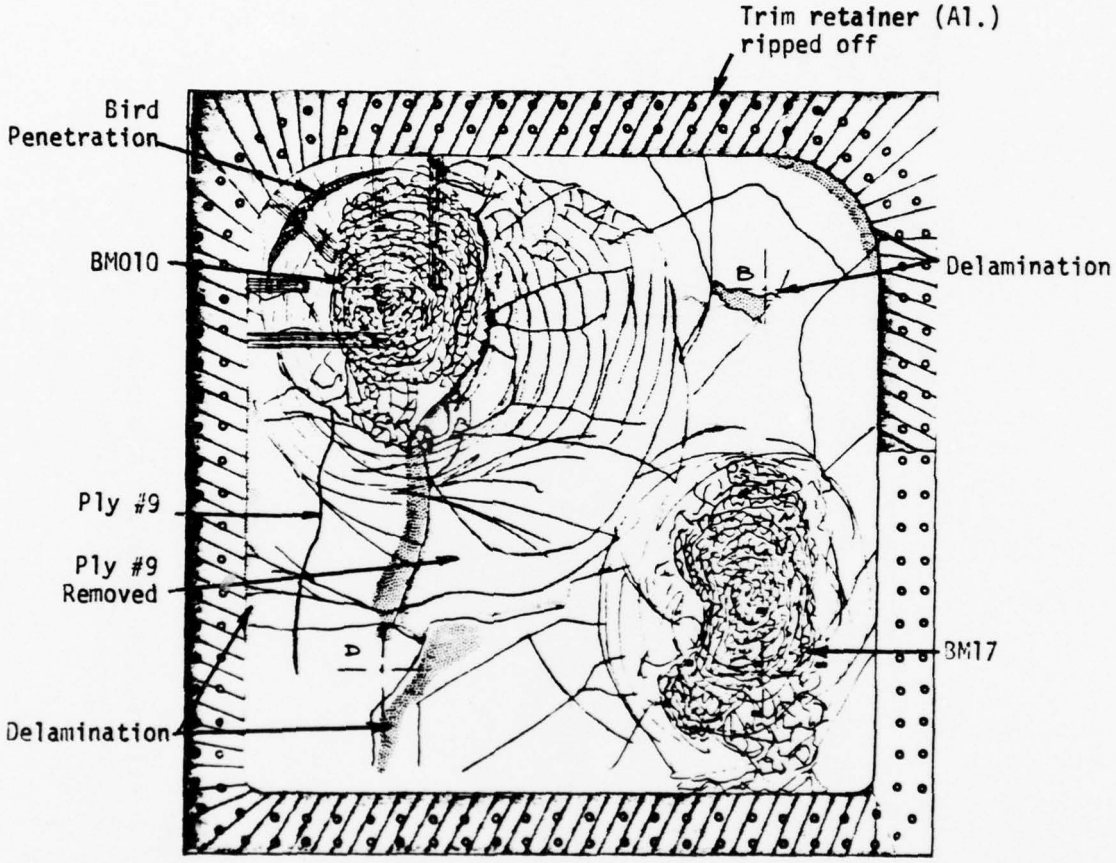

Figure A.6. Simulated aircraft windshield test Specimen Z5942640-501 (SWU001) test Numbers BM010, BM017.

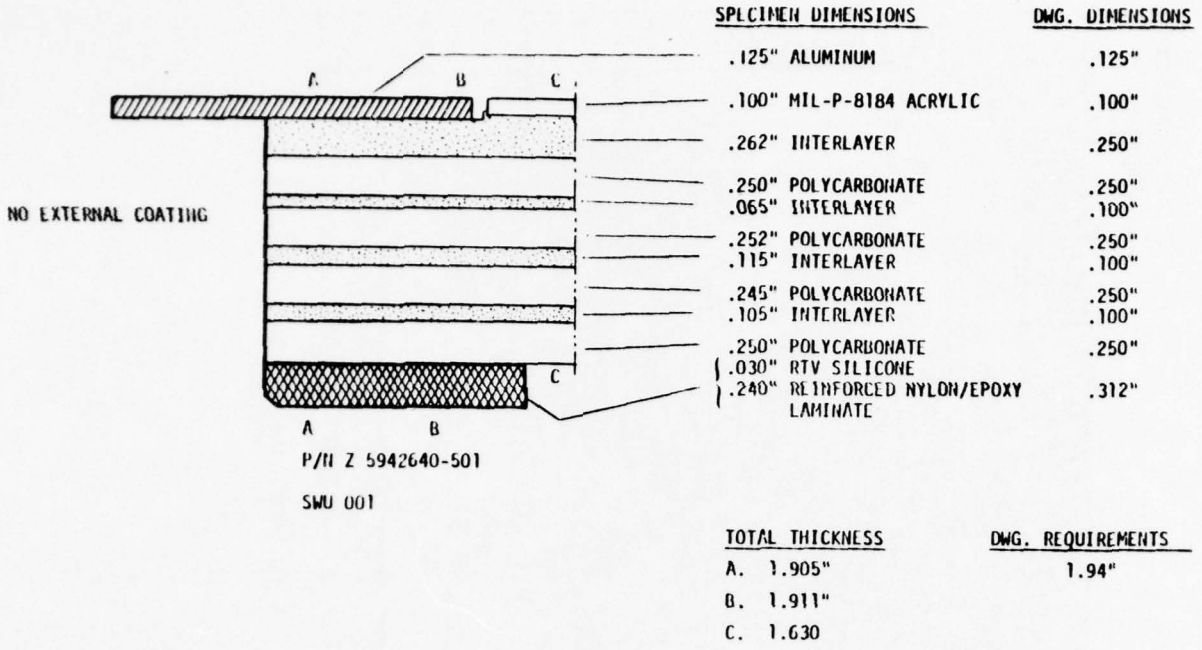

SPECIMEN DIMENSIONS	DWG. DIMENSIONS
.125" ALUMINUM	.125"
.100" MIL-P-8184 ACRYLIC	.100"
.262" INTERLAYER	.250"
.250" POLYCARBONATE	.250"
.065" INTERLAYER	.100"
.252" POLYCARBONATE	.250"
.115" INTERLAYER	.100"
.245" POLYCARBONATE	.250"
.105" INTERLAYER	.100"
.250" POLYCARBONATE	.250"
.030" RTV SILICONE	
.240" REINFORCED NYLON/EPOXY LAMINATE	.312"

TOTAL THICKNESS	DWG. REQUIREMENTS
A. 1.905"	1.94"
B. 1.911"	
C. 1.630	

Figure A.7. Material identification and dimensional verification, test specimen Z5942640-501 (SWU001).

TABLE A.4.

FAILURE ANALYSIS
OF
WINDSHIELD SPECIMENS
(SWU-002)

TEST ENCLOSURE	Z5942640-501	
PART NUMBER	SWU-002	
TEST NUMBER	BM-011	BM-016
SHOT LOCATION	A	C
IMPACT VELOCITY (fps)	960	369
TEST TEMPERATURE	Ambient	Ambient
WINDOW TEMPERATURE	Ambient	Ambient
NO. BOLT HOLES	Two (2)	Two (2)
TYPE OF ENCLOSURE	Multi-layer Polycarbonate/Silicon Laminate	
TEST RESULTS	Bird Penetration	No Penetration

BM-011

Visual Examination

The 4-pound bird penetrated and punctured through the upper "A" corner of the test enclosure as shown in Figure A.8. All polycarbonate plies were cracked or ruptured. Severe delamination occurred in all the laminated plies. Large amounts of interlayer delamination were present in #6 and #8 interlayer plies, which extended into the lower portion of the test panel, again indicating poor adhesion of the silicone based interlayer to the P.C. plies. A large series of primary concentric arched cracks and fissures emanated from all the bird impacted plies of P.C. A series of secondary cracks, primarily in #9 P.C. ply, emanated from the primary arched cracks and fissures. The entire aluminum trim retainer was removed. All attachment holes looked good, and internal hole quality looked exceptionally clean and smooth.

Material Identification and Dimensional Verification

Test enclosure P/N Z5942640-501 - SWU-002 material identification and dimensional verification were very close to the drawing requirements, except that the interlayer thickness varied slightly. See

Figure A.9 for detailed material and dimensional comparison.

Discussion

The rationale of the failure mode for the BM-011 bird penetration is exactly the same failure mechanism as reported in BM-010 shot. Immediate and severe delamination occurred upon initial impact, resulting in a series of concentric shear and tensile/shear cracking of individual Polycarbonate plies.

BM-016

Visual Examination

BM-016 shot was identical to BM-011, except the V (fps) was 369 as compared to 960, and there was no bird penetration. There was only superficial, small cracks in the thin outer acrylic ply covering a very small panel area. The aluminum trim retainer was peeled back, covering about 10 attachment holes. There was one secondary crack in the outer acrylic ply, starting and terminating near the attachment holes. All the strain gauges appeared to be intact. All attachment holes looked to be in good condition. (Figure A.8)

Material Identification and Dimensional Verification

Test enclosure P/N Z5942640-501 - SWU-002 material identification and dimensional verification were very close to the drawing requirements, except that the interlayer thickness varied slightly. See Figure A.9 for detailed material and dimensional comparison.

Discussion

The low speed and ambient temperature bird test shot into the "C" corner bounced the bird successfully and produced only superficial damage.

The composite transparent test enclosure resisted the bird impact shot because the interlayer did not delaminate, and acted as an intact composite structure.

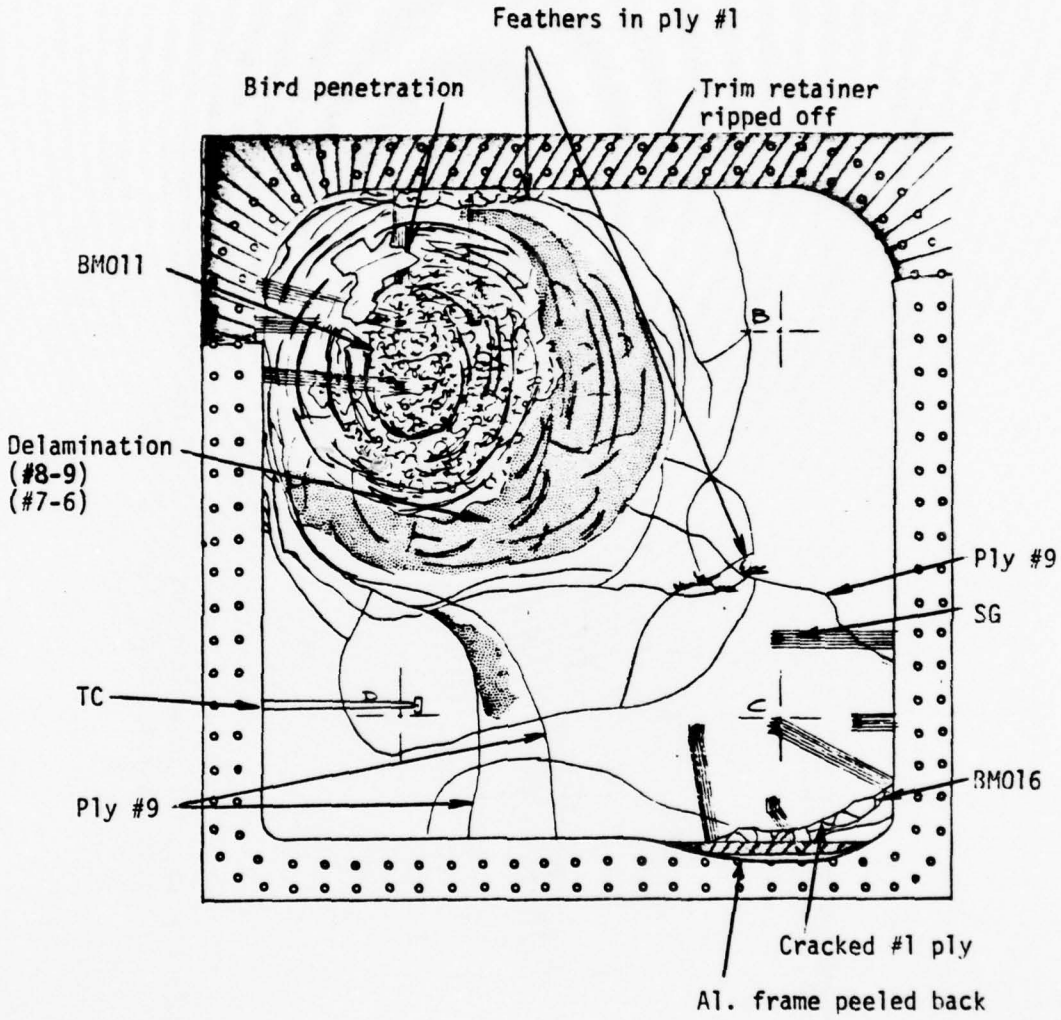

Figure A.8. Simulated aircraft windshield test Specimen Z5946240-501 (SWU002), test Numbers BM011, BM016.

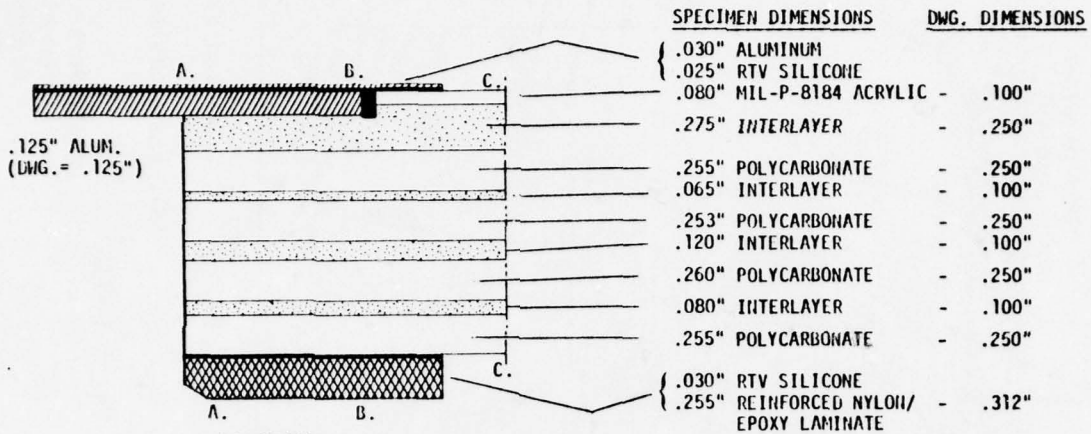

Figure A.9. Material identification and dimensional verification, test specimen Z5942639-503 (SWU002).

TABLE A.5.

FAILURE ANALYSIS
OF
WINDSHIELD SPECIMENS
(PPG-001)

TEST ENCLOSURE	Z5942639-501	
PART NUMBER	PPG-001	
TEST NUMBER	BM-012	BM-013
SHOT LOCATION	A	A
IMPACT VELOCITY (fps)	943	948
TEST TEMPERATURE	Ambient	Ambient
WINDOW TEMPERATURE	Cold	Ambient
NO. BOLT HOLES	One Row	
TYPE OF ENCLOSURE	Laminated Glass	
TEST RESULTS	No Bird Penetration	

Visual Examination

The initial bird impact shot, BM-012, ruptured only the initial ply of 1/2-inch thick fully tempered glass ply. The outer chemically strengthened ply didn't rupture. The origin of both glass failures emanated from the center of the impacted area. The small size of the glass particles indicates a high temperature and a good center tension value for both glass plies. It was difficult and time consuming to conduct a more quantitative analysis of the inherent stress that was either thermally or chemically (ion exchange) induced in each ply of glass.

The second bird impact shot BM-013 at ambient temperature in the same corner successfully bagged the bird and did not allow any penetration.

All plies of glass were ruptured during the second shot at the same corner. The interlayer held the broken pieces of glass fairly well.

The attachment holes looked very good. Strain gauge and thermocouples appeared to be in good condition also. (Figure A.10)

TABLE A.5. (Continued)

Material Identification and Dimensional Verification

The material identification and dimensional verification was very close to the requirements as specified in P/N Z5942639-501 Drawing. See Figure A.11 for detailed comparison.

Discussion

The laminated glass test enclosure displayed its capability of successfully bagging two high velocity bird shots in the same corner without bird penetration. The PPG-112 new interlayer exhibited good impact properties by its ability in bagging the bird and toughness by preventing bird penetration.

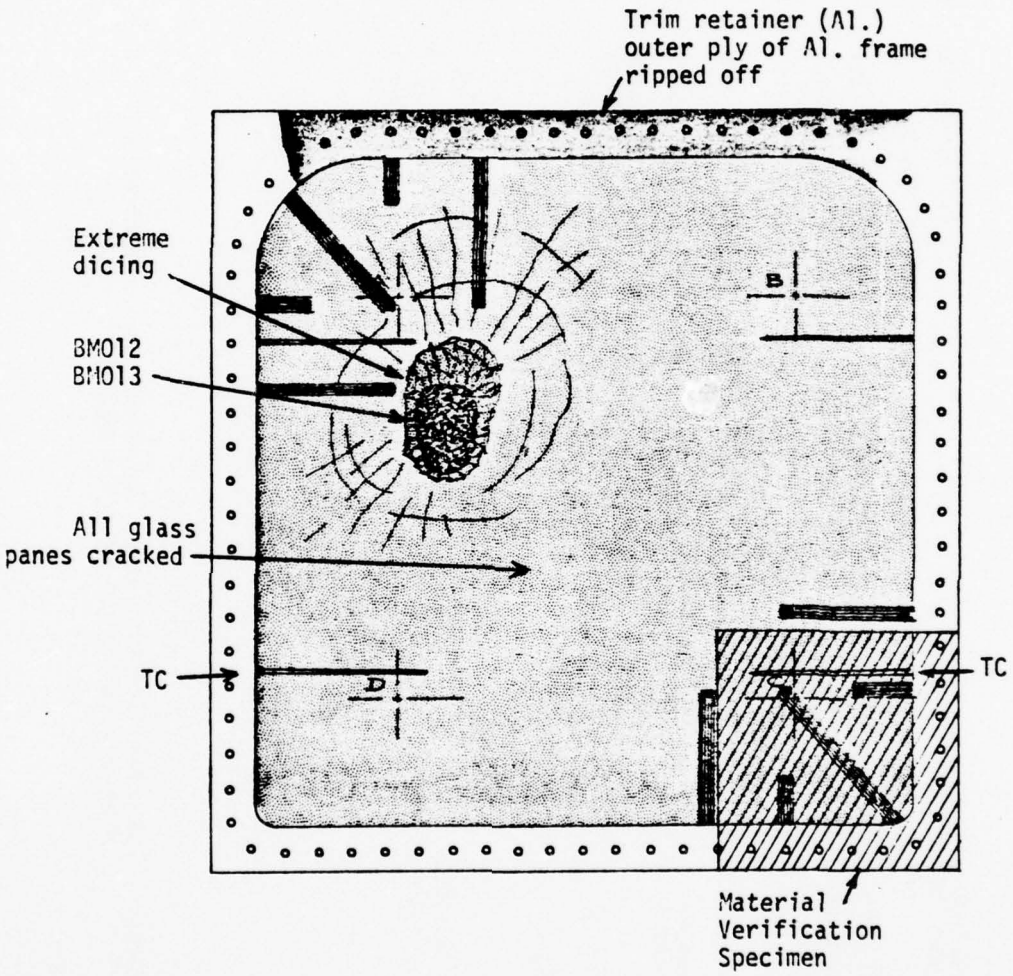

VIEW LOOKING INBOARD

Figure A.10. Simulated aircraft windshield test specimen Z5942639-501 "B" (PPG001), Test Numbers BM012, BM013.

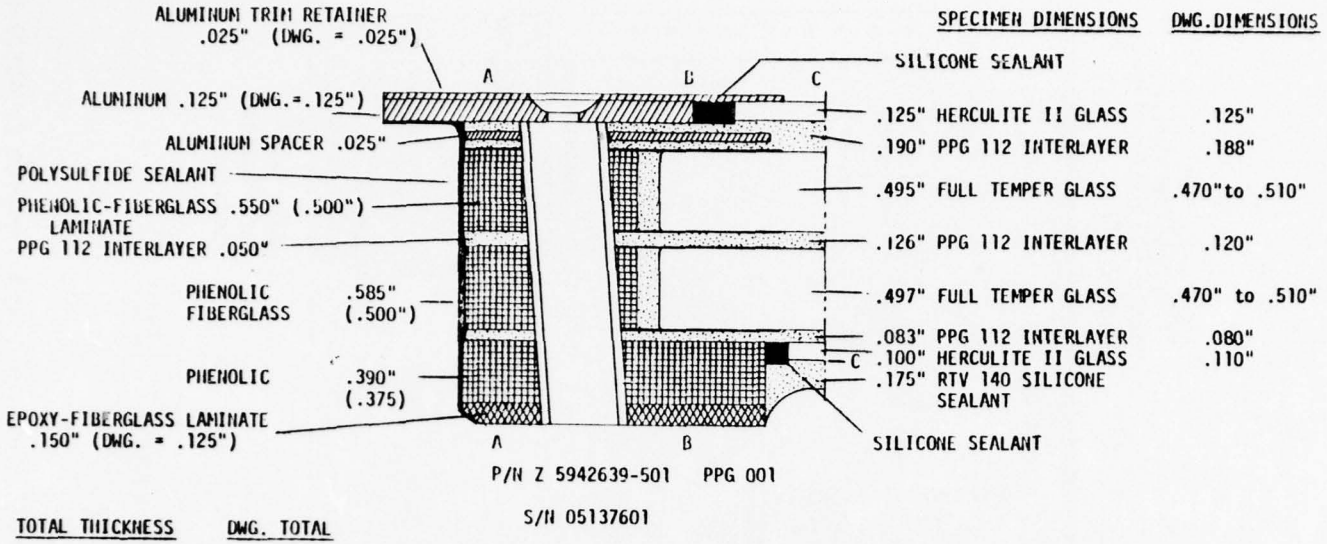

TOTAL THICKNESS	DWG. TOTAL
A. 2.039"	1.980
B. 2.049"	
C. 1.582"	

Figure A.11 Material identification and dimensional verification, test specimen Z5942639-501 (PPG001)

TABLE A.6.

FAILURE ANALYSIS

OF

WINDSHIELD SPECIMENS
(PPG-002)

TEST ENCLOSURE	5942639-501 Dwg. Change B	
PART NUMBER	PPG 002	
TEST NUMBER	BM-014	BM-015
SHOT LOCATION	C	E
IMPACT VELOCITY (fps)	939	515
TEST TEMPERATURE	Ambient	
WINDOW TEMPERATURE	90°F	
NO. BOLT HOLES	One	One
TYPE OF ENCLOSURE	Laminated Glass	
TEST RESULTS	No Bird Penetration	

Visual Examination

The initial bird shot in corner "C" ruptured both the 1/2-inch thick plies of thermally tempered glass without rupturing both external chemically strengthened glass plies. The second shot "E" centrally located between "A" and "B" corners did not again rupture the external chemically strengthened plies. Both bird shots sucessfully bagged the bird without penetration. Figure A.12 depicts the bird impact area, and dark shading indicates extremely heavy dicing, producing a translucent appearance.

This test panel exhibited extraordinary phenomena, by taking two fairly high velocity bird shots without rupturing both external chemically strengthened glass plies.

There was no measurable deformation in the test enclosure. Part of the aluminum retainer was removed during bird impact.

Material Identification and Dimensional Verification

The material identification and dimensional verification was not made on this test enclosure. It was agreed that this panel be shipped to PPG for additional examination and analysis.

TABLE A.6. (Continued)

Discussion

This bird impacted test enclosure exhibited the excellent impact resistance of thin chemically strengthening glass. The superior physical and mechanical properties of ion exchanged glass was quite evident in both bird shot.

The thermally tempered 1/2-inch glass plies exhibited fine and uniform dicing characteristics, indicating good compression tempering process with a fairly high center tension. The toughness of the PPG's 112 interlayer was quite evident in bagging the bird and maintaining the glass particles without penetrating the external chemically strengthened glass plies.

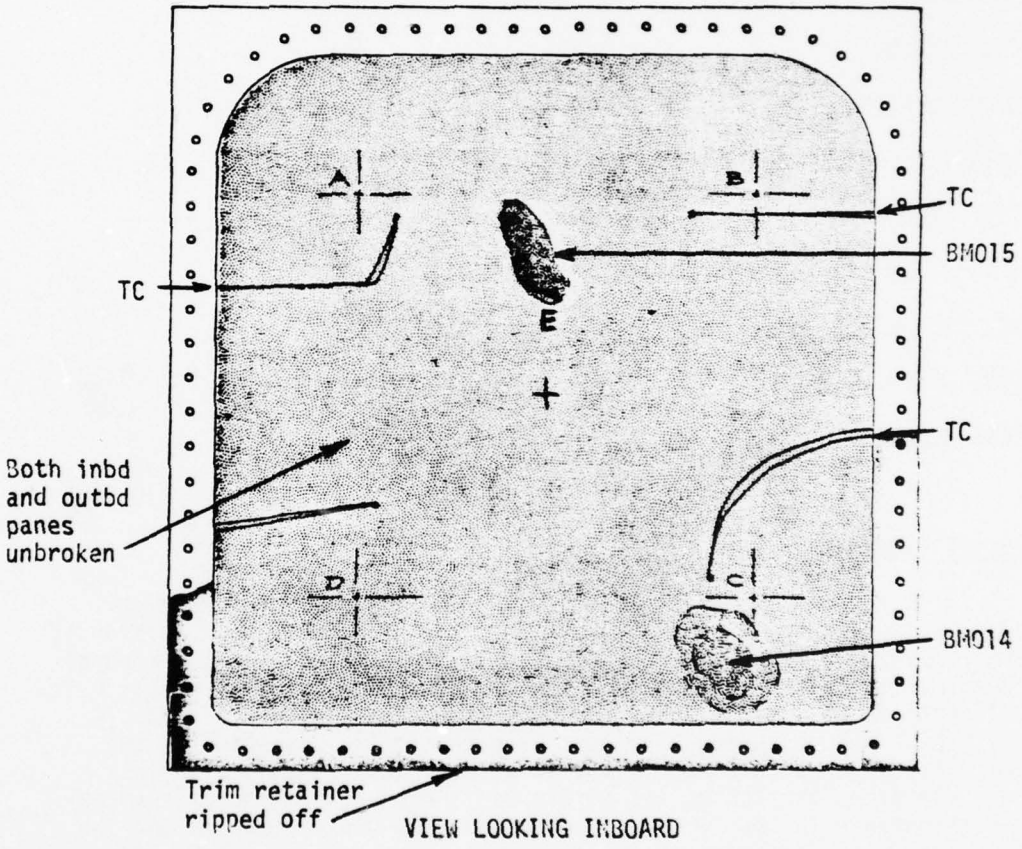

Figure A.12 Simulated aircraft windshield test Specimen Z5942639-501"B" (PPG002), test Numbers BM014, BM015.

AD-A071 814 DOUGLAS AIRCRAFT CO LONG BEACH CALIF F/G 1/3
HIGH SPEED BIRD IMPACT TESTING OF AIRCRAFT TRANSPARENCIES.(U)
JUN 78 M J COKER, R H MAGNUSSON F33615-75-C-3105
UNCLASSIFIED MDC-J7184 AFFDL-TR-77-98 NL

3 OF 3
AD
A071814

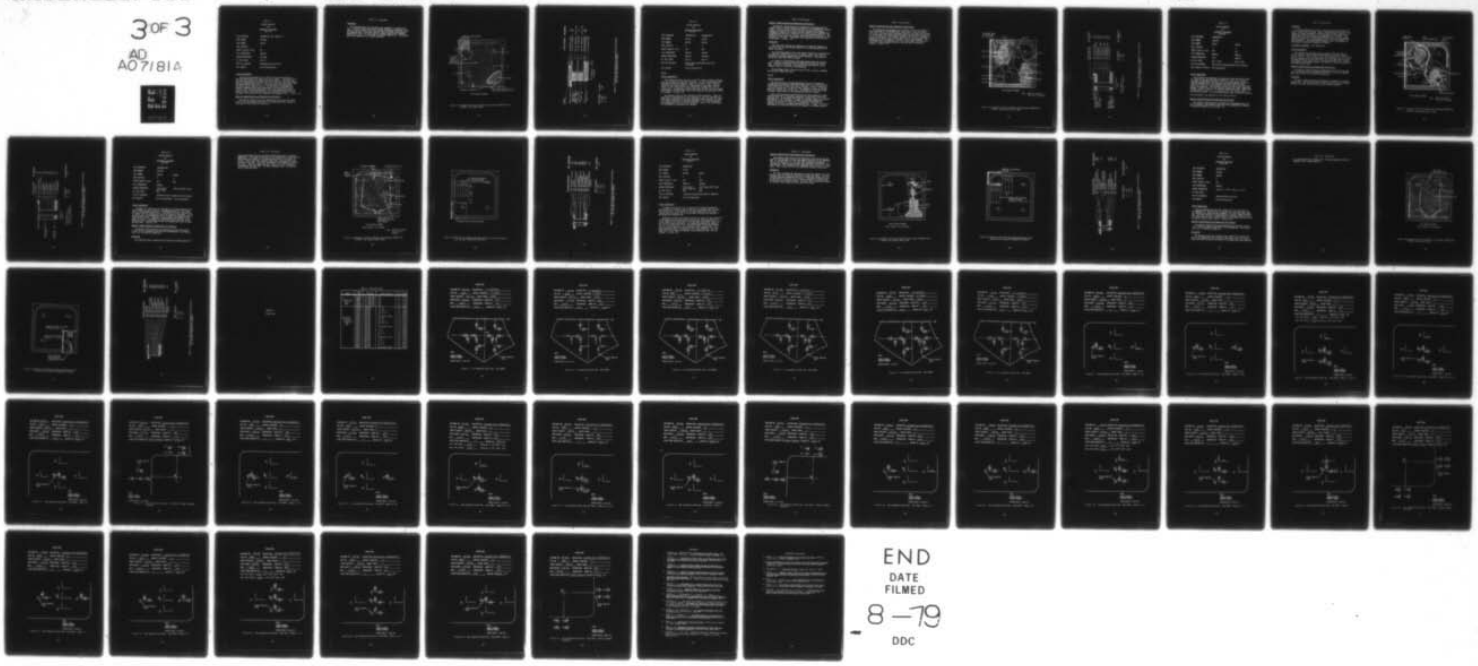

END
DATE FILMED
8-79
DDC

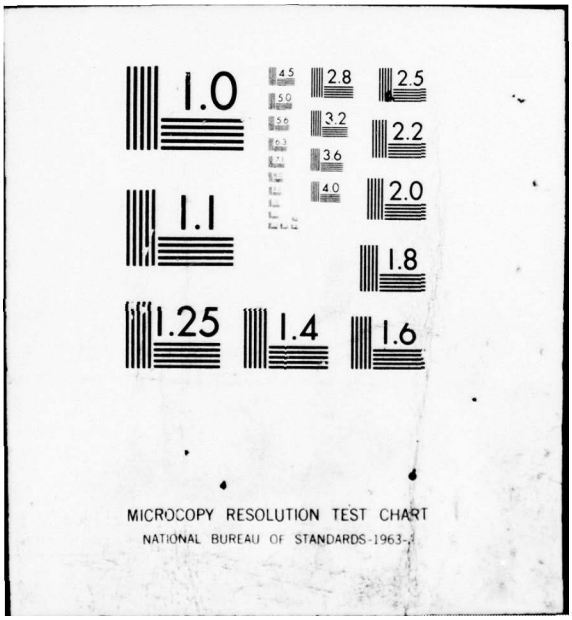
1.0
1.1
1.25
1.4
1.6
1.8
2.0
2.2
2.5
2.8
3.2
3.6
4.0
4.5
5.0
5.6
6.3
MICROCOPY RESOLUTION TEST CHART
NATIONAL BUREAU OF STANDARDS-1963-A

TABLE A.7.

FAILURE ANALYSIS
OF
WINDSHIELD SPECIMENS
(PPG-003)

TEST ENCLOSURE	5942639-501 Dwg. Change "B"
PART NUMBER	PPG-003
TEST NUMBER	BM-019
SHOT LOCATION	C
IMPACT VELOCITY (fps)	971
TEST TEMPERATURE	Ambient
WINDOW TEMPERATURE	Elevated
NO. BOLT HOLES	One (1)
TYPE OF ENCLOSURE	Laminated Glass Enclosure
TEST RESULTS	No Bird Penetration

Visual Examination

The bird shot impacted the "C" corner of the test enclosure at elevated temperatures and ruptured all glass panels. A good portion of the aluminum retainer was removed during bird impact. The outer panel bowed out approximately one inch, while the inner laminated panels bowed out approximately three inches. The entire panel was translucent, obviously with no residual vision. The chemically strengthened and thermally tempered glass panels exhibited a uniform and small glass particle size, indicating the panels had a high compression stress exterior surface in the tempered glass, and good center tension and ion exchange in the exterior of the chemically strengthened glass. (Figure A.13)

Material Identification and Dimensional Verification

The material identification and dimensional verification was very close to the requirements specified in P/N 5942639-501 Dwg., Change "B". See Figure A.14 for detailed comparison.

TABLE A.7. (Continued)

Discussion

The laminated glass test enclosure was successful in bagging the bird. The bird impact and elevated window temperature caused the interlayer to deflect significantly and resulted in permanent deformation in the impacted area. This test seemed to demonstrate the bird bagging capability of PPG's 112 interlayer at elevated temperature. The attachment holes appeared to be in good condition.

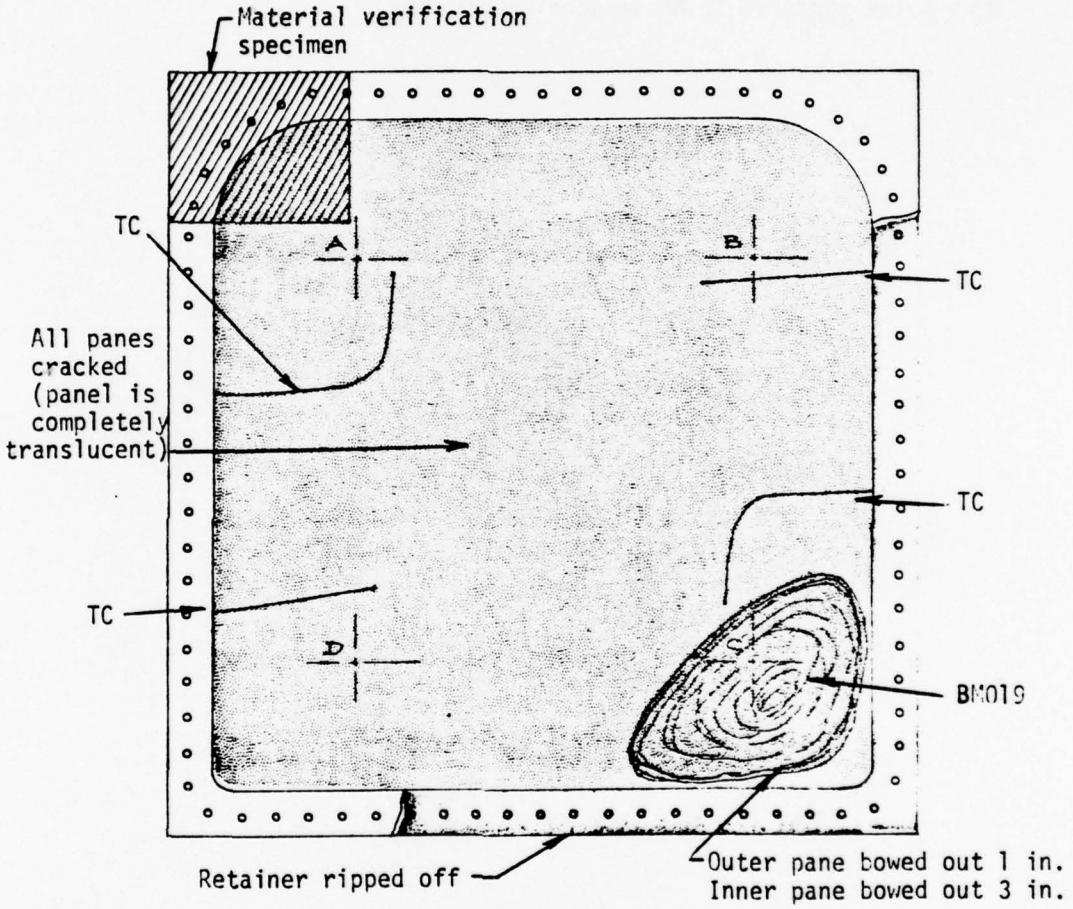

Figure A.13 Simulated aircraft windshield test specimen Z5942639-501"B" (PPG003), test Number BM019.

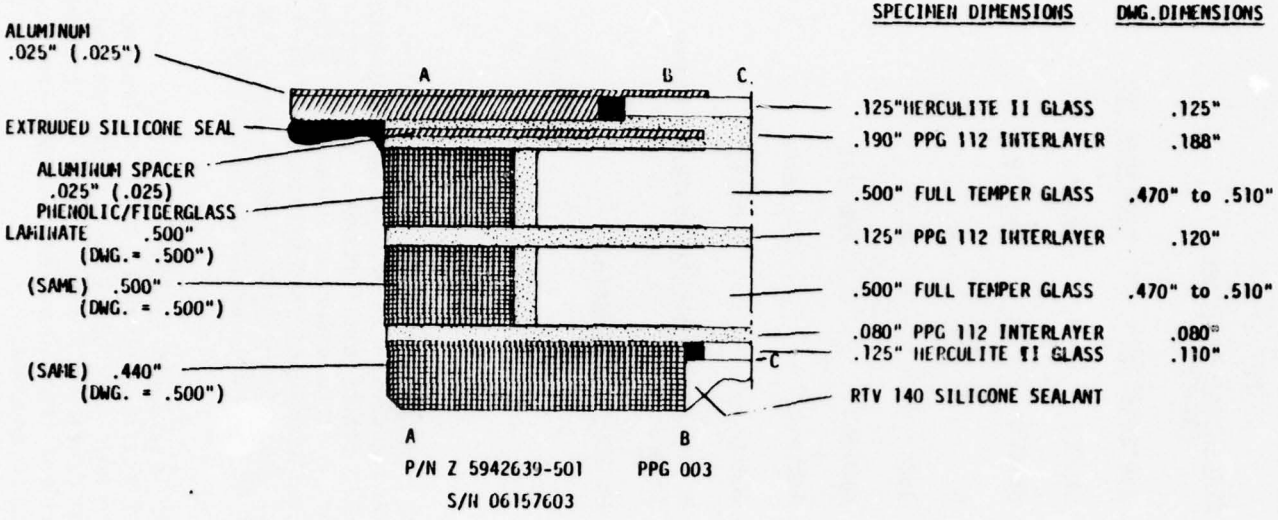

TOTAL THICKNESS	DWG. TOTAL
A. 2.020"	1.980
B. 2.029"	
C. 1.578"	

Figure A.14 Material identification and dimensional verification, test specimen Z5942639-501 (PPG003).

TABLE A.8.

FAILURE ANALYSIS
OF
WINDSHIELD SPECIMENS
(SK-001)

TEST ENCLOSURE	Z5942640-501	Z5942640-501
PART NUMBER	SK-001	SK-001
TEST NUMBER	BM-020	BM-018
SHOT LOCATION	A	C
IMPACT VELOCITY (fps)	958	847
TEST TEMPERATURE	Ambient	Ambient
WINDOW TEMPERATURE	Ambient	Elevated
NO. BOLT HOLES	One (1)	One (1)
TYPE OF ENCLOSURE	Multi-layer polycarbonate/silicone Interlayer	
TEST RESULTS	No Bird Penetration	

BM-020

Visual Examination

The 4-pound bird that was shot at the "A" corner at ambient temperature did not penetrate the test enclosure. All the polycarbonate plies exhibited primary and secondary cracks and fissures. Very little delamination was noted, however, a large amount of interlayer internal "tear" or tear fissures was quite evident just outside this bird impacted area. The presence of these interlayer fissures are quite common to elastomeric polymer under high strain condition that may occur during bird impact. (Figure A.15)

The exterior layer of the interlayer failed cohesively. There was absolutely no delamination of any interlayer at the bird impacted area. Some cracks terminated at the edge attachment holes; however, no cracks or fissures propagated to the panel periphery. All of the attachment holes appeared to be in excellent condition. Most of the strain gauge and thermocouples appeared to be unbonded.

TABLE A.8. (Continued)

Material Identification and Dimensional Verification

The material identification and dimensional verification was extremely close to the requirements specified in P/N Z5942640-501 Drawing, except a 1/8-inch thick x 1-1/4 inch wide reinforced nylon/epoxy laminate was bonded with RTU-630 Silicone sealant to the aluminum edge attachment and the first (interior) ply of polycarbonate material. The drawing calls out that the silicone interlayer should extend out to the periphery of the panel. Attachment holes appeared to be drilled at a slight angle. (Figure A.16)

Discussion

This test panel depicts the importance of interlayer adhesion to the multi-plies of polycarbonate material for achieving maximum bird impact resistance.

The oustanding observation is the lack of unbonding or delamination of interlayer, especially in the bird impacted area. This shot was conducted at elevated temperatures, which provided a large amount of deflection under high velocity impact.

All layers of polycarbonate exhibited primary shear and tensile/shear concentric cracks and fissures emanating from the bird strike area. A series of secondary slow tensile and tensile/shear cracks emanated from all the plies of polycarbonate.

The attachment holes, relative to hole finish, ovality, alignment and crazing, looked very good.

BM-018

Visual Examination

The high velocity, elevated temperature bird shot successfully bounced the bird package, producing minimum cracks. All four plies of polycarbonate had at least one crack or fissure. There is hardly any notice of primary shear or tensile shear concentric cracks or fissure emanating from the bird strike area. The majority of the cracks were secondary, smooth ductile, fast propagating tensile fracture.

Again, the outstanding observation was the total absence of interlayer delamination or unbonding, especially in the plies in the bird impacted area. An extremely small area of incipient "tears" or "fissure" was present in the interlayer. Perhaps the elevated temperatures affected the modular of elasticity of elastomeric interlayer, as compared to the previous ambient temperature shot. Figure A.15 depicts the absence of cracks and fractures, and removal of aluminum retainer.

TABLE A.3. (Continued)

Material Identification and Dimensional Verification

The dimensional requirements were extremely close to the requirements specified in P/N Z5942640-500, except that a 1/8-inch thick X 1-1/4 inch reinforced wide nylon/epoxy laminate was bonded with RTU-630 silicone sealant to aluminum edge attachment, and the first (exterior) ply of polycarbonate. The drawing specifies the silicone interlayer to extend out to the periphery of the panel with no reinforcement. The attachment holes all appeared to be on a slight angle, resulting in a little more edge attachment material than the panels prepared by Swedlow. (Figure A.16)

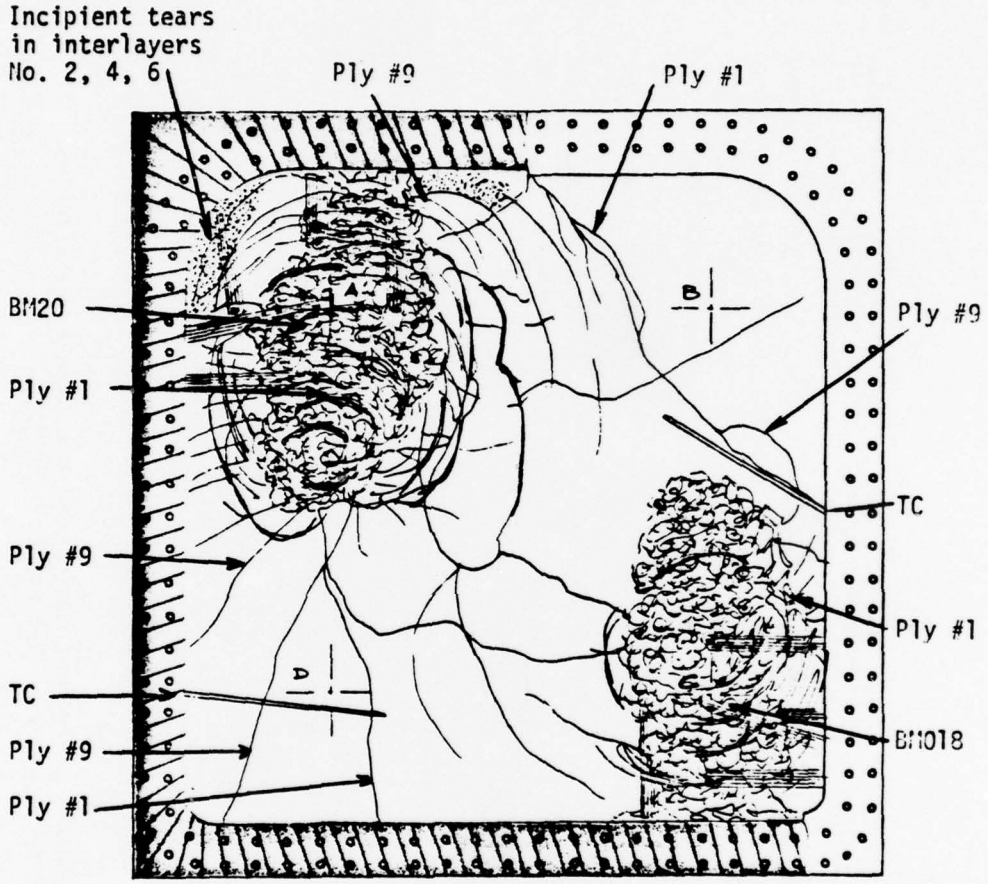

VIEW LOOKING INBOARD

Note: Refer to Figure 6
for ply I.D. numbers.

Figure A.15 Simulated aircraft windshield test Specimen Z5942640-501 (SK001), test Numbers BM018, BM020.

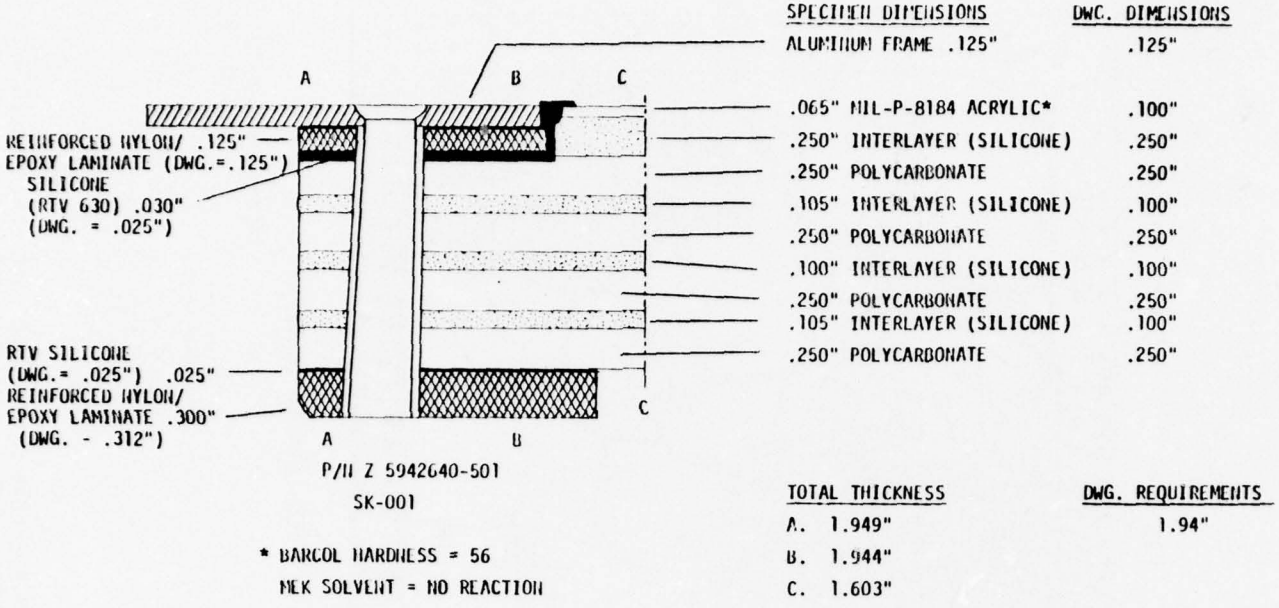

Figure A.16 Material identification and dimensional verification, test specimen Z5942640-501 (SK001).

TABLE A.9.

FAILURE ANALYSIS

OF

WINDSHIELD SPECIMENS
(SWU-003)

TEST ENCLOSURE	Z5942640-501	
PART NUMBER	SWU-003	
TEST NUMBER	BM-021	BM-022
SHOT LOCATION	A	C
IMPACT VELOCITY (fps)	960	847
TEST TEMPERATURE	Ambient	Ambient
WINDOW TEMPERATURE	Cold	Ambient
NO. BOLT HOLES	One (1) Row	One (1) Row
TYPE OF ENCLOSURE	Multi-layer polycarbonate/silicon laminate	
TEST RESULTS OF BM-021	Bird Penetration	

Visual Examination

The 4-pound bird penetrated and punctured a hole through the upper "A" corner of the test enclosure as shown in Figure A.17. Severe interlayer delamination occurred in all plies and extended concentric from the impacted area. The unbonded and bonded interlayer both exhibited a series of minute internal tears or fissure, indicating high strain rate exposure. The aluminum trim retainer was almost completely removed. Several inches of the aluminum frame was missing. These areas are depicted in Figure A.17. A large piece of (#9) polycarbonate ply was also missing. All polycarbonate plies were cracked and ruptured.

Edge attachment holes appeared to be in good condition.

Material Identification and Dimensional Verification

The material identification and dimensional requirements were very close to material and dimension specified in P/N Z5942640-501 Drawing. For detailed comparison, see Figure A.18.

TABLE A.9. (Continued)

Discussion

The failure mode was identical to the previous SWU fabricated 36 inch x 36 inch test enclosure. Again, severe delamination upon initial impact, followed by concentric shear and tensile shear cracking and rupturing of individual plies of polycarbonate was evidenced. The impact resistance of the delaminate composite test panel was reduced basically to 4 plies of polycarbonate, with 4 plies of unbonded silicone interlayer. The polycarbonate seemed to have large amounts of contamination dispersed throughout the sheets.

Test Result of BM-022 - Bird Penetration

Visual Examination

The 4-pound bird penetrated and punctured through the lower "C" corner, leaving a fairly large residual opening as shown in Figure , and Figure A.17. Even though the shot was conducted at ambient temperature as compared to the low temperature shot, the same type of failure and mode of failure occurred as in the previous BM-021 shot. Primary and secondary cracks were slightly less because of ambient temperature and slower impact speed.

Material Identification and Dimensional Verification

The material identification and dimensional verification was very close to the materials and dimensions specified in Dwg. P/N Z5942640-501. See Figure A.18 for detailed comparisons.

Discussion

The failure mode and ruptured surface was the same as in previous BM-021 shots. New findings were not observed, other than the residual opening left after the shot, which was the largest observed.

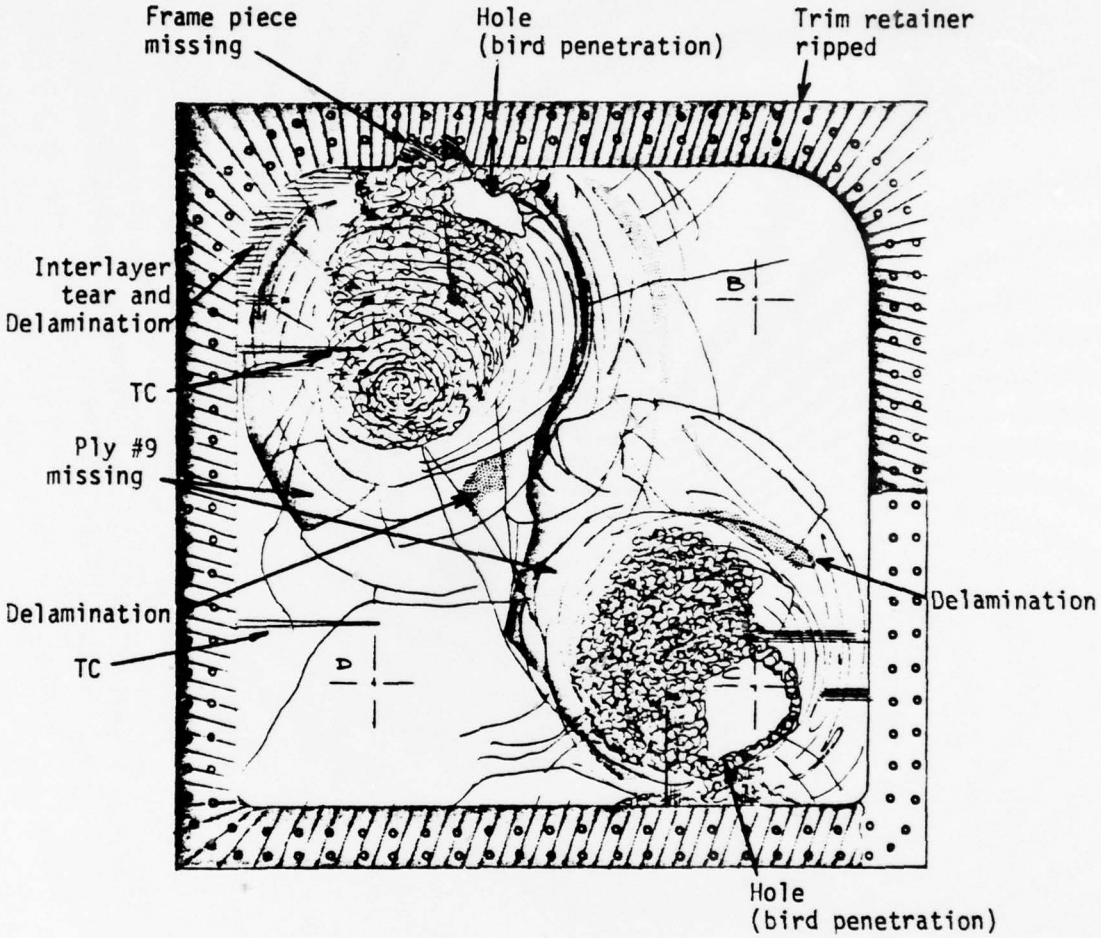

VIEW LOOKING INBOARD

Note: Refer to Figure 6 for ply I.D. number

Figure A.17 Simulated aircraft windshield test Specimen Z5942640-501 (SWU003), Test Numbers BM021, BM022.

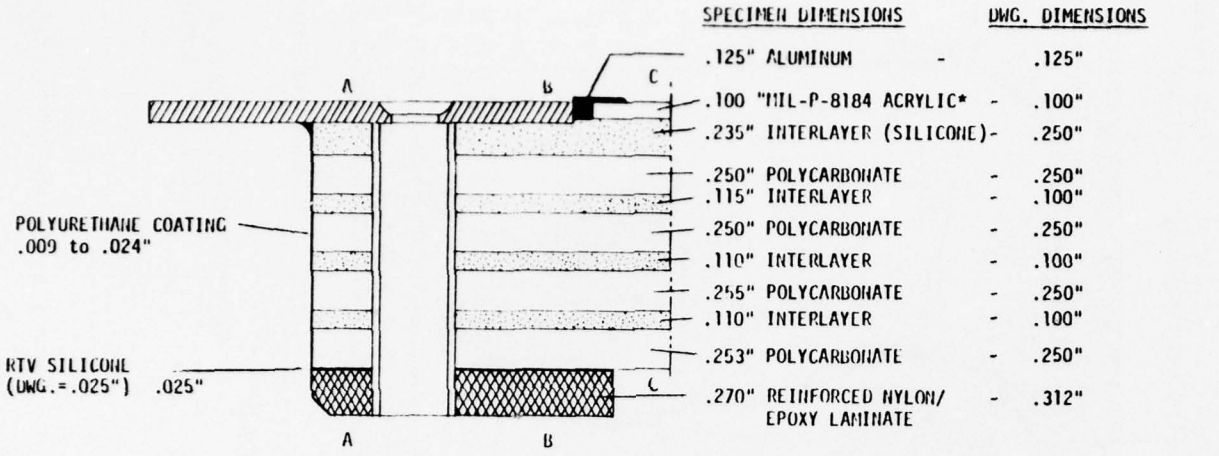

Figure A.18 Material identification and dimensional verification, test specimen Z5942640-501 (SWU003).

TABLE A.10

FAILURE ANALYSIS

OF

WINDSHIELD SPECIMENS
(PPG-004)

TEST ENCLOSURE	Z5942639-503	
PART NUMBER	PPG 004	
TEST NUMBER	BM-023	BM-028
SHOT LOCATION	C	B
IMPACT VELOCITY (fps)	953	940
TEST TEMPERATURE	Ambient	
WINDOW TEMPERATURE	161°F Outer/ 131°F Inner	-23°F outer/35°F Inner
NO. BOLT HOLES	One	
TYPE OF ENCLOSURE	Laminated Plastic Composite Test Enclosure	
TEST RESULTS	No Bird Penetration	Bird Penetration

Visual Examination

The upper "C" corner was bird impacted at elevated temperature and only cracked the outer chemically strengthened glass ply. All other plies of transparency were intact. The BM-028 bird shot impacted the "B" corner at a low temperature, and bird penetration was made. The #3, #5 and #7 plies of polycarbonate failed in shear and a combination of tensile/shear cracks. There was slight permanent deformation in the upper "B" corner. The chemically strengthened glass particle dicing characteristics indicated good surface ion exchange and center surface tension value. (Figure A.19)

Material Identification and Dimensional Verification

The material identification and dimensional verification agreed closely to the requirement specified in P/N 5942639-503. See Figures A.20, A.21 for detailed comparison.

Discussion

The laminated plastic composite test enclosure exhibited good bird

TABLE A.10. (Continued)

bouncing characteristics on the initial BM-023 test shot at elevated temperature. The second shot BM-028 at low temperature resulted in bird penetration and cracked all the polycarbonate plies in the upper "B" corner. These cracks were primarily shear and a combination of shear and tensile failures. The cracks propagated to the immediate edges of the panel. Specified damage was done. Panel #3 and #5 fractured in approximately the same area. The edge attachment holes all appeared to be in good condition.

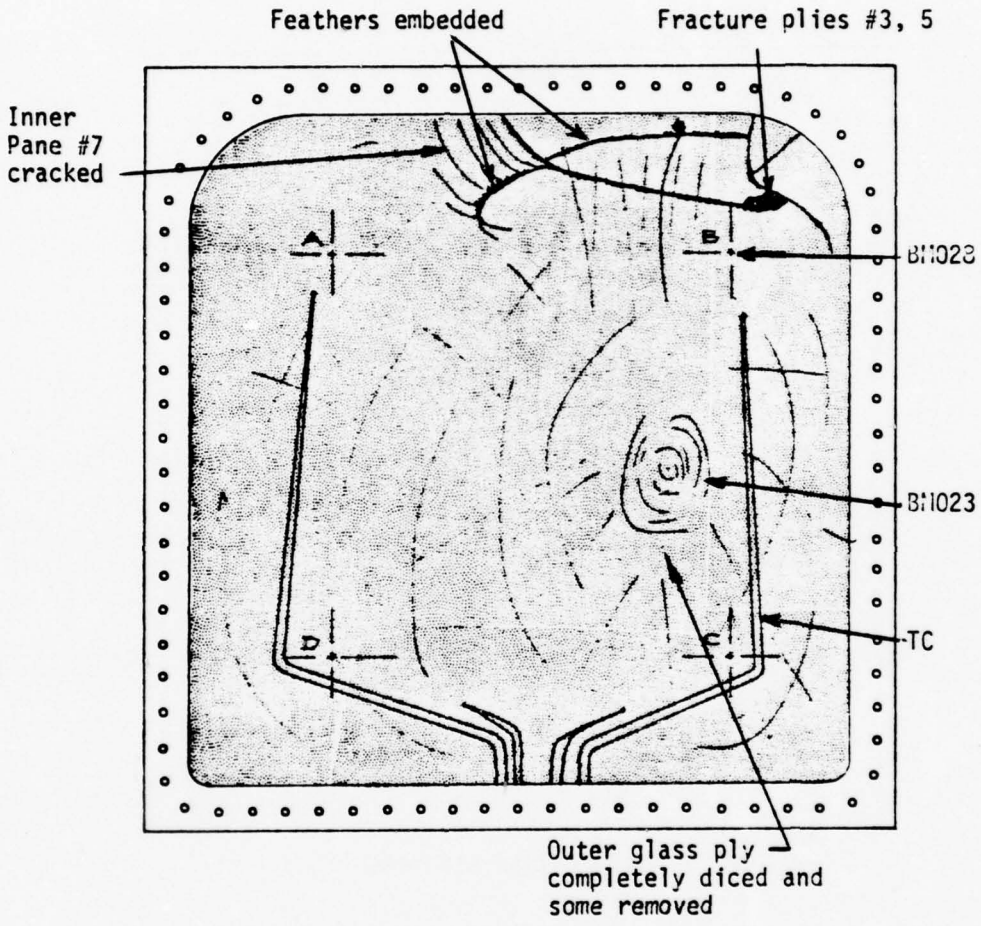

VIEW LOOKING INBOARD

Panel Weight = 97.0 pounds

Note: Refer to Figure 7 for ply I.D. number.

Figure A.19 Simulated aircraft windshield test Specimen Z5942639-503 (PPG004), test Numbers BM023, BM028.

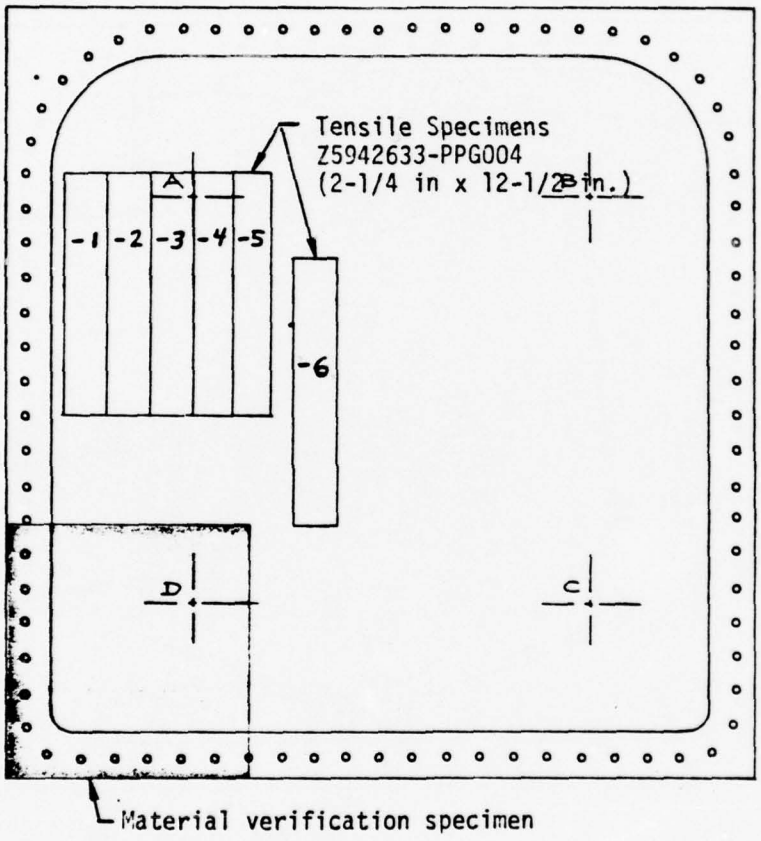

Figure A.20 Material verification specimens, simulated aircraft windshield test Specimen Z5942639-503 (PPG-004).

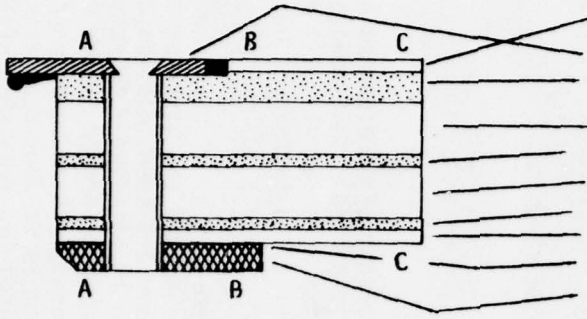

SPECIMEN DIMENSIONS	DWG. DIMENSIONS
.100" HERCULITE II GLASS	.100"
.135" ALUMINUM	.125"
.250" PPG 112 INTERLAYER	.250"
.500" POLYCARBONATE	.500"
.095" PPG 112 INTERLAYER	.100"
.495" POLYCARBONATE	.500"
.095" PPG 112 INTERLAYER	.100"
.125" POLYCARBONATE	.125"
.010" RTV INTERLAYER	
.275" PHENOLIC/FIBERGLASS LAMINATE	.320"

TOTAL THICKNESS	DWG. THICKNESS
A. 1.950"	1.94"
B. 1.953"	
C. 1.670"	

Figure A.21 Material identification and dimensional verification, test specimen Z5942639-503 (PPG004).

TABLE A.11.

FAILURE ANALYSIS

OF

WINDSHIELD SPECIMENS
(SK-002)

TEST ENCLOSURE	5942640-507	
PART NUMBER	SK 002	
TEST NUMBER	BM-026	BM-027
SHOT LOCATION	C	B
IMPACT VELOCITY (fps)	939	920
TEST TEMPERATURE	Ambient	Ambient
WINDOW TEMPERATURE	213°F Outer/ 143°F Inner Ply	-40°F Outer/+35°F Inner Ply
NO. BOLT HOLES	One	One
TYPE OF ENCLOSURE	Laminated polycarbonate plastic composite	
TEST RESULTS	No Bird Penetration	

Visual Examination

A 4-pound bird shot at the "C" corner of an elevated temperature test enclosure successfully bounced the bird and damaged only the outer thin acrylic ply. A few cracks in the outer acrylic ply and interlaminar shear failure of the silicone based interlayer was observed in and around the impacted area.

Another bird strike was conducted at the "B" corner of test enclosure at low temperature and successfully bounced the bird, producing only slight damage of the outer acrylic ply and some interlaminar shear failure of the silicone interlayer. The outstanding observation made was the lack of delamination of the interlayer bonded to the polycarbonate plies at both elevated and low temperature bird impacted shots. The edge attachment holes all appeared to be in good condition. The test panel had a large amount of residual vision remaining after two bird strikes. (Figure A.22)

TABLE A.11. (Continued)

Material Identification and Dimensional Verification

The material identification and dimensional verification was not exactly in accordance with the requirements specified in P/N Z5942640-507. A 1/8-inch thick x 1-1/4 inch wide reinforced nylon/epoxy laminate was bonded to the aluminum edge attachment with RTU-630 silicone sealant. The attachment holes appeared to be drilled at a slight angle. See Figures A.23, A.24 for additional detailed comparisons.

Discussion

This test indicated the importance of interlayer adhesion to transparency plies for achieving maximum bird impact resistance. The outstanding observation made was the lack of interlayer delamination and no rupturing or cracking of the structural transparent plastic plies during a hot and cold bird strike. The panel had a significant amount of residual vision remaining after both bird strikes.

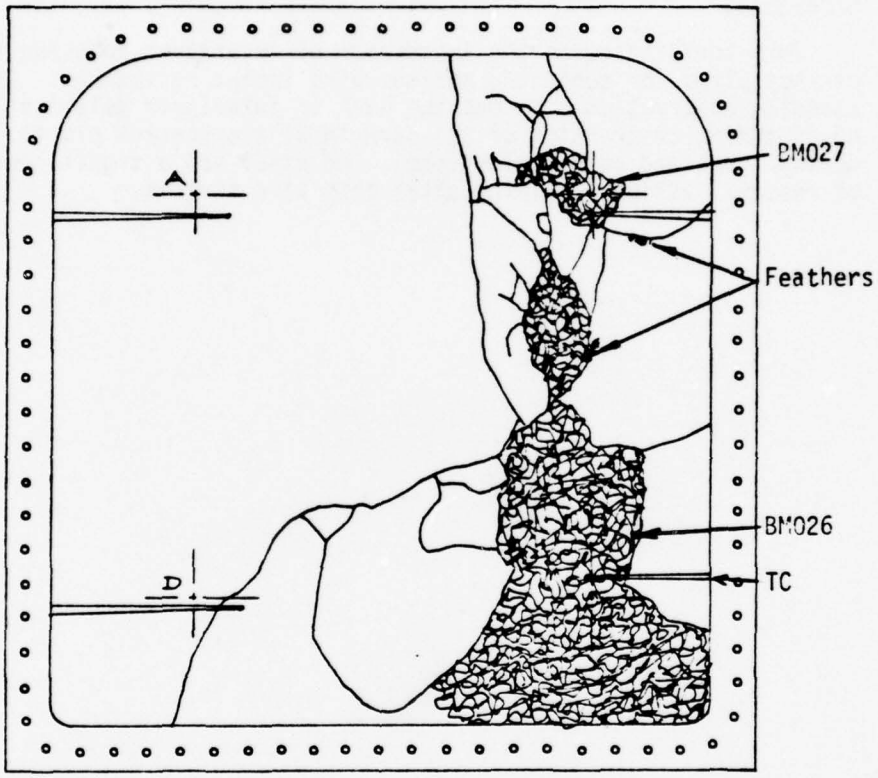

VIEW LOOKING INBOARD

Panel Weight = 37-1/2 Pounds

Figure A.22 Simulated aircraft windshield test Specimen Z5942640-507"B" (SK002), test Numbers BM026, BM027.

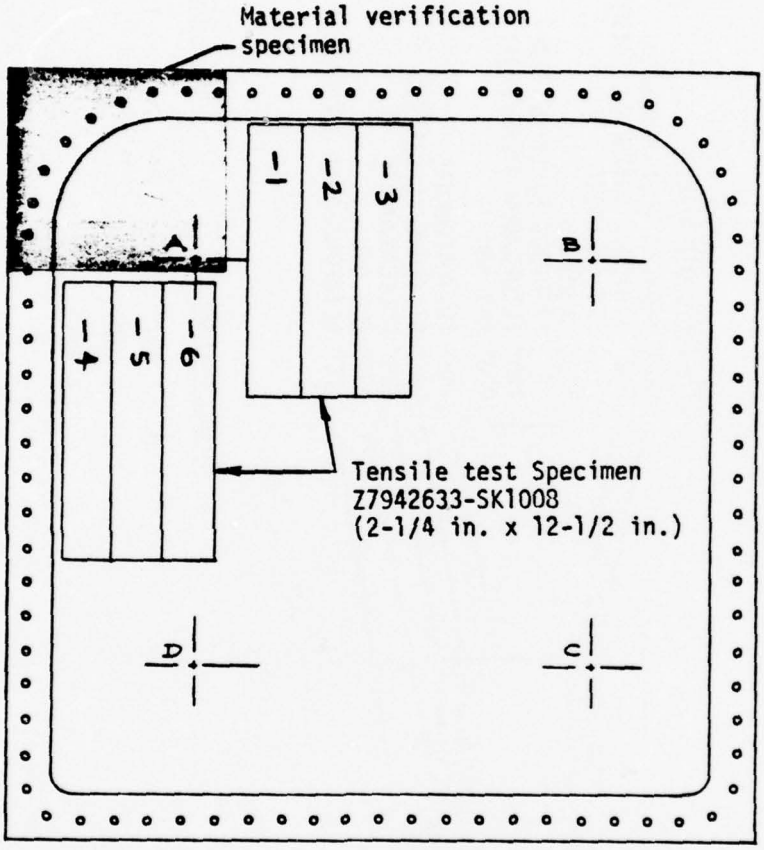

Figure A.23 Material verification specimens, simulated aircraft windshield test Specimen Z5942640-507 (SK002).

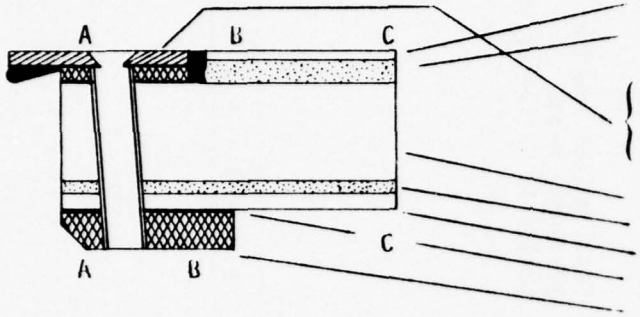

SPECIMEN DIMENSIONS		DWG. DIMENSIONS
.080"	ACRYLIC (MIL-P-8184)	.100"
.242"	SILICONE INTERLAYER (CP) RTV SILICONE	.250"
.125"	ALUMINUM EXTRUDED SILICONE SEAL	.125"
.140"	REINFORCED NYLON/EPOXY	
.020"	RTV 630	
.940"	POLYCARBONATE	.870"
.125"	SILICONE INTERLAYER	.120"
.150"	POLYCARBONATE	.150"
.030"	RTV 630	
.375"	REINFORCED NYLON/EPOXY	.500"

TOTAL THICKNESS	DWG. REQUIREMENTS
A. 1.957"	1.94"
B. 1.948"	
C. 1.535"	

Figure A.24 Material identification and dimensional verification, test specimen Z5942640-507 (SK002).

TABLE A.12.

FAILURE ANALYSIS
OF
WINDSHIELD SPECIMENS
(PPG-005)

TEST ENCLOSURE	5942639-505
PART NUMBER	PPG 005
TEST NUMBER	BM-029
SHOT LOCATION	B
IMPACT VELOCITY (fps)	931
TEST TEMPERATURE	Ambient
WINDOW TEMPERATURE	Outer Ply - 28°F, inner ply + 35°F
NO. BOLT HOLES	
TYPE OF ENCLOSURE	Laminated Glass Enclosure
TEST RESULTS	No Bird Penetration

Visual Examination

The bird impacted the lower "B" corner of the test enclosure at low temperature. There was no bird penetration; only the outer glass ply ruptured into finely divided fragments. No other damage was observed. The outer chemically strengthened ply exhibited a small and uniform glass particle size, indicating good ion exchanged surface, as well as central surface tension value. (Figure A.25)

Material Identification and Dimensional Verification

The material identification and dimensional verification was very close to the requirements specified in P/N Z5942629-505. See Figures A.26, A.27 for detailed comparison.

Discussion

The laminated glass test enclosure was successful in bouncing the bird at low temperature and relatively high speed. PPG's 112 interlayer exhibited sufficient resiliency at low temperature when subjected

TABLE A.12. (Continued)

to a high velocity bird impact shot. The edge attachment holes all appeared to be in good condition.

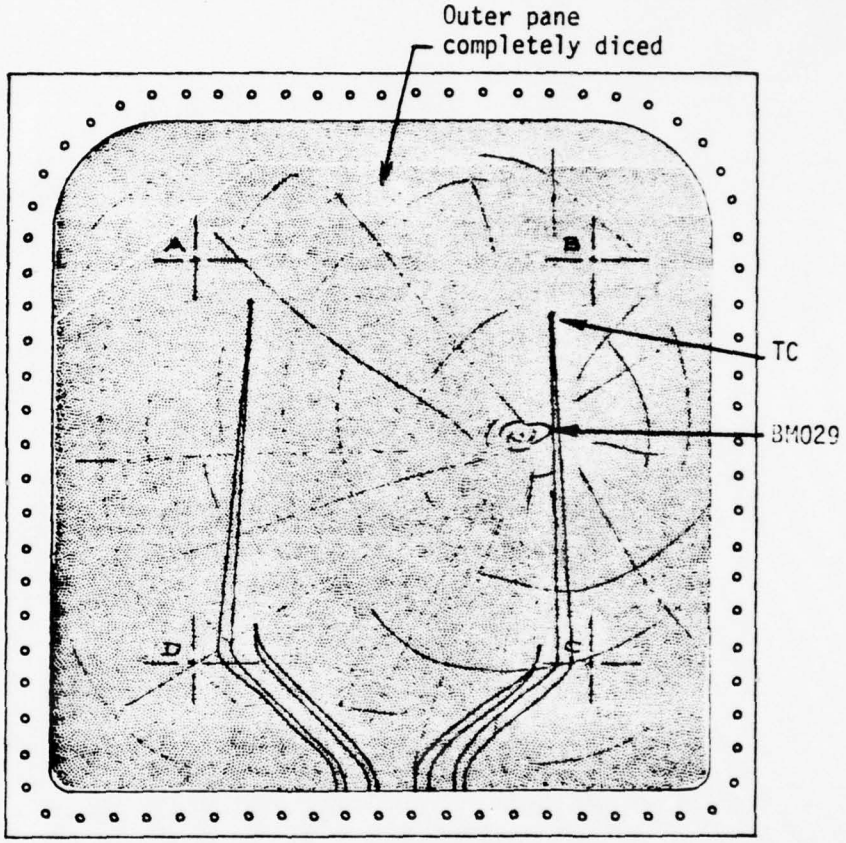

VIEW LOOKING INBOARD

Panel Weight = 94-1/4 Pounds

Figure A.25 Simulated aircraft windshield test Specimen Z5942639-505 (PPG005), test Number BM029.

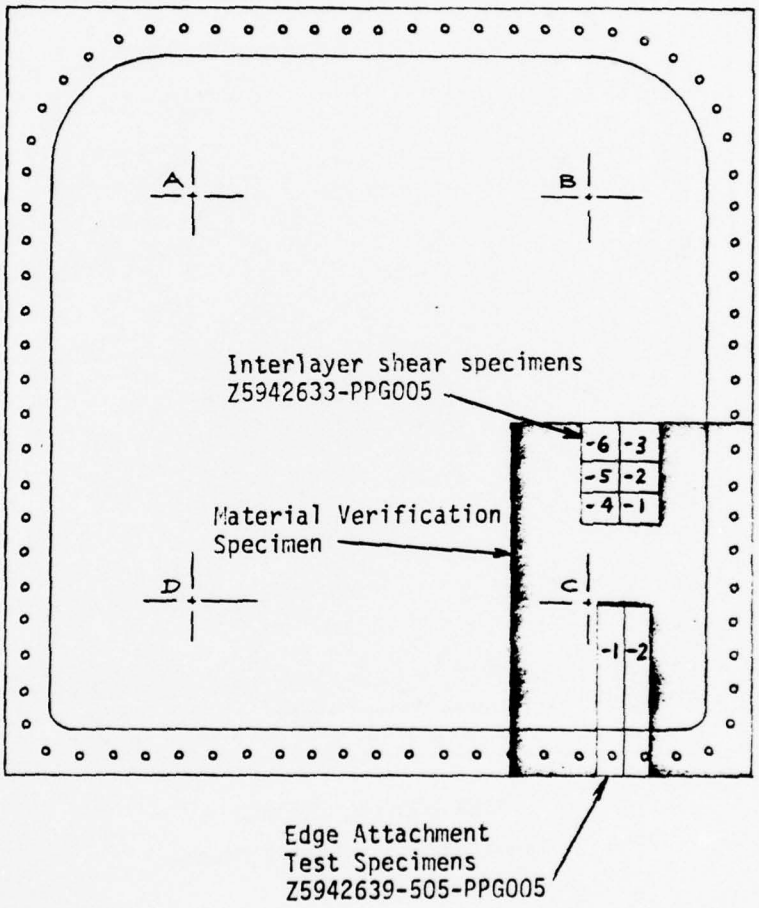

Figure A.26 Material verification specimens, simulated aircraft windshield test Specimen Z5942639-505 (PPG005).

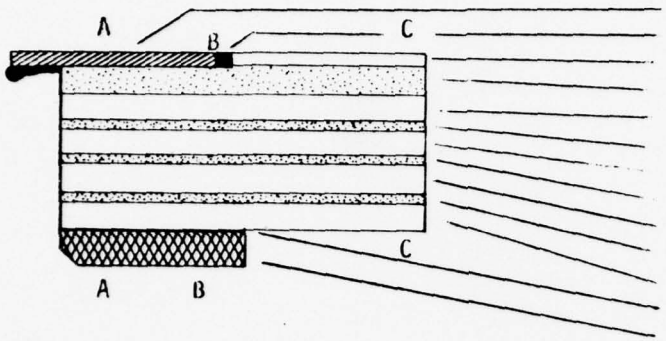

SPECIMEN DIMENSIONS	DWG. DIMENSIONS
.125" ALUMINUM	.125"
.100" RTV 630	
.110" HERCULITE II GLASS	.100"
.255" PPG 112 INTERLAYER	.250"
.245" POLYCARBONATE	.250"
.095" PPG 112 INTERLAYER	.100"
.245" POLYCARBONATE	.250"
.095" PPG 112 INTERLAYER	.100"
.245" POLYCARBONATE	.250"
.095" PPG 112 INTERLAYER	.100"
.245" POLYCARBONATE	.250"
.010" RTV 630	
.320" PHENOLIC/FIBERGLASS LAMINATE	.320"

TOTAL THICKNESS	DWG. THICKNESS
A. 1.957"	1.94"
B. 1.965"	
C. 1.623"	

Figure A.27 Material identification and dimensional verification, test specimen Z5942639-505 (PPG005).

APPENDIX B

STRAIN MAPS

TABLE 8. STRAIN MAP INDEX

TEST	TEST NO.	SPECIMEN	STRAIN GAGE NO.	FIGURE	PAGE
B-1 Windshield Strain Map	BM004	B-1 SWU-108	All	B.1	215
	BM005	B-1 SWU-108	All	B.2	216
	BM006	B-1 SWU-107	All	B.3	217
	BM007	B-1 SWU-107	All	B.4	218
	BM008	B-1 SWU-107	All	B.5	219
	BM009	B-1 SWU-107	All	B.6	220
Simulated Aircraft Windshield Strain Map	BM012	PPG-001	11, 19	B.7	221
	BM012	PPG-001	12, 20	B.8	222
	BM012	PPG-001	13, 15, 17	B.9	223
	BM012	PPG-001	14, 16, 18	B.10	224
	BM012	PPG-001	21	B.11	225
	BM012	PPG-001	On Support Struc.	B.12	226
	BM013	PPG-001	11, 19	B.13	227
	BM013	PPG-001	12, 20	B.14	228
	BM013	PPG-001	13, 15, 17	B.15	229
	BM013	PPG-001	14, 16, 18	B.16	230
	BM013	PPG-001	21	B.17	231
	BM013	PPG-001	On Support Struc.	B.18	232
	BM014	PPG-002	1, 9	B.19	233
	BM014	PPG-002	2, 10	B.20	234
	BM014	PPG-002	3, 5, 7	B.21	235
	BM014	PPG-002	4, 6, 8	B.22	236
	BM014	PPG-002	22	B.23	237
	BM014	PPG-002	On Support Struc.	B.24	238
	BM019	PPG-003	1, 9	B.25	239
	BM019	PPG-003	2, 10	B.26	240
	BM019	PPG-003	3, 5, 7	B.27	241
	BM019	PPG-003	4, 6, 8	B.28	242
	BM019	PPG-003	22	B.29	243
	BM019	PPG-003	On Support Struc.	B.30	244

STRAIN MAP

SPECIMEN NO. SWU-108 DESCRIPTION B-1 Windshield

TEST NO. BM004 SUPPORT STRUCTURE B-1 Module

IMPACT VELOCITY 957 FPS IMPACT POINT Center

BIRD WEIGHT 4.00 lbs. TEMPERATURE - OUTER PLY 76°F

DATE 2-28-76 TEMPERATURE - INNER PLY NA

STRAIN GAGE MOUNTED ON Inside SURFACE OF Inner PLY

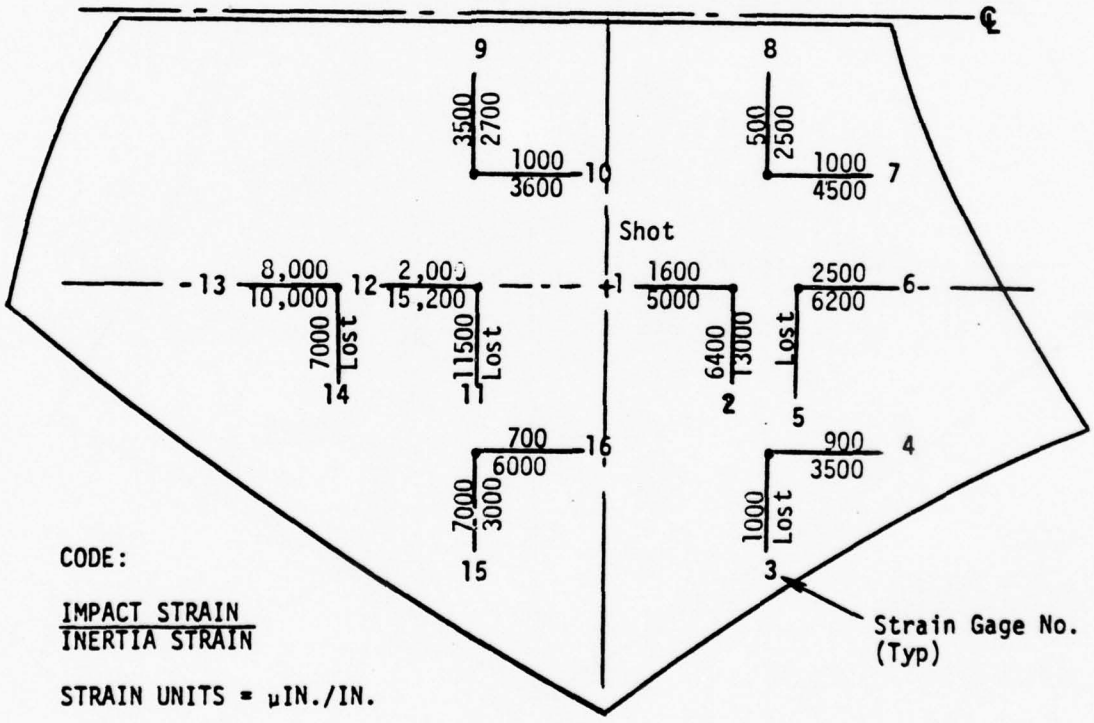

Figure B.1. B-1 Windshield Strain Map - Test BM004.

STRAIN MAP

SPECIMEN NO. SWU 108 DESCRIPTION B-1 Windshield

TEST NO. BM005 SUPPORT STRUCTURE B-1 Module

IMPACT VELOCITY 952 FPS IMPACT POINT Center

BIRD WEIGHT 4.07 lbs TEMPERATURE - OUTER PLY 40°F

DATE 3-09-76 TEMPERATURE - INNER PLY 55°F

STRAIN GAGE MOUNTED ON Inside SURFACE OF Inner PLY

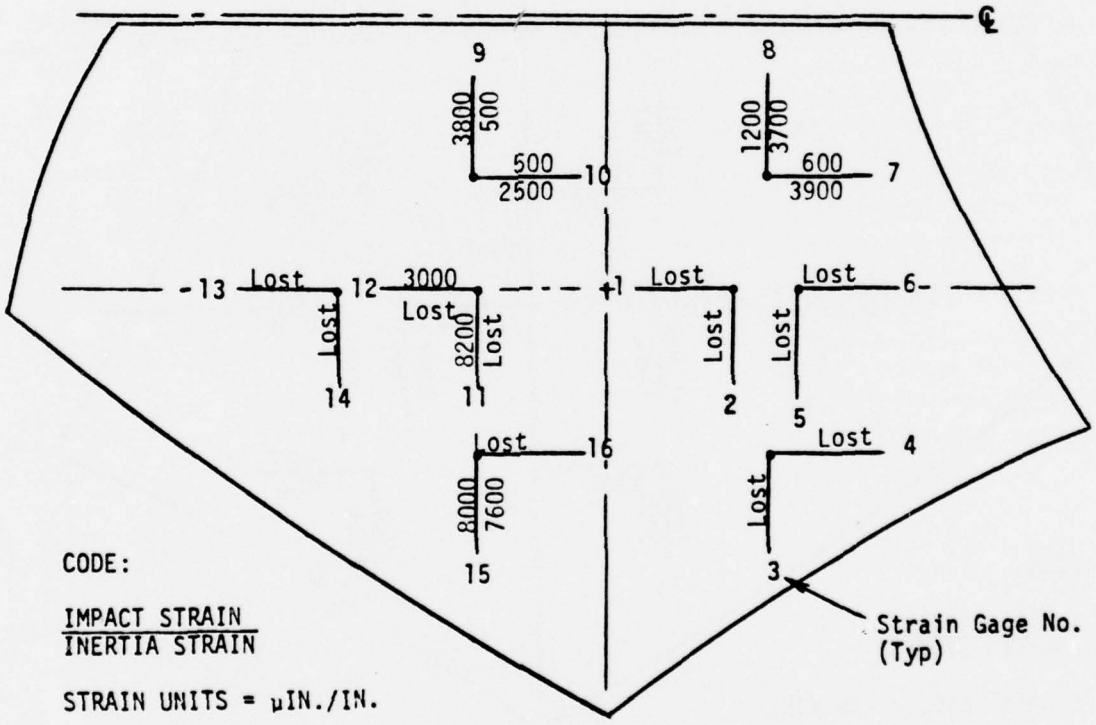

Figure B.2. B-1 Windshield Strain Map - Test BM005.

STRAIN MAP

SPECIMEN NO. SWU 107 DESCRIPTION B-1 Windshield

TEST NO. BM1006 SUPPORT STRUCTURE B-1 Module

IMPACT VELOCITY 967 FPS IMPACT POINT Center

BIRD WEIGHT 4.02 lbs TEMPERATURE - OUTER PLY 58°F

DATE 3-12-76 TEMPERATURE - INNER PLY 71°F

STRAIN GAGE MOUNTED ON Inside SURFACE OF Inner PLY

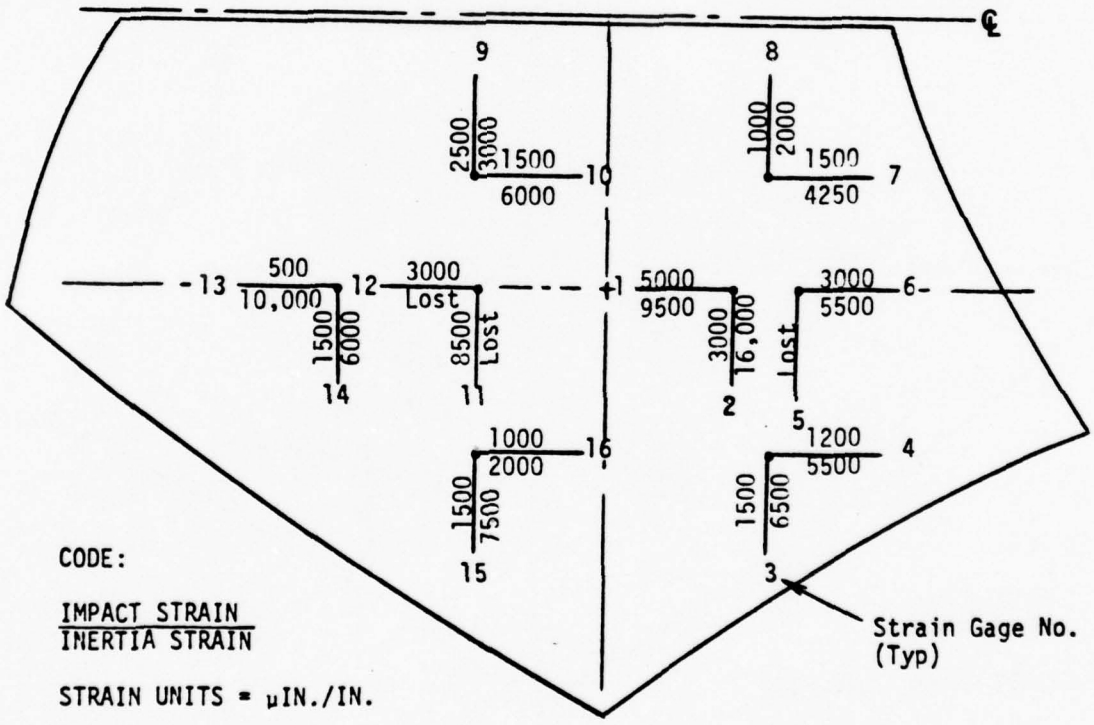

Figure B.3. B-1 Windshield Strain Map - Test BM006.

STRAIN MAP

SPECIMEN NO. SWU 107 DESCRIPTION B-1 Windshield

TEST NO. BM 007 SUPPORT STRUCTURE B-1 Module

IMPACT VELOCITY 936 FPS IMPACT POINT Center

BIRD WEIGHT 4.00 lbs TEMPERATURE - OUTER PLY 54°F

DATE 3-18-76 TEMPERATURE - INNER PLY 56°F

STRAIN GAGE MOUNTED ON Inside SURFACE OF Inner PLY

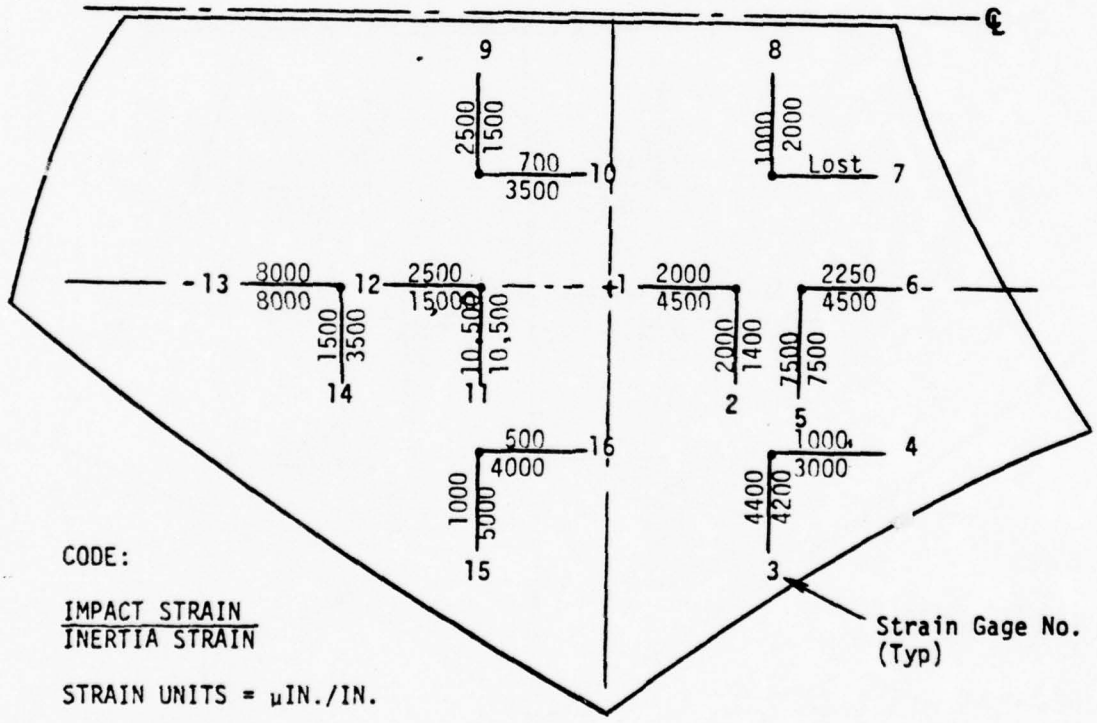

Figure B.4. B-1 Windshield Strain Map - Test BM007.

STRAIN MAP

SPECIMEN NO. SWU 107 DESCRIPTION B-1 Windshield

TEST NO. BM008 SUPPORT STRUCTURE B-1 Module

IMPACT VELOCITY 930 FPS IMPACT POINT Center

BIRD WEIGHT 4.02 lbs TEMPERATURE - OUTER PLY 68°F

DATE 3-20-76 TEMPERATURE - INNER PLY 66°F

STRAIN GAGE MOUNTED ON Inside SURFACE OF Inner PLY

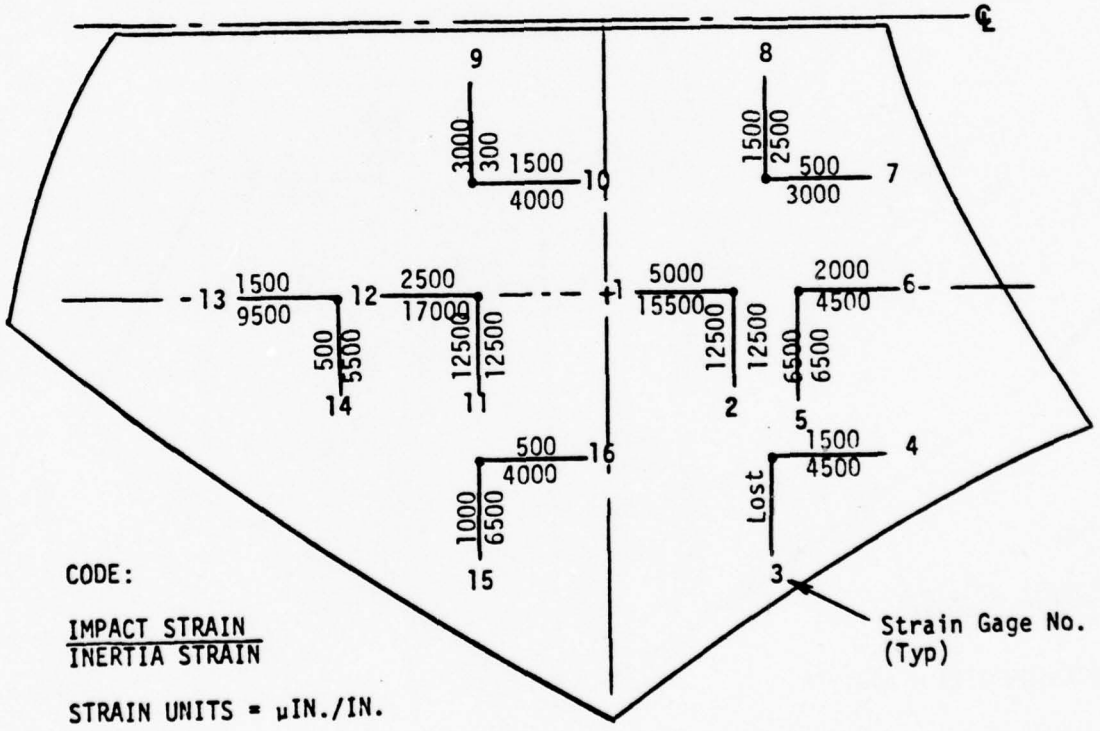

Figure 3.5. B-1 Windshield Strain Map - Test BM008.

STRAIN MAP

SPECIMEN NO. SWU 107 DESCRIPTION B-1 Windshield

TEST NO. BM009 SUPPORT STRUCTURE B-1 Module

IMPACT VELOCITY 952 FPS IMPACT POINT Center

BIRD WEIGHT 6.15 lbs TEMPERATURE - OUTER PLY 69°F

DATE 3-23-76 TEMPERATURE - INNER PLY 74°F

STRAIN GAGE MOUNTED ON Inside SURFACE OF Inner PLY

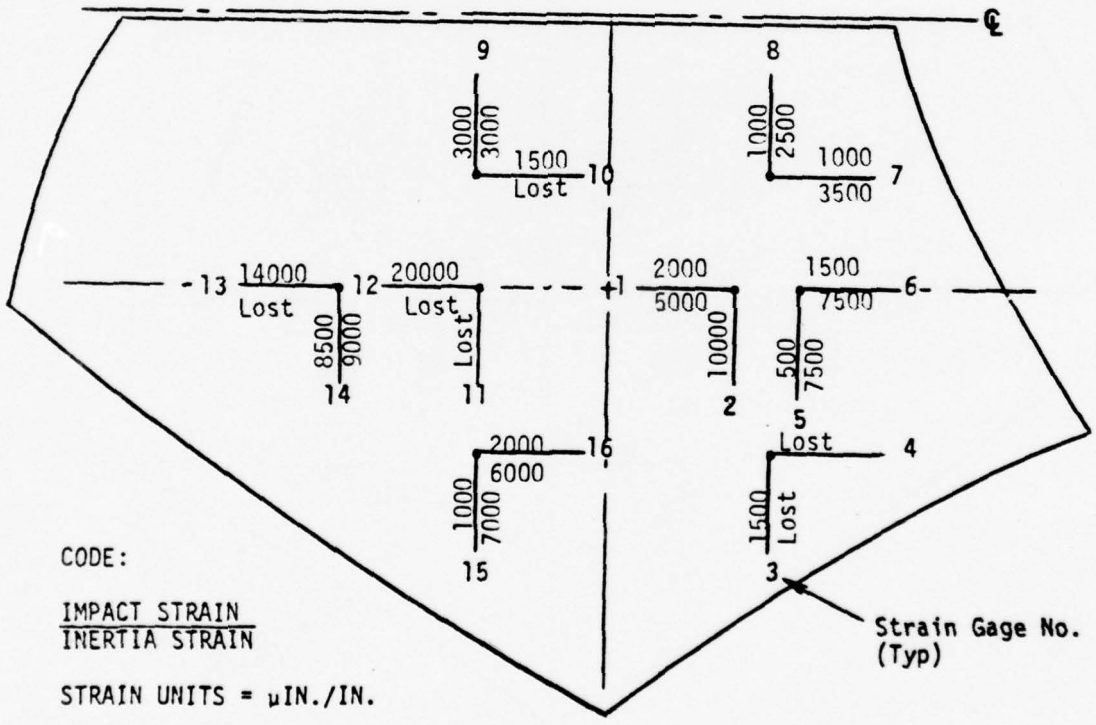

Figure B.6. B-1 Windshield Strain Map - Test BM009.

STRAIN MAP

SPECIMEN NO. PPG 001 DESCRIPTION Laminated Glass (Z5942639-501)

TEST NO. BM012 SUPPORT STRUCTURE GL

IMPACT VELOCITY 943 FPS IMPACT POINT A

BIRD WEIGHT 4.00 lbs TEMPERATURE - OUTER PLY -28°F

DATE 7-16-76 TEMPERATURE - INNER PLY 7°F

STRAIN GAGE MOUNTED ON -9 SURFACE OF outer PLY

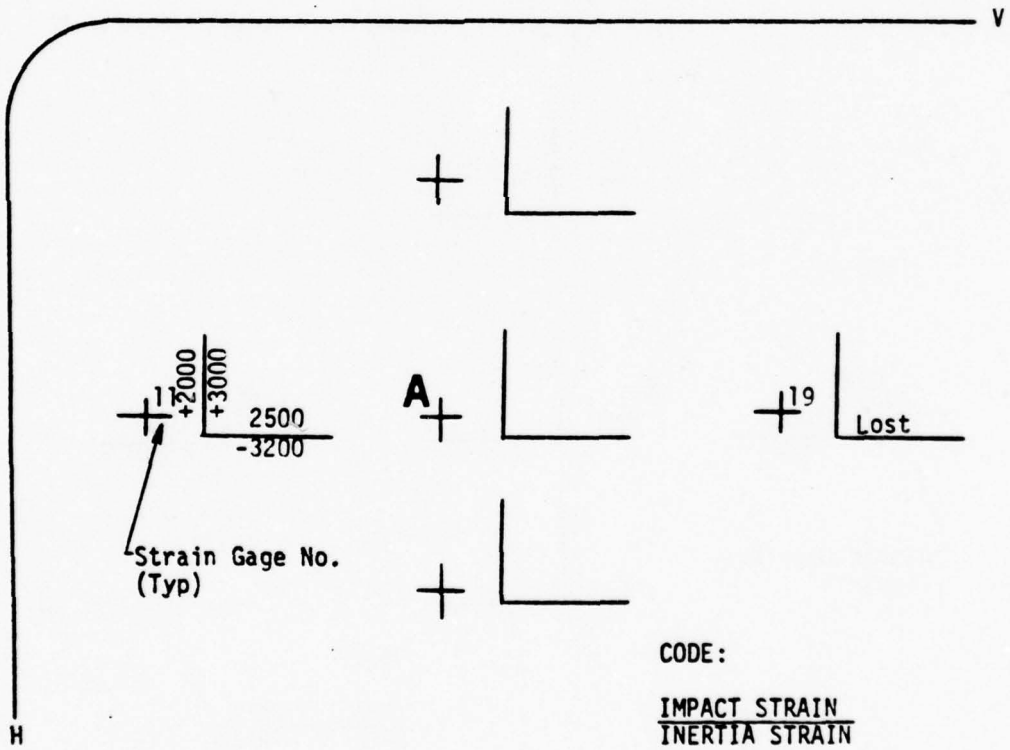

Figure B.7. Test Windshield Strain Map - Test BM012 - Gages 11, 19.

STRAIN MAP

SPECIMEN NO. PPG 001 DESCRIPTION Laminated Glass (Z5942639-501)

TEST NO. BM012 SUPPORT STRUCTURE GL

IMPACT VELOCITY 943 FPS IMPACT POINT A

BIRD WEIGHT 4.00 lbs TEMPERATURE - OUTER PLY -28°F

DATE 7-16-76 TEMPERATURE - INNER PLY 7°F

STRAIN GAGE MOUNTED ON -9 SURFACE OF inner PLY

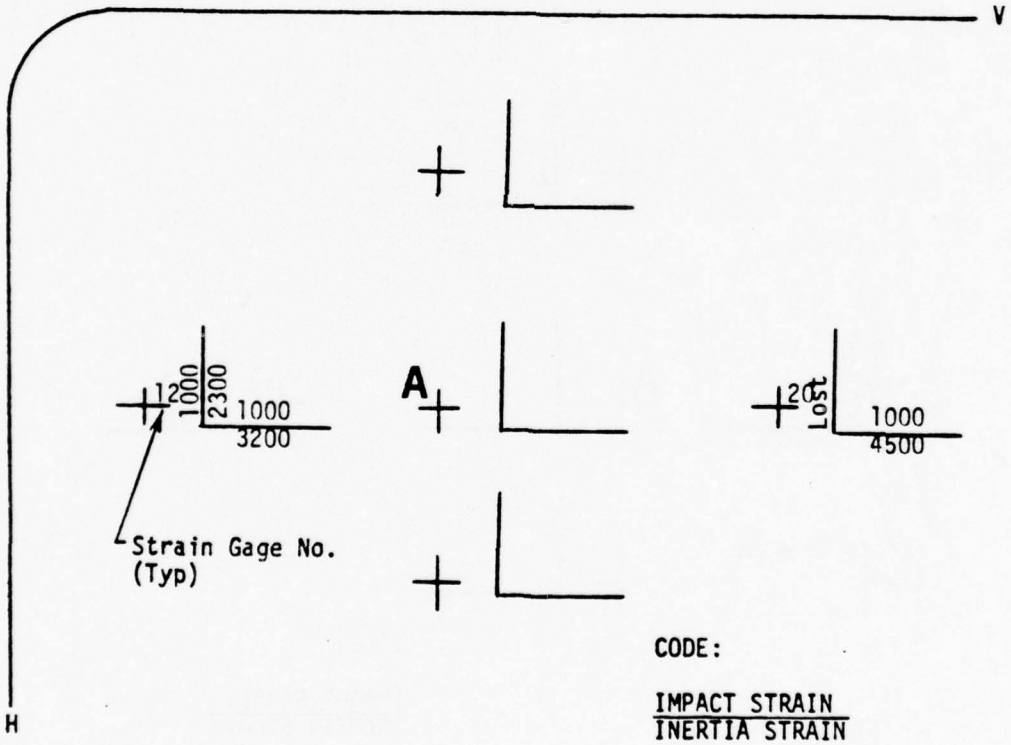

Figure B.8. Test Windshield Strain Map - Test BM012 - Gages, 12, 20.

STRAIN MAP

SPECIMEN NO. PPG 001 DESCRIPTION Laminated Glass (Z5942639-501)

TEST NO. BM012 SUPPORT STRUCTURE GL

IMPACT VELOCITY 943 FPS IMPACT POINT A

BIRD WEIGHT 4.00 lbs TEMPERATURE - OUTER PLY -28°F

DATE 7-16-76 TEMPERATURE - INNER PLY 7°F

STRAIN GAGE MOUNTED ON -7 SURFACE OF outer PLY

REAL TIME IMPACT 13.20 MICRO-SEC ($x10^2$) FROM + GATE

REAL TIME INERTIA 17.20 MICRO-SEC ($x10^2$) FROM + GATE

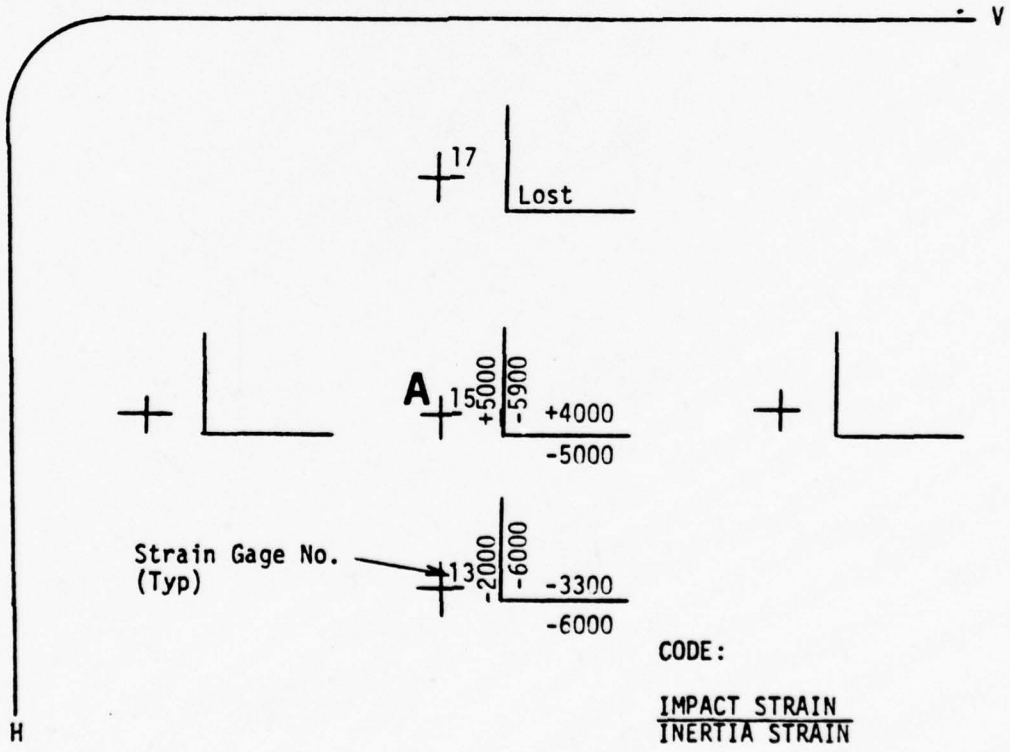

Figure B.9. Test Windshield Strain Map - Test BM012 - Gages, 13, 15, 17.

STRAIN MAP

SPECIMEN NO. PPG 001 DESCRIPTION Laminated Glass (Z5942639-501)

TEST NO. BM012 SUPPORT STRUCTURE GL

IMPACT VELOCITY 943 FPS IMPACT POINT A

BIRD WEIGHT 4.00 lbs TEMPERATURE - OUTER PLY -28°F

DATE 7-16-76 TEMPERATURE - INNER PLY 7°F

STRAIN GAGE MOUNTED ON -7 SURFACE OF inner PLY

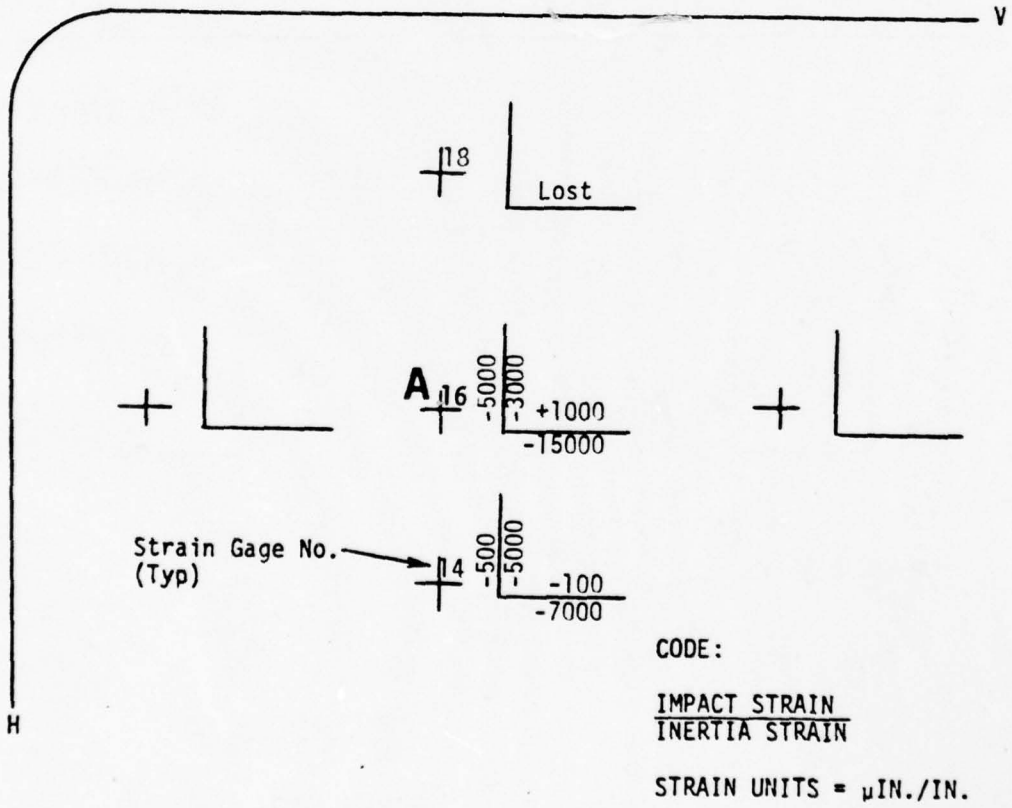

Figure B.10. Test Windshield Strain Map - Test BM012 - Gages, 14, 16, 18.

STRAIN MAP

SPECIMEN NO. PPG 001 DESCRIPTION Laminated Glass (Z5942639-501)

TEST NO. BM012 SUPPORT STRUCTURE GL

IMPACT VELOCITY 943 FPS IMPACT POINT A

BIRD WEIGHT 4.00 lbs TEMPERATURE - OUTER PLY -28°F

DATE 7-16-76 TEMPERATURE - INNER PLY 7°F

STRAIN GAGE MOUNTED ON inner SURFACE OF cockpit PLY

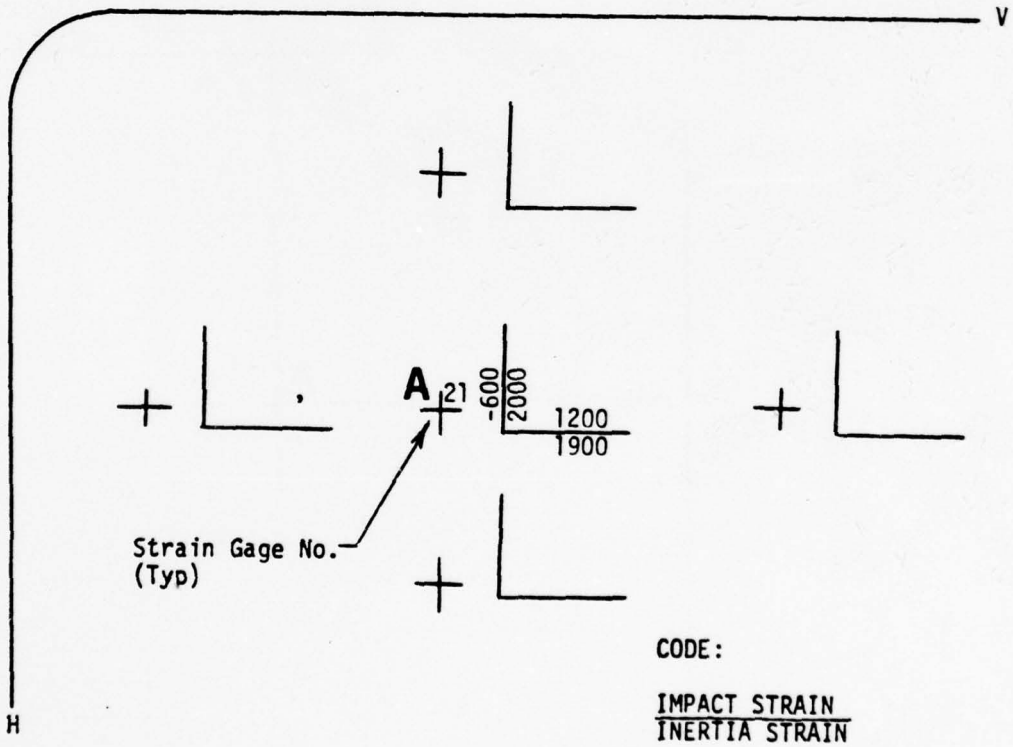

CODE:

IMPACT STRAIN
INERTIA STRAIN

STRAIN UNITS = μIN./IN.

Figure B.11. Test Windshield Strain Map - Test BM012 - Gage 21.

STRAIN MAP

SPECIMEN NO. PPG 001 DESCRIPTION Laminated Glass (Z5942639-501)

TEST NO. BM012 SUPPORT STRUCTURE GL

IMPACT VELOCITY 943 FPS IMPACT POINT A

BIRD WEIGHT 4.00 lbs TEMPERATURE - OUTER PLY -28°F

DATE 7-16-76 TEMPERATURE - INNER PLY 7°F

STRAIN GAGE MOUNTED ON Support Structure SURFACE OF inside PLY

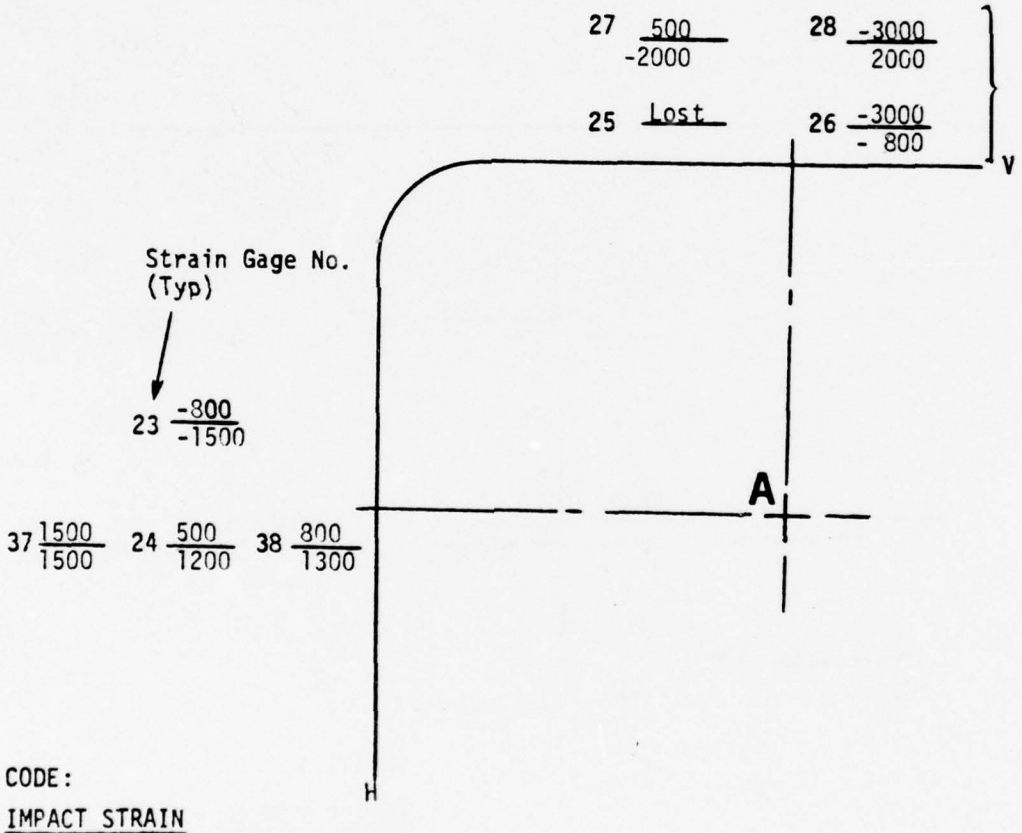

CODE:

IMPACT STRAIN / INERTIA STRAIN

STRAIN UNITS = μ IN./IN.

Figure B.12. Test Windshield Strain Map - Test BM012 - Gages on Support Structure.

STRAIN MAP

SPECIMEN NO. PPG 001 DESCRIPTION Laminated Glass (Z5942639-501)

TEST NO. BM013 SUPPORT STRUCTURE GL

IMPACT VELOCITY 948 FPS IMPACT POINT A

BIRD WEIGHT 4.06 lbs TEMPERATURE - OUTER PLY 80°F

DATE 7-17-76 TEMPERATURE - INNER PLY 80°F

STRAIN GAGE MOUNTED ON -9 SURFACE OF outer PLY

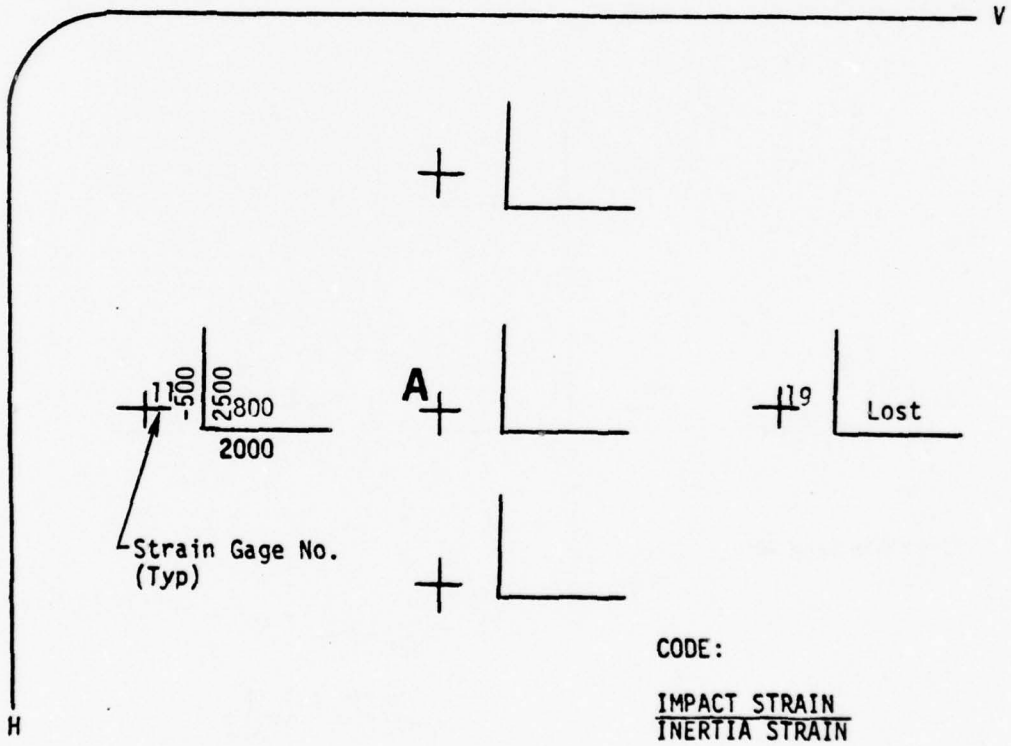

Figure B.13. Test Windshield Strain Map - Test BM013 - Gages, 11, 19.

STRAIN MAP

SPECIMEN NO. PPG 001 DESCRIPTION Laminated Glass (Z5942639-501)

TEST NO. BM013 SUPPORT STRUCTURE GL

IMPACT VELOCITY 948 FPS IMPACT POINT A

BIRD WEIGHT 4.06 lbs TEMPERATURE - OUTER PLY 80°F

DATE 7-17-76 TEMPERATURE - INNER PLY 80°F

STRAIN GAGE MOUNTED ON -9 SURFACE OF inner PLY

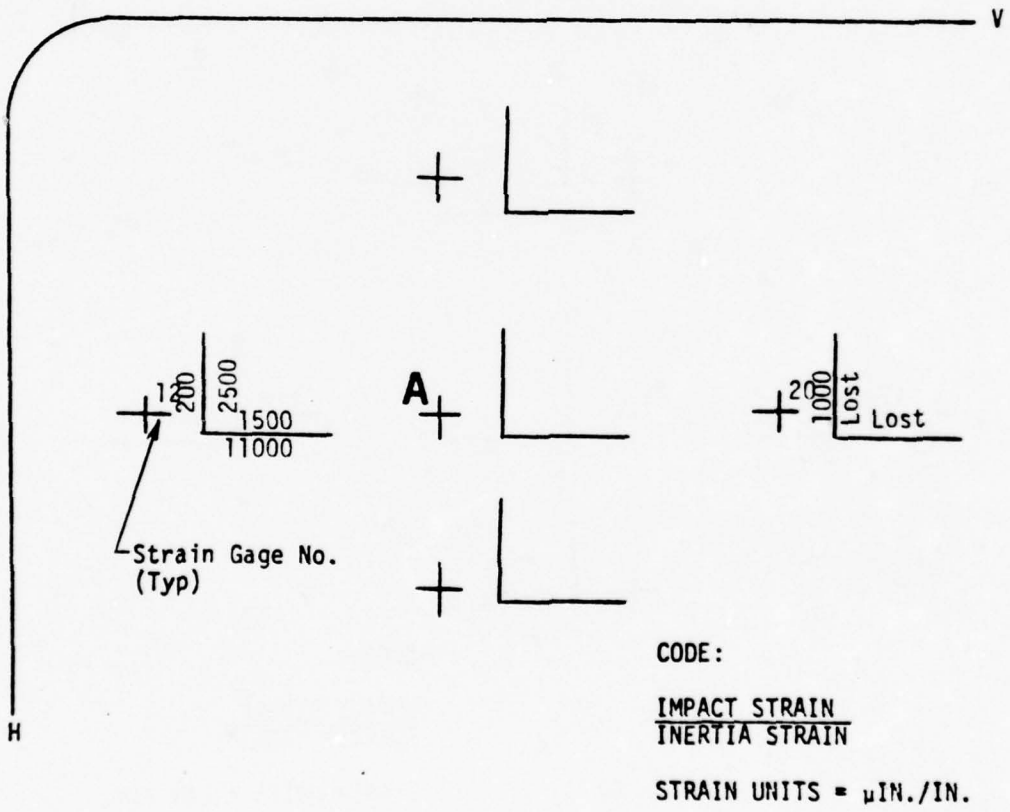

Figure B.14. Test Windshield Strain Map - Test BM013 - Gages 12, 20.

STRAIN MAP

SPECIMEN NO. PPG 001 DESCRIPTION Laminated Glass (Z5942E39-501)

TEST NO. BM013 SUPPORT STRUCTURE GL

IMPACT VELOCITY 948 FPS IMPACT POINT A

BIRD WEIGHT 4.06 lbs TEMPERATURE - OUTER PLY 80°F

DATE 7-17-76 TEMPERATURE - INNER PLY 80°F

STRAIN GAGE MOUNTED ON -7 SURFACE OF Outer PLY

REAL TIME IMPACT 10.20 MICRO-SEC (x 10^2) FROM + GATE

REAL TIME INERTIA 15.20 MICRO-SEC (x 10^2) FROM + GATE

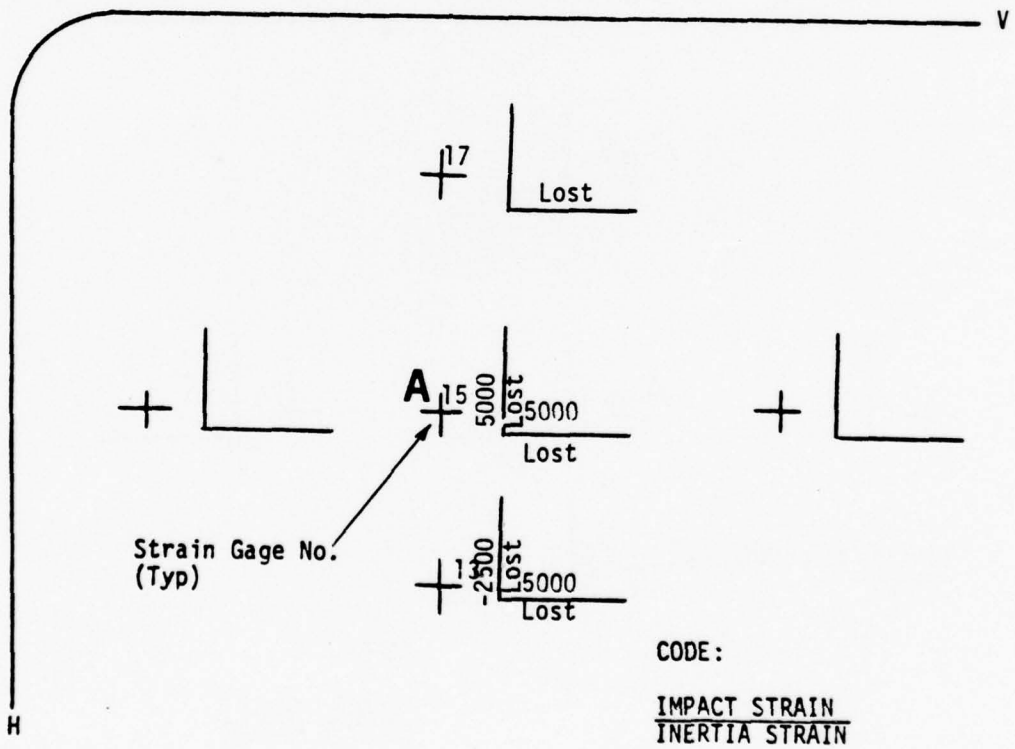

Figure B.15. Test Windshield Strain Map - Test BM013 - Gages 13, 15, 17.

STRAIN MAP

SPECIMEN NO. PPG 001 DESCRIPTION Laminated Glass (Z5942639-501)

TEST NO. BM013 SUPPORT STRUCTURE GL

IMPACT VELOCITY 948 FPS IMPACT POINT A

BIRD WEIGHT 4.06 lbs TEMPERATURE - OUTER PLY 80°F

DATE 7-17-76 TEMPERATURE - INNER PLY 80°F

STRAIN GAGE MOUNTED ON -7 SURFACE OF inner PLY

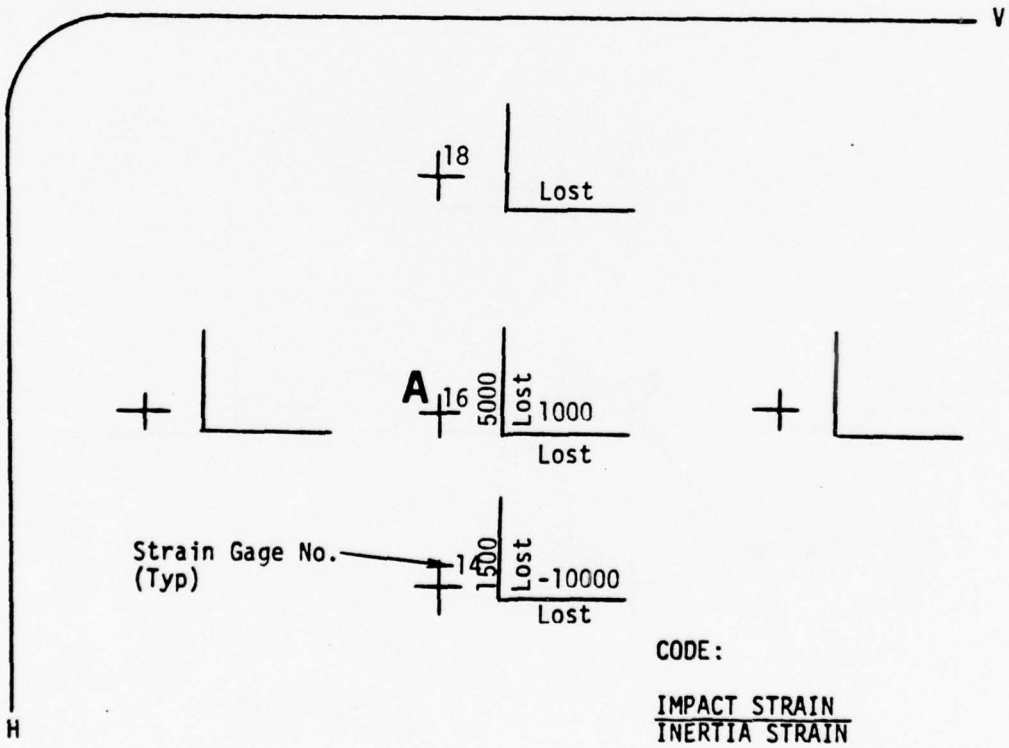

Figure B.16. Test Windshield Strain Map Test BM013 - Gages 14, 16, 18.

STRAIN MAP

SPECIMEN NO. PPG 001 DESCRIPTION Laminated Glass (Z5942639-501)

TEST NO. BM013 SUPPORT STRUCTURE GL

IMPACT VELOCITY 948 FPS IMPACT POINT A

BIRD WEIGHT 4.06 lbs TEMPERATURE - OUTER PLY 80°F

DATE 7-17-76 TEMPERATURE - INNER PLY 80°F

STRAIN GAGE MOUNTED ON inner SURFACE OF cockpit PLY

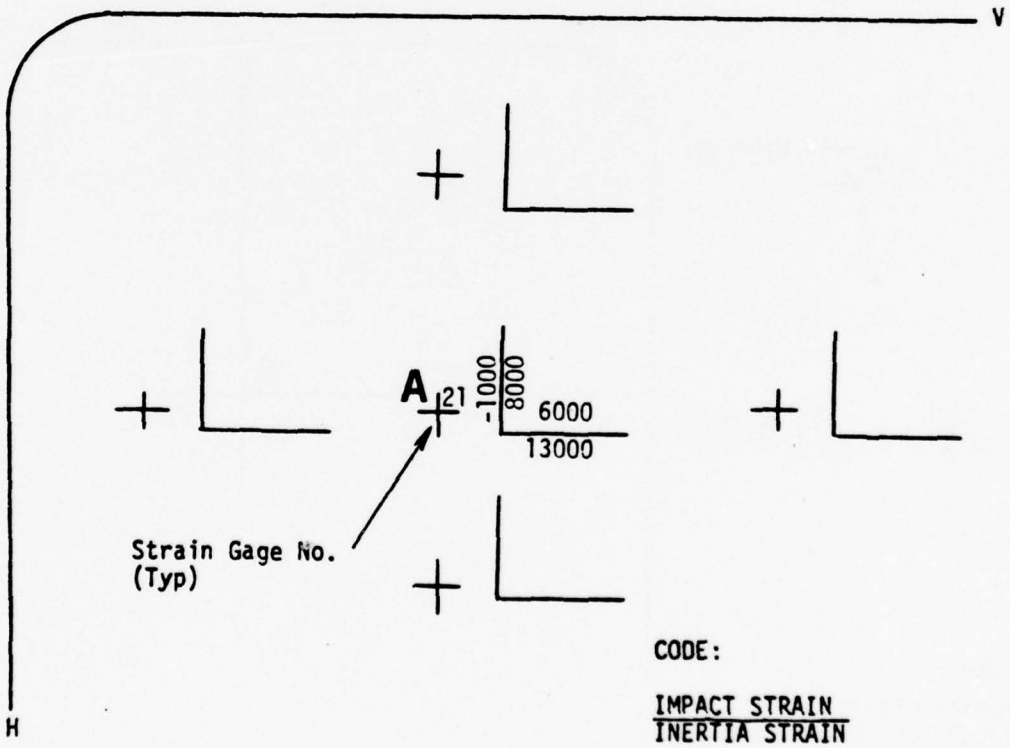

CODE:

IMPACT STRAIN
INERTIA STRAIN

STRAIN UNITS = μIN./IN.

Figure B.17. Test Windshield Strain Map - Test BM013 - Gage 21.

STRAIN MAP

SPECIMEN NO. PPG 001 DESCRIPTION Laminated Glass (Z5942639-501)

TEST NO. BM013 SUPPORT STRUCTURE GL

IMPACT VELOCITY 948 FPS IMPACT POINT A

BIRD WEIGHT 4.06 lbs TEMPERATURE - OUTER PLY 80°F

DATE 7-17-76 TEMPERATURE - INNER PLY 80°F

STRAIN GAGE MOUNTED ON Support Structure SURFACE OF inside PLY

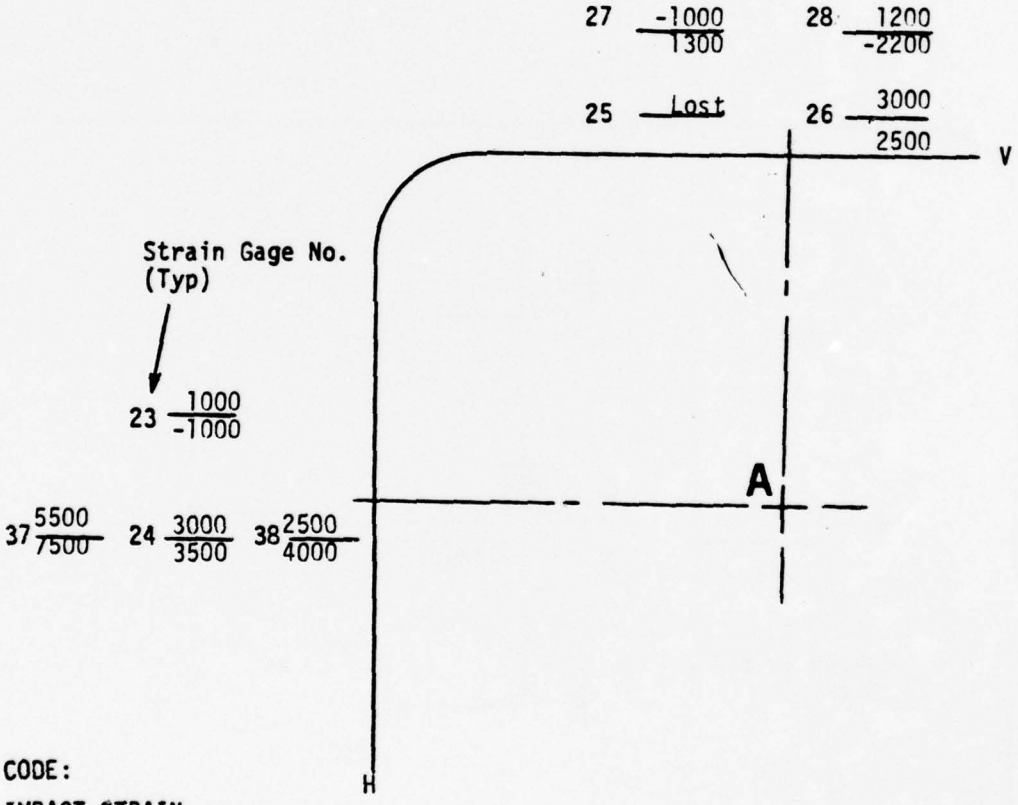

CODE:

IMPACT STRAIN / INERTIA STRAIN

STRAIN UNITS = μ IN./IN.

Figure B.18. Test Windshield Strain Map - Test BM013 - Gages on Support Structure.

STRAIN MAP

SPECIMEN NO. PPG 003 DESCRIPTION Laminated Glass (Z5942639-501)

TEST NO. BM019 SUPPORT STRUCTURE GL

IMPACT VELOCITY 974 FPS IMPACT POINT C

BIRD WEIGHT 4.02 lbs TEMPERATURE - OUTER PLY 190°F

DATE 7-26-76 TEMPERATURE - INNER PLY 160°F

STRAIN GAGE MOUNTED ON -9 SURFACE OF outer PLY

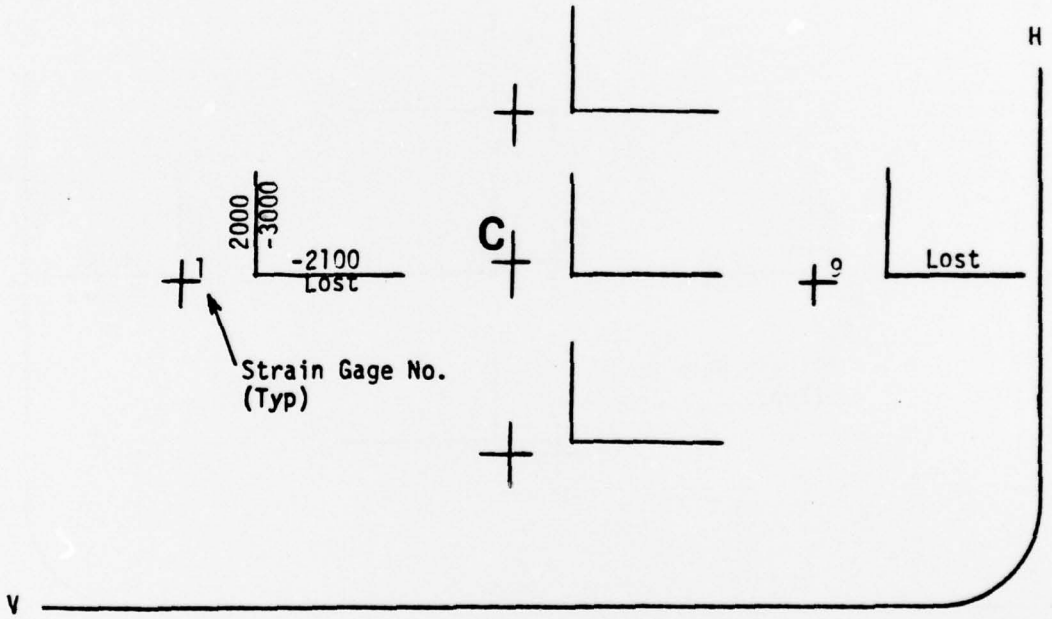

CODE:

IMPACT STRAIN
INERTIA STRAIN

STRAIN UNITS = μIN./IN.

Figure B.19. Test Windshield Strain Map - Test BM019 - Gages 1, 9.

STRAIN MAP

SPECIMEN NO. PPG 003 DESCRIPTION Laminated Glass (Z5942639-501)

TEST NO. BM019 SUPPORT STRUCTURE GL

IMPACT VELOCITY 974 FPS IMPACT POINT C

BIRD WEIGHT 4.02 lbs TEMPERATURE - OUTER PLY 190°F

DATE 7-26-76 TEMPERATURE - INNER PLY 160°F

STRAIN GAGE MOUNTED ON -9 SURFACE OF Inner PLY

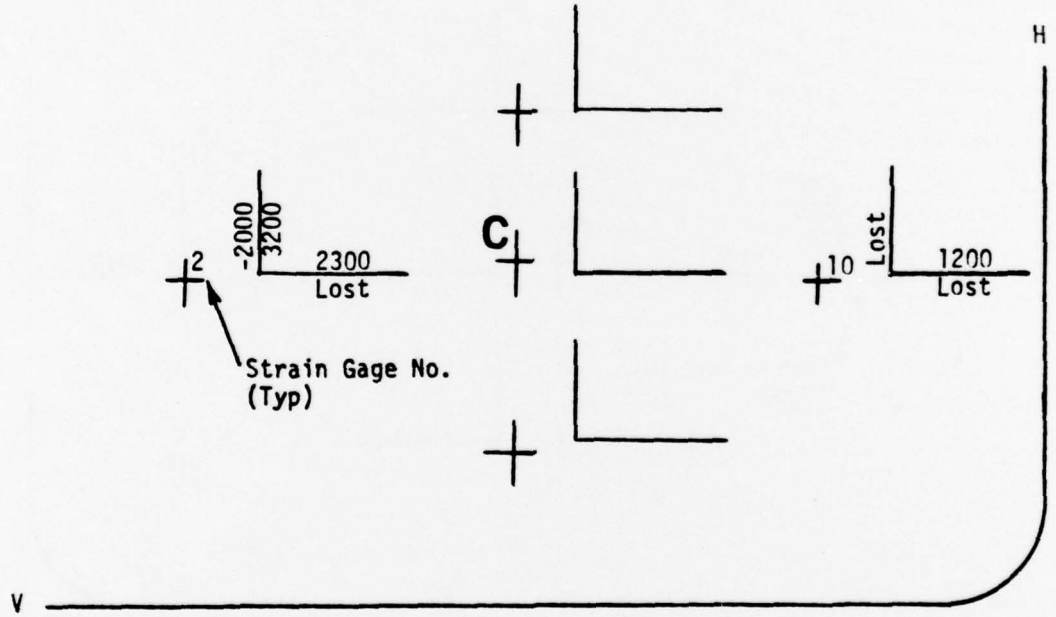

CODE:

IMPACT STRAIN
INERTIA STRAIN

STRAIN UNITS = μIN./IN.

Figure B.20. Test Windshield Strain Map - Test BM019 - Gages 2, 10.

STRAIN MAP

SPECIMEN NO. PPG 003 DESCRIPTION Laminated Glass (Z5942639-501)

TEST NO. BM019 SUPPORT STRUCTURE GL

IMPACT VELOCITY 974 FPS IMPACT POINT C

BIRD WEIGHT 4.02 lbs TEMPERATURE - OUTER PLY 190°F

DATE 7-26-76 TEMPERATURE - INNER PLY 160°F

STRAIN GAGE MOUNTED ON -7 SURFACE OF outer PLY

REAL TIME IMPACT 12.20 μ-SEC ($x10^2$) FROM + GATE

REAL TIME INERTIA 21.20 μ-SEC ($x10^2$) FROM + GATE

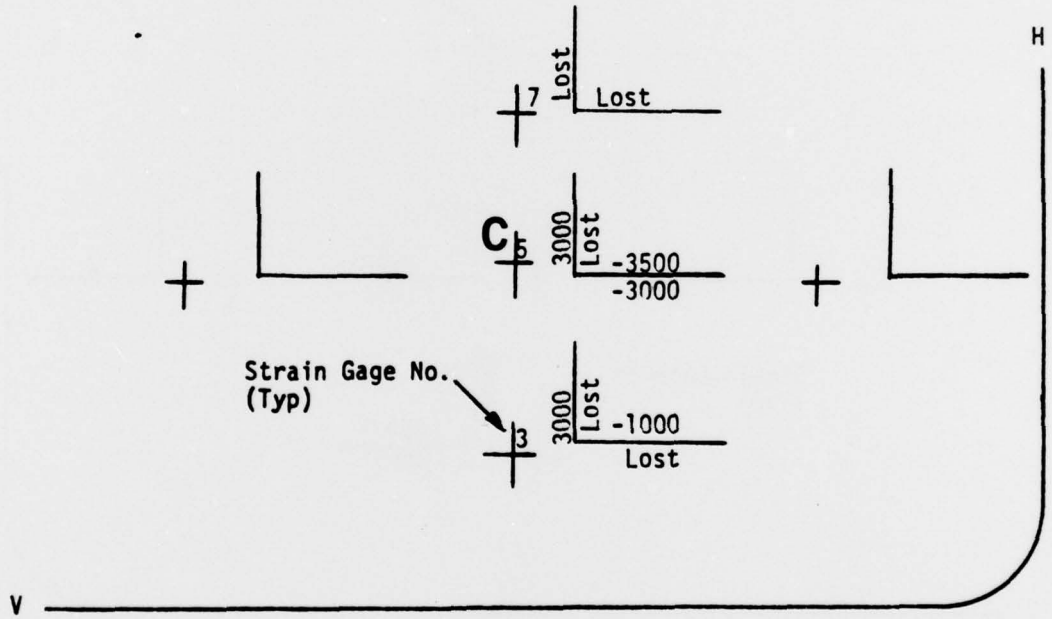

CODE:

IMPACT STRAIN
INERTIA STRAIN

STRAIN UNITS = μIN./IN.

Figure B.21. Test Windshield Strain Map - Test BM019 - Gages 3, 5, 7.

STRAIN MAP

SPECIMEN NO. PPG 003 DESCRIPTION Laminated Glass (Z5942639-501)

TEST NO. BM019 SUPPORT STRUCTURE GL

IMPACT VELOCITY 974 FPS IMPACT POINT C

BIRD WEIGHT 4.02 lbs TEMPERATURE - OUTER PLY 190°F

DATE 7-26-76 TEMPERATURE - INNER PLY 160°F

STRAIN GAGE MOUNTED ON -7 SURFACE OF inner PLY

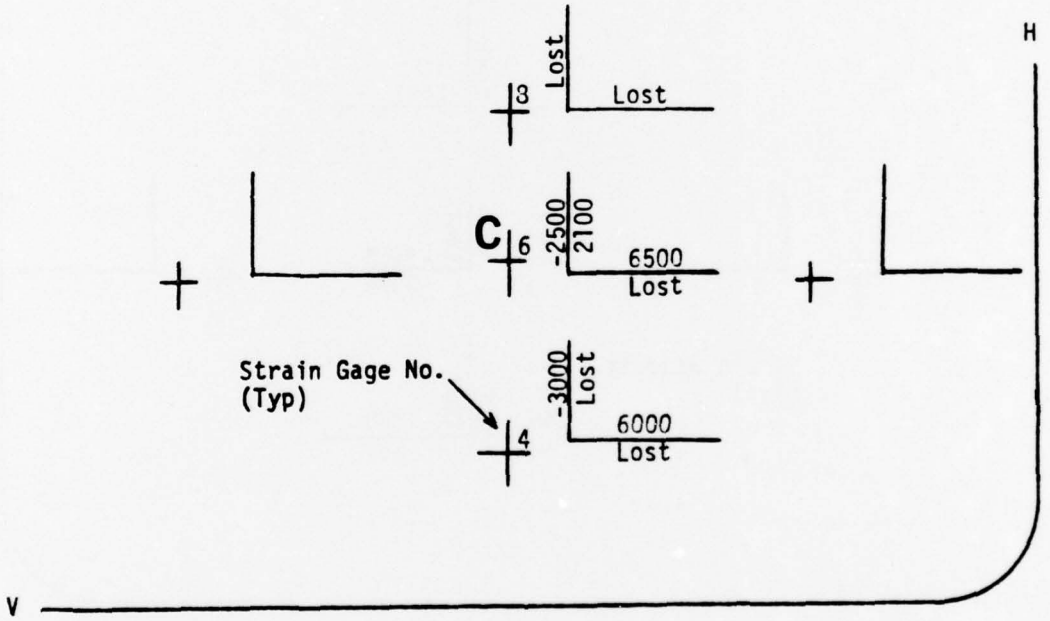

CODE:

IMPACT STRAIN
INERTIA STRAIN

STRAIN UNITS = μIN./IN.

Figure B.22. Test Windshield Strain Map - Test BM019 - Gages 4, 6, 8.

STRAIN MAP

SPECIMEN NO. PPG 003 DESCRIPTION Laminated Glass (Z5942639-501)

TEST NO. BM-19 SUPPORT STRUCTURE GL

IMPACT VELOCITY 974 FPS IMPACT POINT C

BIRD WEIGHT 4.02 lbs TEMPERATURE - OUTER PLY 190°F

DATE 7-26-76 TEMPERATURE - INNER PLY 160°F

STRAIN GAGE MOUNTED ON inner SURFACE OF cockpit PLY

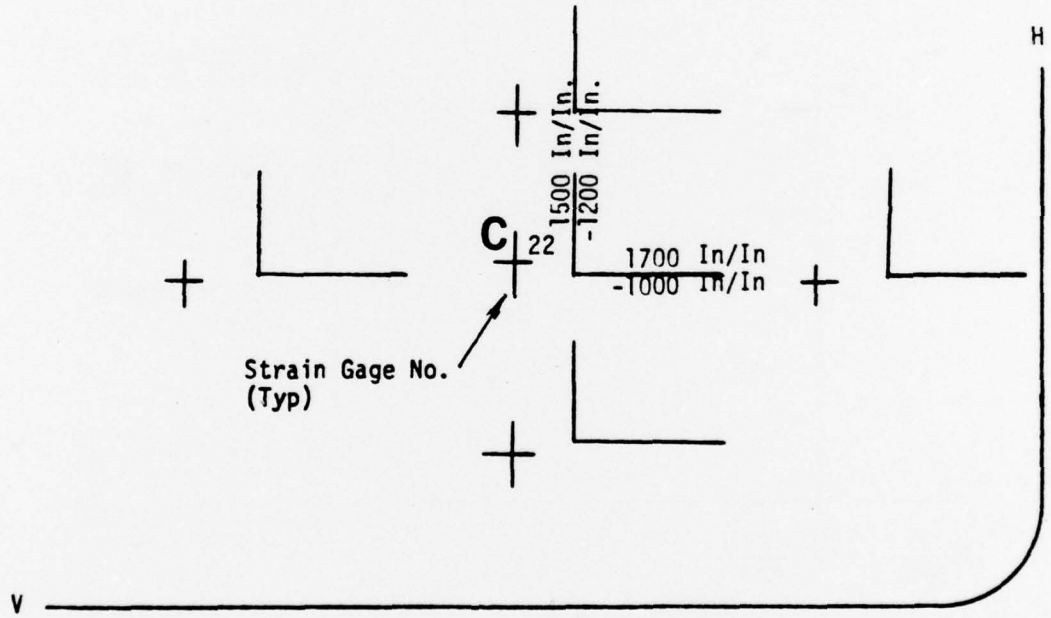

CODE:

IMPACT STRAIN
INERTIA STRAIN

STRAIN UNITS = μIN./IN.

Figure B.23. Test Windshield Strain Map - Test BM019 - Gage 22.

STRAIN MAP

SPECIMEN NO. PPG 003 DESCRIPTION Laminated Glass (Z5942639-501)

TEST NO. BM019 SUPPORT STRUCTURE GL

IMPACT VELOCITY 974 FPS IMPACT POINT C

BIRD WEIGHT 4.02 lbs TEMPERATURE - OUTER PLY 190°F

DATE 7-26-76 TEMPERATURE - INNER PLY 160°F

STRAIN GAGE MOUNTED ON Support Structure SURFACE OF inside PLY

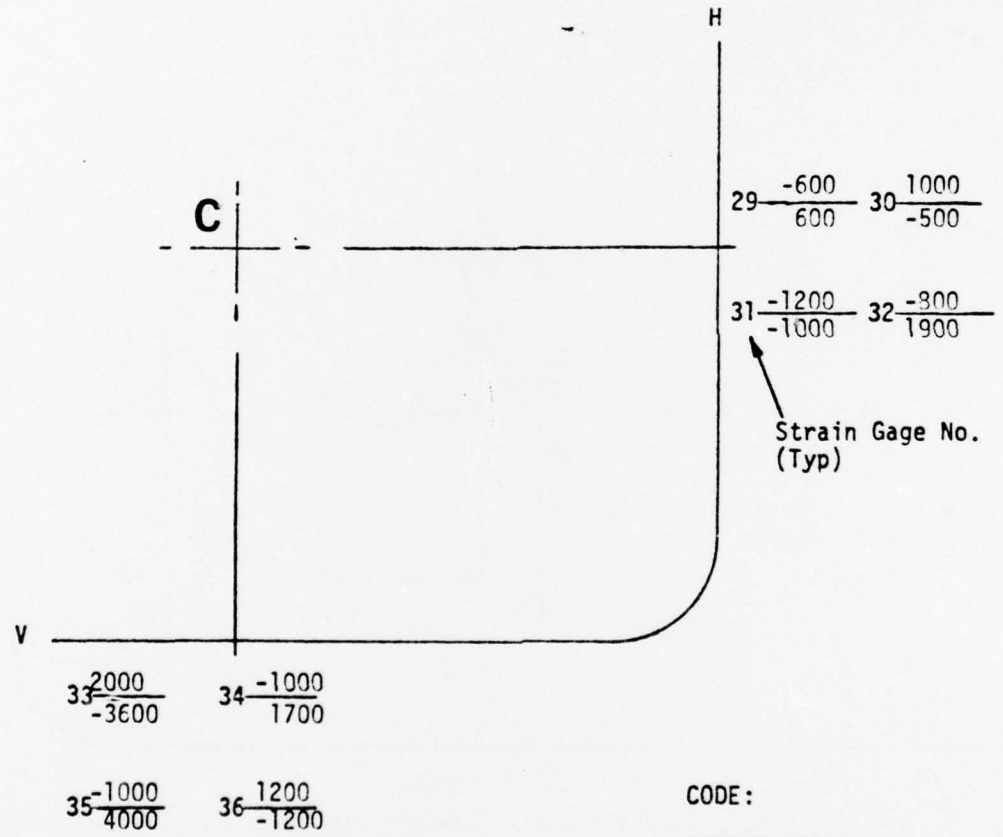

CODE:

IMPACT STRAIN / INERTIA STRAIN

STRAIN UNITS = μIN./IN.

Figure B.24. Test Windshield Strain Map - Test BM019 - Gages on Support Structure.

STRAIN MAP

SPECIMEN NO. PPG 002 DESCRIPTION Laminated Glass (Z5942639-501)

TEST NO. BM014 SUPPORT STRUCTURE GL

IMPACT VELOCITY 939 FPS IMPACT POINT C

BIRD WEIGHT 4.04 lbs TEMPERATURE - OUTER PLY 87°F

DATE 7-20-76 TEMPERATURE - INNER PLY 87°F

STRAIN GAGE MOUNTED ON -9 SURFACE OF Outer PLY

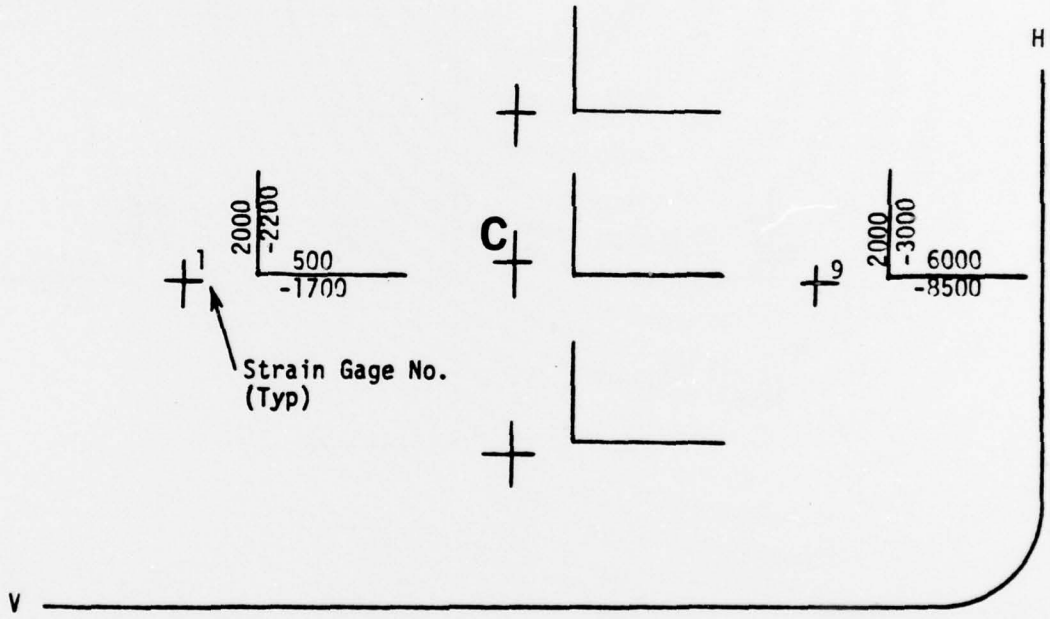

CODE:

IMPACT STRAIN
INERTIA STRAIN

STRAIN UNITS = μIN./IN.

Figure B.25. Test Windshield Strain Map - Test BM014 - Gages 1, 9.

STRAIN MAP

SPECIMEN NO. PPG 002 DESCRIPTION Laminated Glass (Z5942639-501)

TEST NO. BM014 SUPPORT STRUCTURE GL

IMPACT VELOCITY 939 FPS IMPACT POINT C

BIRD WEIGHT 4.04 lbs TEMPERATURE - OUTER PLY 87°F

DATE 7-20-76 TEMPERATURE - INNER PLY 87°F

STRAIN GAGE MOUNTED ON -9 SURFACE OF Inner PLY

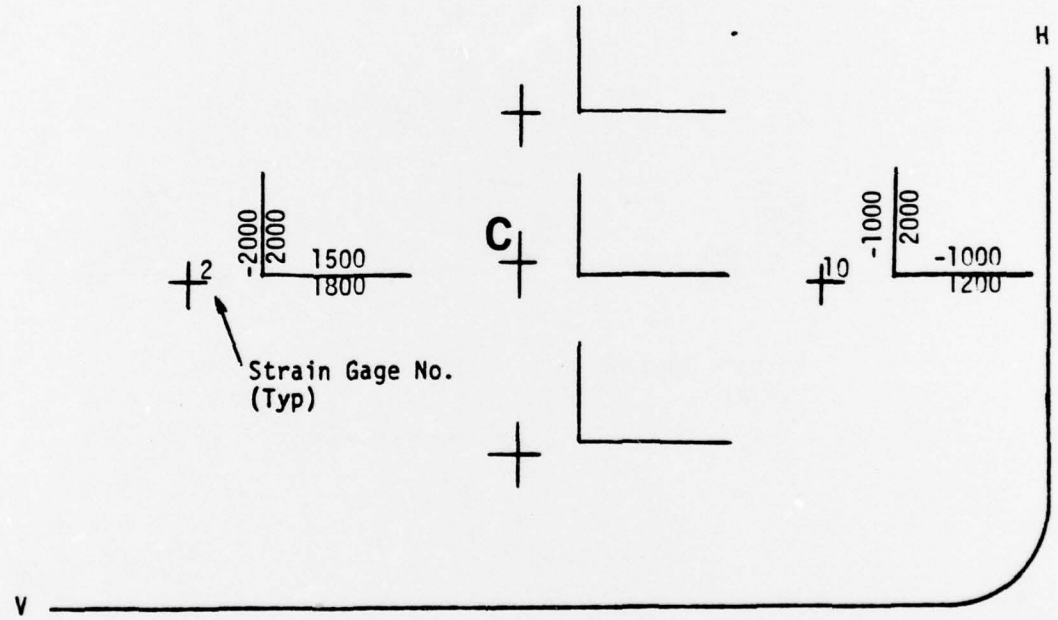

CODE:

IMPACT STRAIN
INERTIA STRAIN

STRAIN UNITS = μIN./IN.

Figure B.26. Test Windshield Strain Map - Test BM014 - Gages 2, 10.

STRAIN MAP

SPECIMEN NO. PPG 002 DESCRIPTION Laminated Glass (Z5942639-501)

TEST NO. BM014 SUPPORT STRUCTURE GL

IMPACT VELOCITY 939 FPS IMPACT POINT C

BIRD WEIGHT 4.04 lbs TEMPERATURE - OUTER PLY 87°F

DATE 7-20-76 TEMPERATURE - INNER PLY 87°F

STRAIN GAGE MOUNTED ON -7 SURFACE OF outer PLY

REAL TIME IMPACT 12.20 μ-SEC ($x10^2$) FROM + GATE

REAL TIME INERTIA 19.20 μ-SEC ($x10^2$) FROM + GATE

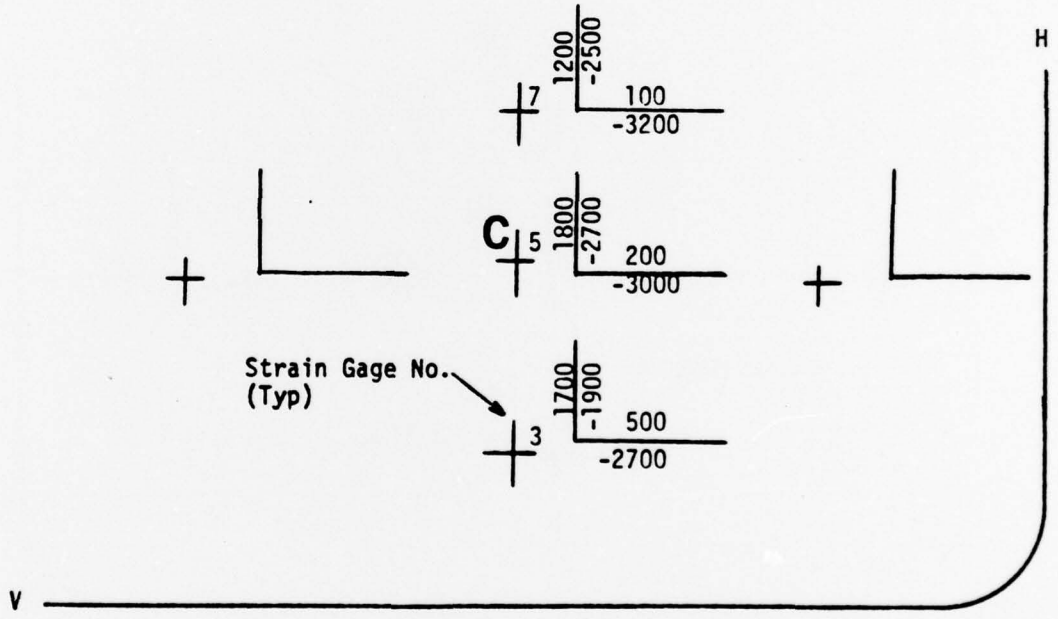

CODE:

IMPACT STRAIN
INERTIA STRAIN

STRAIN UNITS = μIN./IN.

Figure B.27. Test Windshield Strain Map - Test BM014 - Gages 3, 5, 7.

STRAIN MAP

SPECIMEN NO. PPG 002 DESCRIPTION Laminated Glass (Z5942639-501)

TEST NO. BM014 SUPPORT STRUCTURE GL

IMPACT VELOCITY 939 FPS IMPACT POINT C

BIRD WEIGHT 4.04 lbs TEMPERATURE - OUTER PLY 87°F

DATE 7-20-76 TEMPERATURE - INNER PLY 87°F

STRAIN GAGE MOUNTED ON -7 SURFACE OF inner PLY

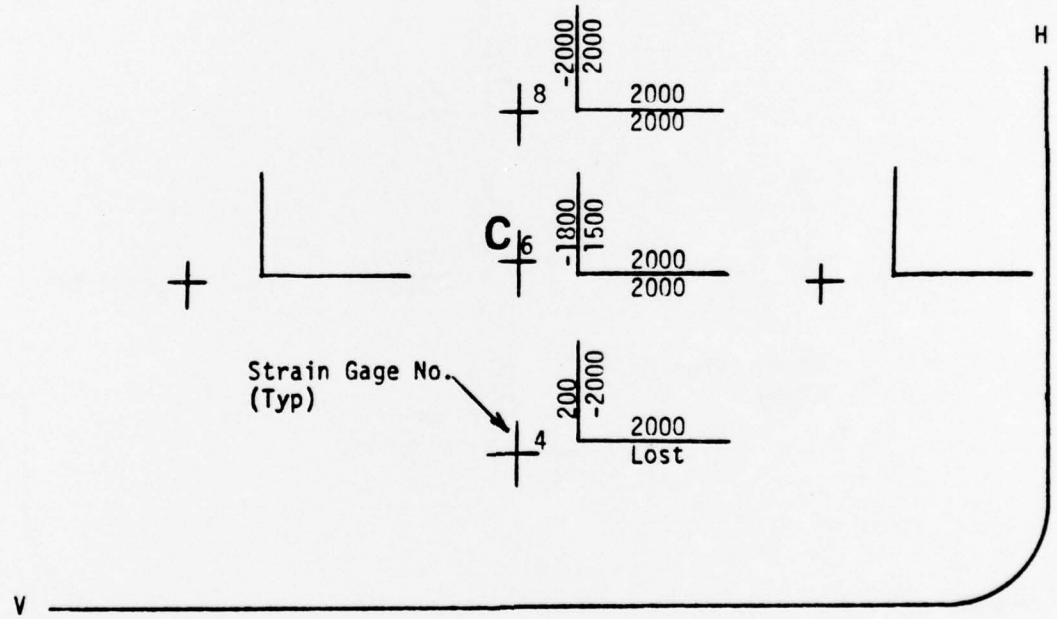

CODE:

IMPACT STRAIN
INERTIA STRAIN

STRAIN UNITS = μIN./IN.

Figure B.28. Test Windshield Strain Map - Test BM014 - Gages 4, 6, 8.

STRAIN MAP

SPECIMEN NO. PPG 002 DESCRIPTION Laminated Glass (Z5942639-501)

TEST NO. BM014 SUPPORT STRUCTURE GL

IMPACT VELOCITY 939 FPS IMPACT POINT C

BIRD WEIGHT 4.04 lbs TEMPERATURE - OUTER PLY 87°F

DATE 7-20-76 TEMPERATURE - INNER PLY 87°F

STRAIN GAGE MOUNTED ON Inner SURFACE OF Cockpit PLY

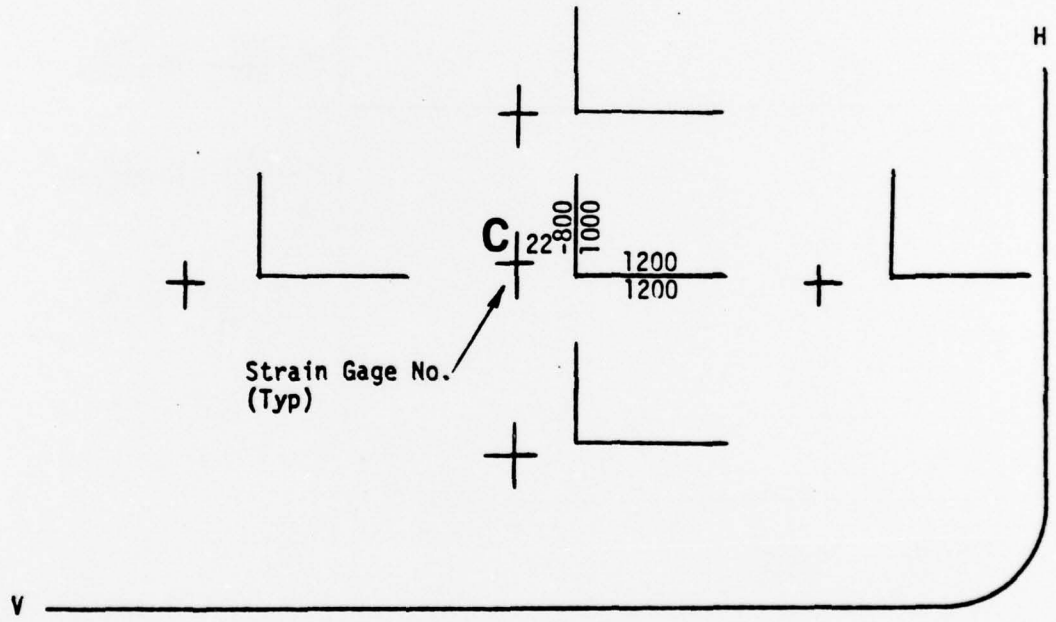

CODE:

IMPACT STRAIN
INERTIA STRAIN

STRAIN UNITS = μIN./IN.

Figure B.29. Test Windshield Strain Map - Test BM014 - Gage 22.

STRAIN MAP

SPECIMEN NO. PPF 002 DESCRIPTION Laminated Glass (Z5942639-501)

TEST NO. BM014 SUPPORT STRUCTURE GL

IMPACT VELOCITY 949 FPS IMPACT POINT C

BIRD WEIGHT 4.04 lbs TEMPERATURE - OUTER PLY 87°F

DATE 7-20-76 TEMPERATURE - INNER PLY 87°F

STRAIN GAGE MOUNTED ON Support Structure SURFACE OF Inside PLY

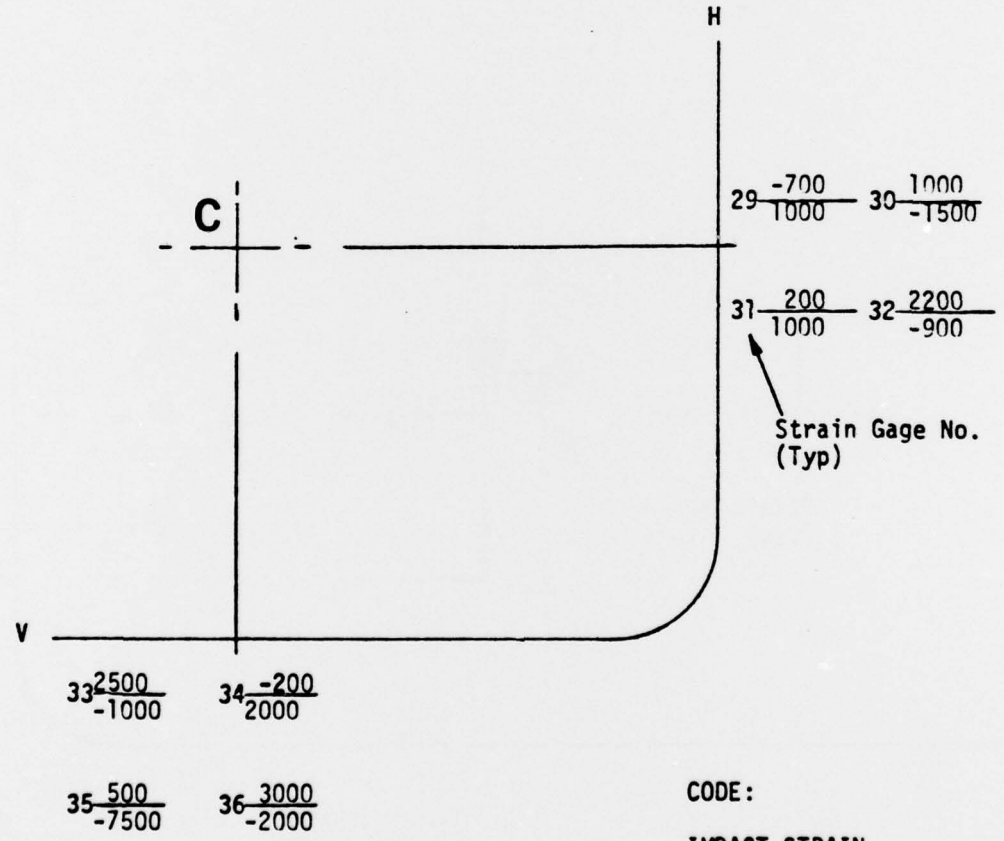

CODE:

IMPACT STRAIN / INERTIA STRAIN

STRAIN UNITS = μIN./IN.

Figure B.30. Test Windshield Strain Map - Test BM014 - Gages on Support Structure.

REFERENCES

1. Islander, L. Magnusson, R.H., Preliminary Bird Impact Tests, MDC Report J6947, Revision C, Douglas Aircraft Company, September 1976.

2. Sanders, E. J., Results of Further Tests to Evaluate the Bird Impact Resistance of Windshields for the B-1 Aircraft, AEDC-DR-76-43, May 1976.

3. Sanders, E. J., Results of Bird Impact Testing of Prototype B-1 Windshields and Support Structure Design, AEDC-DR-76-100, December 1976.

4. Sanders, E. J., Results of Qualification Testing of Bird Resistance Windshields for the B-1 Aircraft, AEDC-DR-75-87, September 1975.

5. Structural Test Programs, "DVT Crew Module X-5 Bird Impact Tests Strain Gage Instrumentation Package", Rockwell International Report TFD-75-353, May 1975.

6. Metcalf, J. M., Development of a Turbine Engine Inlet Device for Protection Against Bird Ingestion, Project 520-004-03H, July 1969.

7. Littell, Jr., H. E., Improved Windshield and Canopy Protection Development Program, AFFDL-TR-74-75, June 1974.

8. Ingelse, A. O., Wintermute, G. E., Gaynes, M. H. Waters, E. L., Bird Strike Capabilities of Transparent Aircraft Windshield Materials, AFML-TR-74-234, Part I, December 1974, and Part II, October 1975.

9. McQuilkin, F. T., "The Design Development of a Birdproof Windshield for B-1 Strategic Bomber", Conference on Transparent Aircraft Enclosures, Las Vegas, Nevada, February 1973; Technical Report AFML-TR-73-126, Wright-Patterson AFB, Ohio, P. 531-557.

10. Starkey, G. W., Haviland, G. P., B-1 Program Development Test and Evaluation Plan, NA-70-550-3-2, May 1971.

11. Denke, P. H., Hoffman, J. B., The Determination of Deflection and Stress Distribution for a Transparent Laminated Beam, AFML-TR-76-114, March 1977.

12. Roark, R. J., Formulas for Stress and Strain, Fourth Edition McGraw-Hill Book Company, 1965.

13. Green, F. E., Testing for Mechanical Properties of Monolithic and Laminated Polycarbonate Materials, AFFDL-TR-77-96, March 1978.

14. Lawrence, J. L., Jr., etal., Windshield Technology Demonstrator Program - Detail Design Options Study, AFFDL-TR-77-1, Volume 1, 2, and 3, September 1977.

REFERENCES (Continued)

15. Denke, P. H., Aircraft Windshield Bird Impact Math Model, AFFDL-TR-77-99, Part 1, 2 and 3, December 1977.

16. Design and Testing of F-111 Bird Resistant Windshield/Support Structure, University of Dayton Research Institute, June 1976 (AFFPL Contract F33615-75-C-3134).

17. Myklestad, N. O., Vibration Analysis, McGraw-Hill Book Co., 1956.

18. Rhodes, G. F., Damping, Static, Dynamic and Impact Characteristics of Laminated Beams Typical of Windshield Construction, AFFDL-TR-76-156, December 1977.

19. Barber, J. P., Wilbeck, J. S., Characterization of Bird Impacts on a Rigid Plate: Part 1, AFFDL-TR-75-5, January 1975.

20. Barber, J. P., Bird Impact Loading Models for Structural Code Input, VDRI-TM-76-14, University of Dayton Research Institute, May 1976.

21. Lawrence, J. H., Magnusson, R. H., Kelly, R. D., Certification Bird Tests for Windshields and Clearview Windows - Model DC-10, MDC Report J0025, Douglas Aircraft Company, August 1969.